

**Anti-Trypanosomal and Metabolomic Effects of Propolis
Constituents**

**A Thesis Presented for the Degree of Doctor of Philosophy in the
Strathclyde Institute of Pharmacy and Biomedical Sciences at the
University of Strathclyde**

BY

Sultan Saadi Almutairi

2015

Declaration

‘This thesis is the result of the author’s original research. It has been composed by the author and has not been previously submitted for examination which has led to the award of a degree.’

‘The copyright of this thesis belongs to the author under the terms of the United Kingdom Copyright Acts as qualified by University of Strathclyde Regulation 3.50. Due acknowledgement must always be made of the use of any material contained in, or derived from, this thesis.’

Signed:

Date:

Acknowledgments

I am very grateful to my first supervisor, Dr David G. Watson, who gave me the opportunity to undertake this PhD, for teaching, supporting and guiding me while providing a lot of valuable advice. At the same time, I would like to express my sincere appreciation to him for proposing me as a potential candidate to continue this research at postdoctoral level.

My heartfelt thanks are also to my second supervisor, Dr. RuAn Edrada-Ebel, for her guidance, encouragement and assistance.

I would like to express my sincere thanks to Prof. Alexander Gray and Dr. John Igoli for helping with NMR experiments.

I am thankful to Dr. Tong Zhang and all my colleagues in both DW and REE labs for their support and useful time as we shared experiences and information.

I want to express my gratitude to my wife and all my brothers and sisters who have always taken great interest in and cared about my studies. Special appreciation goes to my mother and late father for their support since I was a little child.

Finally, I would like to thank the Ministry of Health of Saudi Arabia for offering me a scholarship to pursue my studies at the University of Strathclyde.

Table of Contents

Declaration	i
Acknowledgments.....	ii
List of tables.....	viii
List of figures	xi
List of Abbreviations.....	xviii
Abstract	xx
Published work from this research.....	xxii
1 GENERAL INTRODUCTION TO PROPOLIS.....	2
1.1 Propolis.....	2
1.1.1 Composition of Propolis	2
1.1.2 Biological Activity of Propolis	7
1.2 Trypanosomiasis.....	9
1.2.1 Introduction.....	9
1.2.2 Distribution of the disease.....	10
1.2.3 African trypanosomiasis.....	11
1.2.4 American trypanosomiasis	11
1.2.5 Treatments for Trypanosomiasis.....	11
1.2.6 Currently available drugs and their limitations.....	14
1.3 Instrumental methods	17
1.3.1 Introduction.....	17
1.3.2 High resolution mass spectrometry.....	17
1.3.3 Orbitrap	19
1.3.4 HPLC with evaporative light scattering (ELSD) detection	20
1.3.5 Medium pressure liquid chromatography	22
1.3.6 NMR Techniques: DEPT, COSY, HMBC, HMQC and NOESY.	24

1.4	Metabolomics	27
1.4.1	Mass Spectrometry in Metabolomics.....	27
1.4.2	Metabolomics Applications	30
1.4.3	Sample Preparation	30
1.4.4	Software in Metabolomics	32
1.4.5	Trypanosome Metabolomics.....	33
1.5	Aims and Objectives	37
2	MATERIALS AND METHODS.....	39
2.1	Chemical reagents	39
2.2	Laboratory Equipment and tools	39
2.3	Propolis samples.....	39
2.4	Extraction of propolis samples	40
2.4.1	Extraction of propolis used for LC-MS Profiling	40
2.4.2	Extraction of propolis used for fractionation and purification.....	40
2.5	Preparative Chromatographic Methods.....	41
2.5.1	Column Chromatography.....	41
2.5.2	Medium Pressure Liquid Chromatography	42
2.5.3	Semi-preparative HPLC	44
2.6	Analytical Chromatographic Methods	44
2.6.1	HPLC-UV-ELSD	45
2.6.2	Thin Layer Liquid Chromatography (TLC).....	45
2.7	Measurement of Optical Rotation	46
2.8	Data Extraction and Database Searching	46
2.9	NMR Methods	47
2.10	Bioassay.....	48
2.10.1	Trypanocidal assay.....	48

2.10.2	Anti-mycobacterial Assay	49
3	CHEMICAL AND BIOLOGICAL PROFILING OF PROPOLIS	51
3.1	General screening of propolis samples against <i>Trypanosoma brucei</i>	51
3.2	High resolution mass spectrometry profiles of African propolis samples ..	53
3.3	Development of a Rapid Method for the Analysis of Propolis by LC-MS .	58
3.4	Natural Product Data Base	58
3.5	Discussion	61
4	PROFILING AND ATTEMPTED PURIFICATION OF ANTITRYPANOSOMAL PROPOLIS EXTRACTS.....	65
4.1	Results of Investigation of Nigerian propolis Sample (S95).....	65
4.2	Result of fractionation of Tanzanian Propolis (TP1) Samples.....	72
4.3	Discussion	75
4.4	Conclusion on Nigerian and Tanzanian propolis samples	77
5	FRACTIONATION AND TESTING OF A PROPOLIS SAMPLE FROM GHANA	79
5.1	LC-MS profiling of propolis sample–S87.....	79
5.2	Further Fractionation of Sample S87	87
5.3	Identification and isolation of bioactive compounds of Ghanaian propolis .	87
5.4	Semi-preparative high pressure liquid chromatography.....	87
5.5	Flash chromatography the Grace Reveleris®.....	89
5.6	Characterization of new prenylated stilbenes from Ghanaian propolis.....	91
5.6.1	Structure of Ghana propolis stilbine 1 (F9-1)	93
5.6.2	Structure of Ghana propolis stilbene 2 (F13-11).....	98
5.7	Biological activities of new stilbenes	103
5.7.1	Anti-trypanosomal activity	103
5.8	Discussion	104

6	METABOLOMIC PROFILING OF THE EFFECTS PRENYLATED STILBENES ON <i>T. BRUCEI</i>	106
6.1	Introduction	106
6.2	Materials and Methods	106
6.2.1	Chemicals and solvents	106
6.2.2	Cell extraction	106
6.2.3	Mass spectrometry	107
6.3	Metabolomics data processing	107
6.3.1	The Effect of compound F13-11 on the Metabolome of <i>T. b. brucei</i>	107
6.3.2	Conclusion	110
7	PROFILING, TESTING AND FRACTIONATION OF SAUDI ARABIAN PROPOLIS	120
7.1	Introduction	120
7.2	Methodology	121
7.2.1	Saudi Arabian Propolis	121
7.2.2	Extraction of Saudi Arabian Propolis Metabolites	122
7.2.3	Chromatographic Isolation of Components in Saudi Arabian propolis	122
7.2.4	Analysis of Fractions from Saudi Arabian propolis using LC-MS, LC-UV-ELSD.....	124
7.2.5	NMR experiment.....	125
7.3	Results	126
7.3.1	The yields obtained and bioactivity fractions of KSA1 extracts.....	132
7.3.2	Identification and Structure Elucidation of main compound from fraction 4 (CF4).....	135
7.3.3	Characterisation of CF4 (Flavonoid compound).....	136

7.3.4	Further characterisation of bioactive Fractions obtained from KSA propolis extracts	141
7.3.5	Identification and Structure Elucidation of Purified Compounds from CF6 and CF7	144
7.4	Biological Testing of Components Isolated from Saudi Arabian Propolis	168
7.4.1	Anti-Trypanosomal and Anit-mycobacterium activity	168
7.5	Discussion	169
8	GENERAL DISCUSSION.....	173
9	CONCLUSIONS AND FUTURE WORK	179
10	REFERENCES.....	181
11	Appendix I: Publication	190

List of tables

Table 1.1: Common compounds occurring in raw propolis.....	3
Table 1.2: The available of trypanocidal drugs (Bouteille et al., 2003, Legros et al., 2002)	13
Following ion formation the determination of these ions is performed by a mass analyser which acts to separate and distinguish the ions based on their respective mass/charge ratios. The ability of a mass spectrometer to distinguish very closely related masses determines its resolving power. Table 1.3: Comparison of common high resolution mass analyser (Krauss et al., 2010).....	18
Table 1.4: Common examples of nuclei and their spin quantum numbers.....	26
Table 2.1: EtOAc and EtOH extractions weight for biologically active propolis samples.....	41
Table 2.2: Sequence of MPLC solvent systems for EtOAc extracts of propolis	43
Table 2.3: Sequence of fractions collected on the Grace Reveleris® flash system for EtOAc extracts (S87F13)	44
Table 3.1: The most potent propolis samples tested against <i>T. brucei</i> initially at 20µg/ml and then MIC was determined.....	52
Table 3.2: Summary of the data obtained from the samples observed to putatively contain propolones according to LC-MS profiles.....	55
Table 4.1: The %yield of fractions obtained of sample 95 by SP.....	65
Table 4.2: Anti-trypanosomal activity of the fractions from propolis sample S95....	67
Table 4.3: Shows the most abundant compounds in fractions 3-5. These elemental compositions could correspond to a range of structural types including triterpenes, lignans or propolones.....	69
Table 4.4: The yield of fractions obtained of sample TB1 by normal phase on MPLC	72

Table 5.1: The compounds in the crude extract of S87 which are the most abundant by response when analysed by reversed phase LC-MS in positive ion mode.	80
Table 5.2: Summary for the weights and anti-trypanosomal and anti-mycobacterium activities obtained from S87 extracts. The brown cells indicate the highest activity. Fractions in pink have been isolated and identified.	82
Table 5.3: ¹ H NMR (400 MHz) and ¹³ C NMR (100 MHz) data of new prenylated compounds F9-1 and F13-11	92
Table 5.4: MIC of the stilbenes isolated from Ghanian propolis along with positive controls against <i>T. brucei brucei</i>	103
Table 6.1: The effects of fraction 11-13 on the metabolic profile of <i>T. brucei</i> comparison of 4 h or incubation fraction vs control and 24 h incubation fraction vs control	113
Table 7.1: Sequence of Column Chromatography Solvent Systems and propolis extracts collected	123
Table 7.2: The compounds in the crude extract of Saudi propolis which are the most abundant by response when analysed by reversed phase LC-MS in positive ion mode.	127
Table 7.3: Yields and activities of pooled fractions obtained from KSA1 extract the fractions which are highlighted had strong activity, while pink highlight indicates the compounds which were identified	132
Table 7.4: The most abundant in mixture fraction 5 when analysed by reversed phase LC-MS in positive ion mode	134
Table 7.5: ¹ H and ¹³ C NMR data of compound CF4 (400 MHz, CHCl ₃)	138
Table 7.6: ¹ H and ¹³ C chemical shifts for Anadanthoside and CF6-F5 (400MHz, d ₆ -DMSO)	147
Table 7.7: ¹ H NMR (400 MHz) and ¹³ C NMR (100 MHz) data of compounds CF6-F6 (400 MHz, DMSO- d ₆)	153

Table 7.8: ^{13}C NMR (100 MHz) and ^1H NMR (400 MHz) chemical shifts for CF7-M2 (400MHz, CDCl_3) and Diterpene 3 (75MHz, pyridine- d_5).....	158
Table 7.9: ^1H NMR (400 MHz) and ^{13}C NMR (100 MHz) data of compound 4 in CDCl_3 . Highlighted rows indicate the differences from Compound 3.	167
Table 7.10: MIC against <i>M. marinum</i> and <i>T. brucei</i>	168

List of figures

Figure 1.1: The structures of some flavonoids and phenolics identified in propolis. . . 5	5
Figure 1.2: Structures of some terpenes and the phenolic esters identified in propolis. 6	6
Figure 1.3: The structures of some prenylated benzophenones identified in propolis. 7	7
Figure 1.4: Distribution of Human African Trypanosomiasis in sub-Sahara Africa and Latin American countries (Hamilton, 2014, Anon, 2008). 10	10
Figure 1.5: Melarsoprol is converted in the host to Melarsen Oxide, which is concentrated by the P2 purine transporter to react with trypanothione to form Mel T or to react with other targets (Fairlamb, 2003). 15	15
Figure 1.6: Structures of drugs used to treat (a) early stage and (b) late stage trypanosomiasis..... 16	16
Figure 1.7: A: LTQ Orbitrap. B: Schematic of the basic components of a mass spectrometer (Snider, 2014). 20	20
Figure 1.8: Principle of HPLC-ELSD detection of compounds during analysis (SHIMADZU, 2015). 22	22
Figure 1.9: The main components of a medium pressure liquid chromatography system (Claeson et al., 1993). 23	23
Figure 1.10: Basic element of classical NMR spectrometer. 24	24
Figure 1.11: Overall comparison of metabolomes: (A) a normal mammalian cell; (B) bloodstream stage of the African Trypanosome, <i>T. brucei</i> . Pathways are coloured as follows: purple for fatty acid and sterol metabolism; orange for carbohydrate metabolism and electron transport; green for amino acids and related metabolites; light blue for, pyrimidine, purine and nucleic acid metabolism; yellow for co-enzyme biosynthesis (Fairlamb, 2002). 36	36

Figure 3.1: General screening of propolis samples from different regions of Africa for activity against against <i>T. brucei</i>	51
Figure 3.2: Phloroglucinol	58
Figure 3.3: The structure of Hyperforin.....	62
Figure 3.4: LC-MS spectral analysis for phloroglucinone present in St John's Wort63	
Figure 4.1: Testing of crude extract of S95 and its fractions for anti-trypanosomal activity.....	66
Figure 4.2: Extracted ion traces for the main compounds in fraction 3. The masses and elemental compositions were as follows: A: m/z 515.23±0.03 (C ₂₉ H ₃₉ O ₈), B: m/z 531.25±0.01 (C ₂₉ H ₃₉ O ₉), C: m/z 537.23±0.03 (C ₃₁ H ₃₇ O ₈) and D: m/z 517.222±0.11 (C ₂₉ H ₄₁ O ₈). These elemental compositions match that of propolones. The peak numbers -denote compounds that possibly exist as isomers in the fraction.	68
Figure 4.3: Shows ions for co-eluting compounds present in the peak at 25.7 min which appears to be the most abundant peak in the samples.	69
Figure 4.4: Extracted ion traces for the main compounds in fraction 4. The masses and elemental compositions were as follows: A: m/z 515.23±0.03 (C ₂₉ H ₃₉ O ₈), B: m/z 531.25±0.01 (C ₂₉ H ₃₉ O ₉), C: m/z 537.23±0.03 (C ₃₁ H ₃₇ O ₈) and D: m/z 517.222±0.11 (C ₂₉ H ₄₁ O ₈). These elemental compositions match that of propolones. The peak numbers denote compounds that possibly exist as isomers in the fraction.....	70
Figure 4.5: Extracted ion peaks for the main compounds present in fraction 5. The masses and elemental compositions were as follows: A: m/z 515.23±0.03 (C ₂₉ H ₃₉ O ₈), B: m/z 531.25±0.01 (C ₂₉ H ₃₉ O ₉), C: m/z 537.23±0.03 (C ₃₁ H ₃₇ O ₈) and D: m/z 517.222±0.11 (C ₂₉ H ₄₁ O ₈). These elemental compositions match that of propolones. The peak numbers denote compounds that possibly exist as isomers in the fraction.	71
Figure 4.6: Extracted ion peaks for the main compounds present in fraction 6-7 obtained from Tanzanian Propolis. The masses and elemental compositions were as follows: A: m/z 314.48±1.00 (C ₁₇ H ₁₅ O ₆), B: m/z 424.75±1.00 (C ₂₆ H ₄₉ O ₄), C: m/z	

308.62±1.00 (C ₂₀ H ₃₇ O ₂) and D: m/z 427.38±0.20 (C ₃₀ H ₅₁ O). The compound in chromatogram A corresponds to a dimethyl flavanone whereas compounds in B-C are not as unsaturated and may correspond to terpenoids.....	74
Figure 4.7: Proton NMR spectrum (400 MHz in CDCl ₃) of fraction 6-7 showing mainly aliphatic protons.....	75
Figure 4.8: Phloroglucinone compounds (Almutairi et al., 2014)	76
Figure 5.1: Extracted ion chromatogram and mass spectrum for S87-1 which is the most abundant compound by response in S87 when analysed by reversed phase LC-MS in positive ion mode.	81
Figure 5.2: Fractions from MPLC containing compound S87-1	81
Figure 5.3: Extracted ion chromatogram and mass spectrum for S87-2 which is the second most abundant compound by response in S87 when analysed by reversed phase LC-MS in positive ion mode.....	83
Figure 5.4: Fractions from MPLC containing compound S87-2	84
Figure 5.5: Extracted ion chromatogram and mass spectrum for S87-3 which is the third most abundant compound by response in S87 when analysed by reversed phase LC-MS in positive ion mode.....	85
Figure 5.6 Fractions from MPLC containing compound S87-3	85
Figure 5.7: Extracted ion chromatogram and mass spectrum for S87-12 which is the 12 th most abundant compound by response in S87 when analysed by reversed phase LC-MS in positive ion mode.....	86
Figure 5.8: Fractions from MPLC containing compound S87-12	86
Figure 5.9: ¹ H NMR spectrum (400 MHz, in CDCl ₃) of crude S87 showing mainly aliphatic protons.	87
Figure 5.10: Semi-prep (A) and Analytical HPLC (B) column chromatograms for 87F9-1 Conditions as in section 2.5.3.....	89

Figure 5.11: ^1H NMR spectrum (400 MHz, in CDCl_3) fraction 13 from MPLC separation of S87.....	90
Figure 5.12: LC-UV-ELSD chromatogram of fraction F13-11 purified from fraction 13 by MPLC (Conditions as in section 2.5.2.2).....	91
Figure 5.13: New prenylated stilbenes.....	91
Figure 5.14: LC-MS trace and ESI mass spectrum of F9-1.....	94
Figure 5.15: ^1H NMR of F9-1 (400 MHz, CDCl_3). The peaks denoted by X represent signals from ethyl acetate.....	95
Figure 5.16: The correlation of the protons in a COSY spectrum of F9-1 labelled in blue prenyl substituents and pink (aromatic system).	96
Figure 5.17: Expansion of the HMBC of F9-1 highlighted and labelled the correlations between olefinic protons and the resorcinol ring and another different correlation which is different from that of the chalcone poinsettifolin B.	97
Figure 5.18: Prenylated stilbenes 1 (87F9-1)1 and poinsettifolin B with highlighting of the different groups.....	98
Figure 5.19: Key HMBC correlations ($\text{H} \rightarrow \text{C}$) for compound F9-1.....	98
Figure 5.20: ^1H NMR of F13-11 (400 MHz, Acetone- d_6).	99
Figure 5.21: The DEPT ^{13}C NMR spectrum F13-11.	100
Figure 5.22: LC-MS trace and ESI mass spectrum of F13-11.....	100
Figure 5.23: Expansion of the HMBC of F13-11. The labelled correlations show how the location of the signals for the open chromenol ring differs from those of F9-1.101	
Figure 5.24: Key HMBC correlations ($\text{H} \rightarrow \text{C}$) for compounds F13-11.	102
Figure 5.25: geranylated stilbenes f13-11 (2) and some Related Compounds.	102
Figure 6.1: Deamidation of phenylalanine and histidine when normal grown in culture.....	110

Figure 6.2: Extracted ion trace showing increased levels of sedoheptulose phosphate in <i>T. b. brucei</i> treated with fraction 11 for 24 h.	111
Figure 7.1: Distribution of <i>Apis mellifera jemenitica</i> Ruttner in the Arabian Peninsula and northeastern Africa (Alqarni et al., 2011).	121
Figure 7.2: Saudi Arabian propolis.	122
Figure 7.3: ¹ H NMR spectrum (400 MHz, DMSO-d ₆) of crude Saudi propolis.	128
Figure 7.4: Extracted ion traces (A-E) for the the most abundant components in a crude extract of Saudi propolis. These elemental compositions could correspond to a range of structural type diterpenes and flavonoids as shown inTable 7.2	129
Figure 7.5: Extracted ion chromatogram and mass spectrum for the third most abundant compound by response in crude extract of Saudi propolis. The elemental composition corresponds to that of the diterpene abietic acid.	130
Figure 7.6: Structure of diterpene abietic acid.	130
Figure 7.7: Extracted ion chromatogram and mass spectrum for the fourth most abundant compound by response in a crude extract of Saudi propolis. The elemental composition shown corresponds to casticin.	131
Figure 7.8: Structure of casticin.	131
Figure 7.9: Extracted ion traces (A-D) for the main compounds present in fraction 5 run in positive ion mode. Their elemental composition are as shown inTable 7.4..	134
Figure 7.10: LC-UV-ELSD chromatogram of fraction 4 (CF4) methods as in section 7.2.3. Pink trace UV absorbance (290 nm) and brown trace ELSD response.	135
Figure 7.11: HR-ESIMS ion chromatogram and mass spectrum of the main component in CF4	136
Figure 7.12: ¹ H NMR of CF6-f6 (400 MHz, CDCl ₃).....	137
Figure 7.13: ¹³ C NMR spectrum of CF6-F6 (100 MHz, CDCl ₃).....	137
Figure 7.14: HMBC correlations (H → C) for compound in F4.	140

Figure 7.15: Structure of CF4 (psiadiarabin 2)	141
Figure 7.16: TLC analysis of CF 6 from a Saudi propolis extract using 60:40% EtOAc/ hexane as a mobile phase. The spots were observed with anisaldehyde spray and also under short UV light λ 254 nm.	142
Figure 7.17: LC-UV-ELSD chromatogram of fraction 6(CF6) of KSA propolis extracts methods as in section 7.2.3 (Pink traces ELSD and blue trace UV at 290 nm).	143
Figure 7.18: LC-UV-ELSD chromatogram of fraction 7(CF7) of KSA propolis extracts methods as in section 7.2.3 (brown trace ELSD and blue trace UV at 290 nm).	143
Figure 7.19: LC-UV-ELSD chromatogram of CF6-F5 purified from CC (Section 7.2.3.1) (Pink traces ELSD and blue trace UV at 290 nm).....	145
Figure 7.20: HR-ESIMS ion chromatogram and mass spectrum of CF6-F5.....	145
Figure 7.21: Structure of CF6-f5. (Fisetinidol): 3, 4-dihydro-2-(3, 4-dihydroxyphenyl)-2H-chromene-3, 7-diol.....	145
Figure 7.22: COSY spectrum of the compound present in CF6-F5 (400 MHz, d-DMSO).....	149
Figure 7.23: COSY correlations of F6-f5. The coloured arrows show the correlations corresponding COSY correlations in Figure 7-22.	149
Figure 7.24: The structure anadanthoside (Piacente et al., 1999) that data were compared to proposed structure for F6-F5.....	150
Figure 7.25: Structure of CF6-F6 psiadiarabin 1	151
Figure 7.26: LC-UV-ELSD chromatogram of CF6-F6 purified from CC (conditions in section 7.2.3.1).....	151
Figure 7.27: HR-ESIMS ion chromatogram and mass spectrum of CF6-F6.....	152
Figure 7.28: ^1H NMR of CF6-f6 (400 MHz, DMSO-d ₆).	154

Figure 7.29: ^{13}C NMR spectrum of CF6-F6 (100 MHz, $-\text{DMSO-d}_6$).....	155
Figure 7.30: Psiadiarabin 1 structure (El-Feraly et al., 1990).....	155
Figure 7.31: Chemical structure of CF7-M1.....	157
Figure 7.32: Positive ion HR-ESIMS extracted ion chromatogram and mass spectrum of CF7-M1.....	159
Figure 7.33: LC-UV-ELSD Chromatogram of CF7-M1 Purified from Grace flash chromatography (in section 7.2.3.2) ELSD trace in pink.....	159
Figure 7.34: ^1H NMR of CF7-M1 (400 MHz, CDCl_3)	160
Figure 7.35: The DEPT Q ^{13}C NMR spectrum of CF7-M1 (100 MHz, CDCl_3)	160
Figure 7.36: COSY spectrum of the CF7-M1 structure showing the correlations mentioned in the discussion above and shown in figure 7-31.	161
Figure 7.37: Key HMBC (\rightarrow) and COSY correlations. The colours arrows show the corresponding to the COSY correlations in Figure 7-36.	161
Figure 7.38: HMBC correlations of CF7-M1.	162
Figure 7.39: nOe interactions observed in the NOESY spectrum for CF7-M1 (compound 3)	163
Figure 7.40: Fragmentation of m/z 319.2256 $[\text{M}+\text{H}]^+$. (A) Mass spectrum for ion using the LTQ-Orbitrap. (B) The proposed fragmentation pathway of compound 3 ($\text{C}_{20}\text{H}_{31}\text{O}_3$).....	164
Figure 7.41: CF7-M5 structure compound 4. The differences between this compound and Compound 3 are highlighted.	166
Figure 7.42: Flavonoids and diterpenes isolated of Psiadia species (Albar, 2014)..	171

List of Abbreviations

μM	Micromolar
^{13}C NMR	Carbon nuclear magnetic resonance
2D NMR	Two dimensional nuclear magnetic resonance spectroscopy
Brs	Broad singlet
CC	Column chromatography
CDCl_3	Deuterated Chloroform
COSY	^1H - ^1H Correlation Spectroscopy
D	Doublet
Dd	Doublet of a doublet
DEPT	Distortionless Enhancement by Polarization Transfer
DMSO	Dimethyl sulphoxide
EI	Electrospray
ELSD	Evaporative light scattering detection
EtOAc	Ethyl acetate
FAB	Fast Atom Bombardment
H	Hour
^1H NMR	Proton nuclear magnetic resonance
HAT	Human African Trypanosomiasis
HMBC	Heteronuclear Multiple Bond Coherence
HMQC	Heteronuclear Multiple Quantum Coherence
HPLC	High performance liquid chromatography
HR-ESIMS	High resolution electrospray ionisation mass spectrometry
Hz	Hertz
LC-MS	Liquid chromatography mass spectrometry
M	Multiple
M. aurum	Mycobacterium aurum

Mg	milligram
MHz	Megahertz
MIC	Minimum inhibitory concentration
ml	millilitre
MPLC	Medium pressure liquid chromatography
MS	Mass Spectroscopy
NMR	Nuclear Magnetic Resonance
No.	Number
NOESY	spectroscopy Nuclear Overhauser effect
°C	Celsius
S	Singlet
SP	straight phase
T	Triplet
T.brucei	Trypanosoma brucei
TLC	Thin layer Chromatography
TMS	Tetramethylsilane
UV	Ultraviolet light
WHO	World Health Organization

Abstract

Propolis, a product from honeybees, is a resinous material composed of beeswax and resin obtained from plant secondary metabolites. It has been used as a folk remedy by humans since ancient times for treatment of many ailments such as wounds, inflammation and peptic ulcer disease. This study investigated the parasiticidal and metabolomic effects of propolis on *Trypanosoma brucei*, the etiologic agent for sleeping sickness which is an endemic parasitosis in sub-Saharan Africa as well as anti-mycobacterial effects.

Propolis samples (n=91) which were mainly from Africa were extracted and profiled by high resolution LC-MS. The active samples which were available in high abundance were subjected to a series of chromatographic separations (open column, MPLC and HPLC) and screening techniques including HR-LCMS and NMR (1D & 2D) in order to separate and identify biologically active compounds present in the extracts. Fractionation was carried out on four samples as follows: S95 (Nigeria), S87 (Ghana), P1 (Tanzania) and KSA1 (Saudi Arabian) which possessed high potency against trypanosomes. Metabolomic effects were also investigated on blood stream form trypanosomes for a compound isolated from S87.

Two new anti-trypanosomal prenylated stilbenes [(*E*)-5-(2-(8-hydroxy-2-methyl-2-(4-methylpent-3-en-1-yl)-2*H*-chromen-6-yl)vinyl)-2-(3-methylbut-2-en-1-yl)benzene-1,3-diol (F9) and 5-((*E*)-3,5-dihydroxystyryl)-3-((*E*)-3,7-dimethylocta-2,6-dien-1-yl)benzene-1,2-diol] (F13-11) were isolated from ethyl acetate extracts of the Ghanaian sample (S87). Both compounds exhibited moderate activity against *T. brucei* with MICs of 6.73 and 16.45 μ M, respectively. A new diterpene psiadin [(*ent*)-2-oxo-kaur-16-en-6,18-diol] (4) along with three known flavonoids 3,4-dihydro-2-(3,4-dihydroxyphenyl)-2*H*-chromene-3,7-diol (1), psiadiarabin (2), psiadiarabin (5) and a known diterpene psiadin (3) were isolated from the Saudi Arabian sample. Compound 1 was inactive at the initial concentration tested against *T. brucei* and *M. marinum* while compounds 2–4 had MICs at 30.9, 78.1, and 78.1 μ M against *T. brucei* and 312.1, 312.1 and 69.1 μ M against *M. marinum*, respectively. Psiadiarabin (5) showed considerable activity (0.6 % of control) during the initial screening at 20 μ g/ml concentration.

A new stilbene compound (F13-11) exhibited more interesting biological activity and was isolated in higher quantities than F9-1, another stilbene, which made the former a suitable candidate for metabolomic profiling on *T. brucei*. Treatment of *T. brucei* with F13-11 revealed significant metabolomic changes including alterations in levels of some of the essential amino acids, elevation of some of the sugars, particularly sedoheptulose, and minor increments in lipids.

Overall, this work has revealed new propolis constituents with significant activity against *T. brucei* and has confirmed the presence of some potential therapeutic compounds in propolis which could be employed as leads in new drug discovery.

Published work from this research

1. **Almutairi, Sultan**, Ben Eapen, Sai Maneesha Chundi, Adnan Akhalil, Weam Siheri, Carol Clements, James Fearnley, David G. Watson, and RuAngelie Edrada-Ebel. "New anti-trypanosomal active prenylated compounds from African propolis." *Phytochemistry Letters*, 10 (2014): 35-39.
2. **Almutairi, Sultan**, RuAngelie Edrada-Ebel, James Fearnley, John O. Igoli, Waqas Alotaibi, Carol J. Clements, Alexander I. Gray, and David G. Watson. "Isolation of diterpenes and flavonoids from a new type of propolis from Saudi Arabia." *Phytochemistry Letters* 10 (2014): 160-163.
3. Zhang, Tong, Ruwida Omar, Weam Siheri, **Sultan Al Mutairi**, Carol Clements, James Fearnley, RuAngelie Edrada-Ebel, and David Watson. "Chromatographic analysis with different detectors in the chemical characterisation and dereplication of African propolis." *Talanta*, 120 (2014): 181-190.

CHAPTER ONE:

GENERAL INTRODUCTION TO PROPOLIS, TRYPANOSOMIASIS, METABOLOMICS AND INSTRUMENTAL METHODS

1 GENERAL INTRODUCTION TO PROPOLIS

1.1 Propolis

Propolis is a resinous bee product composed of beeswax blended with resins collected by honey bees from exudates of various plants within their environment. The substance is utilized by the bees to seal and maintain hives, and may be generally used as an anti-infective substance (Burdock, 1998, Bertelli et al., 2012); hence the reason why propolis is often called bee glue. The Greek origins of the word highlight its meaning: *pro-* (in defence or before) and *polis-* (the city); that is, the defence of the city or the hive (Salatino et al., 2011). Another function of propolis is to protect the colony of bees against diseases caused by fungi or bacteria since it displays both antifungal and antibacterial activities respectively. Propolis appears as a highly resinous, sticky gum and, like other lipophilic substances, its consistency changes according to temperature, becoming elastic and sticky when warm, but hard and brittle when cold (Hausen et al., 1987). Its colours vary from yellowish- green to dark brown depending on its age and source and it has a pleasant aroma since it often contains lower terpenoids (Marcucci, 1995).

1.1.1 Composition of Propolis

For over a decade ago, it has been claimed (in Table 1-1) that temperate propolis, the one which has been investigated to the greatest extent, normally contains approximately 55 % of the total components in form of resinous substances and balsams, 30 % wax, 10% aromatic and essential oils, 5% pollen and 5% in form of various other substances such as organic debris(Burdock, 1998). However, the components of raw propolis differ depending on the harvest season, geographical location, and plant source; its composition varies because of the broad range of plants foraged by honey bees while collecting it (Crane, 1990).

Table 1.1: Common compounds occurring in raw propolis

Ingredient	Group of Ingredients	Amount
Resins	Flavonoids, Esters and Phenolic Acids	45-55%
Waxes and Fatty Acids	Beeswax and Plant Origin	23-35%
Essential Oils	Volatiles	10%
Pollen	Proteins (16 free amino acids>1%) Arginine and Proline, together 46% of total	5%
Other Organics and Minerals	14 traces of minerals, zinc and iron most common; lactones, quinines, ketenes, steroids, benzoic acid, sugar and vitamins	5%

There are currently many studies in literature that describe the chemical information, including molecular structures and biological activities, of various individual components isolated from propolis. In recent years, researchers employing advanced techniques of separation, purification and analysis, including medium pressure liquid chromatography (MPLC), HPLC, and gas chromatography (GC), alongside identification techniques such as mass spectrometry and nuclear magnetic resonance (NMR), have characterised over 300 constituents isolated from propolis including flavonoids (flavones, flavonols, flavanones, chalcones) (Inui et al., 2012, Li et al., 2008), terpenoids (monoterpenes, sesquiterpenes, di- and tri-terpens) (Oliveira et al., 2010, Popova et al., 2010), phenolics (phenylpropanoids, lignans and stilbenes) (Petrova et al., 2010), hydrocarbons, and mineral elements. Some structures of these chemical compounds are presented in Figures 1-1 and 1-2. However, given the complexity of propolis material and the dependence of its composition on its ethno-geographical source (Seidel et al., 2008), existing data on its profile is hardly exhaustive.

Fairly extensive reviews by de Castro Ishida et al. (2011), Hernandez et al. (2005) and Matsuhisa et al. (2002) have, in the past decade, described several of the prenylated benzophenones and benzoylphloroglucinol compounds isolated from Cuban and Brazilian propolis (de Castro Ishida et al., 2011, Hernández et al., 2005, Matsuhisa et al., 2002). These compounds include: propolones A-D, nemorosone, xanthochymol, and hyperibones, examples of which are shown in figure 1-3.

Terpenoids give propolis its characteristic resinous odour and this plays a vital role in determining the quality of propolis thus enabling one to distinguish authentic samples from poor or fake ones. Being the main compounds among the volatile components in propolis, terpenoids also contribute to a variety of propolis' biological activities including antimicrobial and antioxidant, despite the volatiles constituting only 10% of the total constituents (Huang et al., 2014).

Flavonoids, various phenolics and aromatics are biologically important key compounds occurring within propolis. Flavonoids play a major role as the pigments of many plant species. However, the flavonoids present in propolis are unlike those normally found in plants. Propolis flavonoids do not contain sugar molecules in their chemical structure to any great extent (i.e. they are not glycosides), while, in the majority of plants, flavonoids have sugar molecules within their structures (Greek, 1997).

The components of propolis differ depending on the geographical origin of the sample; propolis from temperate areas, such as Europe, contains phenolic compounds (e.g. flavonoids, aromatic acids and their esters) (Marcucci, 1995). In contrast, propolis from tropical areas, such as Brazil, contains clerodane and several labdane-type diterpenoids. The latter are not present in propolis in temperate areas, because these plants are enriched by various diterpenes and with polyprenylated benzophenones. Nevertheless, flavonoids have been reported in tropical propolis because they are widespread within the plant kingdom (Banskota et al., 2001). So far, more than 38 flavonoids have been identified in propolis including kaempferol, pinobanksin, galangin, pinocembrin, chrysin, quercetin, pinostrobin, tectochrysin and isalpinin (Schmidt, 1992). There are also aromatic acids and alcohols which include

cinnamic acid, benzoic acid, benzyl alcohol, caffeic, and ferulic acid, vanillin and cinnamyl alcohol.

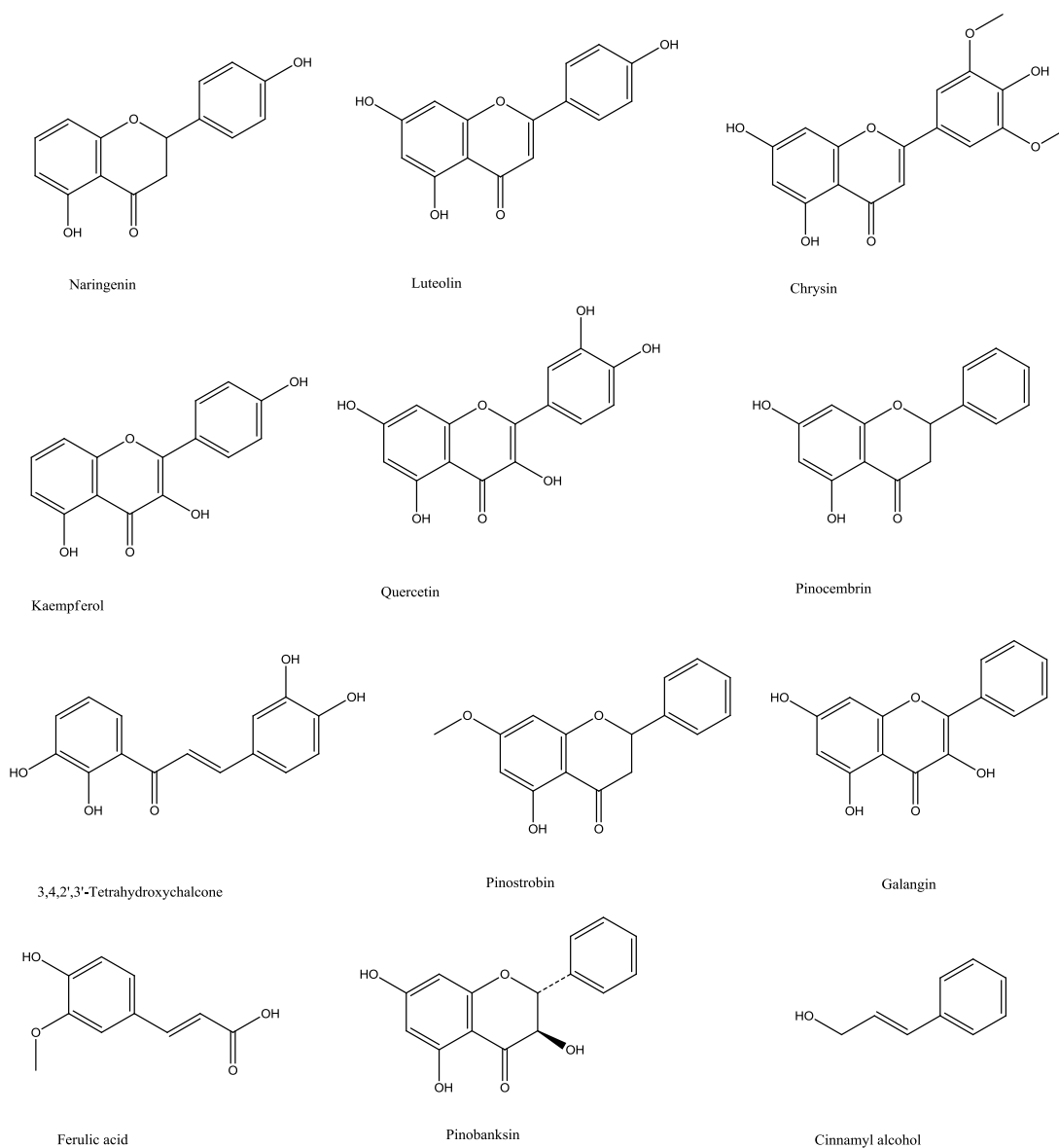
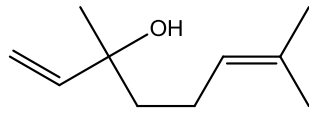
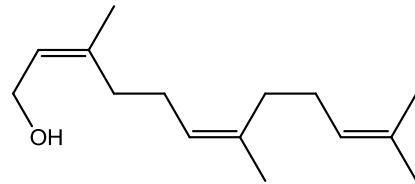


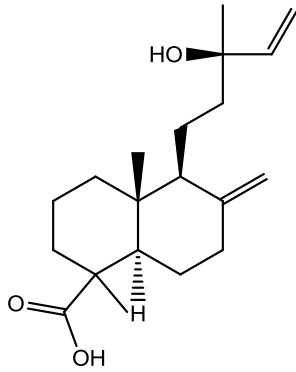
Figure 1.1: The structures of some flavonoids and phenolics identified in propolis.



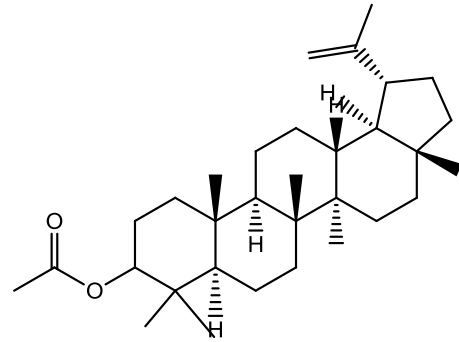
Linalool



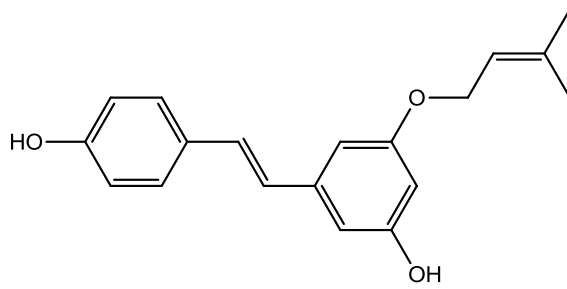
Farnesol



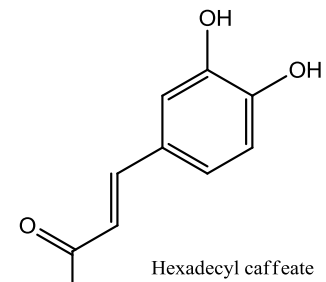
13-Hydroxy-8(17),14-labddien-19-oic acid



lupeol acetate



5,4'-Dihydroxy-3-prenyloxy-E-stilbene



Hexadecyl caffeate

Figure 1.2: Structures of some terpenes and the phenolic esters identified in propolis.

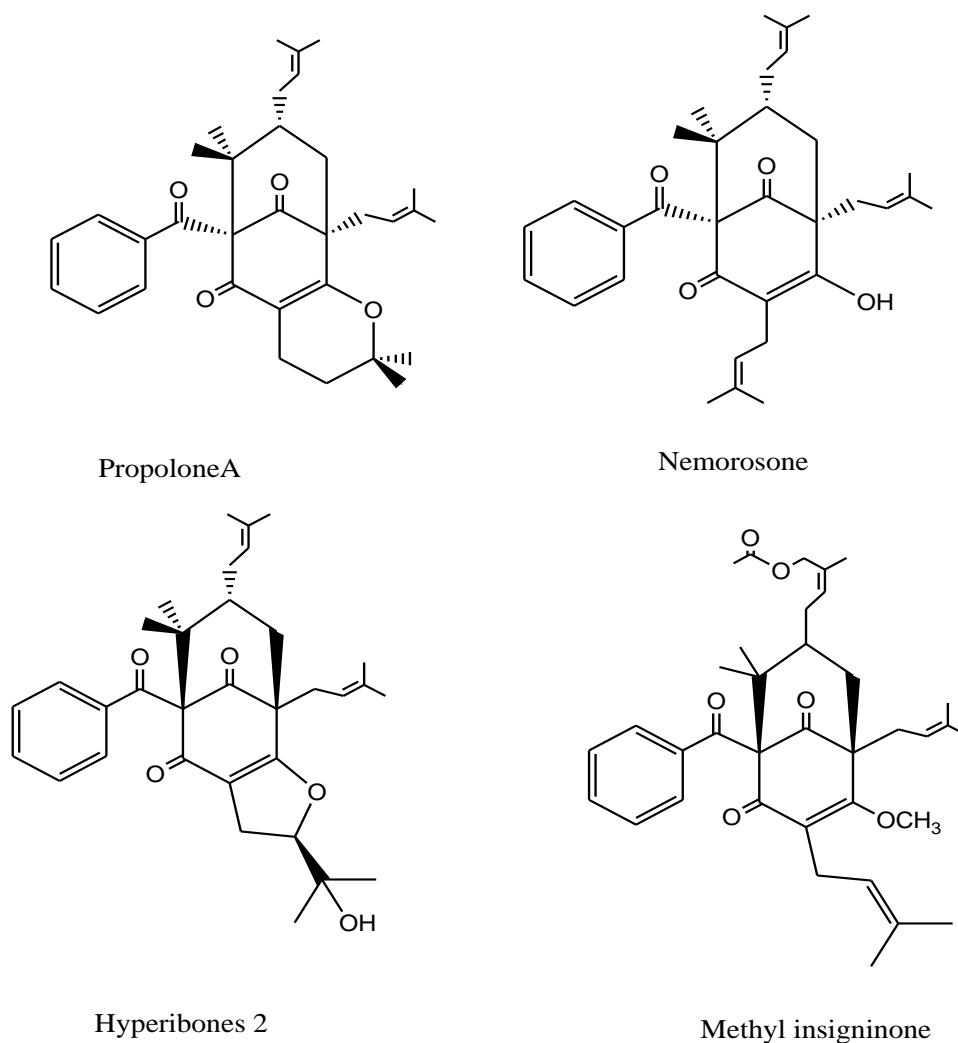


Figure 1.3: The structures of some prenylated benzophenones identified in propolis.

1.1.2 Biological Activity of Propolis

Propolis has been used as a medical agent since the ancient times. According to Tezuka, et al., (2001) it was used in traditional medication as early as the 300 BC for inflammation, cosmetic purposes, and wound healing. It has been used in folk medicine both internally and externally because it is believed to kill fungi, bacteria, viruses, to possess local antiulcer, anti-inflammatory and anaesthetic properties (Lotfy, 2006, Banskota et al., 2001). It also stimulates the immune system and at the same time lowers blood pressure. The products of propolis have also been used for body energy production and health support for many years (Rai et al., 2012). Many cultures such as Asia, Middle East, and European have used propolis to kill microbes

and heal festering wounds such as diabetic ulcers and bedsores for more than 2000 years.

Chou, et al., (2005) reported that propolis possesses antibacterial activities against several encountered Gram-positive and cocci rods, including the human tubercle bacillus, but displays limited activities against Gram-negative bacilli (Lu et al., 2005, Tezuka et al., 2001). Gram-negative bacteria include *Escherichia coli*, *Salmonella enteric* and *Pseudomonas aeruginosa*. Gram-positive bacteria include the species *aureus*, with *Staphylococcus aureus* being the most susceptible to treatment with propolis (Rai et al., 2012). The resins possess growth inhibitory mechanisms against the bacteria, curing nosocomial and communitarian infections in humans. It is important to know that antibacterial activities of propolis may be due to a synergistic process between its distinct components (Wojtyczka et al., 2013). Propolis has also been used in dental and oral preparations as it has a role in minimizing oral ulcers and tooth decay, and also promotes the health of injured/affected teeth (Wagh, 2013). The biological activities of propolis have been attributed mainly to its flavonoid content (Ikegaki and Koo, 2013).

Kelly, in his study showed that the chemical composition of propolis compounds had a positive correlation with trypanocidal activity, some phenolic and prenylated derivatives. The derivatives included 3, 5-diprenyl-4-hydroxycinnamic acid 4 (DHCA4) and 2, 2-dimethyl-6-carboxyethenyl-2H-1-benzopyran (DCBEN). The compounds were considered as the most active constituents of propolis against trypanosomes. The overall research on the activity of propolis on trypanasoma indicates that the substance contains trypanocidal active ingredients that reduce the level of parasites (parasitaemia level) on the tested parasites (Salomao et al., 2008).

Previous reports have also shown that the cytotoxicity of propolis and its constituents have inhibited the growth of tumour cells and tumours in animals, active compounds include terpenes, flavonoids, and caffeic acid phenethyl esters (Wagh, 2013, Chou et al., 2005). Moreover, it has been confirmed that the extracts from propolis can economically reduce the cost of the treatment of cancer (Banskota et al., 2001). Propolis constituents having the ability to kill the cells have been applied on cancerous cells to reduce the tumour effects of the cells (Chou et al., 2005). Many

phenolic compounds have been studied to investigate their effective usage as chemopreventive substances. However, studies are underway to determine the real effect of such substances as cancer treatment agents.

Other biological effects have been reported by Ikegaki and Koo (2013). Propolis exhibits extensive medicinal uses such as antifungal, antioxidant and antiparasitic effects. An antioxidant is a molecule that protects another molecule from being damaged by a radical through oxidation. Propolis compounds have exhibited this antioxidation effect and have been used to protect the destruction of other compounds (Tezuka et al., 2001) thus are potential useful preservatives. Propolis also has effects on fungi such as *Candida albicans*. Caffeic acid, ferulic acid and cinnamic acid are amongst the known compounds that have antifungal effects. Parasitic diseases such as leishmaniasis can effectively be cured by propolis. Propolis also may exhibit some allergic reactions with the irritations of the mucous and skin membranes (Lotfy, 2006, Shaw et al., 1997).

1.2 Trypanosomiasis

1.2.1 Introduction

Trypanosomiasis is an infectious disease that is prevalent in the African and South American continents and is caused by infection with protozoal parasites. This type of protozoa belongs to the trypanosoma genus and is transmitted to humans by insect bites and there are various types of trypanosome but it is only sleeping sickness and Chagas' disease that are human diseases caused by trypanosomes (Barrett et al., 2003) both of these disease are listed by the WHO as neglected tropical diseases (Fairlamb, 2003). There are three kinds of trypanosomiasis that include the two types of African disease which are also called sleeping sickness. The parasite is transmitted by the bite of the tsetse fly (*Glussina* genus) that is infected with the parasites. The symptoms of the disease develop in two phases. Firstly, when a human becomes infected, the protozoa multiply in the lymphatic tissues and blood causing fever, severe headaches, extreme tiredness, rashes and joint pains. People who are infected may or may not show signs of the disease immediately; these symptoms relate to the early stage, or hemolymphatic, phase. The second, or neurological, phase starts when the parasite crosses the blood-brain barrier and invades all organs of the body

including the heart and central nervous system, the latter leading to apathy, convulsions, mental dullness, sleepiness tremors and coma (Barrett et al., 2003).

1.2.2 Distribution of the disease

Trypanosomiasis is prevalent in Africa (Figure 1-4) threatening 1,000,000 people in 36 countries of sub-Saharan Africa, and thus constitutes a serious public health issue in Africa. It is mostly a problem in central Africa where approximately 500,000 people contract human African trypanosomiasis (HAT). It has achieved epidemic proportions in four countries with a prevalence reaching 50% in some places such as the Democratic Republic of Congo, Southern Sudan, Uganda and Angola (Smith et al., 1998, Moore and Richer, 2001, Brun et al., 2010).

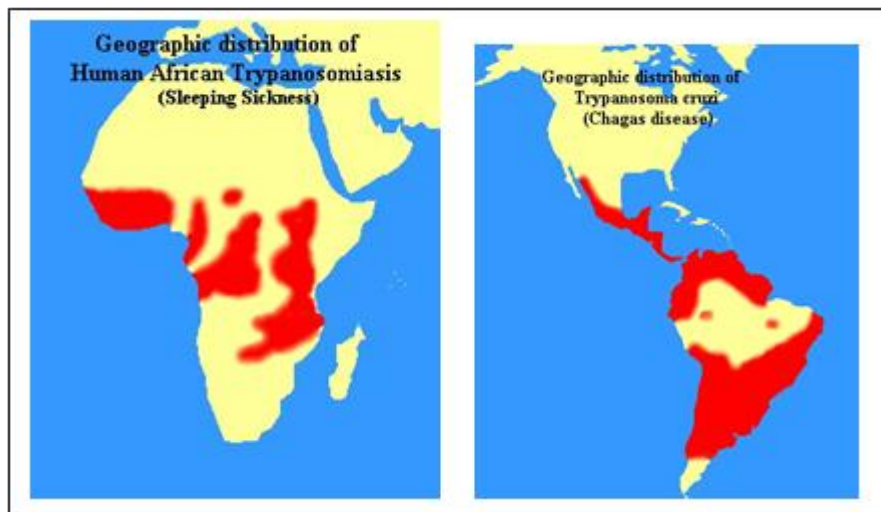


Figure 1.4: Distribution of Human African Trypanosomiasis in sub-Sahara Africa and Latin American countries (Hamilton, 2014, Anon, 2008).

Epidemics of this disease are considered one of the greatest causes of mortality in affected communities, greater than HIV/AIDS (WHO, 2013). According to the World Health Organization (WHO), about a half a million people have HAT and will die if left untreated (Robinson et al., 2011).

In 2005 WHO reported that the number of new cases had decreased between 1998 and 2004. The number of both acute and chronic forms of HAT fell from 37,991 to 17,616. This means that actual cases average was between 50,000 and 70,000. By

2009, after continued efforts to control the disease, the number had fallen to 10,000, the lowest in 50 years. Therefore, the number of actual cases is currently 30,000 (WHO, 2013).

1.2.3 African trypanosomiasis

The two types of African disease are caused by *Trypanosoma brucei gambiense* which causes the chronic disease in West Africa and *Trypanosoma brucei rhodesiense* that causes the acute disease in East Africa (Lee and Maurice, 1983).

1.2.4 American trypanosomiasis

Trypanosomiasis cruzi, also known as Chagas disease, is caused by Reduviid Bugs including the Assassin Bugs and Rhodnius which infect people when they evacuate. It occurs in 21 Latin American countries from Mexico to Argentina (de Chagas, 2009).

The first symptoms of *Trypanosoma cruzi* infection may appear after a few hours when local lesions (chagoma) arise at the primary infection site. In acute infections there is often fever, vomiting, loss of appetite, rash, severe anemia, and muscle pain. The symptoms of chronic infection include megacolon, neurological disorders (including dementia), megaesophagus, and damage to the heart muscle (de Chagas, 2009).

1.2.5 Treatments for Trypanosomiasis

Sleeping sickness is considered invariably fatal in either of the two stages and there have been only a few drugs available in the past 40 years to treat it (Bouteille et al., 2003, Hoet et al., 2004). The treatment used depends on whether or not the parasite has caused disease of the hemolymphatic system, associated with the early stage, or has progressed to the later neurological stage, and also upon the causative agent (Barrett et al., 2007). Depending on the stage of the disease a suitable type of treatment can be chosen. The drugs employed in the 1st stage of the disease are easier to administer and of lower toxicity. The drugs used in the 2nd stage are, however, only successful when they have the ability to cross the blood-brain barrier to attack the parasite. They are toxic and this makes them difficult to administer (WHO, 2013).

So far the options regarding chemotherapy are limited. There are only two compounds which are utilized against both stages of sleeping sickness as seen in Table 1-2. Drugs used in the 1st stage of the disease are pentamidine and suramin. Drugs used in the 2nd stage of the disease are eflornithine, which is only suitable for *Trypanosoma brucei gambiense*; melarsoprol that is affective against *Trypanosoma brucei rhodesiense* and *Trypanosoma brucei gambiense*; and nifurtimox which was registered for the treatment of Chagas disease or American Trypanosomiasis and can be used alone or in combination with other medications such as eflornithine (Barrett et al., 2007).

Table 1.2: The available of trypanocidal drugs (Bouteille et al., 2003, Legros et al., 2002)

Drug*	Activity	Stage of disease	Route	First marketed	Comments
Suramin	T.b. rhodesiense	Stage 1	I.V.	1922	Not recommended for <i>T. b. gambiense</i>
	T.b. gambiense				
Pentamidine	T. b. gambiense	Stage1	I.M.	1937	Treatment failures
Diminazene aceturate	T. b. gambiense	Stage1	I.V.	1960	Veterinary use
Melarsoprol	T. b. gambiense	Stage 2	I.V.	1949	2 to 12% mortality rates, reactive encephalopathy, treatment failures
	T. b. rhodesiense				
Eflornithine	T. b. gambiense	Stage 2	I.V.	1981	Difficult to administer Not effective against <i>T.b. rhodesiense</i>
Nifurtimox	T. b. gambiense	Stage 2	Per os (orally)	1960	Not approved for sleeping sickness Effects on <i>T. b. rhodesiense</i> unknown

* See Figure 1-6, page 16 for structures.

1.2.6 Currently available drugs and their limitations

The drugs already used in the early stage of sleeping sickness are the following [see Fig.1-6, page 16].

1.2.6.1 Suramin

Suramin (Germanin ®; Bayer), is an older product produced in the early half of the last century by Bayer. Suramin is colorless, has a negative charge and a high molecular weight. It is a polyanionic sulfonated naphthylamine which is chemically associated with Paul Ehrlich's Trypan Red [Fairlamb 2003]; it has been known as a drug option for a long time, as a treatment of the hemolymphatic phase (1st stage) of *Trypanosoma brucei gambiense* and *rhodesiense* infections. Nevertheless, it is ineffective in the later neurological stages of the disease owing to its inability to cross the blood brain barrier (Bouteille et al., 2003, Fairlamb, 2003).

1.2.6.2 Pentamidine

Pentamidine (pentamidine isethionate BP, pentacarinat ®) produced by Aventis, entered the market in the 1940s. It is an aromatic diamidine with a positive charge at physiological pH (Bouteille et al., 2003). This drug is another option for the 1st stage of *Trypanosoma brucei gambiense* and is only used as a second-line drug when suramin has failed (Pepin and Milord, 1994). It has undesirable side-effects, however. It is also effective against antimony resistant leishmaniasis and *Pneumocystis carinii* infections when patients refuse trimethoprim-sulphamethoxazole. The major side effect is damage to essential organs such as the liver and kidneys (Fairlamb, 2003).

1.2.6.3 Diminazene aceturate

Diminazene (Berenil®) is similar to Pentamidine and its use has been reported to be effective in treating some patients against the first stages of both *Trypanosoma brucei rhodesiense* and *gambiense* (Dumas et al., 1999). It is recommended for use in veterinary therapy (Fairlamb, 2003).

Drugs used in the late stage of the disease are as follows:

1.2.6.4 Melarsoprol

Melarsoprol (Mel B, Arsobal®), a melaminophenyl-based organic arsenical, was produced in the middle of the last century by Sanofi-Aventis. It remains the most broadly used medication against both stages of *Trypanosoma brucei rhodesiense* and *gambiense* although it is extremely toxic and complex to administer. Its use therefore is only recommended when Trypanosomiasis is in the late stage (Bouteille et al., 2003). It is a pro-drug in which the reactivity of the trivalent arsenic moiety is masked with 2,3-dimercaptopropanol (British anti-Lewisite, or dimercaprol) (Friedheim, 1949, Fairlamb, 2003) and in the body it is rapidly converted into melarsen oxide (Figure1-5).

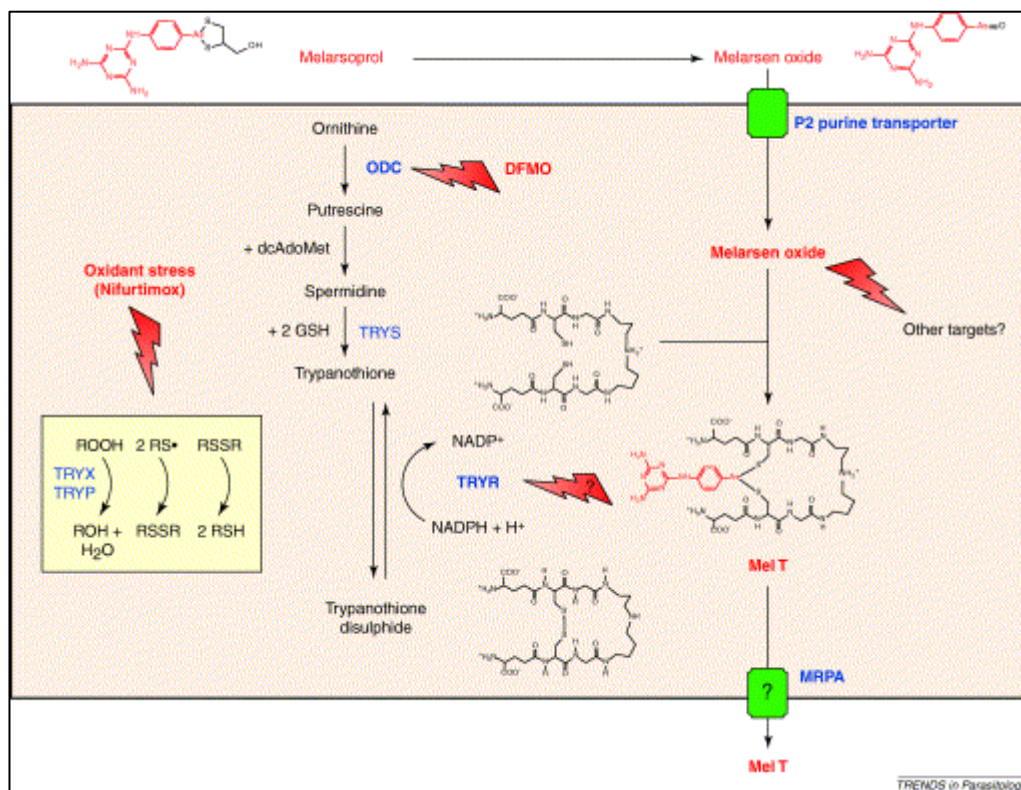


Figure 1.5: Melarsoprol is converted in the host to Melarsen Oxide, which is concentrated by the P2 purine transporter to react with trypanothione to form Mel T or to react with other targets (Fairlamb, 2003).

1.2.6.5 Eflornithine

Eflornithine (DFMO, Ornidyl®), D, L-a-difluoromethylornithine was produced in 1980S by Aventis. The drug is effective against *Trypanosoma brucei gambiense* in both stages; nevertheless, against *Trypanosoma brucei rhodesiense* its use is restricted (Barrett et al., 2007) because it is difficult to administer, and costly.

1.2.6.6 Nifurtimox

Nifurtimox (Lampit®) is a 5-nitrofuran derivative and was produced in 1969 by Bayer for the treatment of Chagas disease or American Trypanosomiasis.

It is effective against both stages of *Trypanosoma brucei gambiense* infection, but whether it can treat *Trypanosoma brucei rhodesiense* is unknown. It has been registered for use in some Latin American countries (Fairlamb, 2003).

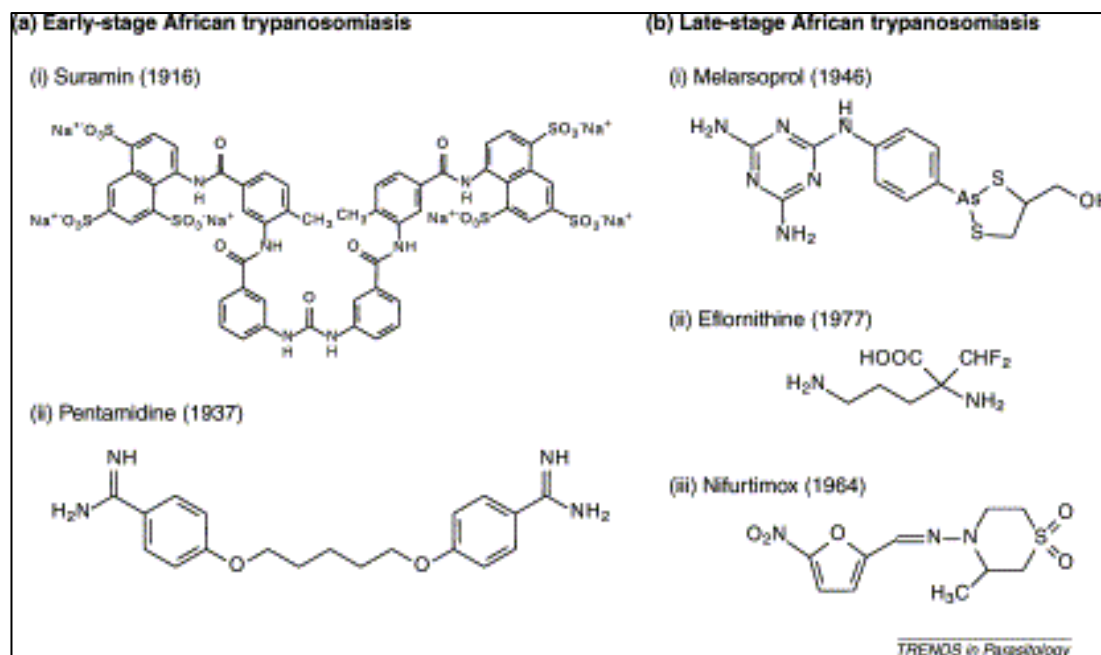


Figure 1.6: Structures of drugs used to treat (a) early stage and (b) late stage trypanosomiasis.

1.3 Instrumental methods

1.3.1 Introduction

As mentioned previously, propolis is a complex material composed of bees wax and secondary metabolites of plant origin. Therefore, investigation of its composition is normally carried out via traditional phytochemical methods such as chromatographic and spectroscopic techniques to isolate and detect constituents and this is followed by structural determination using mass spectrometry and NMR. In most cases this approach leads to the discovery of novel chemical components.

1.3.2 High resolution mass spectrometry

Despite the fact that GC-MS is a powerful technique for identification of volatile compounds, and HPLC is an excellent tool for assessing UV-absorbing substances both techniques are still not considered the best tools for evaluation of propolis due to its complex composition which also depends on the geographic source. In recent years, the coupling of HPLC to MS (LC-MS) has become more suitable for analysis of this diversity of propolis constituents (Midorikawa et al., 2001) and it has been used effectively for evaluation and assays of propolis from different regions (Falcão et al., 2010, Volpi and Bergonzini, 2006). This technique works not only for natural products and pharmaceuticals analysis but also plays a vital role in comprehensive analysis of metabolite changes in biological samples (metabolomics), proteomics and genomics. In addition HPLC-MS and MS/MS have also been the most preferred techniques for most analyses performed at all stages of new drug development (Korfmacher, 2005).

Briefly a typical mass spectrometer, in Figure 1-7, consists of an ion source, a mass analyser, detector and computer. Its concept is to produce ions in the gaseous phase from analytes in the ion source unit and accelerate them towards the mass analyser which can separate the given ions based on their mass to charge ratio (m/z). The resulting data are then collected by the detector which then converts them to signals which can be displayed on a computer monitor (Kang, Snider, 2014).

There are different modes of producing ions within the ionisation chamber of the mass spectrometer. The ionisation source provides an interface between the

chromatographic system used for the separation of analytes and the rest of the mass spectrometer. Thus ion production is achieved either by ionizing a neutral substance through electron capture, or ejection, protonation or deprotonation, cationization or by converting molecule charge into a charged form in the gas phase (Kang, 2012). Also ionisation modes are distinguished by their ability to either fragment analytes or maintain them largely intact during ion formation. The former are known as hard ionisation techniques (e.g. electron impact ionisation) while the latter are termed soft ionisation techniques (e.g. electrospray ionisation). The most commonly used ionisation techniques in LCMS today include electrospray ionization (ESI), matrix assisted laser desorption/ ionization (MALDI), and atmospheric pressure chemical ionization (APCI) all of which are soft ionisation techniques.

Following ion formation the determination of these ions is performed by a mass analyser which acts to separate and distinguish the ions based on their respective mass/charge ratios. The ability of a mass spectrometer to distinguish very closely related masses determines its resolving power. Table 1.3: Comparison of common high resolution mass analyser (Krauss et al., 2010)

Mass spectrometer	Mass accuracy (ppm)	Resolving power	Dynamic range
Fourier transform ion cyclotron resonance (FT-ICR)	Less than 1	1,000,000	10 ⁴
Orbitrap	2	100,000	10 ³ -10 ⁴
Time-of-flight (TOF)	3	20,000	10 ² -10 ³
Quadrupole ion trap	50	10,000	10 ³

Nowadays the highest resolution mass analysers available include Fourier transform ion cyclotron resonance (FT-ICR) mass spectrometers, Orbitraps and time of flight (TOF) instruments (Xian et al., 2012).

1.3.3 Orbitrap

The Orbitrap mass analyser is one of the fairly recent technologies for mass measurement in modern spectrometers which was invented by Alexander Makarov in late 1990's (Hu et al., 2005) and entered the market in 2005. The principle of its operation involves utilising two specially designed electrodes, the outer one of which is barrel-like (C-Trap) for trapping and temporary storage of ions while the inner one is spindle-shaped. Application of a voltage causes ions in the C-trap to accelerate towards the inner spindle-shaped electrode where a specially-applied voltage causes them to circulate round the electrode, thereby getting trapped in their motion (Hu et al., 2005).

The arising spiral motion round the spindle-shaped electrode is maintained because of the balance between the resulting outward centrifugal force originating from the initial tangential velocity upon ion injection and inward electrostatic attraction towards the central electrode. Mass measurement is based on the frequency of transients generated by vibrating ions and is independent of both the spatial spread of the ions and the energy of the ions themselves. The development of Orbitraps was inspired mainly by the need to overcome resolution and accuracy problems associated with previous technologies. It offers high mass resolution of around 150,000, high mass accuracy (about 1-2 ppm), high m/z range around 6000, and dynamic range around 10^4 (Hu et al., 2005). This dynamic range means that the MS can detect analytes that differ in concentration by a factor of up to 10^4 . This is essential during the analysis of low levels of one analyte in the presence of another at a much higher level, for example during impurity profiling studies.

The highly accurate and highly mass resolving hybrid technique can be employed to screen suspected components with or without reference standards and even unknown compounds. It offers a great deal of data thus enabling not only knowledge of the mass of molecules or atoms and their molecular formula but also some detailed structural information via fragmentation patterns produced through MS/MS (Krauss et al., 2010).

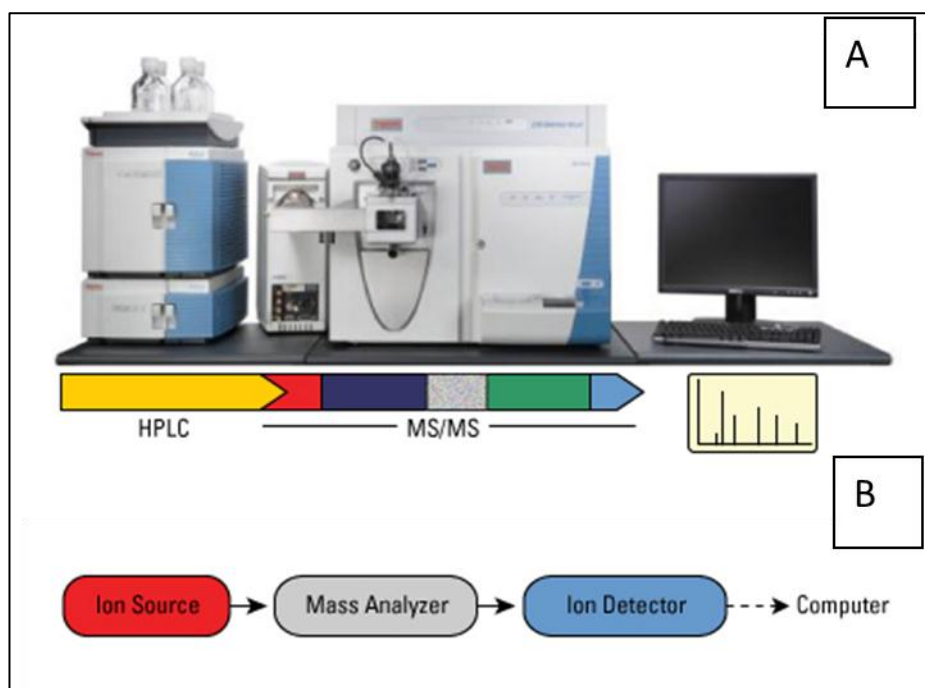


Figure 1.7: A: LTQ Orbitrap. B: Schematic of the basic components of a mass spectrometer (Snider, 2014).

1.3.4 HPLC with evaporative light scattering (ELSD) detection

Determination and separation of constituents of natural products by chromatography can be accomplished by several techniques including TLC and GC. However, the HPLC system is considered the main analytical technique which can achieve the best results in a phytochemical study. Evaporative light scattering detection (ELSD) is commonly used as a semi-universal detector for HPLC detection of compounds that have poor UV absorption due to lack of chromophores in their structures. Recently, reverse phase-HPLC with ELSD detection has become the ideal choice for the detection of different classes of natural products and it also finds considerable analytical application in the analysis of beverages, food, and in the development of pharmaceuticals (Dvořáčková et al., 2014). In addition, being relatively non-selective and linear, it allows detection of approximate quantities of various constituents in a complex mixture, even if it contains unknown compounds (Cebolla et al., 1997).

Thus the main advantage of using ELSD over UV detectors in phytochemical screening is that it can detect various ranges of compounds that do not absorb significantly in the UV range such as terpenoids, glycosides, and saponins. The main

drawback associated with the technique is that it is considered destructive and there is a variation of response depending on the solvent composition in the mobile phase (Looney, 2012).

The principle of LC-ELSD is based on three successive processes that include mobile phase nebulization, eluent evaporation, and then measurement of scattered light of retained analytes as showed in figure 1-8.

The analytes will be separated in the column and these together with mobile phase are converted by the nebulizer into a fine spray of uniform droplets suspended within a N₂ carrier gas. The atomized spray is moved to a drift tube which is heated to allow only the mobile phase to evaporate, leaving the remaining target components in the evaporation tube to convert into dried particle aggregates that are then detected by means of light scattering (Young and Dolan, 2003). In the detection unit, the light source is directed at the solid particles as a target and scattered light is measured by a photodiode or photomultiplier (Looney, 2012). The higher the concentration of target components in a samples the higher the amount of scattered light (SHIMADZU, 2015).

The relationship between the peak area (A) of evaporative light scattering detection and the quantity of analyte in the samples (m) is represented by the equation:

$$A = a m^b,$$

Where *a* and *b* are constants.

Thus a plot of the log of peak area against the log of analyte concentration will be linear (i.e., $\log A = a + b \log m$), with slope *b*, and y-intercept *a*. The value of *b* lies between 1 and 2, and seems to vary from one detector to another depending on the specific design of the detector, especially of the nebulizer component. Useful linearity is attained when when *b* is close to 1 (Young and Dolan, 2003).

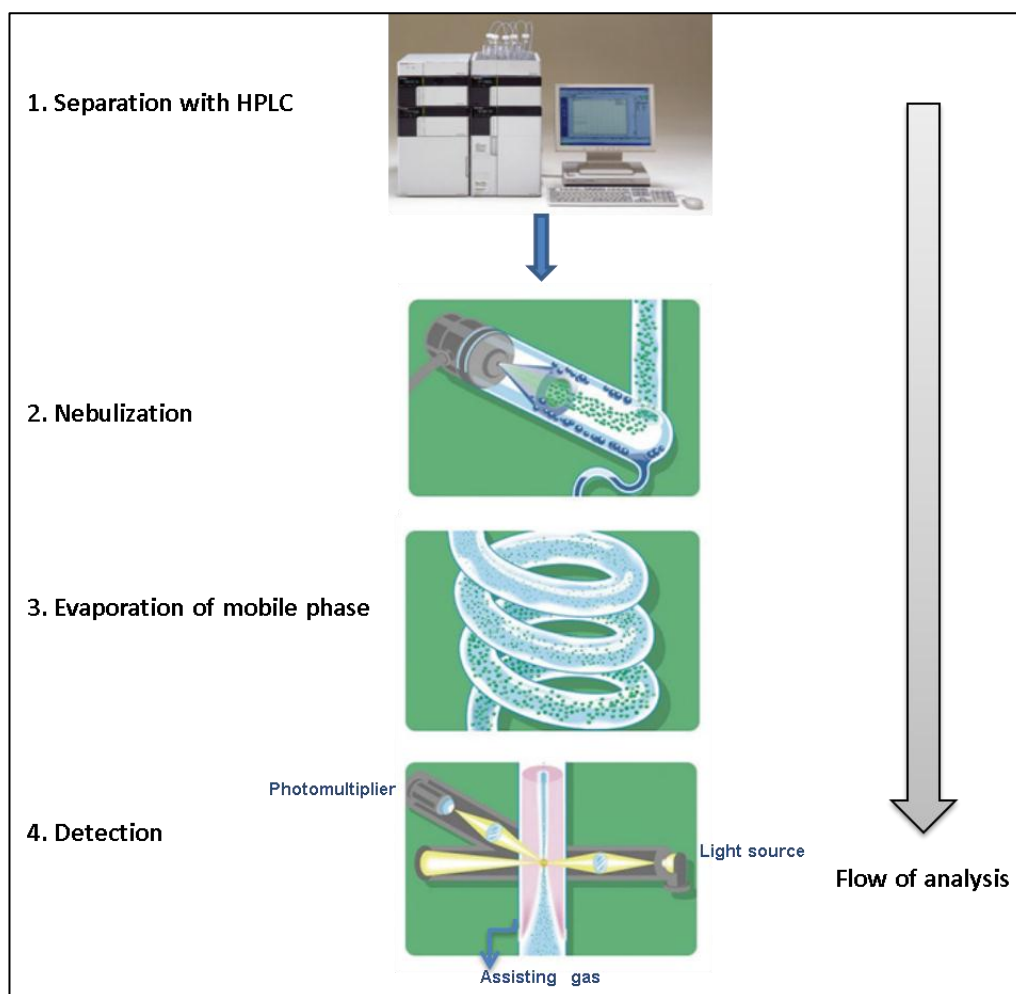


Figure 1.8: Principle of HPLC-ELSD detection of compounds during analysis (SHIMADZU, 2015).

1.3.5 Medium pressure liquid chromatography

Medium pressure liquid chromatography (MPLC) is a preparative separation technique used for large scale isolation and purification of compounds from crude materials before being subjected to further purification with techniques such as prep-HPLC due to its higher throughput and sample loading as well as its lower cost (Cheng et al., 2010).

MPLC is a complement to flash chromatography and the pressure required is within the range of 5-20 bars which is generated through a piston pump with an adjustable flow rate. This distinguishes it from flash chromatography and other low pressure techniques which require low pressures in the range of 1-5 bar (Weber et al., 2011).

The medium pressures employed in MPLC allow sample elution through the column at a faster rate. Additionally, good resolution enables separation of compounds with a broad range of polarities from semi-purified samples. Samples loading of up to 50 g can be used in a single run. The obtained fractions can be re-chromatographed for further purification of the obtained extracts and reproducibility of the packing of columns and separation can all be attained (Claeson et al., 1993, Still et al., 1978).

The principal components of an MPLC system are outlined in the schematic diagram below (Fig 1-9) and should be similar for any type of such equipment.

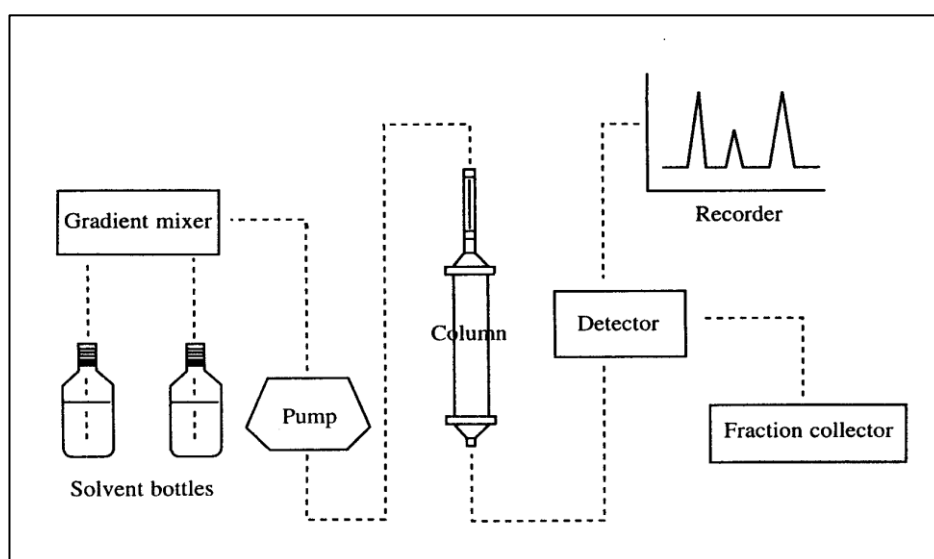


Figure 1.9: The main components of a medium pressure liquid chromatography system (Claeson et al., 1993).

For this purpose, two models of MPLC systems were used in this research. These were the BÜCHI flash chromatography which has two pumps: the Buchi Pump Manager C-615 coupled to binary pumps Modules C-601 and contained of versa flash SUPELCO column. It is capable of using binary solvent gradients with a wide range of flow rates (2.5 to 250 ml/min). The other system used was the Grace Reveleris® iES flash chromatography system equipped with variable wavelength UV detectors at 280 nm and 210 nm wavelengths and an ELSD detector. The use of simultaneous UV and ELSD detectors in the device serves to permit detection of

both weakly or non-chromophoric compounds such as terpenoids as well as chromophoric ones such as flavonoids in complex extracts during a single run.

1.3.6 NMR Techniques: DEPT, COSY, HMBC, HMQC and NOESY.

Nuclear magnetic resonance (NMR) is considered to be a key analytical technique in pharmaceutical analysis with particular application in the structure elucidation of natural products leading to identification and confirmation of chemical compounds. NMR was first discovered in 1946 by two individual physicists groups when they detected radiofrequency signals of proton nuclei in water and paraffin when introduced into a magnetic field (Abraham and Mobli, 2009).

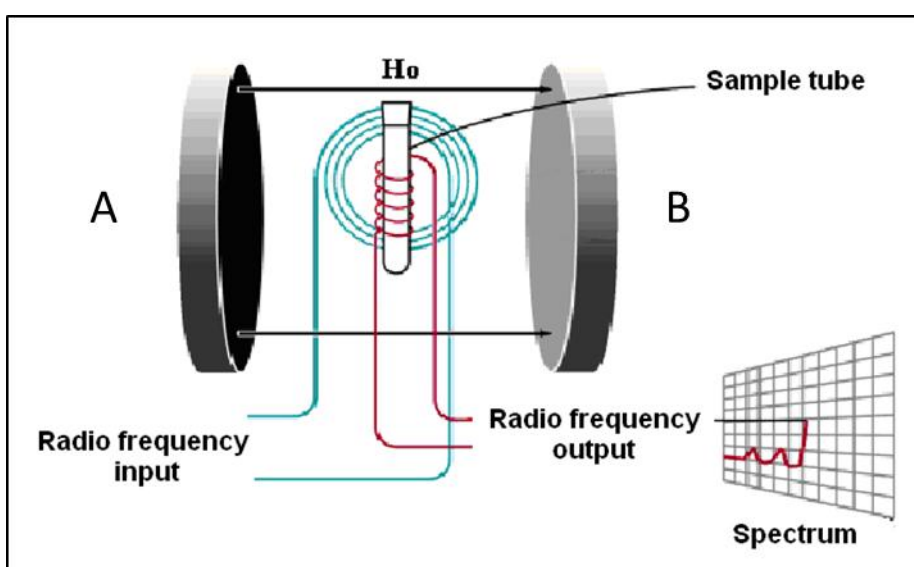


Figure 1.10: Basic element of classical NMR spectrometer.

The NMR signal (Fig 1-10) results from transitions between different Zeeman levels of spin active atomic nuclei when placed in a magnetic field (Cummins and Jones, 2000). It is well known that an atomic nucleus consists of protons and neutrons and each of them has property of individual nuclear spin. The total vector of individual spins of protons and neutrons determine the total nuclear spin I . The spin quantum number I can be an integer, half-integer or zero depending on the atomic number (number of protons) and atomic mass minus atomic number (number of neutrons) in that nucleus. This number I is a physical constant for a particular nucleus and determine the number of spin states $(2I+1)$ that is possible for that nucleus. When $I=$

$\frac{1}{2}$, there are 2 (i.e. $2 \times \frac{1}{2} + 1 = 2$) spin states as occurs in active nuclei. For any nucleus to be NMR applicable, it must have a nuclear magnetic moment, the nuclear magnetic moment (μ) is directly proportional to the spin quantum I of the nucleus: $\mu = \gamma I h / 2\pi$.

Nuclei with spins $I = 0$ include ^{12}C , ^{16}O and ^{32}S ; these isotopes are not spin active and they are called NMR silent. The commonly used nucleus for most NMR experiments is hydrogen (^1H) whose natural abundance is 99.98% and has a spin quantum number $I = \frac{1}{2}$. Hence only 2 spin states are allowed based on the equation $2I+1$ [$2(\frac{1}{2}) + 1 = 2$]. The two permitted spin states are thus: $+\frac{1}{2}(\alpha)$ and $-\frac{1}{2}(\beta)$ (Pavia et al., 2009).

Nuclei with spin quantum number $I = \frac{1}{2}$ such as ^1H and ^{13}C are called dipolar nuclei. They are spherical in appearance, with a uniform distribution of charge density over their entire surface. This shape means that ^1H and ^{13}C nuclei are able to interact equally with a probing electromagnetic field irrespective of its direction. This results in a strong, sharp NMR signal (Kühl, 2008).

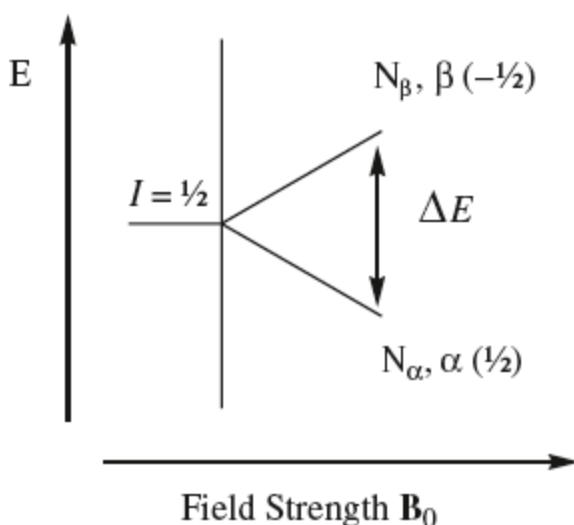


Figure 2: A transition energy for a nucleus in NMR (Kühl, 2008).

In organic and pharmaceutical chemistry, ^1H and ^{13}C are the most important nuclei for NMR analysis and both of these have half-integral spin numbers ($I = \frac{1}{2}$). The spin numbers of common nuclei are summarized in Table 1-4.

Table 1.4: Common examples of nuclei and their spin quantum numbers.

Spin number (<i>I</i>)	Number of protons	Number of neutrons	Examples
Zero	Even	Even	^{16}O , ^{32}S , ^{12}C ,
Half-integer	Odd	Even	^1H , ^{31}P , ^{15}N , ^{19}F
Half-integer	Even	Odd	^{13}C , ^{73}Ge
Integer	Odd	Odd	^2H , ^{14}N

Several NMR techniques were employed in this work:

One dimensional spectrum including ^1H NMR and ^{13}C NMR/ ^{13}C DEPT Q normally provide less information in comparison to two-dimensional spectra. ^1H NMR and ^{13}C NMR spectra reveal important information about the number and type of protons and carbon atoms respectively that are present in a molecule as well as their chemical shifts. On the other hand, ^{13}C DEPT Q (Distortionless Enhancement by Polarization Transfer) NMR spectroscopy detects additional details about the carbon which can distinguish between primary, secondary, tertiary, and quaternary carbon atoms.

Two-dimensional NMR spectra are powerful tools for determining unknown structure connectivity in chemical compounds. They include Correlation Spectroscopy (COSY), Heteronuclear Multiple Bond Coherence (HMBC), Heteronuclear Multiple -Quantum Correlation (HMQC) and Nuclear Overhauser Effect Spectroscopy (NOESY). ^1H - ^1H COSY directly detects neighbouring protons. The correlations between protons and carbons to which they are directly attached on the chain are displayed through Heteronuclear Multiple Quantum Correlation (^1H - ^{13}C HMQC) which shows a proton and its directly attached carbon. On the other hand, Heteronuclear Multiple Bond Coherence (^1H - ^{13}C HMBC) gives considerable structural details through longer carbon-proton coupling up to four bonds apart. Nuclear Overhauser Effect Spectroscopy (NOESY) detection in the ^1H - ^1H COSY square format identifies closely spatially related protons in large molecules (Breitmaier, 1993). This improves the ability to determine exact molecular

orientations and structures during structure elucidation of unknown organic compounds.

1.4 Metabolomics

The term ‘metabolomics’ was first documented in 1998 and was used in the context of description of the metabolic conduct of microbial systems. Since that time, the term has been used by scientific community not only in the area of microbiology. The suffix –ome in the word ‘metabolomics’ indicates the aspiration of the field to “direct attention to holistic abstractions” based only on those observations that are possible although being only part of that whole (Oldiges et al., 2013). Currently, there are four different approaches to metabolomic studies and these are: metabolic profiling, target analysis, foot-printing and metabolic fingerprinting (Oldiges et al., 2013). Indeed, the ultimate goal of metabolomics is to identify, quantify, and classify all cellular metabolites. For this reason, metabolomics, a rapidly emerging field, can be described as a comprehensive study of all metabolites – the end products of regulatory developments in a cell (Fiehn, 2001). The level of metabolites indicates the reaction of biological systems to environmental and genetic changes (Fiehn, 2002). In response to the changes, biological systems synthesize a set of metabolites which makes up its metabolome. The analysis of metabolomes can help to explain how metabolite levels vary in response to such changes as single mutation and other genetic and environmental alterations (Fiehn, 2001). In a broader context, the analysis of metabolomes is important for understanding of cellular function; it helps to unveil the dynamic nature of metabolism by supplying profound knowledge about types and quantities of existing metabolites, and the environment which exists in cell systems and living organisms (Tomita and Nishioka, 2006). Better understanding of metabolism leads to a better understanding of the overall physiological state of organisms. In metaphorical terms, metabolomics has been described as a direct ‘functional readout of the physiological state’ of a living organism (Roessner and Bowne, 2009). Despite its seeming specificity – focus on metabolites, metabolomics is a powerful tool capable of shaping the knowledge of underlying principles of the function of living organisms.

1.4.1 Mass Spectrometry in Metabolomics

Of the four different approaches to metabolomic studies mentioned above, there are two main research directions: metabolic profiling and metabolic fingerprinting. Metabolic profiling is concerned with analysis of a set of metabolites which are related to specific biochemical pathways or a group of compounds (Dettmer et al., 2007). In pharmacology, the aim of metabolic profiling is to determine the catabolic outcome of administered drugs (Fiehn, 2002). Metabolic profiling is often hypothesis-driven rather than hypothesis-generating: metabolites are selected for investigation on the basis of the hypothesis. Hence, the constraints of metabolic profiling are obvious: while this method can corroborate or refute the hypothesis, its capacity to reveal new aspects is limited. Another disadvantage of metabolic profiling is that it is not global due to its focus on specific groups of metabolites (Dettmer et al., 2007).

Metabolic fingerprinting is focused on comparison of changing patterns of metabolites. Metabolic fingerprinting is widely used as a diagnosis tool in medicine: it allows identifying and separating diseased subjects, and assessing the dynamics of biotic, abiotic, and genetic perturbations (Ellis et al., 2007). Metabolic fingerprinting can be performed on a wide variety of biomaterial: urine, tissues, cells and so on. Unlike metabolic profiling, metabolic fingerprinting is a true 'omics' approach, since it can be applied concurrently to a wide range of metabolites. In other words, metabolic fingerprinting is a more global method (Dettmer et al., 2007). Both metabolic profiling and metabolic fingerprinting rely on various analytical tools. One such tool is nuclear magnetic resonance (NMR) technology, which allows screening samples for varieties of patterns. The strength of NMR is that it is non-destructive, implying that the sample can be used for further analysis by other techniques, and it is highly selective, with the ability to distinguish between several closely related chemical compounds. In addition, NMR sets forth minimal requirements for sample preparation. The disadvantage of the technique is that it allows for identification of medium and high-level metabolites. This is because the NMR tool has limited sensitivity. In particular, it is estimated that no more than 60 different metabolites can be assessed in a biological sample (Scalbert et al., 2009).

This limitation can be overcome with mass spectrometry (MS) analysis. MS is a highly selective and sensitive instrument which potentially can identify metabolites. MS techniques provide spectral information such as fragmentation patterns and the precise mass of molecular ion which allows for identification of the metabolites. For this reason, one may witness a rapid increase of MS-based metabolomics studies.

MS analysis is often used in combination with liquid chromatography (LC) analysis. Such a combination is often referred to as LC-MS based metabolomics. In LC-MS analysis prepared biological samples are introduced into a mass spectrometer through LC. In simple terms, LC-MS analysis works as follows: comparative abundances of metabolites are estimated, data is processed, and data analysis is conducted (Chen et al., 2007). The development of LC-MS technology was primarily driven by pharmaceutical industry: the industry requires high sensitivity and precision for studying xenobiotics, drugs and their metabolic effects (Lindon et al., 2011). LC-MS analysis is applied in studying of drug metabolism, invasive ovarian carcinomas and ovarian borderline tumors, inducers of myocardial injury and so on (Lewis et al., 2008).

In metabolic profiling MS serves as a separation technique, it differentiates metabolites based on their mass-to-charge ratio. LC technique alone is not able to provide a comprehensive analysis due to its limited sensitivity and selectivity. However, in combination with MS, a higher degree of sensitivity and specificity is feasible to achieve. For instance, pyrolysis-MS is able to identify metabolic markers that distinguish certain bacteria species and to classify bacteria species. Also, it is reported that MS-technology was applied to distinguish fungi species (Fiehn, 2002).

In metabolic fingerprinting the role of LC-MS analysis is not so much to differentiate the analyte but to provide as accurate as possible data for further identification and analysis of biomarkers. This task also requires a high degree of sensitivity which the LC-MS technique provides. The primary advantage of the MS technique in metabolic fingerprinting is that its capability to render high mass accuracy which, in its turn, provides good anatomic structure of data. It further means that the number of potential identities for candidate markers is reduced (Theodoridis et al., 2013). Hence, the overall process of identification and analysis is facilitated.

1.4.2 Metabolomics Applications

Metabolomics has a number of applications. Traditionally, metabolite profiling has been conducted for medical and diagnostic purposes. In addition, metabolomics advanced classification and description of plants and fungi. For instance, detection and quantification of mycotoxins cover a path to characterization of fungi. The study of mycotoxins was also used to advance regulations related to food safety (Nielsen and Jewett, 2007). Also, metabolomics is an important instrument in functional genomics. Specifically, it helps discovering the role of genes. For instance, metabolomics provided classification of molecular signatures which account for phenotype of unknown and silent mutations. In addition, metabolome studies were used to characterize features which account for a silent plant phenotype. Metabolomics tools allowed developing hypotheses about an impact of a certain phenotype on amino acid and carbohydrate metabolism (Nielsen and Jewett, 2007).

Metabolomics has also potential application in evolution studies. The point is that certain secondary metabolites are very species-specific and such metabolites are considered to be potential markers for phylogenetics and taxonomy (Roessner and Bowne, 2009). Therefore, they can help to reveal the evolution of certain species.

Metabolomics research is widely used in pharmacology for purposes of drug discovery and development. Specifically metabolomics is applied in lead compound discovery. Furthermore, metabolomics helps to identify biomarkers which are necessary to monitor diseases and to assess drug efficiency. Also, metabolomics is used in drug metabolism studies. Finally, metabolite research is a part of drug toxicity assessment, clinical trials and post-approval drug monitoring (Wishart, 2008). Thus one may observe that metabolomics accompanies virtually all stages of drug development – from discovery to post-approval maintenance.

1.4.3 Sample Preparation

Metabolomics research requires adequate methods of sample preparation. Methods of sample preparation are essential for successful analysis. As a rule sample preparation involves the following activities: termination of enzymatic activities by

application of various freezing techniques and subsequent extraction of metabolites (Dettmer et al., 2007). At the same time, sample preparation methods vary considerably depending on the analytes studied. For instance, to detect and examine metabolites in parasites, specific sample preparation methods are necessary. Shin et al (2010) has studied metabolites in *Saccharophagus degradans*, a Gram-negative bacterium. To stop enzymatic activity the researchers applied cold methanol quenching (Shin et al., 2010). The alternative technique and fast filtration was also applied. As far as methanol quenching is concerned, the samples were quenched with 70% (v/v) methanol at -70°C . When fast filtration and cold methanol quenching are compared, the latter technique caused significant cell leakage and subsequently led to a considerable loss of intracellular metabolites. Next the samples were rinsed with 2.3% NaCl. The researchers note that the washing with 2.3 % sodium chloride resulted in a serious loss of intracellular metabolites. The researchers also compared the efficiency of extraction solvents. They found that acetonitrile/methanol/water mixture and water/isopropanol/methanol are more effective extraction solvents for *Saccharophagus degradans* than acetonitrile/water and pure methanol (Shin et al., 2010). The significance of this research is that it shows the peculiarities of sample preparation for studying the metabolites of parasites. Specifically it suggests that fast filtration may be a better freezing technique than cold methanol quenching, since the latter results in a significant loss of metabolites. Also, it suggests what solvents can be more suitable for sample preparation, as far as the metabolite research of parasites is concerned.

T'Kindt et al [2010] also comprehensively described the sample preparation protocol for another parasite - *Leishmania*, kinetoplastid protozoans, which are transmitted to mammals by sand flies. To arrest metabolite activity the researchers applied chloroform/methanol/water 20:60:20 (v/v/v) quenching at 0°C . This solvent, unlike the other tested solvents (aqueous methanol, aqueous ethanol, aqueous acetonitrile, and aqueous isopropanol) provided visual cell disruption under cold conditions. Then the samples were washed three times in phosphate-buffered saline (PBS), the extraction was performed by heating and vortexing. Finally the extracted samples were centrifuged (t'Kindt et al., 2010). The researchers reported that thorough washing with PBS helped to prevent cell leakage after quenching. It shows how

certain problems of the sample preparation process can be cured: the use of adequate solvent that can work under cold conditions and the use of the rinsing compound that helps to avoid the loss of metabolites. Overall, the sample preparation protocol for metabolome research of parasites follows general principles of preparation: freezing enzymatic activity, rinsing, and extraction. However, specific biological structures of parasites require specific methods of sample preparation. The research conducted by Shin et al [2010] suggests that methanol-based quenching is a suitable technique for arresting metabolite processes in samples. Also, it is evident that sodium chloride may not be the best washing compound since significant loss of analytes occurs, while PBS can be more suitable.

1.4.4 Software in Metabolomics

Metabolomics uses various statistical methods for data analysis. The choice of the method depends upon the objective of the study. Thus, if the objective is to classify samples and if there is no prior information about the sample identity, then principal component analysis (PCA), hierarchical clustering analysis (HCA) and independent component analysis (ICA) are applied for study to find out properties of biomarkers and if the sample identity is known, then such supervised methods as soft-independent method of class analogy (SIMCA) and partial least squares (PLS) can be used (Dettmer et al., 2007).

PCA is one of the most popular statistical methods. This tool is used to reduce complexity or number of parameters. PCA identifies an optimal linear conversion for a group of data points such as characteristics of the sample studied. PCA allows observation of differences among samples and identifying the main contributors to such differences. Also, PCA is a powerful visualization tool; it allows visual detection of sample patterns. The visualization is achieved through projection of multidimensional data on 2D and 3D sketches.

HCA is an unsupervised method which produces a 'tree-like' dendrogram. It, as well as other clustering methods, is used to evaluate in a multivariate way the similarity of set of samples on the basis the metabolite profiles of these samples. The application of the HCA allows classifying unknown samples according to their closeness to the

known ones. This method, however, is criticized as poorly reproducible and mathematically unjustified. It is also claimed that this method lacks adequate measurement for the quality of clusters (Goodacre et al., 2004).

SIMCA is a statistical method that identifies properties of the cluster studied, analyzes them and based upon this analysis assigns metabolites to certain class. SIMCA is good classificatory when it comes to known compounds. It is known that SIMCA was applied to classify various teas from around the world (Moreda-Piñeiro et al., 2003). In metabolomics SIMCA was applied to evaluation of anabolic treatment traces in cattle urine (Trygg et al., 2007).

1.4.5 Trypanosome Metabolomics

The application of metabolomics can be especially useful for trypanosome research, since *Trypanosoma brucei* has relatively few metabolic pathways. Indeed, in the metabolome of the bloodstream form of *T. brucei* many essential metabolic pathways are absent when compared to the metabolome of typical mammalian cell. The following demonstrates how the application of trypanosome metabolomics can be useful for development of drugs curing trypanosome-induced diseases. Fairlamb [2002] compared the known glutathione and polyamine of *T. brucei* and the same pathways in the human host. The purpose of comparison was to discover enzymes that are shared by the host and parasite or those are unique for parasites or that are unique for the host discovered, among others that the pathways involving glutathione reductase are unique to the host. The pathways involving ornithine, putrescine and spermidine are shared by the host and parasite. The pathways involving GspdSH and T(SH)₂ are unique to parasite (Fairlamb, 2002). These findings potentially enable the development of a target discovery tool.

The study of metabolism in trypanosomes started in the 1980s. First, there was identification of certain metabolites in *T. brucei*. Thus, the use of LC- MS analysis allowed identifying the glycolytic intermediates. Also, the properties of the thiol intermediate and polyamines were determined. The early research, however, was not confined to identification activities. There was also a quantitative analysis. For instance, Moreno et al. (2000) employed NMR techniques to map out abundant

phosphorylated compounds (Moreno et al., 2000). In addition, the researchers used NMR methods to assess abundant metabolites. Trypanosome metabolomics research followed the principles described earlier (section 1.4.3). First, freezing of enzyme activity in trypanosome was performed: the cells studied were put in an ice-ethanol bath. Second, metabolites were extracted using centrifugal shaking and elution (Barrett et al., 2010). Later trypanosome research took advantage of MS analysis. In one of the studies the extracts collected were directly injected into a Fourier transform ion cyclotron resonance mass spectrometer. Many of the peaks detected by MS were associated with the trypanosome liposome (Barrett et al., 2010).

The researchers, however, accepted that such results can be attributable to the possible suppression of ionization of many non-lipid metabolites (Barrett et al., 2010). Furthermore, ultra-high resolution mass spectrometry (UHRMS) was used to the metabolome of *T. brucei* and its host setting. Specifically, metabolite mass differences were assessed with high precision. The differences were further used to verify metabolite identification and to forecast biological association between the masses (Breitling et al., 2006).

Now the standard approach to trypanosome metabolomics is hydrophilic interaction liquid chromatography which relies on HILIC columns to resolve hydrophilic compounds. This approach enabled the identification of hundreds of metabolites. The data obtained through this technique was then used to develop procedures improving accuracy of mass spectra by calibration based on detected ions (Barrett et al., 2010). Metabolomics research showed that certain regulatory mechanisms in *T. brucei* when trypanosome lives in mammals, it is provided with a ready source of glucose. The accumulation of glucose at extreme levels can damage living organisms, unless there is no special regulatory mechanism. As far as trypanosome is concerned, the question is how it survives the influx of glucose from the bloodstream of mammals. There must be some kind of metabolic regulation that protects trypanosome. Metabolomics helps to discover such regulation. Trypanosomes have glycosomes - peroxisome-like organelles. In these organelles trypanosome glycolysis is processed as follows: the first 7 enzymes of glycolysis and 2 which participate in glycerol metabolism are located there (Haanstra et al., 2008).

Metabolite research also revealed the processes in acidic organelles (acidocalcisomes) of trypanosome. The research covered *T. brucei* procyclic and bloodstream forms. *T. brucei* bloodstream forms were isolated from infected mice and rats. The acidic organelles were extracted by centrifugation and rinsed twice. *T. brucei* procyclic forms were grown at 28 °C. The main research method used was NMR spectroscopy. The research showed that acidocalcisomes are essentially the subcellular localization of the abundant polyphosphates. From that it suggests that acidocalcisomes are common for all investigated trypanosomatids: the spectra of content of acidic organelles of *T. brucei*, *T. cruzi*, and *Leishmania major* are very similar. Discovery of the content of acid organelles in trypanosomatides potentially sheds a light of their role in metabolite process. It is suggested that acidocalcisomes serve as energy stores and/or chelators of metal ions. Also, the experiment showing that pyrophosphates and tripolyphosphate are hydrolyzed by enzymes to inorganic phosphates and the observation that acidocalcisomes lose their high electron density through light permeabilization with formaldehyde and subsequent treatment with yeast inorganic pyrophosphatase suggest that the polyphosphate structure of acidocalcisomes are involved in storage and transportation of cations (Moreno et al., 2000).

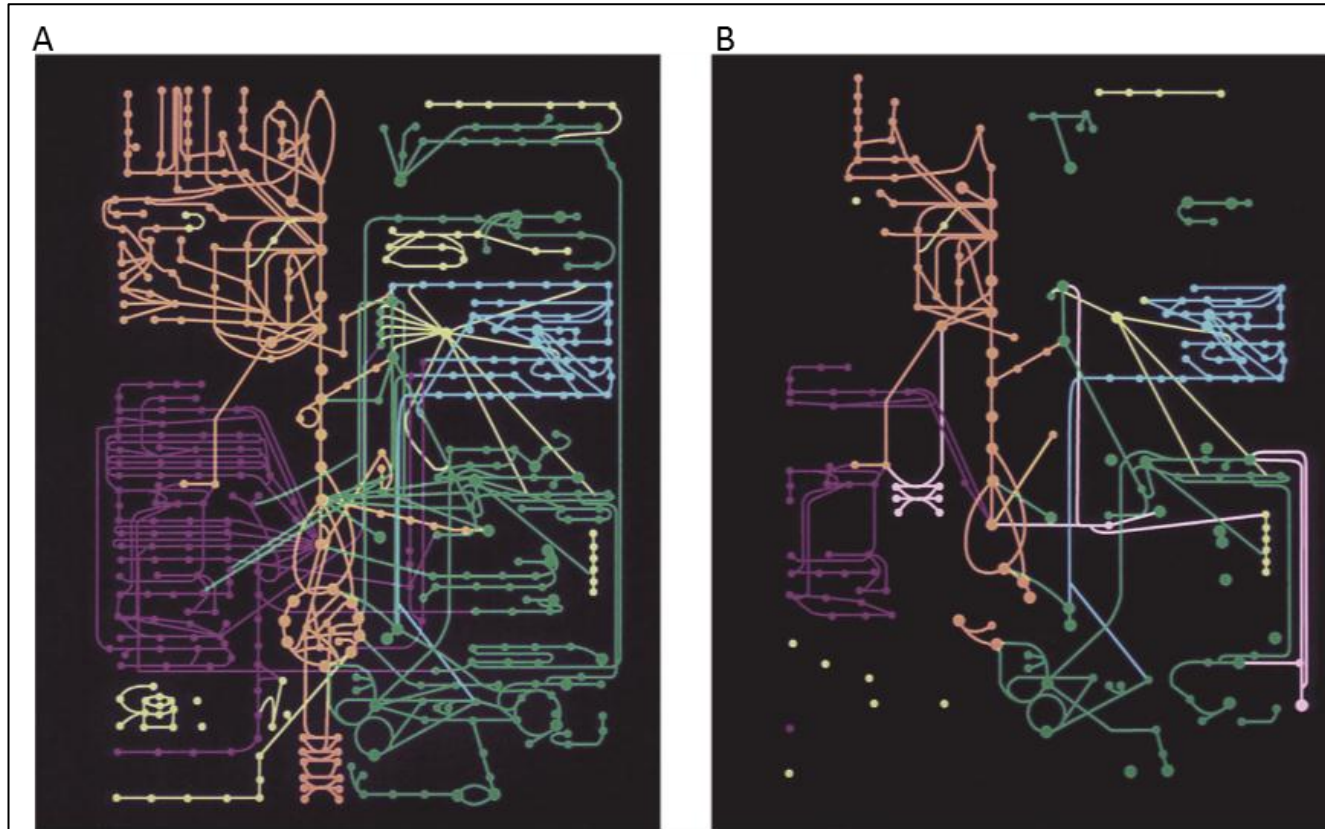


Figure 1.11: Overall comparison of metabolomes: (A) a normal mammalian cell; (B) bloodstream stage of the African Trypanosome, *T. brucei*. Pathways are coloured as follows: purple for fatty acid and sterol metabolism; orange for carbohydrate metabolism and electron transport; green for amino acids and related metabolites; light blue for, pyrimidine, purine and nucleic acid metabolism; yellow for co-enzyme biosynthesis (Fairlamb, 2002).

1.5 Aims and Objectives

The aims of the present research were:

- Investigations of the chemical composition and biological activity of propolis from different geographical origins using high resolution mass spectrometry and HPLC-ELSD profiling.
- Evaluation of the most active components possessing anti-parasitic activity against *Trypanosoma brucei* and ante-bacterial *Mycobacterium marinum* and then subjecting them to further study in order to isolate and identify the bioactive compounds using appropriate fractionation and identification techniques.
- To employ a metabolomics approach to examine the metabolomic effects of active separation of individual compounds in propolis on *T. brucei*.

CHAPTER 2:
MATERIALS AND GENERAL METHODS

2 MATERIALS AND METHODS

2.1 Chemical reagents

Hexane, methanol, ethyl acetate, acetonitrile and ethanol were purchased from Fisher Scientific, Loughborough, UK and Acetone from Sigma Ltd, Dorset UK. All solvents used were of HPLC grade and water was produced in the lab using a Millipore water purification system. Deuterated NMR solvents used including Chloroform, Acetone and dimethylsulfoxide (DMSO) were purchased from Sigma Aldrich, Dorset UK. Anisaldehyde was obtained from FSA laboratory, UK.

2.2 Laboratory Equipment and tools

The syringes and Acrodisc filters were obtained from Fisher Scientific, Loughborough, UK. In addition, a rotary evaporator (Buchi, Switzerland), Ultrasonic Bath (Scientific Laboratory Supplies, Ltd.) was obtained from Fisher Scientific, Loughborough UK. Automatic pipettes (Gilson) were from Anachem, UK and NMR tubes (5mm 300 MHz, 187 mm L, from NORELL, USA) were obtained from Sigma Aldrich, Dorset UK. The UV detector (wavelengths 254 and 366 nm) was obtained from UVP, UK. Erlenmeyer flasks, beakers, vials were from FISHERBAND, column chromatography (CC) from Rotaflo, UK and the TLC plates (Si60 F254) were obtained from Merck, Germany.

2.3 Propolis samples

Propolis samples (n=91) that had been collected from some various parts of the world were provided by BeeVital (Whitby, UK) while Saudi Arabian samples were supplied by a local beekeeper (Rijal Alma'a village, Saudi Arabia). The majority of the samples supplied by BeeVital had been collected from Africa in the countries of Tanzania (n=6; codes S75, S92, S83, S136, S137, P1), South Africa (n=7; codes S43, S48, P6, S198, S1F19, F19, SA9), Zambia (n=10; codes S143, 144, S40, S147, S198, S145, S140, S156, S150, S156), Kenya (n=6; codes S133, S217, S101, S151, S76, S65), Uganda (n=7; codes S149, S16, S155, S166, S80, S152, S94), Cameroon (n=6; codes S60, P7, P5, C20, C45, C24), Nigeria (n=7; codes S95, S97, S96, P3, P4, N2, N1) and Ghana (S87). The rest originated from China (S61), Lithuania (S54), Brazil (S126) and Saudi Arabia (KSA1).

However information regarding the origin of the following propolis samples was not available: S277, S257, D46, S264, S239, S273, S272, S239, S256, S260, S275, S243, S278, S244, S251, S261, S240, S253, S269, S276, S242, S238, S245, S270, S252, S248, CU21, S271, E47, S403, S520, CU22, S259 and S262. Samples were stored at room temperature in the laboratory.

2.4 Extraction of propolis samples

Extraction techniques for propolis samples were performed at close to room temperature without applying any thermal agitation to avoid thermal degradation. Different polarity solvents (EtOAc, EtOH) were used in the bioassay-guided extraction in order to obtain the active constituents in the fractions.

2.4.1 Extraction of propolis used for LC-MS Profiling

Approximately 200 mg amounts of propolis samples were weighed into 50 ml vials and dispersed in 3ml of Ethyl Acetate. The samples were extracted by sonication at 30° C for 30 min and the extracts were then filtered using syringe filters. Thereafter the ethyl acetate supernatant was blown off under nitrogen gas. The residue was dissolved in HPLC grade methanol, then vortexed and diluted to give a nominal final concentration of 1mg/ml. In the case of more hydrophobic, poorly soluble samples, the diluents was prepared by mixing an amount of HPLC grade methanol with chloroform (1:2 ratio) to avoid analyte precipitation of less polar analytes. These extracts were then subjected to LC-MS using the method and conditions described in section 2.6.3.1.

2.4.2 Extraction of propolis used for fractionation and purification

The bulk biologically active propolis resins were initially coarsely ground into small pieces using a mortar and pestle. They were then subjected to three successive steps of cold extraction using different polarity solvents.

The first stage of extraction was carried out in a 1000 ml flask, using 3 successive portions each of 250 ml of HPLC grade Acetone by cold extraction on the magnetic stirrer for three hours for two cycles and then, for one cycle, was left overnight at room temperature. After the process was completed the extract was filtered using a

vacuum filter and the acetone decanted into a round bottomed flask. The sample was then concentrated on a rotary evaporator at a temperature of 40⁰C.

The remaining residue was extracted in a similar way with 250 ml of HPLC grade methanol. The acetone and methanol extracts were then combined and evaporated to complete dryness or oiliness using the rotary evaporator.

The obtained extracts were subjected to liquid-liquid fractionation by partitioning between 150 ml each of EtOAc and water, three times, in a separating funnel. The ethyl acetate was removed by using a rotary evaporator and the yield calculated as shown in Table 2-1.

Table 2.1: EtOAc and EtOH extractions weight for biologically active propolis samples

<i>Sample Code</i>	<i>Origin sample</i>	<i>Weight of resin (g)</i>	<i>Weight of extract (g)</i>	<i>% Yield</i>
S 95	Nigeria	12.163	6.52 ¹	53.60
S P1	Tanzania	145.41	58 ¹	39.88
S 87	Ghana	104	28.5 ¹	27.41
KSA1	Saudi Arabia	7.05	4.8 ²	68.08

¹ EtOAc

² EtOH

2.5 Preparative Chromatographic Methods

In this work, a number of modern and conventional techniques were used for fractionation and purification of compounds in the crude extracts.

2.5.1 Column Chromatography

The classical system column chromatography (CC) is a common and useful purification technique which allows one to isolate and collect the compounds individually from a crude extract or fraction. The CC employs glass columns with different lengths and diameters. The packing of the glass column is made manually with silica stationary phase and the sample is placed loosely at the top of the column.

The crude extracts were subjected to CC; the glass column (55 x 3 cm) was packed with about 70 g of silica gel 60. The silica gel was initially mixed with a small amount of nonpolar solvent (hexane) in a beaker (slurry method) to form a homogeneous mixture. The mixture was then poured carefully into the column. The hexane (solvent) was allowed to flow through the column to remove any air bubbles and cracks. A portion of the propolis sample (e.g. KSA-1, 4.8 g) obtained previously in 2.4.2 was dissolved in a minimum amount of EtOAc and then mixed with a small quantity of silica gel. The mixture was then left to dry completely under a vacuum hood. The dried extract was then loaded onto the top of the column and then elution was carried out sequentially using different solvent systems containing varying proportions of polar and nonpolar solvents as further described in section 7.2.3. Fractions were collected in vials and were examined by TLC with suitable solvent systems.

2.5.2 Medium Pressure Liquid Chromatography

Ethyl acetate extracts which were usually sticky and complex and were fractionated by using two different advanced flash chromatography techniques to fractionate the extracts.

2.5.2.1 BÜCHI System

Preliminary fractionations of biologically active fractions were done through a BÜCHI flash chromatography which consists of versa flash SUPELCO and Büchi Pump Manager C-615 coupled to binary pumps Modules C-601.

The crude extracts obtained were dissolved in 30% EtOAc in Hexane and adsorbed on to a small amount of kieselguhr or diatomaceous earth (Celite), then left under a vacuum hood until the homogenous mixture completely dried for dry loading. The extracts were then loaded into a cartridge that was subsequently connected to the top of the silica gel MPLC column. Sample elution was carried out by using a gradient method as detailed in Table 2-2. The fractions were collected and evaporated by a rotary evaporator and then similar fractions were pooled together based on the TLC and LC-MS results.

Table 2.2: Sequence of MPLC solvent systems for EtOAc extracts of propolis

Fractions	Time (min)	B% (Hexane)	A% (EtoAc)	Flow rate (ml/min)
0-4	0	100	0	100
5	5	100	0	100
6-35	35	0	100	100
36-40	40	0	100	100

2.5.2.2 Reveleris system

Some of the fractions that did not attain sufficient purity were subjected to flash chromatography on the Reveleris system. S87F13 (2.7 g) was further purified using a Grace Reveleris® iES Flash Chromatography System equipped with variable length UV detectors at 210 nm and 280 nm wavelengths and ELSD detector that can detect both non- chromophoric and chromophoric compounds in complex extracts during a single run. This system was acquired about half way through the PhD period and the ELSD detector allowed targeting of fractions in which there was a lot of compound to be carried out.

The extracts intended for purification on the Reveleris system were dissolved in a small amount of appropriate solvent (EtOAc) and mixed with celite; then the mixture was left under a vacuum hood until completely dried. The extract was then loaded into special cartridges at Reveleris® iES system and fractionated on a silica gel column (GraceResolv Silica 24 g/32 ml) with gradient elution as shown in table 2-3, with flow rate at 12 ml/min. The detection wavelength was set at 210 nm UV1, 280 nm UV2 and 3mV for LCD. Data were collected and processed using Reveleris® Navigator™ Windows.

Table 2.3: Sequence of fractions collected on the Grace Reveleris® flash system for EtOAc extracts (S87F13)

Time (min)	Hexane B%	EtOAc A%	Fractions obtained
12	90	10	1-3
12	80	20	4-5
12	75	25	6-7
12	70	30	8-9
12	65	35	10
10	55	45	11
10	40	60	12
10	20	80	13
10	0	100	

2.5.3 Semi-preparative HPLC

The semi- preparative liquid chromatographic system contained of a Spectra SYSTEM AS3000 autosampler (equipped with a Type 7010-150 Rheodyne injection valve (100 µl loop)), a Spectra SYSTEM P2000 gradient pump and a Spectra SYSTEM UV 1000 detector (Thermo Separation Products, Inc.). The semi-prep column was an ACE silica gel column 250 mm×10 mm I.D., 5µm particle size, (HiChrom Ltd) with ethyl acetate-Hexane, isocratic 10:90 at a flow rate of 5 ml/min. The detection wavelength was set 295 nm and 320 nm. Data were acquired and processed using ChromQuest software.

2.6 Analytical Chromatographic Methods

Preliminary characterisation of crude extracts or fractions – whether pure or semi-pure was performed using different chromatographic techniques including the versatile HPLC-ELSD system which allows detection of almost all components in the sample.

2.6.1 HPLC-UV-ELSD

Approximately 1 ml of a 1 mg/ml solution of each sample was dried under nitrogen and reconstituted in 1 ml of the starting composition of the mobile phase LC gradient to form a 1 mg/ml solution. A reversed phase column (4.6×150 mm, 3µm C18) (Hichrom, Reading UK) was used for separation with mobile phases water (A) and ACN (B). A linear gradient elution was used (5% to 100% B over 35 min) at a flow rate of 0.400 µl/min. At the end of the gradient, a 5-min hold up preceded a 5 minute re-equilibration so that the total chromatographic run time was 45 min. The HPLC-UV-ELSD equipment was an Agilent 1100 system (Agilent Technologies, Germany) equipped with a quaternary pump, a diol UV detective- detector (at 290 and 320 nm wavelengths) and an Evaporative Light Scattering Detector (ELSD) (SEDEX75 SEDERE, France). The data was collected and processed using Clarity software from DataApex.

2.6.2 Thin Layer Liquid Chromatography (TLC)

TLC is among the simplest and most easily performed preliminary polarity tests for sample mixtures to allow selection of appropriate solvent systems for further separation methods such as medium pressure liquid chromatography (MPLC) and column chromatography (CC). TLC normal phase was used on silica aluminium plates (Si60 F254) from Merck and each crude extract or chromatographic fractions were spotted on a TLC plate and introduced into a chamber containing a mobile phase combination of varying proportions of hexane and ethyl acetate. They were then separated according to their polarity. After development was completed the plates were dried and examined non-destructively using short (254 nm) and long (366 nm) wavelength ultraviolet detection and then visualised by applying anisaldehyde and heating to permit a chromogenic detection. LC-MS Methods

LCMS provides a reliable and sensitive technique, considered to be one of most versatile analytical techniques, in the quality control of various propolis samples. The sample data were captured on the instrument and processed by Xcalibur software (Thermo Fisher Corporation, Hemel Hempstead, UK).

2.6.2.1 Profiling of Propolis Extracts

The samples from crude or fractions were prepared at 1mg/ml in HPLC grade methanol and then analysed on an LTQ Orbitrap system. The system consists of a Surveyor HPLC pump hyphenated to an LTQ Orbitrap mass spectrometer (Thermo Fisher Scientific, Hemel Hempstead, UK). The column used was a reversed phase C18 (4.6×50 mm, 3µm C18) (Atlantis, Ireland) and eluting with mobile phase consisting of 0.1% v/v formic acid in water (solvent A) and 0.1% v/v formic acid in acetonitrile (solvent B). Elution was carried out gradient-wise using a profile as described previously in section (2.6.1) at a flow rate of 0.4 ml/min. The ESI interface was employed in positive ionisation mode to permit detection of $[M+1]^+$ ions. The spray voltage for both Capillary and cone were set at 4.5 kV and 35 V respectively. The flow rate for the sheath and auxiliary gases were 50 and 15 arbitrary units, ion transfer capillary temperature was set at 275 °C and full scan data were obtained from m/z 75-1500. The data were handled using Xcalibur 2.1.0 software (Thermo Fisher Scientific, UK).

2.7 Measurement of Optical Rotation

The specific rotation for some pure compounds obtained was using a Perkin–Elmer 241 polarimeter with a sodium lamp at 20 °C (PerkinElmer Inc., USA) to measure their optical rotation. 1mg of each of the compounds was dissolved in solvent (chloroform) to get 1mg/ml. The average ten readings were taken and then optical rotation was calculated using the equation:

$$[\alpha]_{\lambda}^T = \frac{100 \times \alpha}{l \times c}$$

Where $[\alpha]$ is the specific rotation at wavelength λ , α is the average of the measured rotation ($^{\circ}$), T is the temperature at 20 °C, l is the path length in decimetres, and c is the concentration of the solution in g/mL.

2.8 Data Extraction and Database Searching

The data obtained for crude propolis samples which exhibited high potency against trypanosomes and which from the LC-MS profiling seemed to contain possibility of propolones (phloroglucinones) were processed using m/z mine. The high-resolution

mass spectral data obtained from Xcalibur 2.1 were imported into MZMine 2.10 (Pluskal et al., 2010). The data set was deconvoluted and deisotoped and then sorted with MZmine; the chromatogram builder was set to detect the peaks in the samples and blanks. Parameters were set at minimum for time span and height to 0.5 and 3.0E4 respectively, and m/z tolerance 0.001 m/z or 5.0 ppm. Mass ion detects were isolated with a centroid detector threshold that was set to 10000 and an MS level of 1. Chromatogram deconvolution was carried out to detect the individual peaks and set as follows: local minimum search algorithm, chromatographic threshold: 90%, search minimum in (RT range, relative height, absolute height and ratio of peak top/edge) were: 0.4, 5 %, 3.0E4 and 3 respectively, and peak duration range was at 0.3–5 min. The deisotoped was set at (m/z tolerance: 0.001 m/z or 5.0 ppm, retention time tolerance: 0.2 absolute (min) with maximum charge: 1 and representative isotope: most intense). These parameters were followed by normalising of retention time (m/z and RT tolerance: 0.001 m/z or 5.0 and 5.0 absolute (min) respectively, and then minimum standard intensity: 5.0E3). Aligner parameters were set to m/z tolerance: 0.001 m/z or 5.0 ppm, weight for both m/z and RT: 15, retention time tolerance: 5.0 relative (%) to reduce variation of inter-group. The gap filling was used to detect missing peaks at intensity tolerance: 1.0%, m/z and retention time tolerance: 0.001 m/z or 5.0 ppm and 0.5 absolute (min) respectively. The processed data set was coupled to the created library (in-house propolone database) to perform molecular formula prediction and then Hits identification exported to a CSV file.

2.9 NMR Methods

Approximately 10 or/and 20 mg of each sample was dissolved in 750 μ L of deuterated solvent such as DMSO- d_6 , acetone and $CDCl_3$ which were selected based on appropriate solubility of the compounds and were prepared into the standard NMR tubes (5mm x 7in L). The NMR spectroscopic data were carried out on a JEOL-LA400 -NMR spectrometer system (^{13}C NMR at 100 MHz, 1H NMR at 400 MHz) (JEOL Ltd, UK) using TMS as internal standard, Chemical shifts are given in ppm and coupling constants are in Hz. MestReNova 8.1.2 was used to process the NMR spectroscopic data. 1D: 1H and ^{13}C NMR, DEPT 135; 2D: 1H - 1H -COSY,

heteronuclear single quantum correlation (HSQC), HMBC, NOESY] were employed to elucidate the structure of each sample.

2.10 Bioassay

2.10.1 Trypanocidal assay

Anti-trypanosomal activity of isolated compounds and propolis extracts were determined by using the alamar blue™ 96-well microplate assay (Ráz et al., 1997) against the blood stream form of *Trypanosoma brucei brucei* (S427).

Samples were prepared as stock solutions at a concentration of 10 mg/ml in 100 % DMSO. Trypanosomes were counted using a haemocytometer and diluted to a concentration of $2 - 3 \times 10^4$ trypanosomes/ml.

Each propolis sample whether pure or as a fraction was initially tested against *T. brucei brucei* at a single concentration of 20 µg /ml or 20µM (n=3) in order to determine the initial activity *in vitro*. The stock solution (10 mg/ml) of each sample was diluted with HMI-9 medium to give an intermediate concentration of 1 mg/ml. Next, 4µl of the intermediate test solution were mixed with 96 µl HMI-9 medium on a dilution plate to obtain a concentration of 40 µg/ml. The final concentration of 20µg/ml was obtained after a 1:1 dilution with the trypanosome suspension on the assay plate.

The screening 96 plate was arranged as follows: in the column 1 were added both sterility controls and negative controls (DMSO), in column 2-11 were added test samples and in column 12 were added a concentration range of suramin as positive control. 100 µl of the trypanosomes suspension was added to each well of the assay plate with the exception of well A1 (sterility check) and the plate was incubated at 37°C, 5% CO₂ with a humidified atmosphere for 48 hours. After that 20µl of Alamar blue, which is a redox indicator, was added to incubate again for 24 hours. A fluorescence reading was taken using the Wallace Victor Spectrofluorimeter (Excitation 530 nm and Emission 590 nm). The results were calculated as a percent of the DMSO control values.

Finally, minimum inhibitory concentration (MIC) values were determined for active samples (which showed < 10 % of control values) and performed in duplicate. 200 µg/ml test solutions were added in column 2 by pipetting 4µl of test stock solution (10 mg/ml) and adding 196 µl HMI-9 medium into each well. 100 µl of HMI-9 medium was added into each well of column 1 and 3-12 whereas suramin (10 µM) was added in column 12 with a concentration range of 0.008 to 1.0 µM of suramin (10 µM). An inoculum of 100 µl of the trypanosome suspension (3 x10⁴ /ml) was added to each well with exception A1 (sterility check) and then the method was continued as described in the above paragraph.

The MIC values were determined as the lowest active compound concentration which gave < 5 % of the control values.

2.10.2 Anti-mycobacterial Assay

The Samples were also tested against *M. marinum* TCC.BAA535. The anti-bacterial bioassays against *M. marinum* were performed in 96-well microtitre plates using a modification of the well-established AlamarBlue™ method (Franzblau et al., 1998). The samples were tested in duplicate over a concentration range of 100–0.19 mg/ml and negative and positive controls were included containing 1–0.0019% DMSO and 100–0.78 mg/ml gentamycin respectively. The turbidity of a suspension of *M. marinum* was matched to that of a 0.5 McFarland standard (~1 x 10⁸ FUs/ml) and diluted with MHB to give a final concentration of ~0.5x10⁷ FUs/ml in the assay microplate. The assay microplate was incubated at 31 °C for 6 days, after which 10% Alamar Blue TM was added and the incubation was continued for a further 24 h.

CHAPTER 3

CHEMICAL AND BIOLOGICAL PROFILING OF

PROPOLIS SAMPLES

3 CHEMICAL AND BIOLOGICAL PROFILING OF PROPOLIS

3.1 General screening of propolis samples against *Trypanosoma brucei*

The results (Table 3-1) showed that many of the propolis samples were active against trypanosoma whereas no activity was observed against the bacterium (*M. marinum*).

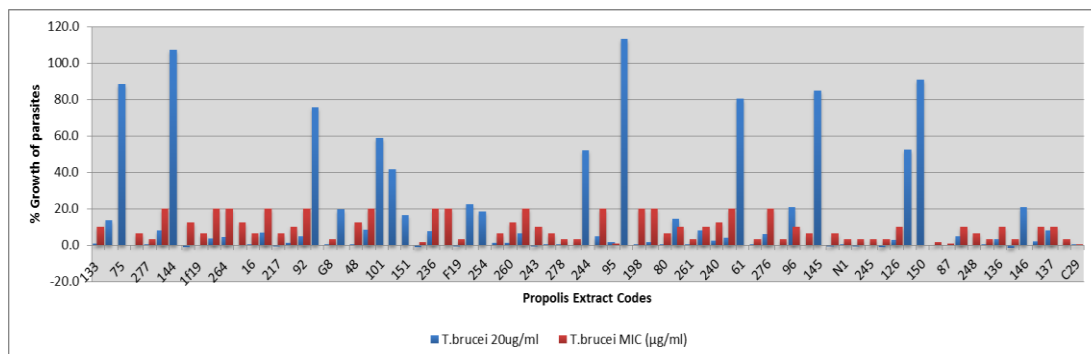


Figure 3.1: General screening of propolis samples from different regions of Africa for activity against against *T. brucei*

Propolis samples collected from different countries within Africa were assayed against *T. brucei* with suramin as the drug control. Figure 3-1 shows the results from screening some of some of the propolis samples. The results indicated varying activity against *T. brucei*, some samples having strong activity and most samples had some degree of activity. C29 was shown to be the most active with minimum inhibitory concentration of 0.39%. Both S95 and S87 were also shown to be highly effective against *T. brucei*, giving a similar MIC percentage of (0.87%). Samples S270 and S272 were quite effective and samples P7 and S94 were considered to be moderately active. Other propolis samples were judged to have low or no activity against *T. brucei*. Table 3-1 summarizes the propolis samples showing stronger antitrypanosomal activities and these were subjected to further investigation.

Table 3.1: The most potent propolis samples tested against *T. brucei* initially at 20µg/ml and then MIC was determined.

No.	Country/region	Extract code	20µg/ml % control	MIC (µg/ml)	Potency
1		C29	0.1	0.39	Highly
2	Jema'a, Nigeria	S 95	1.7	0.78	active
3	Axim, Ghana	S 87	0.0	0.78	
4		S 272	-1.3	1.56	
5		S 270	-0.2	1.56	
6	Cameroon	P7	0.2	3.12	Moderate
7		S 262	0.4	3.12	activity
8		S 277	0.0	3.12	
9		S G8	0.3	3.12	
10		F19	-0.7	3.12	
11		S 278	0.2	3.12	
12	Kampala, Uganda	S 166	-0.3	3.12	
13		S 261	0.4	3.12	
14		S 269	0.4	3.12	
15	East Kenya	S 54	-0.4	3.12	
16		N1	0.1	3.12	
17		S 245	-0.3	3.12	
18	Chua, Uganda	S 152	-1.1	3.12	
19		Cu21	0.5	3.12	
20		S 271	-1.5	3.12	
21	Uganda	S 94	-0.5	3.12	
22	Ethiopia, addis Ababa	P2	0.8	6.25	Low- moderate
23	Nigeria, Zaria,Kauduna state	P4	0.5	6.25	activity
24	Cameroun	P5	0.4	6.25	

25	Copperbelt province,Zambia	S143	-0.5	6.25
26		1f19	-0.1	6.25
27	Uganda,Mbarara	S 16	0.1	6.25
28	Paidha, Uganda	S 155	1.2	6.25
29		C20	0.5	6.25
30	Bundibugyo, Uganda	S 80	0.3	6.25
31	Central Province, Zambi	S 148	-0.2	6.25
32		S 242	-0.7	6.25
33		S 248	-0.3	6.25
+ve Control (Suramin)				0.162

3.2 High resolution mass spectrometry profiles of African propolis samples

Following on from earlier work we were initially interested in the presence of propolones in these samples which we had found in a sample of propolis from Cameroon where the MIC was as low as 0.1 µg/ml when tested against trypanosomes. In order to get some idea of the compounds present in the propolis samples, they were analyzed in positive ion mode by LC- ESI-MS and some samples were found to contain compounds which appeared to be propolones (de Castro Ishida et al., 2011) according to their [M+H] and elemental composition. Among these extracts, strong and moderate antitrypanosomal activities were seen. Further studies, using various techniques, would be required to further identify these compounds. There was some chance of confusing highly oxygenated triterpenoids with propolones; however, the triterpenoids exhibit a lower degree of unsaturation than the phloroglucinones thus a level of unsaturation of >10 was set as the minimum for there to be some confidence in the identification of phloroglucinones in the samples screened. Table 3-2 shows the propolis samples which were found to contain compounds putatively identified as propolones with the elemental composition and

level of unsaturation observed. The table also shows the MIC values for the propolone containing samples. Not all the the propolone containing samples were highly active against *T. brucei* and not all of the highly active samples contained propolones thus there were potentially other active lead compounds in some of the propolis samples from another class of natural products.

Table 3.2: Summary of the data obtained from the samples observed to putatively contain propolones according to LC-MS profiles.

<i>Sample</i>	<i>Code</i>	<i>MIC (μg/ml)</i> against <i>T. brucei</i>	<i>Elemental Compositions observed (MW, RT in min)</i>
Central Province, Zambia	146		C ₂₆ H ₂₉ O ₆ (12.5), C ₂₅ H ₂₇ O ₆ (423.18, 12.5), C ₂₅ H ₂₉ O ₅ (409.20, 11.5), C ₂₆ H ₂₉ O ₇ (453.19, 12.5), C ₂₅ H ₂₉ O ₄ (11.5) C ₂₀ H ₂₁ O ₄ (10.5), C ₃₀ H ₃₅ O ₆ (491.24, 13.5), C ₃₁ H ₃₃ O ₇ (517.22, 15.5)
	276		C ₃₀ H ₃₃ O ₆ (489.23, 14.5), C ₃₀ H ₃₅ O ₆ (491.24, 13.5) C ₃₀ H ₃₃ O ₇ (505.22, 14.5), C ₃₂ H ₃₇ O ₆ (517.25, 14.5) C ₃₃ H ₃₉ O ₆ (531.27, 14.5) C ₃₃ H ₄₁ O ₇ (549.28, 13.5), C ₃₃ H ₄₁ O ₈ (565.27, 13.5) C ₃₄ H ₄₅ O ₆ (12.5), C ₃₃ H ₃₉ O ₆ (14.6), C ₃₅ H ₄₃ O ₉ (607.29, 14.5)
Limbe Buea, SW Cameroon	60	20	C ₂₆ H ₂₉ O ₇ (453.19, 12.5), C ₃₀ H ₃₅ O ₆ (491.24, 13.5), C ₃₀ H ₃₅ O ₇ (505.23, 13.5), C ₃₁ H ₃₇ O ₇ (521.25, 13.5)
Malawi	198	20	C ₂₅ H ₂₉ O ₅ (409.20, 11.5), C ₂₅ H ₂₇ O ₆ (423.18, 12.5), C ₂₆ H ₂₉ O ₆ (437.2, 12.5), C ₂₆ H ₂₉ O ₇ (453.19, 12.5), C ₄₅ H ₄₇ O ₁₁ (763.31, 22.5) C ₄₅ H ₄₅ O ₁₂ (777.29, 23.5), C ₄₅ H ₄₅ O ₁₃ (793.28, 23.5) C ₂₆ H ₂₉ O ₆ (437.2, 12.5)
Uganda, Mbarara	16	6.25	C ₂₅ H ₂₇ O ₅ (407.19, 12.5), C ₃₀ H ₃₅ O ₆ (491.24, 13.5), C ₃₀ H ₃₅ O ₈ (523.23, 13.5)

Kwa Zulu Natal SA	45		$C_{32}H_{43}O_6$ (523.31, 11.5)
	275	20	$C_{30}H_{35}O_6$ (491.24, 13.5), $C_{30}H_{33}O_7$ (505.22, 14.5), $C_{33}H_{41}O_6$ (533.29, 13.5), $C_{33}H_{41}O_7$ (549.28, 13.5), $C_{33}H_{41}O_8$ (565.27, 13.5).
	274		$C_{28}H_{31}O_4$ (431.22, 13.5), $C_{29}H_{33}O_6$ (477.22, 13.5) $C_{35}H_{41}O_8$ (589.28, 15.5) $C_{35}H_{35}O_{10}$ (615.22, 18.5), $C_{35}H_{35}O_{11}$ (631.22, 18.5)
Central Province, Gambia	148	6.25	$C_{33}H_{41}O_5$ (517.3, 13.5)
	273	10	$C_{25}H_{25}O_6$ (421.16, 13.5) $C_{26}H_{27}O_6$ (435.18, 13.5) $C_{31}H_{37}O_7$ (521.25, 13.5), $C_{31}H_{39}O_7$ (523.27, 13.5), $C_{34}H_{31}O_6$ (535.21, 19.5), $C_{34}H_{33}O_6$ (537.23, 18.25) $C_{34}H_{31}O_7$ (553.2, 19.5), $C_{34}H_{33}O_7$ (553.22, 18.5), $C_{35}H_{35}O_7$ (567.24, 18.5), $C_{42}H_{43}O_{11}$ (723.28, 21.5)
	257		$C_{30}H_{35}O_6$ (491.24, 13.5), $C_{32}H_{37}O_6$ (517.25, 14.5), $C_{32}H_{39}O_6$ (517.27, 13.5) $C_{33}H_{41}O_7$ (549.28, 13.5)
Axim, Ghana	87	0.78	$C_{26}H_{29}O_7$ (453.19, 12.5), $C_{33}H_{41}O_6$ (529.28, 13.5), $C_{31}H_{37}O_7$ (521.25, 13.5),

			$C_{33}H_{29}O_{10}$ (585.17, 19.5)
Copper Belt Gambia	145		$C_{25}H_{27}O_6$ (423.18, 12.5), $C_{25}H_{29}O_5$ (409.20, 11.5)
	238	3.12	$C_{25}H_{29}O_7$ (441.19, 11.5), $C_{33}H_{41}O_5$ (517.29, 13.5)
	236	20	$C_{33}H_{41}O_7$ (549.28, 13.5)
Jos, Nigeria	97	10	$C_{32}H_{37}O_6$ (517.25, 14.5), $C_{31}H_{37}O_7$ (521.25, 13.5), $C_{33}H_{21}O_6$ (523.21, 18.5)
Mbarara, Uganda	20	6.25	$C_{33}H_{41}O_7$ (549.28, 13.5), $C_{35}H_{39}O_7$ (571.27, 16.5)

3.3 Development of a Rapid Method for the Analysis of Propolis by LC-MS

In parallel with investigation of propolis composition and its biological activity, a rapid isocratic method using acetonitrile/0.1% formic acid (90:10) was developed for screening samples for propolones with less than 20 minutes retention time. The phloroglucinone hyperforin was used as standard marker compound to develop the method which allowed elution within 20 min.

3.4 Natural Product Data Base

Recently, a searchable database was established “in house” which contains details on more than 25,000 natural products including phloroglucinones which are based on phloroglucinol (Figure 3.2). This database was used to search for these components in the propolis samples and data from this present study obtained from LC-MS was matched with information from this database. Table 3-3 shows the matching of the components in crude sample 87 against this database. It would appear as if there is very little information in the database with regard to phloroglucinones since there are compounds which can be putatively attributed phloroglucinones in the sample but there are few hits against the database. Thus there were many components in the sample which were not found in the database.

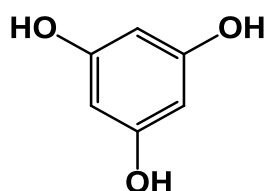


Figure 3.2: Phloroglucinol

Table 3-3: The components in crude sample P87 found from matching against the natural product database

<i>M/Z</i>	<i>Name</i>
409.2008	1,4-Naphthalenedione, 6-ethenyl-4a,5,8,8a-tetrahydro-5-[2-(4-hydroxy-3,5-dimethoxyphenyl)ethenyl]-2,3,4a-trimethyl-, (4aS,5S,8aR)-
423.3619	9,19-Cyclo-9?-lanost-24-en-3-one-2,2-d2 (7CI,8CI)
435.1801	6,10-Methano-1-benzoxacyclotridecin-10,12(11H)-dicarboxaldehyde, 2,5,6,9-tetrahydro-3,7-dimethyl-6-(3-methyl-2-buten-1-yl)-9,11,16-trioxo-
447.2529	1,3,5-Cyclohexanetrione, 6-benzoyl-2,2,4,4-tetra-2-buten-1-yl-
449.2684	Bicyclo[3.3.1]non-3-ene-2,9-dione, 3-benzoyl-4-hydroxy-1,8,8-trimethyl-5,7-bis(3-methyl-2-buten-1-yl)-, (1R,5R,7R)-rel-
455.3519	2H-Benz[e]inden-2-one, dodecahydro-7-hydroxy-6-(hydroxymethyl)-3a,6,9a-trimethyl-3-[(2E,4E)-1,5,9-trimethyl-2,4,8-decatrien-1-ylidene]-,
459.3832	2(1H)-Naphthalenone, octahydro-6-hydroxy-5-(13-hydroxy-4,8,12-trimethyl-3,7,11-tridecatrien-1-yl)-1,1,4a,6-tetramethyl-
467.2063	Tricyclo[3.3.1.13,7]decane-1-propanoic acid, 3-(ethoxycarbonyl)-4,4-dimethyl-?-methylene-2,6,9-trioxo-, 2-phenylethyl ester

471.3468	19-Norlanosta-5,24-diene-7,23-dione, 3,28-dihydroxy-9-methyl-, (3?,4?,9?,10?)-
517.3311	Bicyclo[3.3.1]non-3-ene-2,9-dione, 3-benzoyl-4-methoxy-8,8-dimethyl-1,5,7-tris(3-methyl-2-buten-1-yl)-, (1R,5R,7S)-
517.3312	Bicyclo[3.3.1]non-3-ene-2,9-dione, 3-benzoyl-4-methoxy-8,8-dimethyl-1,5,7-tris(3-methyl-2-buten-1-yl)-, (1R,5R,7S)-
521.2533	2-Cyclohexen-1-one, 2,2'-[3-phenyl-3-(2,3,4-trihydroxyphenyl)propylidene]bis[3-hydroxy-5,5-dimethyl- (9CI)
521.2534	2-Cyclohexen-1-one, 2,2'-[3-phenyl-3-(2,3,4-trihydroxyphenyl)propylidene]bis[3-hydroxy-5,5-dimethyl- (9CI)
603.3677	Bicyclo[3.3.1]non-3-ene-2,9-dione, 3-(3,4-dihydroxybenzoyl)-5-[(2E)-3,7-dimethyl-2,6-octadien-1-yl]-4-hydroxy-8,8-dimethyl-1,7-bis(3-methyl-2-buten-1-yl

3.5 Discussion

The African propolis samples (n=90) were evaluated for anti-trypanosomal activity and activity against *Mycobacterium marinum*. The results presented in Table 3-1 for the ethyl acetate extracts of propolis obviously showed varying degrees of activity against trypanosoma and the samples were categorised as having strong activity at MIC \leq 1.0 μ g/ml, moderate activity with MIC range 2.0-20 μ g/ml, and low activity with MIC $>$ 25.0. None of the samples had significant activity against *M. marinum*. The samples were obtained from various regions and the samples that were used in this study were mainly from Africa but some were from China, Lithuania, and Brazil. Among the African samples S87 (Axim, Ghana) and S95 (Gidan Waya, Jema'a, Nigeria) were found to be highly effective against *T. b. brucei* with similar MIC of 0.87 μ g/ml. However, the samples from Brazil and Lithuania displayed moderate activity with MIC 3.25 and 10.0 μ g/ml, respectively, while the Chinese sample (S61) was inactive. Almost all of the remaining African samples were judged as weakly active (MIC \leq 20 μ g/ml) or as having no activity against *T. b. brucei*. However, the plant source of African propolis also has not been reported yet (Peyfoon, 2009). From previous work it was established that African samples appeared to contain two types of compound which were active against *T. b. brucei*, triterpenoids and phloroglucinone. The triterpenoids exhibited moderate activity and the phloroglucinone containing samples were more potent. At the beginning of the study hyperforin (figure 3.3), a common phloroglucinone present in St John's Wort, was tested against *T. b. brucei*, and was found to have quite strong activity exhibiting a MIC of 3.12 μ g/ml. Thus initially the major interest in the current work was to identify high potency propolis samples and then determine whether or not they contain phloroglucinone compounds. Assay of the antitrypanosomal activity of propolis samples and fractions was carried out in order to identify which had the strongest biological activity. This assay was conducted in parallel with other analysis techniques. Most samples which exhibited high activity were obtained from the African region and subsequently the Nigerian (S95) and Ghanian (S87) samples which had exhibited very high activity were subjected to further fractionation in order to purify the compounds that were responsible for activity. *T. brucei*

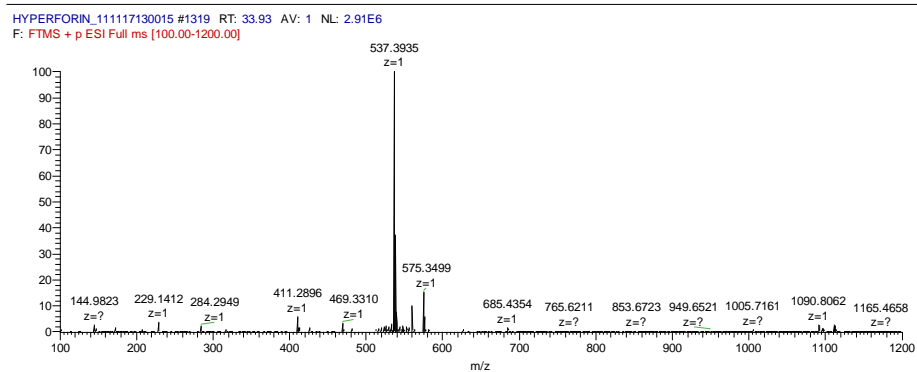
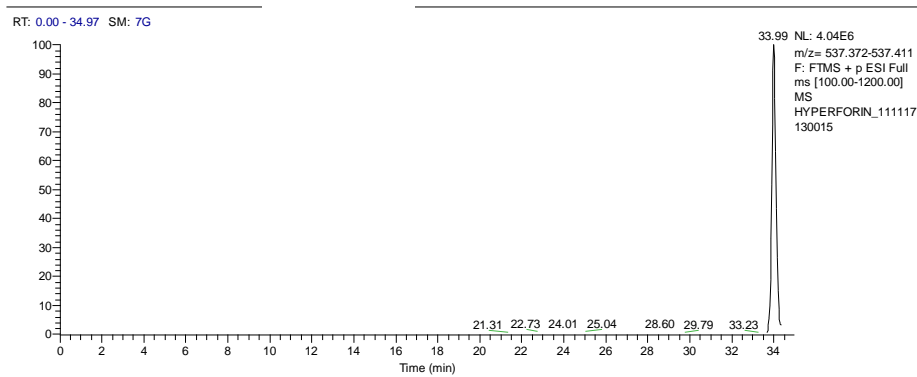


Figure 3.4: LC-MS spectral analysis for phloroglucinone present in St John's Wort

After this initial work a re-run of the profiling work was done for most of the African samples and several members of the lab contributed to this work so it is not reported in this thesis. However, I made a contribution to the study and the published paper resulting from this work is shown in appendix (I), page 190.

CHAPTER 4:
ATTEMPTED PURIFICATION OF ANTI-
TRYPANOSOMAL EXTRACTS OF NIGERIAN
AND TANZANIAN PROPOLIS SAMPLES

4 PROFILING AND ATTEMPTED PURIFICATION OF ANTITRYPANOSOMAL PROPOLIS EXTRACTS

4.1 Results of Investigation of Nigerian propolis Sample (S95)

Sample 95 was found to have a low MIC value for the crude extract and thus it was fractionated by using flash chromatography (MPLC). The weights of the fractions are shown in Table 4-1. The fractions were monitored by TLC as well as by LC-MS. Table 4-2 shows the activity of the different fractions against *T. b. brucei* and it is clear that although the fractions retain good activity the activity was lower than that of the crude extract originally tested although subsequent testing of fractions, as shown in table 4-2, did not yield such high activity for the crude extract. This suggests that the components within the original extracts might display synergistic effects.

Table 4.1: The %yield of fractions obtained of sample 95 by SP

Extract/Fraction	Weights (g)	% yield of fraction
S95F1	0.2886	4.43
S95F2	1.6591	25.45
S95F3	1.016	15.58
S95F4	0.5181	7.95
S95F5	0.5453	8.36
S95F6	0.1985	3.05
S95F7	0.1515	2.32
S95F8	0.2082	3.19
S95F9	0.0983	1.51
95F10	0.0782	1.29
S95F11	0.1158	1.78
S95F12	0.0437	0.67
S95F13	0.2491	3.82

Total crude weight of sample was 6.52 g

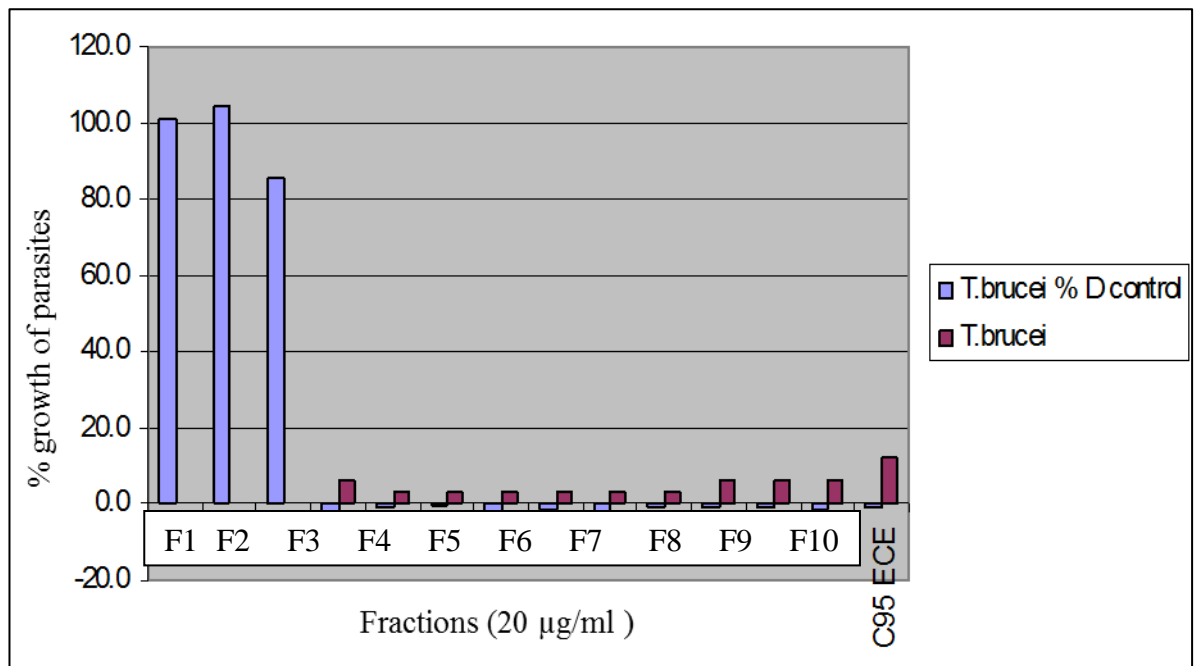


Figure 4.1: Testing of crude extract of S95 and its fractions for anti-trypanosomal activity.

Table 4.2: Anti-trypanosomal activity of the fractions from propolis sample S95

S/no	V. Fraction No.	Extract/Fraction	Anti-trypanosomal activity	
			20µg/ml %control	MIC (µg/ml)
1	1-9	S95F1	101.2	101.2
2	10-11	S95F2	104.3	104.3
3	12-13	S95F3	85.3	85.3
4	14-15	S95F4	-2.9	6.25
5	16-18	S95F5	-1.1	3.12
6	19-21	S95F6	-0.2	3.12
7	22-24	S95F7	-2.1	3.12
8	25-29	S95F8	-1.3	3.12
9	30-32	S95F9	-2.0	3.12
10	33-37	95F10	-1.1	3.12
11	38-40	S95F11	-0.8	6.25
12	41	S95F12	-0.9	6.25
13	42	S95F13	-1.4	6.25
Crude Extract		S95		12.25
+Ve Control		Suramin		0.162

At this stage we were still pursuing the idea that the high activity of African propolis samples against *T. b. brucei* was due to propolones. The peaks with elemental compositions which could correspond to propolones mainly eluted in fractions 3-4 with only partial separation between them. Figure 4-2 shows extracted ion traces for

the main components of the mixture in fraction 3 which had the masses and elemental compositions as follows:

$C_{29}H_{41}O_8$ (517.28), $C_{29}H_{39}O_8$ (515.26), $C_{29}H_{39}O_9$ (531.26) and $C_{31}H_{37}O_8$ (537.25).

However, in fact the compounds with these elemental compositions could also correspond to compounds such as lignans although the number of carbon atoms is not quite correct.

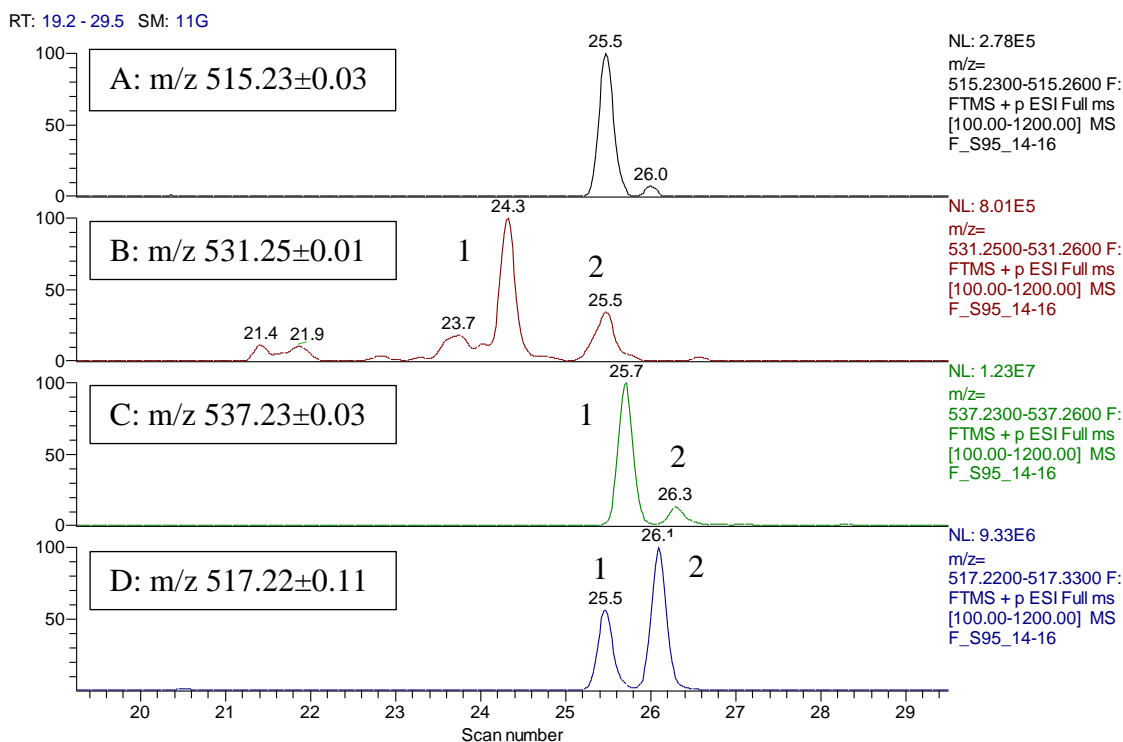


Figure 4.2: Extracted ion traces for the main compounds in fraction 3. The masses and elemental compositions were as follows: A: m/z 515.23±0.03 ($C_{29}H_{39}O_8$), B: m/z 531.25±0.01 ($C_{29}H_{39}O_9$), C: m/z 537.23±0.03 ($C_{31}H_{37}O_8$) and D: m/z 517.22±0.11 ($C_{29}H_{41}O_8$). These elemental compositions match that of propolones. The peak numbers -denote compounds that possibly exist as isomers in the fraction.

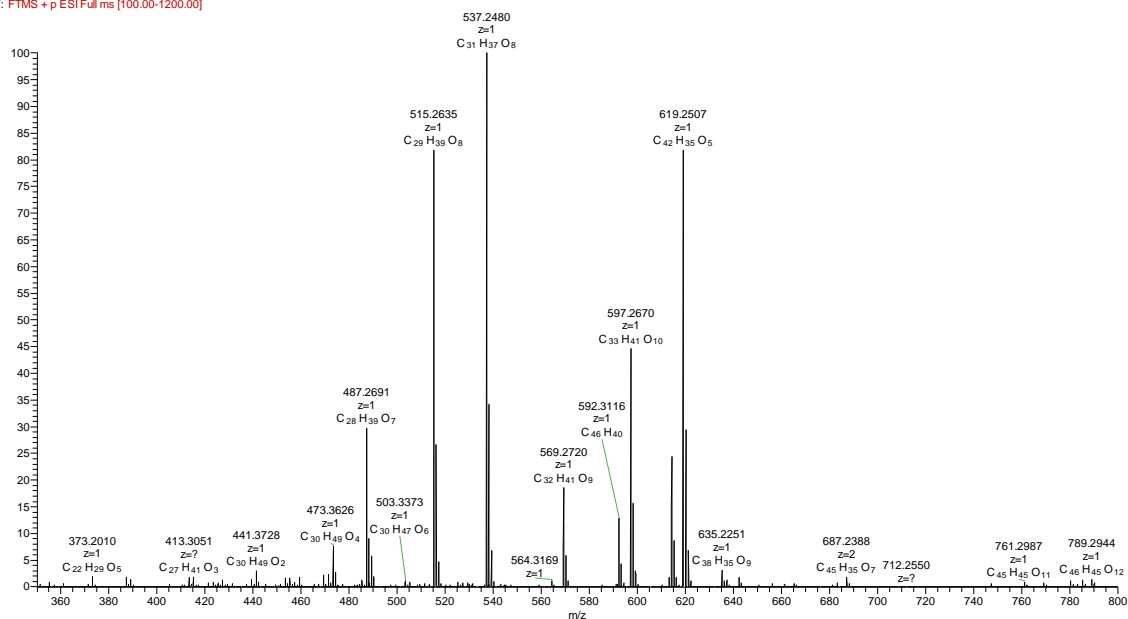


Figure 4.3: Shows ions for co-eluting compounds present in the peak at 25.7 min which appears to be the most abundant peak in the samples.

Table 4.3: Shows the most abundant compounds in fractions 3-5. These elemental compositions could correspond to a range of structural types including triterpenes, lignans or propolones.

m/z	Rt min	RDB	Elemental composition
471.3465	28.4	7.5	C ₃₀ H ₃₇ O ₄
471.3465	30.0	7.5	C ₃₀ H ₃₇ O ₄
473.3619	29.4	6.5	C ₃₀ H ₃₉ O ₄
509.2534	25.6	12.5	C ₃₀ H ₃₇ O ₇
515.2631	25.5	10.5	C ₂₉ H ₃₉ O ₈
517.2789	28.3	9.5	C ₂₉ H ₄₁ O ₈
531.2584	25.4	10.5	C ₂₉ H ₃₉ O ₉
531.2584	28.8	10.5	C ₂₉ H ₃₉ O ₉
537.2478	25.6	13.5	C ₃₁ H ₃₇ O ₈
593.3152	28.3	4.5	C ₂₈ H ₄₉ O ₁₃

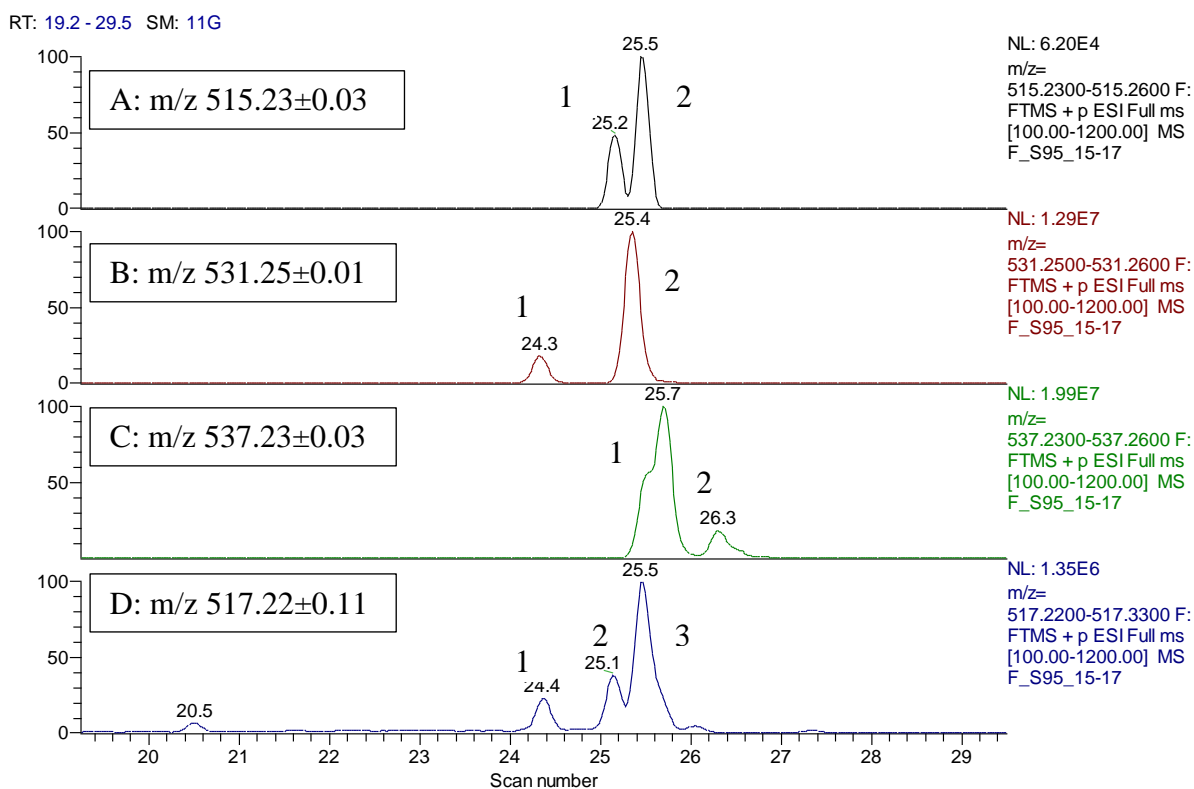


Figure 4.4: Extracted ion traces for the main compounds in fraction 4. The masses and elemental compositions were as follows: A: m/z 515.23±0.03 (C₂₉H₃₉O₈), B: m/z 531.25±0.01 (C₂₉H₃₉O₉), C: m/z 537.23±0.03 (C₃₁H₃₇O₈) and D: m/z 517.22±0.11 (C₂₉H₄₁O₈). These elemental compositions match that of propolones. The peak numbers denote compounds that possibly exist as isomers in the fraction.

The same compounds are present in fraction 4 with the more polar compound with m/z 531.26 being more highly enriched in this fraction. In fraction 5 the intensities of the compound peaks are beginning to fall. It is evident that there are a number of isomers present at each molecular weight.

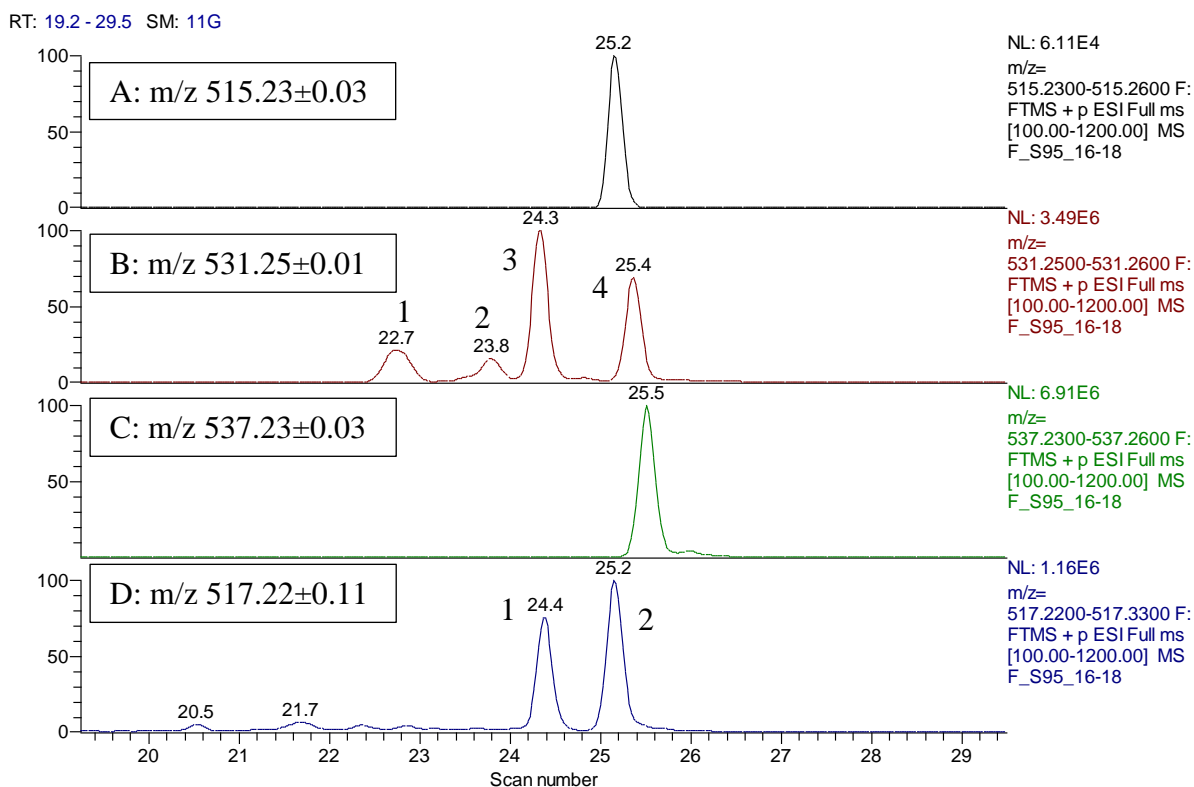


Figure 4.5: Extracted ion peaks for the main compounds present in fraction 5. The masses and elemental compositions were as follows: A: m/z 515.23±0.03 ($C_{29}H_{39}O_8$), B: m/z 531.25±0.01 ($C_{29}H_{39}O_9$), C: m/z 537.23±0.03 ($C_{31}H_{37}O_8$) and D: m/z 517.22±0.11 ($C_{29}H_{41}O_8$). These elemental compositions match that of propolones. The peak numbers denote compounds that possibly exist as isomers in the fraction.

Thus although the MPLC method had separated the propolones from the triterpenoids and other components within the propolis, there was still only partial separation between the propolones themselves. These fractions were tested against *T.brucei* to determine their MICs and fractions 4 and 5 were quite effective while fraction 3 was inactive. Continuing fractionation of the fractions from S95 resulted in a further decrease in activity.

4.2 Result of fractionation of Tanzanian Propolis (TP1) Samples

The Tanzanian sample (TP1) was found to have interesting activity in its fractions although the crude extract was much less active. Fractionation of this sample was accomplished via use of silica column on MPLC. The weights and percentage yields in comparison with the starting weight for the fractions are shown in table 4-4. The fractions were monitored by both TLC and LC-MS.

Table 4.4: The yield of fractions obtained of sample TB1 by normal phase on MPLC

<i>Fraction No.</i>	<i>Fraction</i>	<i>Weights (g)</i>	<i>% yield</i>	<i>Anti-trypanosomal activity</i>	
				<i>20µg/ml % control</i>	<i>MIC (µg/ml)</i>
1-9	TP1F1	0.3585	0.62	100.8	
10	TP1F2	2.6265	4.53	105.9	
11	TP1F3	0.4862	0.84	109.5	
12-13	TP1F4	4.0531	7.0	88.4	
14-15	TP1F5	0.3344	0.58	28.0	
16-17	TP1F6	1.0864	1.87	0.9	12.5
18-19	TP1F7	0.1665	0.29	-0.6	12.5
20-21	TP1F8	0.1144	0.27	2.5	25
22-24	TP1F9	0.0868	0.15	22.8	
25-26	TP1F10	0.1433	0.25	6.8	25
27-28	TP1F11	0.2015	0.35	7.0	25
29-40	TP1F12	0.1725	0.37	109.0	
41	TP1F13	0.0332	0.15	6.8	25
42	TP1F14	0.2183	0.38	58.0	
+Ve Control	(Suramin)				0.162

The fractions obtained from the sample from Tanzania were profiled by using LC-MS. The mass spectra obtained from the fraction showed elemental compositions which did not correspond to propolones. This implies that the activity displayed by this sample may have been due to another class of natural products such as triterpenoids or flavonoids. The strongest activity was observed in fraction 6-7 whose extracted ion chromatogram is shown in Figure 4.6 representing the main components of this mixture of fraction. This fraction contained peaks with elemental compositions and masses as follows: $C_{17}H_{15}O_6$ (315.09), $C_{26}H_{49}O_4$ (425.37), $C_{20}H_{37}O_2$ (309.28) and $C_{30}H_{51}O$ (427.39). $C_{17}H_{15}O_6$ would seem to correspond to possibly a dimethyl flavanone whereas the other compounds are not as unsaturated and may correspond to terpenoid compounds. This supported by the proton spectrum shown in Figure 4.7 where the majority of protons are due to aliphatic compounds with small signals in the aromatic region which may correspond with flavonoid detected in the sample.

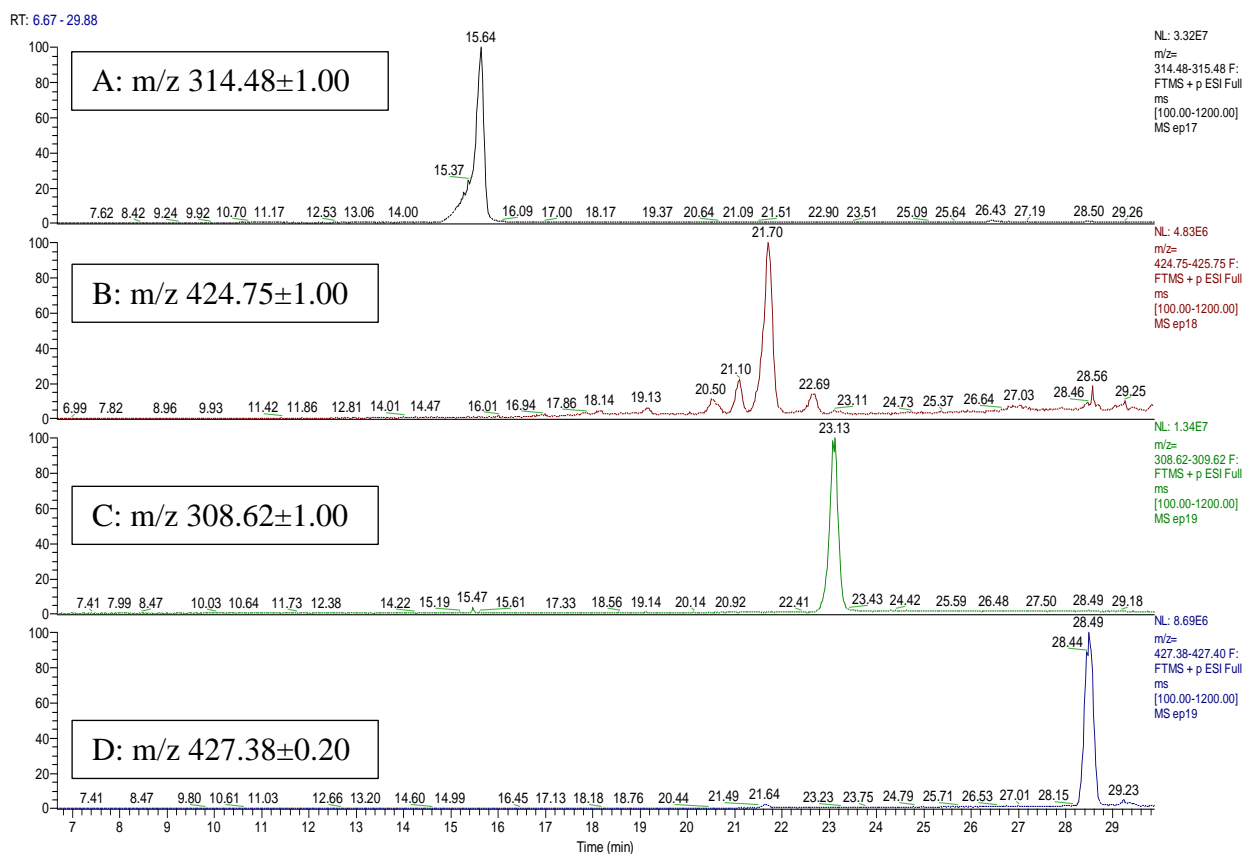


Figure 4.6: Extracted ion peaks for the main compounds present in fraction 6-7 obtained from Tanzanian Propolis. The masses and elemental compositions were as follows: A: m/z 314.48±1.00 (C₁₇H₁₅O₆), B: m/z 424.75±1.00 (C₂₆H₄₉O₄), C: m/z 308.62±1.00 (C₂₀H₃₇O₂) and D: m/z 427.38±0.20 (C₃₀H₅₁O). The compound in chromatogram A corresponds to a dimethyl flavanone whereas compounds in B-C are not as unsaturated and may correspond to terpenoids.

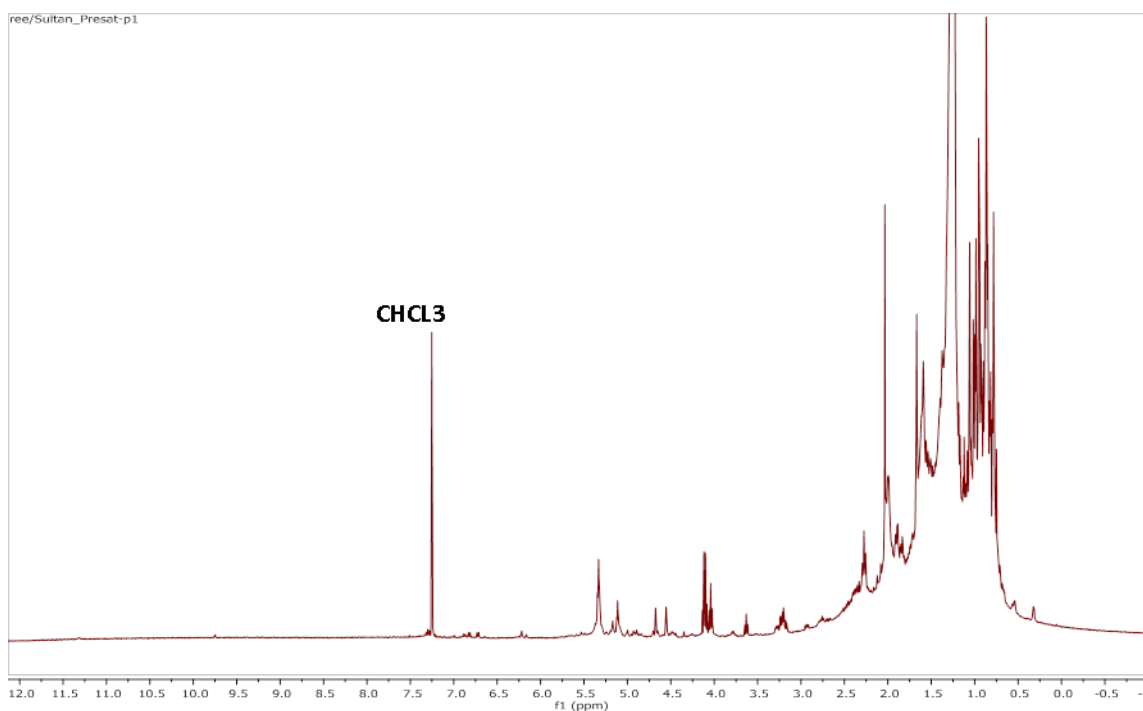


Figure 4.7: Proton NMR spectrum (400 MHz in CDCl_3) of fraction 6-7 showing mainly aliphatic protons

4.3 Discussion

Several of the propolis samples contained propolones but not all the highly active propolis samples contain them. Thus there may be more than one target compound type with regard to activity against *T. b. brucei*. The data base used to search the samples appeared to contain few propolones thus it will be necessary to build up a predicted database based on the existing literature on the propolones found in propolis. From the data shown in Table 3.2 in the previous chapter it is clear that some of the compounds can be related to the propolone structures shown in Figure 4.8. These structures contain a benzoyl group and addition or subtraction of isoprenyl units or the benzoyl group would result in carbon skeletons composed of C_{21} , C_{26} , C_{31} , C_{33} , C_{36} , and C_{38} . In the case of hyperforin a butyl group is present in place of benzoyl group and this would result in a skeleton with C_{20} , C_{21} , C_{25} , C_{30} , C_{31} , and C_{40} . Both these skeleton types appear to be in the African propolis samples. In addition, these compounds are classified as belonging to the polycyclic polyisoprenylated benzophenone (PPBs) class which are reported to be labile compounds which are sensitive to heat, light and oxygen and have been found to

degrade during the extraction or purification particularly when non polar solvents are used for the purification (Piccinelli et al., 2009).

The crude extracts from S95, S87 and T1 which had shown high activity were further fractionated using normal phase flash chromatography and most of their fractions displayed activity against *T. b. brucei*. In addition they appeared to contain an abundance of propolones, thus suggesting that propolones may be responsible for this toxicity or synergism in combination with other phenolic components.

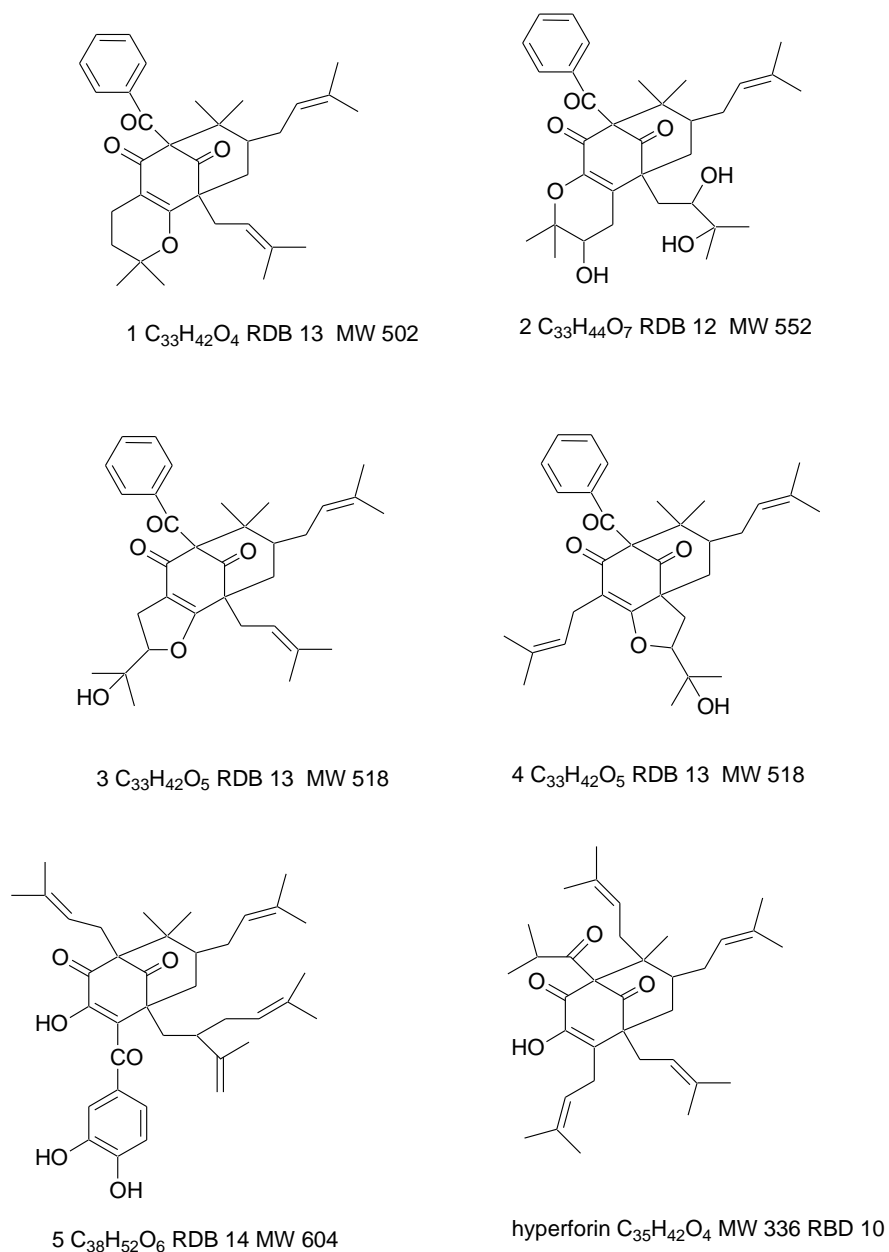


Figure 4.8: Phloroglucinone compounds (Almutairi et al., 2014)

4.4 Conclusion on Nigerian and Tanzanian propolis samples

We can conclude that the propolis sample from Nigeria (S95) possessed significant biological activity against *Trypanosoma brucei brucei* for both crude extracts and fractions with MIC values of 12.25 µg/ml and 3.12-6.25 µg/ml, respectively. Thirteen fractions were obtained from flash chromatography after elution based on their difference in polarities; most of these fractions displayed relatively good activity against *T. b. brucei* although there was little if any improvement in activity as a result of purification. This activity could possibly be due to the presence of a range of structurally diverse compounds including lignans, propolones and triterpenes. The primary goal of our analysis of this sample was to investigate for the presence of propolones which we had found to be very active against *T. b. brucei*. LC-MS analysis indicated that the propolones mainly eluted in fraction 3-4 based on chromatographic peak elemental composition, although this might have been due to another class of related compounds such as lignans.

The Tanzanian sample displayed moderate activity in some of its fractions. However, unlike the Nigerian sample, this sample did not seem to contain propolone compounds after the initial screen by both LC-MS and Proton NMR. Thus the observed biological activity could be attributed to more than one target compound present in the samples. In the end it proved difficult to isolate and characterise the components in the active fractions from S95 and T1. In the case of S95 this may be due to the known instability of the propolone compounds in non-polar organic solvents. In the case of T1 the fractions only proved to be of moderate activity and although we had a large quantity of this sample it was decided that it would be better to focus on samples with higher activity.

CHAPER 5:
FRACTIONATION AND TESTING OF A
PROPOLIS SAMPLE FROM GHANA

5 FRACTIONATION AND TESTING OF A PROPOLIS SAMPLE FROM GHANA

During the preliminary investigations on anti-trypanosomal activity of African propolis, it was found that an ethyl acetate extract of Ghanaian propolis exhibited the lowest MIC (0.78 µg/ml) in a bioassay test. As a result, this sample was selected for subsequent successive fractionation using various chromatographic techniques including HPLC and flash chromatography in order to isolate and purify the active compounds present.

5.1 LC-MS profiling of propolis sample–S87

LC-MS profiling of sample S87 was carried out by using a more rapid the rapid LC-MS method described in section 2.6.3.1. At this stage we were less focused on propolones as targets for activity since it seemed that many types of compounds in propolis showed some degree of activity against *T. b. brucei*. Table 5.1 shows the most abundant compounds in sample S87. The extract of S87 was also fractionated by MPLC on silica gel and the weights of the fractions and their activities are shown in Table 5.2. Figure 5.1 shows the mass spectrum (MH^+) of the most abundant compound by response in the crude extract of S87. The elemental composition $C_{25}H_{27}O_6$ (S87-1) could correspond to a number of structural types but the most common type of structures with this formula are prenylated flavonoids. Figure 5.2 shows the abundance of S87-1 in the different fractions described in Table 5.2.

Table 5.1: The compounds in the crude extract of S87 which are the most abundant by response when analysed by reversed phase LC-MS in positive ion mode.

Compound	m/z	Rt min	RDB*	Elemental composition
1	423.1796	2.6	12.5	C ₂₅ H ₂₇ O ₆
2	439.1749	2.2	12.5	C ₂₅ H ₂₇ O ₇
3	269.0806	1.7	10.5	C ₁₆ H ₁₃ O ₄
4	285.0757	1.7	10.5	C ₁₆ H ₁₃ O ₅
5	409.2005	2.2	11.5	C ₂₅ H ₂₉ O ₅
6	491.2432	5.1	13.5	C ₃₀ H ₃₅ O ₆
7	453.1905	2.8	13.5	C ₂₆ H ₂₉ O ₇
8	385.1278	1.9	11.5	C ₂₁ H ₂₁ O ₇
9	369.1131	1.9	11.5	C ₂₁ H ₂₁ O ₆
10	437.1955	2.7	12.5	C ₂₆ H ₂₉ O ₆
11	421.1643	4.0	13.5	C ₂₅ H ₂₅ O ₆
12	489.2271	9.0	14.5	C ₃₀ H ₃₃ O ₆
13	449.2683	2.4	11.5	C ₂₉ H ₃₇ O ₄
14	507.2373	4.0	13.5	C ₃₀ H ₃₅ O ₇
15	341.1382	1.7	10.5	C ₂₀ H ₂₁ O ₅

*RDB stands for relative double bond

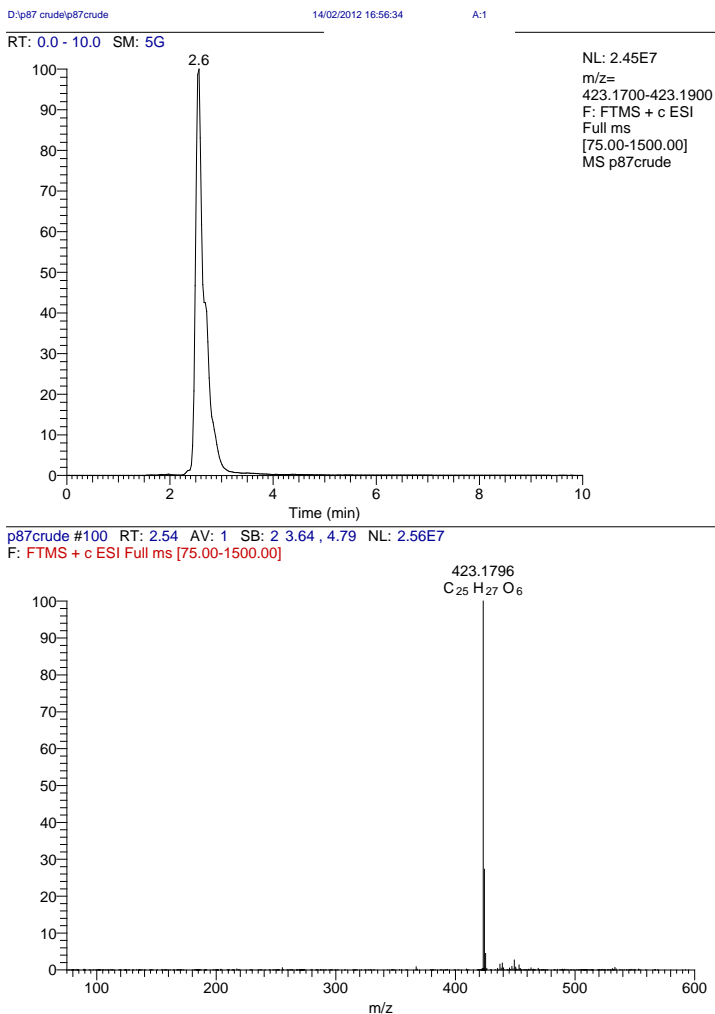


Figure 5.1: Extracted ion chromatogram and mass spectrum for S87-1 which is the most abundant compound by response in S87 when analysed by reversed phase LC-MS in positive ion mode.

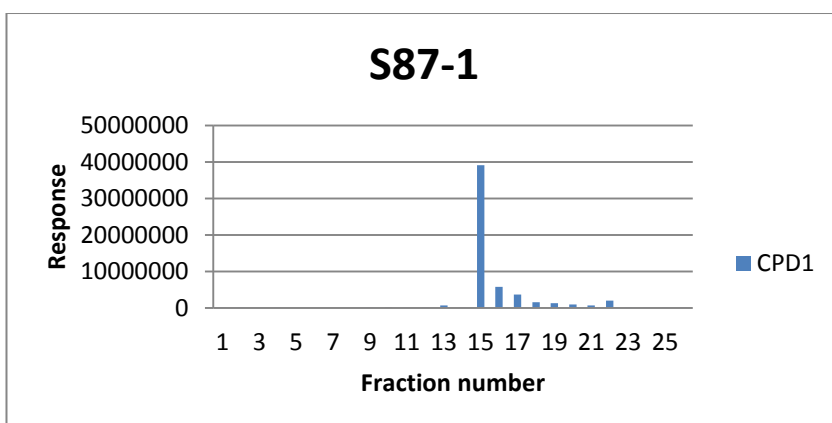


Figure 5.2: Fractions from MPLC containing compound S87-1

Table 5.2: Summary for the weights and anti-trypanosomal and anti-mycobacterium activities obtained from S87extracts. The brown cells indicate the highest activity. Fractions in pink have been isolated and identified.

Fraction number	Flask MPLC numbers	Yield (mg)	Inhibition of <i>T.b.brucei</i> 20µg/mL	Inhibition of <i>M. marinum</i> 100 µg/mL
M-1	2 -3	425.7	94.4	39.0
M-2	4-5	365.4	96.1	51.2
M-3	6-8	19.2	91.5	48.1
M-4	9	185.4	92.4	50.5
M-5	10	202.4	90.9	70.4
M-6	11	381.6	85.8	26.5
M-7	12	653.9	74.2	51.2
M-8	13	335.9	1.6	26.2
M-9	14	330.9	0.3	6.2
M-10	15	659.2	3.4	20.4
M-11	16	893	3.4	11.1
M-12	17	866.8	6.7	2.6
M-13	18-20	2729.7	3.8	2.7
M-14	21-23	2619.7	3.6	18.1
M-15	24-26	2930.5	2.0	3.3
M-16	27-29	2348.6	3.5	37.6
M-17	30-31	1788.1	3.5	36.2
M-18	32-41	11908.7	2.6	82.6
M-19	42	2654	4.6	40.1

It can be seen from Figure 5.2 that S87-1 is most abundant in fraction 15 which is also the highest weight fraction and which has good activity against both *T. b. brucei* and *M. marinum*. The mass spectrum for the second most abundant compound (S87-2) in the crude extract is shown in Figure 5.3 and this would correspond to the hydroxylated version of S87-1. The occurrence of this compound in the fractions from MPLC is shown in Figure 5.4. As would be predicted the addition of a hydroxyl

group causes it to elute later from silica gel based MPLC and it is most abundant in fraction 19 which is another high weight fraction with good activity against *T. b. brucei* although less activity against *M. marinum*.

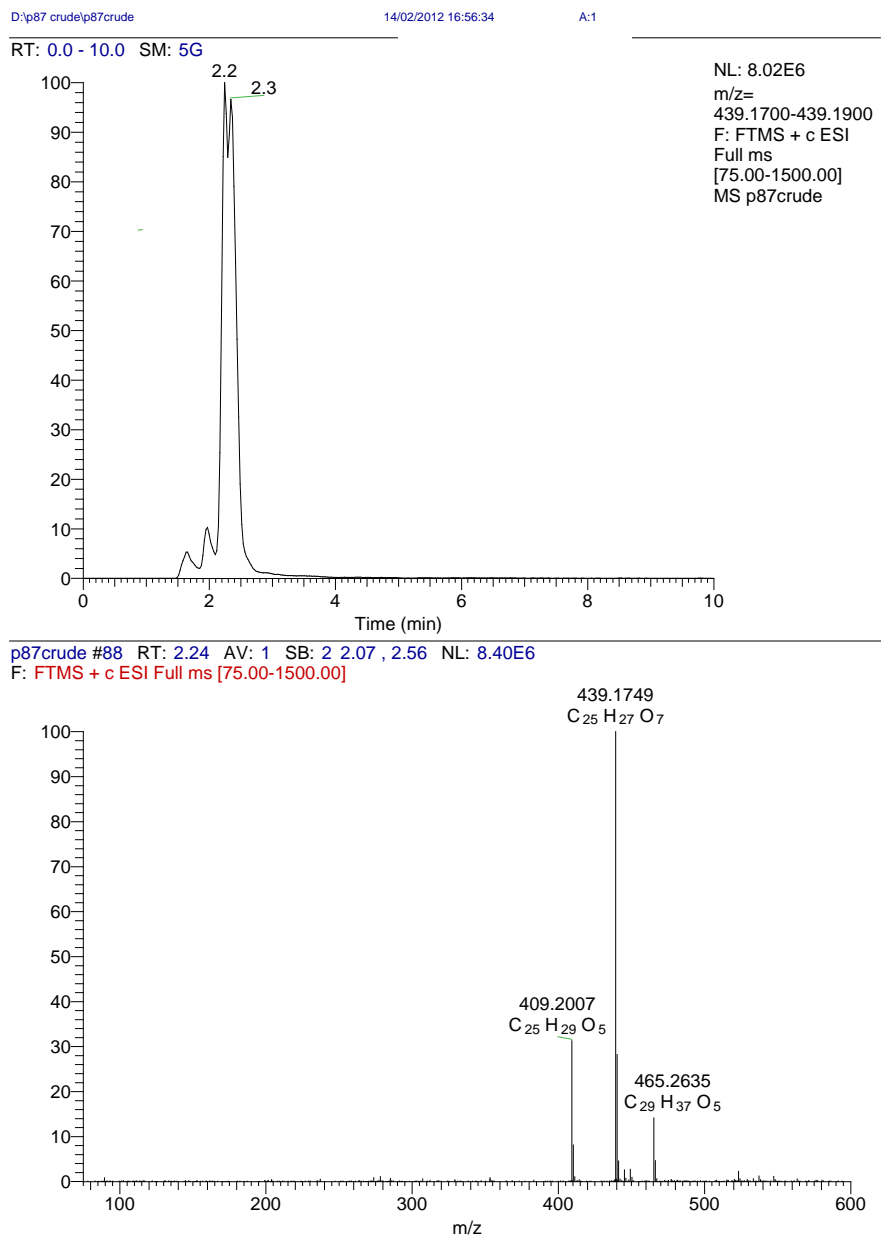


Figure 5.3: Extracted ion chromatogram and mass spectrum for S87-2 which is the second most abundant compound by response in S87 when analysed by reversed phase LC-MS in positive ion mode

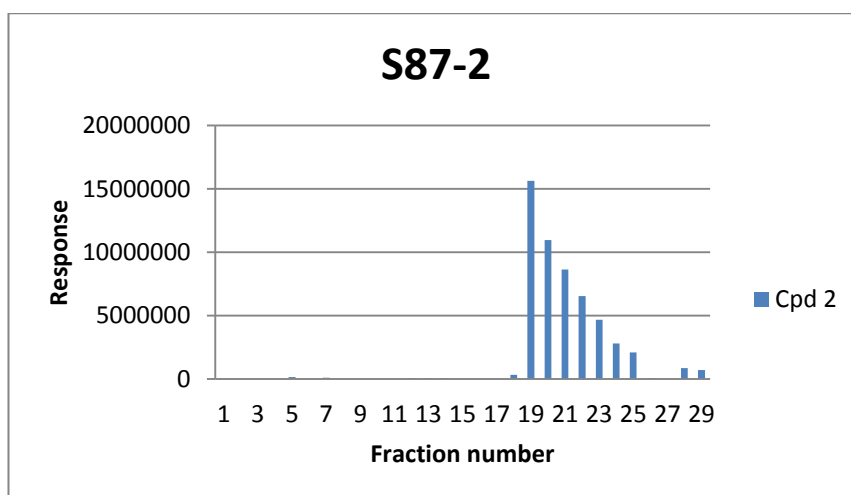


Figure 5.4: Fractions from MPLC containing compound S87-2

The third most abundant compound by response is very interesting since it has the composition $C_{16}H_{12}O_4$ (S-87-3 Figure 5.5) and this has a composition corresponding to methylpinocembrin which is a common flavonoid in temperate European propolis rather than in tropical propolis (de Groot et al., 2014). The mass spectrum shown in Figure 5.5 also contains an ion at m/z 285 which would correspond to methylpinobanksin another constituent of European propolis. Figure 5.6 shows the fractions which contain S-87-3. As might be expected for a smaller more polar molecule it ran in the later fractions, mainly 23 and 24. These fractions were not tested for biological activity. Fraction 13 was a high weight fraction but seems to contain less dominant components. The 12th most abundant component (S87-12) is quite abundant in this fraction (figure 5.8) and has the elemental composition $C_{30}H_{33}O_6$ (figure 5.7) for the MH^+ . This composition could correspond to a lignan and a neolignan with this composition with strong anti-leishmanial activity has been isolated from a Nepalese plant (Suzuki et al., 2009). The above analysis of the data has been retrospective and it would have been useful to analyse before the preparative chromatography steps. However, preparative chromatography was carried out without having carried out detailed analysis of the LC-MS data as described in the sections below.

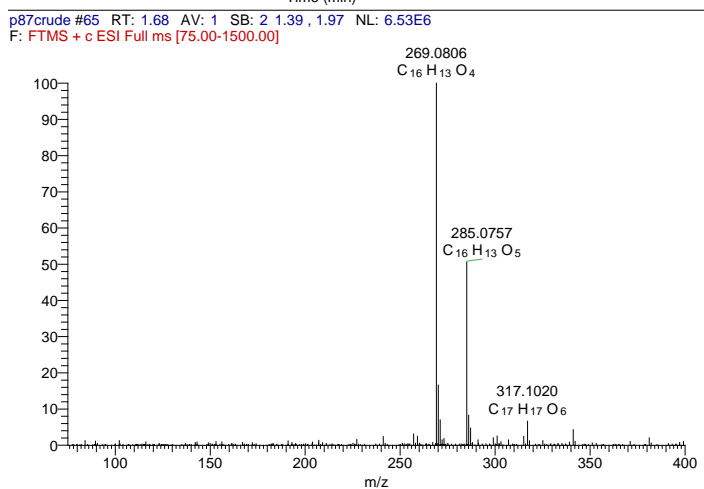
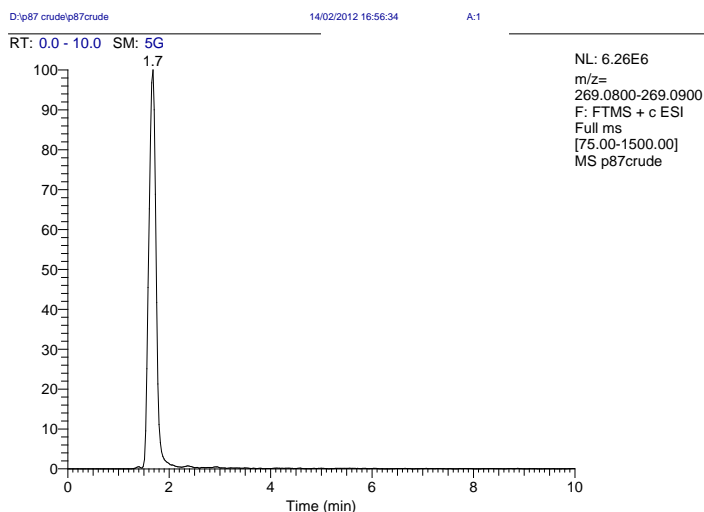


Figure 5.5: Extracted ion chromatogram and mass spectrum for S87-3 which is the third most abundant compound by response in S87 when analysed by reversed phase LC-MS in positive ion mode.

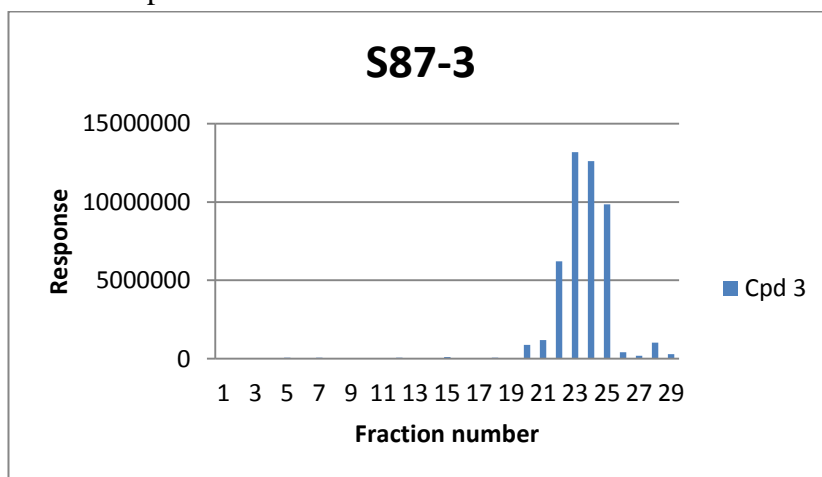


Figure 5.6 Fractions from MPLC containing compound S87-3

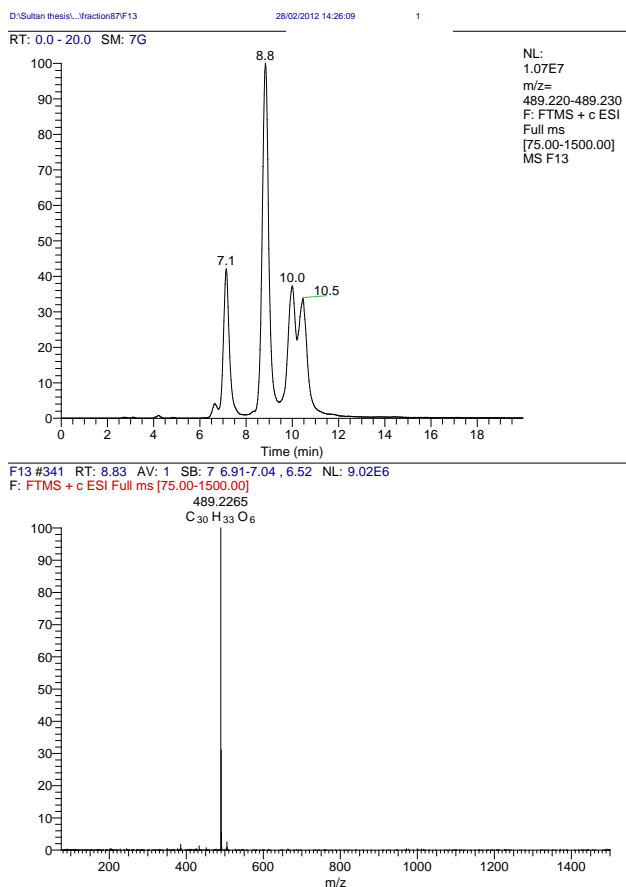


Figure 5.7: Extracted ion chromatogram and mass spectrum for S87-12 which is the 12th most abundant compound by response in S87 when analysed by reversed phase LC-MS in positive ion mode.

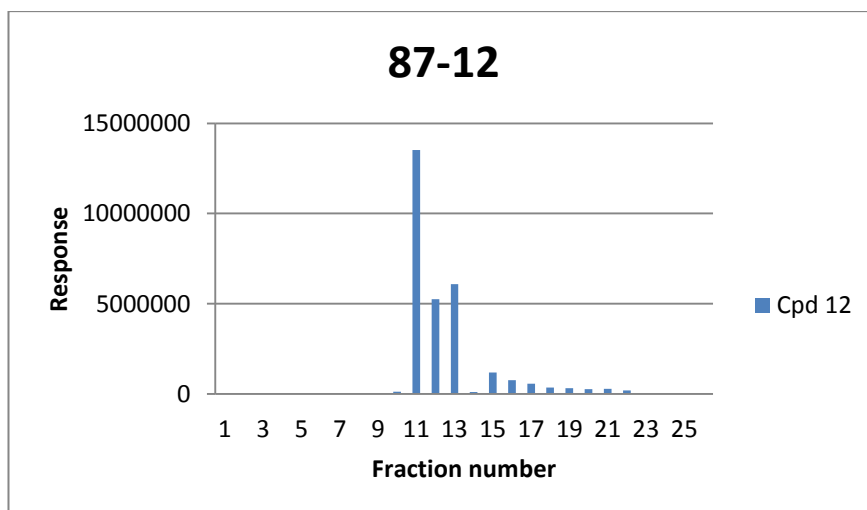


Figure 5.8: Fractions from MPLC containing compound S87-12

5.2 Further Fractionation of Sample S87

Figure 5.9 shows the proton NMR spectrum of crude S87 extract and it is possible to see from this that although it contains proton signals in the aromatic region these are much less than the large aliphatic signals.

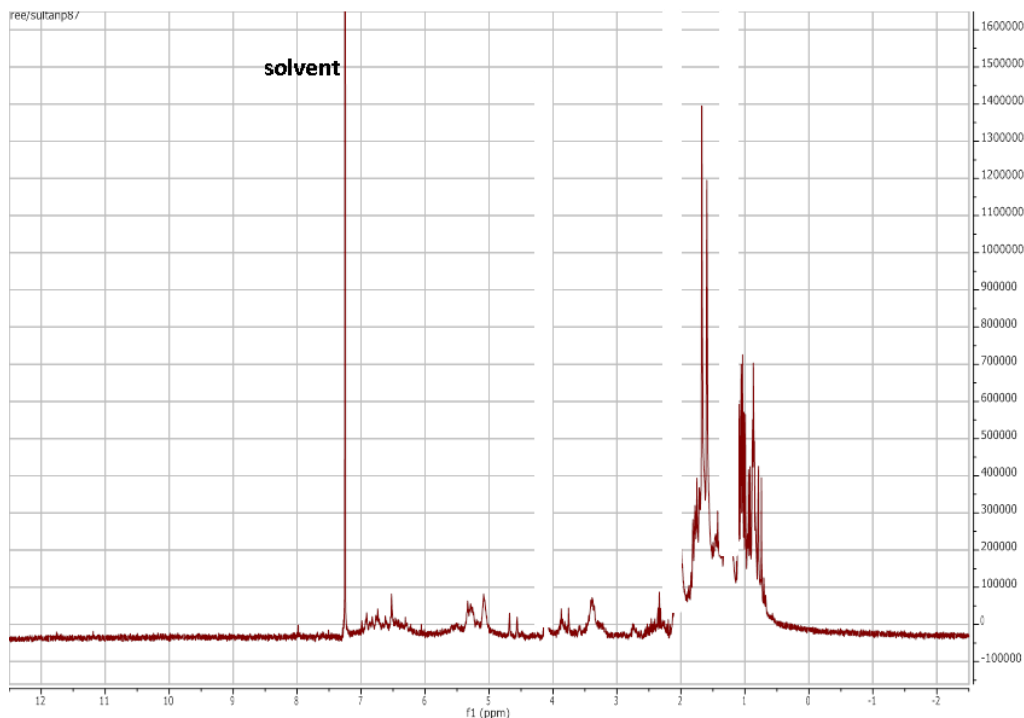


Figure 5.9: ¹H NMR spectrum (400 MHz, in CDCl₃) of crude S87 showing mainly aliphatic protons.

5.3 Identification and isolation of bioactive compounds of Ghanaian propolis

Bioassay guided fractionation yielded two pure stilbene compounds. These were isolated from ethyl acetate extracts of Ghanaian Propolis by a combination of medium pressure liquid chromatography on silica gel followed by high pressure liquid chromatography on a semi-preparative scale to isolate F9-1, whereas the Grace Reveleris® iES Flash Chromatography alone yielded F13-11.

5.4 Semi-preparative high pressure liquid chromatography

Semi-preparative HPLC is a good tool for isolation and collection of individual compounds on a small scale and it led to a purified stilbene (87F9-1). An analytical scale silica column was initially used to determine the most appropriate run conditions that would give best resolution and peak shape of the target compound.

After this, the method was transferred on to the semi preparative column in order to purify the biologically active compounds as discussed in methods chapter (2.5.3).

A semi preparative silica gel HPLC column was chosen for further purification of fraction 9 (Table 5-2, 330.9 mg) and used isocratic elution with ethyl acetate: hexane (10:9) which yielded compound 1 (4.5 mg) at a retention time of 36.25 min (in Figure 5.10) and coded as 87F9-1.

This was the purest fraction and it showed moderate anti-trypanosome activity (Table 5-4) and five semi-preparative runs were performed to yield sufficient amount of material enough for further analysis.

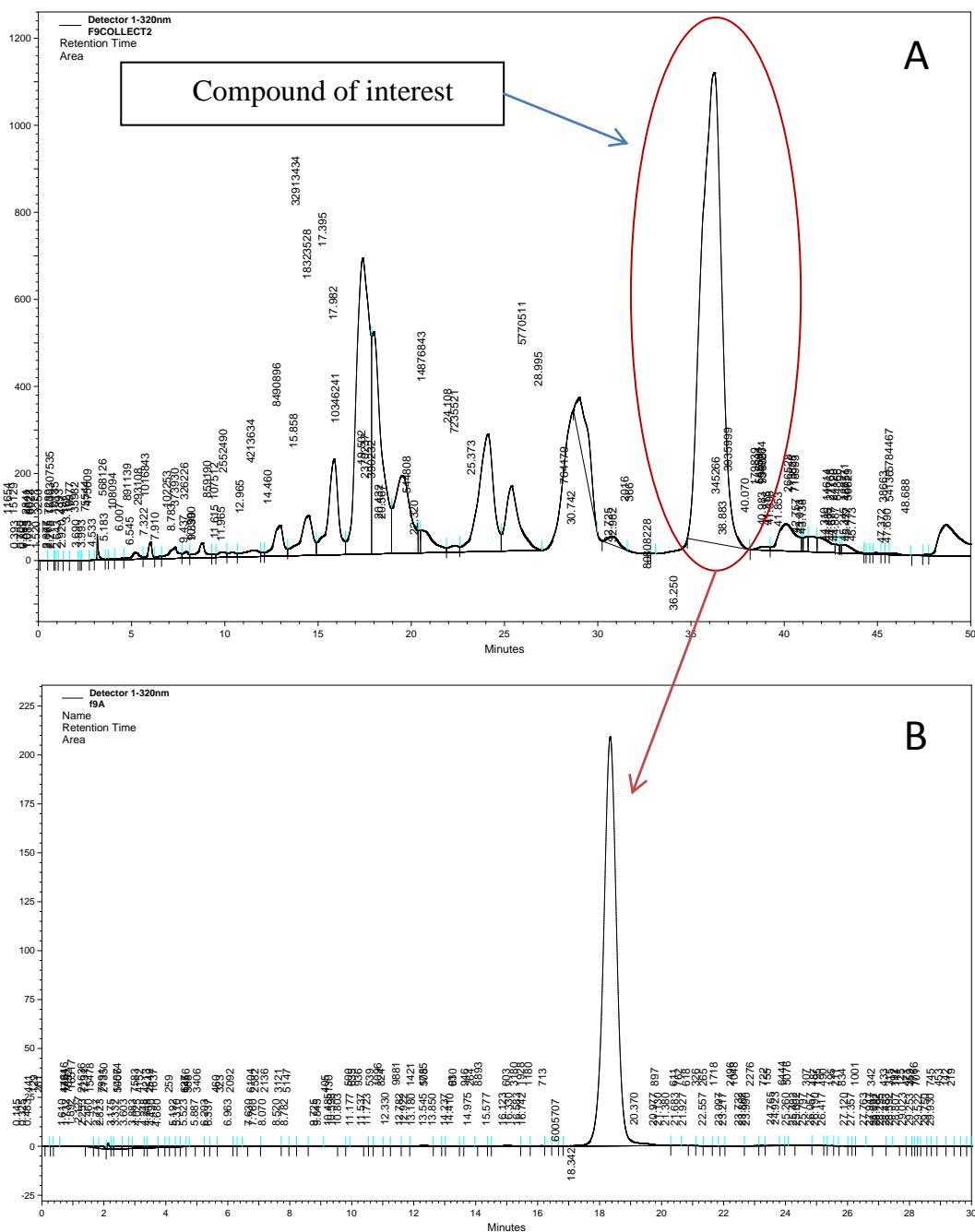


Figure 5.10: Semi-prep (A) and Analytical HPLC (B) column chromatograms for 87F9-1 Conditions as in section 2.5.3.

5.5 Flash chromatography the Grace Reveleris®

It can be seen in the case of fraction 13 (Figure 5-11) in comparison with crude S87-1 (Figure 5-9) that there was considerable enrichment of the signals for aromatic protons.

Fraction 13 was not sufficiently pure and so it was subjected to further flash chromatography in order to further purify it. This was done by using a Grace Reveleris® iES Flash Chromatography System equipped with variable length UV detectors at 280 nm and 210 nm wavelengths and ELSD detector that can detect non-chromophoric and chromophoric compounds in complex extracts during a single run.

A sample of fraction 13 (2.7 g) was first dissolved in a small amount of ethyl acetate and mixed with celite. The dried extracts were fractionated over silica gel with a gradient solvent system (hexane and ethyl acetate) on Grace- MPLC as described in section 2.5.2.2. Thirteen fractions were obtained in total and the compound of interest (compound 2, 55mg) was found in fraction 11 which eluted at a retention time of 59.30 min. It was examined by LC-MS and HPLC-ELSD (chromatogram is shown in Figure 5.12) and coded as (F13 -11).

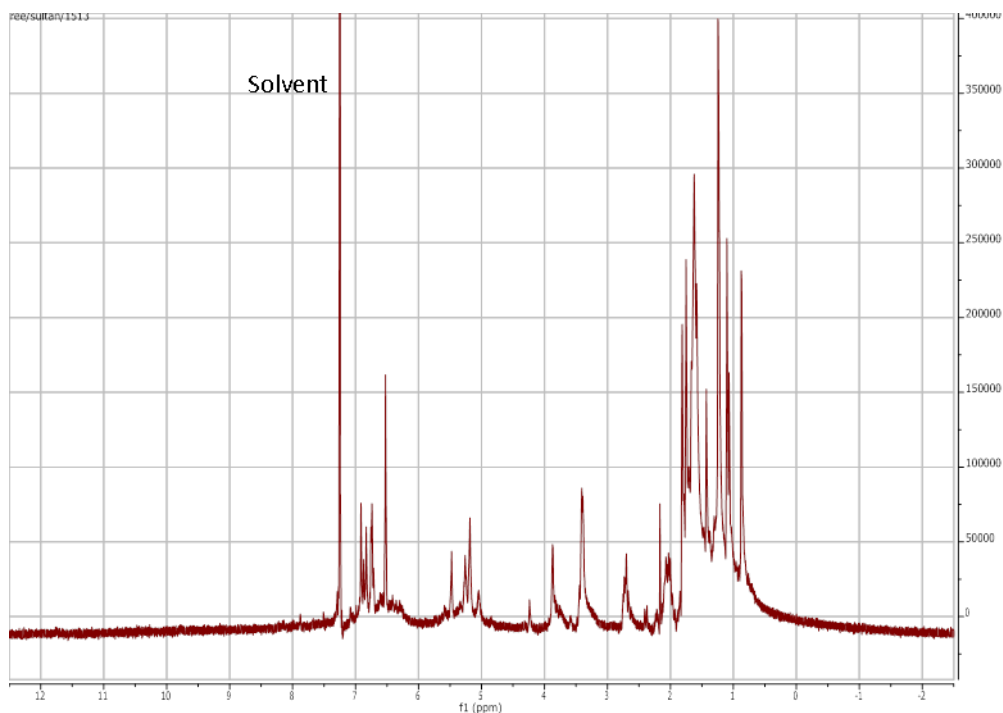


Figure 5.11: ¹H NMR spectrum (400 MHz, in CDCl₃) fraction 13 from MPLC separation of S87.

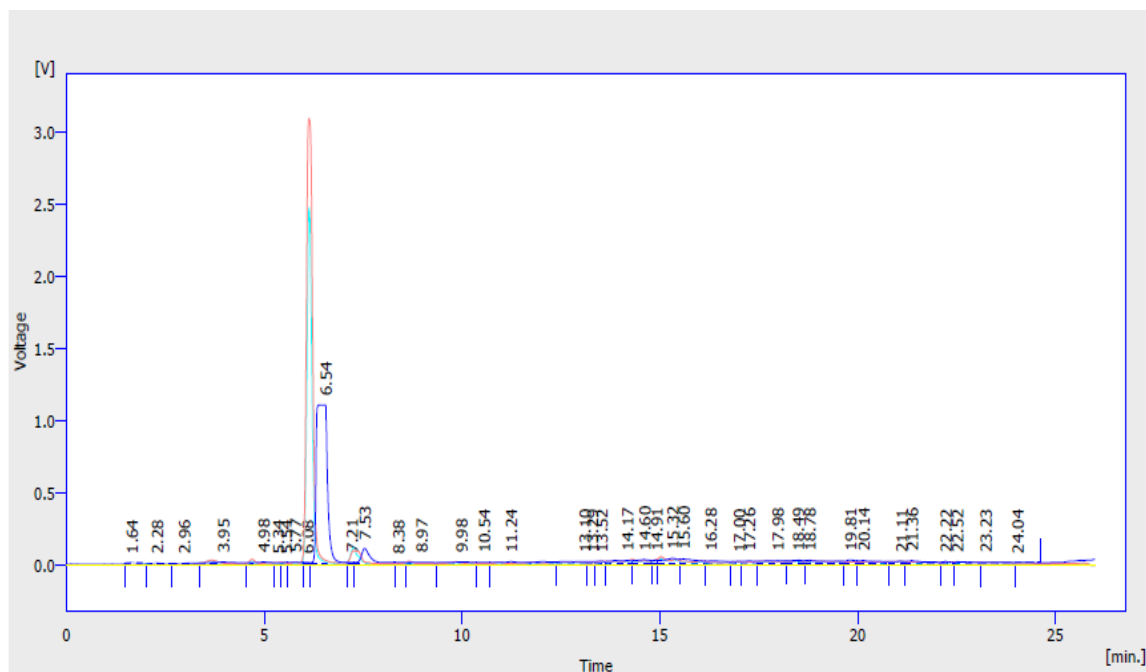


Figure 5.12: LC-UV-ELSD chromatogram of fraction F13-11 purified from fraction 13 by MPLC (Conditions as in section 2.5.2.2)

5.6 Characterization of new prenylated stilbenes from Ghanaian propolis

Two new prenylated stilbenes (F9-1, F13-11, Figure 5-13) were isolated from Ghanaian propolis extracts using Flash chromatography including MPLC, Grace Reveleris® iES and semi-preparative HPLC. Elemental composition for the compounds was determined by HR-ESI-MS, 1D and 2D NMR. The NMR data are summarized in Table 5.3.

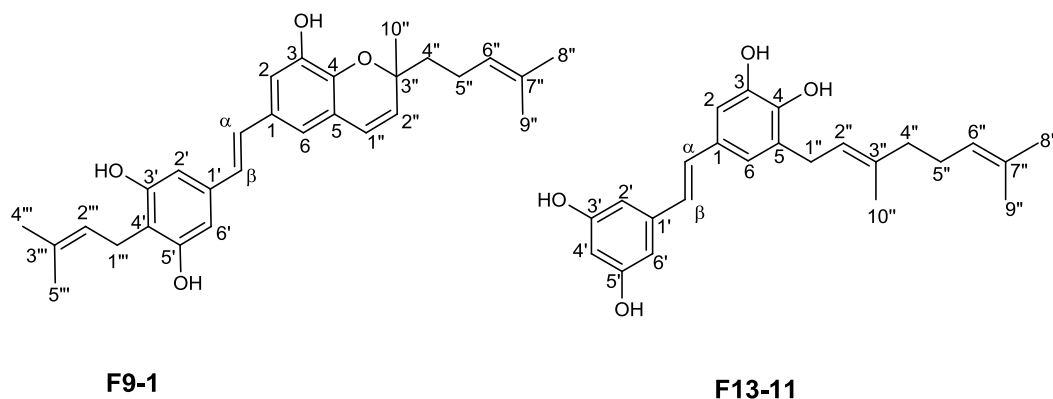


Figure 5.13: New prenylated stilbenes

Table 5.3: ^1H NMR (400 MHz) and ^{13}C NMR (100 MHz) data of new prenylated compounds F9-1 and F13-11

Position	F9-1*			F13-11*		
	δ_{H} , mult., J	δ_{C}	^{13}C type	δ_{H} , mult., J	δ_{C}	^{13}C type
1		130.5	C		128.6	C
2	6.94, d, 1.7	113.1	CH	6.95, d, 1.8	110.5	CH
3		145.0	C		140.0	C
3-OH	5.42, s			7.39, s		
4		139.9	C		143.5	C
4-OH				8.62, s		
5		121.3	C		119.6	C
6	6.68, d, 1.7	116.9	CH	6.82, d, 1.8	120.0	CH
α	6.86, d, 16.2	128.7	CH	6.91, d, 16.3	129.3	CH
β	6.76, d, 16.2	126.5	CH	6.76, d, 16.3	126.3	CH
1'		137.9	C		125.6	C
2'	6.53, br s	106.7	CH	6.49, br d, 2.0	104.9	CH
3'		155.7	C		159.3	C
3'-OH	5.35, s			8.37, s		
4'		113.2	C	6.24, br t, 2.0	101.1	CH
5'		155.7	C		159.3	C
5'-OH	5.35, s			8.37, s		
6'	6.53, br s	106.7	CH	6.49, br d, 2.0	104.9	CH
1''	6.34, d, 10.0	123.1	CH	3.34, d, 7.2	28.7	CH ₂
2''	5.59, d, 10.0	130.3	CH	5.36, t, 7.2	122.5	CH
3''		80.8	C		135.4	C
4''	1.74, m	41.6	CH ₂	2.02, m	40.1	CH ₂
5''	2.06, m	31.0	CH ₂	2.05, m	29.7	CH ₂
6''	5.07, br t, 6.3	124.2	CH	5.08, m	124.7	CH
7''		132.6	C		130.6	C
8''	1.65, s	26.1	CH ₃	1.74, s	15.9	CH ₃
9''	1.57, s	18.1	CH ₃	1.57, s	17.5	CH ₃
10''	1.41, s	27.0	CH ₃	1.63, s	25.6	CH ₃

1'''	3.41, br d, 7.0	22.9	CH ₂
2'''	5.26, br t, 7.0	122.0	CH
3'''		135.2	C
4'''	1.75 s	26.2	CH ₃
5'''	1.81 s	18.3	CH ₃

*In CDCl₃ and Acetone-d₆ respectively.

5.6.1 Structure of Ghana propolis stilbine 1 (F9-1)

Compound F9-1 had a molecular formula of C₂₉H₃₅O₄ with a protonated molecular ion [M+H]⁺ at *m/z* 447.2526 (calcd. 447.2530) (Figure 5.14), UV absorbance maxima at λ 244, 289, and 328 nm; [α]_D +2.78 (c. 0.10, CHCl₃).

The NMR data for compound F9-1 was comparable to that of the chalcone poinsettifolin B (Figure 5-18) (Tsopmo et al., 1998) previously isolated from the leaves of *Dorstenia poinsettifolia* var. *anyusta* Engl. (Moraceae), a scrambling herb indigenous to the humid forests of Cameroon. Compound F9-1 differed from poinsettifolin B by the absence of a keto group which occurred at δ_C 191.7. A further difference was that the unsubstituted methine protons in the resorcinol moiety of 1 were *meta*-coupled, whereas; in poinsettifolin B, these protons were *ortho*-coupled. Thus, due to a symmetrical substitution pattern on the resorcinol ring, H-2' and H-6' as well as OH-3' and OH-6' protons were found to be equivalent yielding singlets at δ_H 6.53 and 5.35, respectively. Two *trans*-olefinic protons assigned as α and β protons were observed at δ_H 6.86 and 6.76 (*J* = 16.2 Hz) (Figure 5.15), respectively.

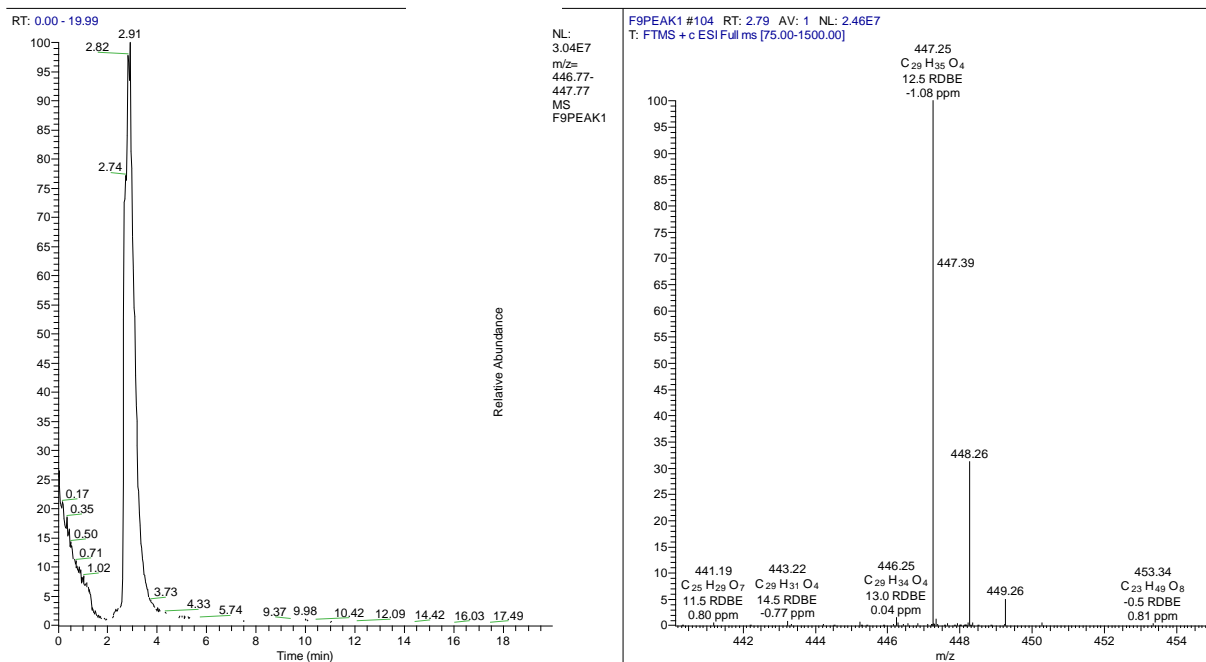


Figure 5.14: LC-MS trace and ESI mass spectrum of F9-1

The ¹H NMR spectra of F9-1 (Figure 5.15) displayed the presence of an asymmetrical stilbene skeleton (δ 6.53 ppm, 2H, br s, H-2' and H-6') with both an AA' benzene ring system and an AB benzene ring system (δ 6.94 ppm, 1H, d, H-2 and δ 6.68 ppm, 1H, d, H-6). Also as presented in the ¹H NMR spectrum shown in figure 5.15, F9-1 showed four aromatic proton 6.94 ppm, H-2 (d, $J=1.7$) 1H, δ 6.68 ppm H-6 (d, $J=1.7$) 1H, 6.53 ppm, 2H, br s H-2' and H-6'. Two methine protons assigned as α and β protons were observed at δ_H 6.86 and 6.76 ($J=16.2$ Hz). In addition there was a signal for a prenyl substituent (H-4'' 1.74, m; H-5'' 2.06, m; H-6'', 5.07, br t, $J=6.3$; H-8'', 1.65, s; H-9'', 1.57, s; H-10'', 1.41, s) and another prenyl group was located on B- ring at C-4' and assigned as H-1''', 3.41, br d, 7.0; H-2''', 5.26, br t, 7.0; H-4''', 1.75 s; H-5''', 1.81 s.

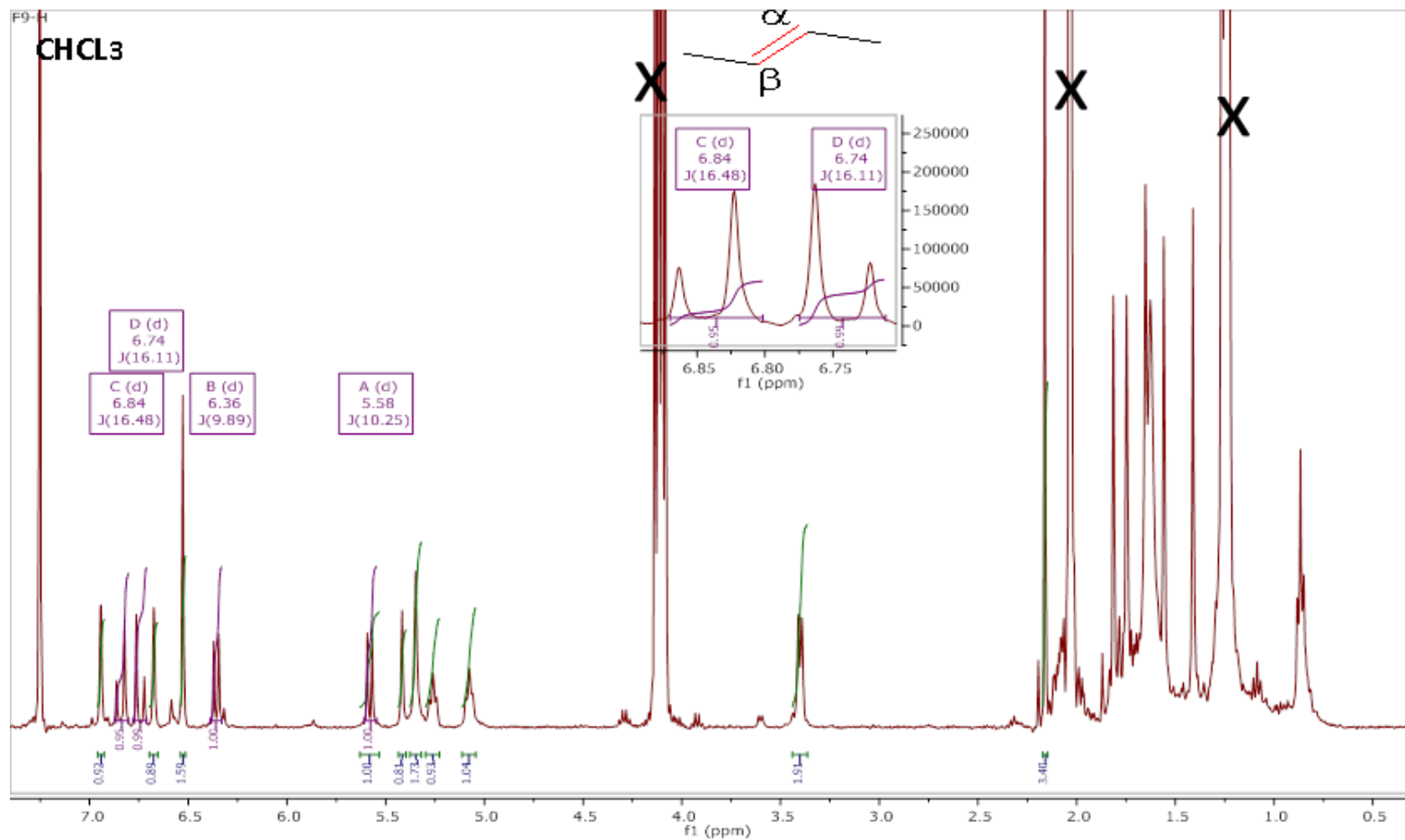


Figure 5.15: ^1H NMR of F9-1 (400 MHz, CDCl_3). The peaks denoted by **X** represent signals from ethyl acetate.

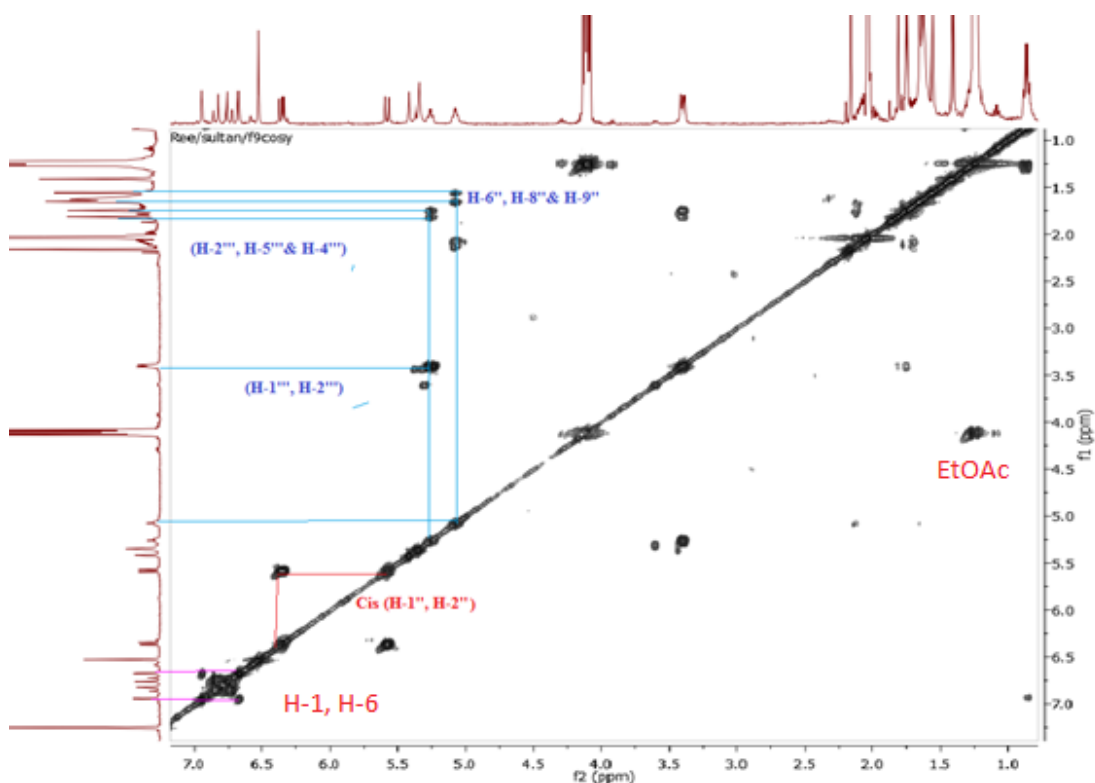


Figure 5.16: The correlation of the protons in a COSY spectrum of F9-1 labelled in blue prenyl substituents and pink (aromatic system).

From the COSY spectrum of F9-1, two methine protons at δ_{H} 5.07 and δ_{H} 5.26 ppm H-6', H-2''' respectively were clearly coupling to two $-\text{CH}_3$ groups each (at δ_{H} 1.65, 1.57 and 1.81, 1.75) and were also coupling to a doublet $-\text{CH}_2$ at 3.39 ppm and multiplet at 2.06 ppm that belonged to the prenyl groups that were located on each ring. Also showed the two doublets at δ_{H} 5.59 and 6.34 ppm which were deshielded and were coupling to each other with $J=10\text{Hz}$ thus this indicated cis/trans coupling since H-1'' and H-2'' were cis to each other. The second spin system clearly evident in the COSY was assigned to the olefinic region of the stilbene, the doublets at δ_{H} 6.86 and 6.76. The aromatic protons assigned to H-2 and H-6 showed coupling to each other. The COSY correlations are presented in Figure 5.16.

In the HMBC spectrum (Figure 5.17) the β -proton gave strong HMBC correlations to C-1', C-2' and 6' of the resorcinol ring while the α -proton correlated to C-2, C-6 of the chromenol moiety. These key HMBC correlations between the *trans*-olefinic

protons and the carbons of the resorcinol unit confirmed the absence of the keto group as illustrated in Figure 5.19.

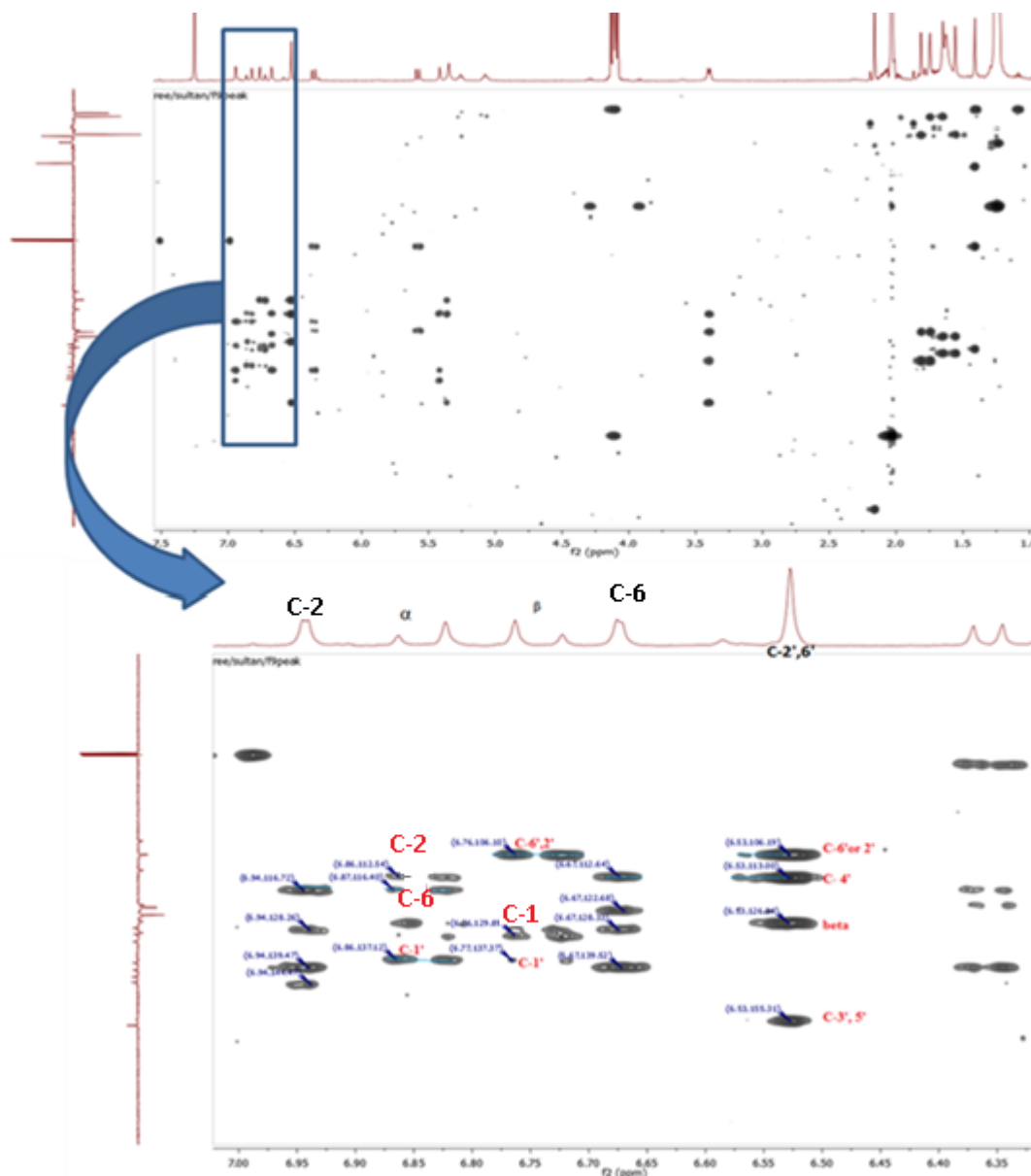


Figure 5.17: Expansion of the HMBC of F9-1 highlighted and labelled the correlations between olefinic protons and the resorcinol ring and another different correlation which is different from that of the chalcone poinsettifolin B.

Accordingly, the structure of compound 1 was elucidated as (*E*)-5-(2-(8-hydroxy-2-methyl-2-(4-methylpent-3-en-1-yl)-2*H*-chromen-6-yl) vinyl)-2-(3-methylbut-2-en-1-yl) benzene-1, 3-diol which was derived from a geranyl-substituted stilbene.

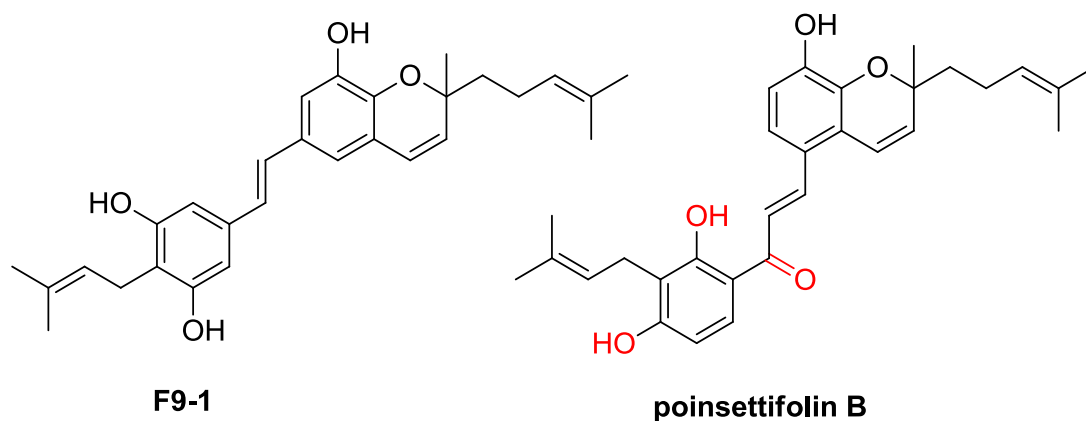


Figure 5.18: Prenylated stilbenes 1 (87F9-1)1 and poinsettifolin B with highlighting of the different groups

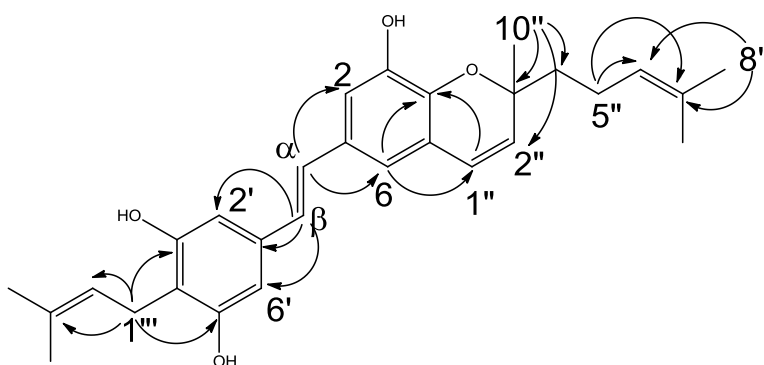


Figure 5.19: Key HMBC correlations (H → C) for compound F9-1

5.6.2 Structure of Ghana propolis stilbene 2 (F13-11)

Compound 2 (F13-11) is shown in Figure 5.25. It displayed a protonated molecular ion $[M+H]$ at m/z 381.2061 (calcd. 381.2060 for $C_{24}H_{29}O_4$) by HRESI-MS. It had UV absorbance maxima at λ 231 and 325 nm.

This suggested that 2 diverged from compound 1 by the absence of an isoprene unit and two protons. 1H , ^{13}C , and DEPT NMR data are presented in Table 5.3. Devoid of an isoprene unit on the resorcinol moiety of 2, the NMR data of 2 resulted in a spectrum almost similar to that of mappain [see Figure 5-25] (van der Kaaden et al., 2001) a cytotoxic prenylated stilbene earlier isolated from the leaves of a Hawaiian species *Macaranga mappia* (Euphorbiaceae). However, the NMR data of 2 were obtained in $(CD_3)_2CO$ due to the solubility problems encountered with $DMSO-d_6$ as well as in $CDCl_3$, the solvents used for mappain in the literature.

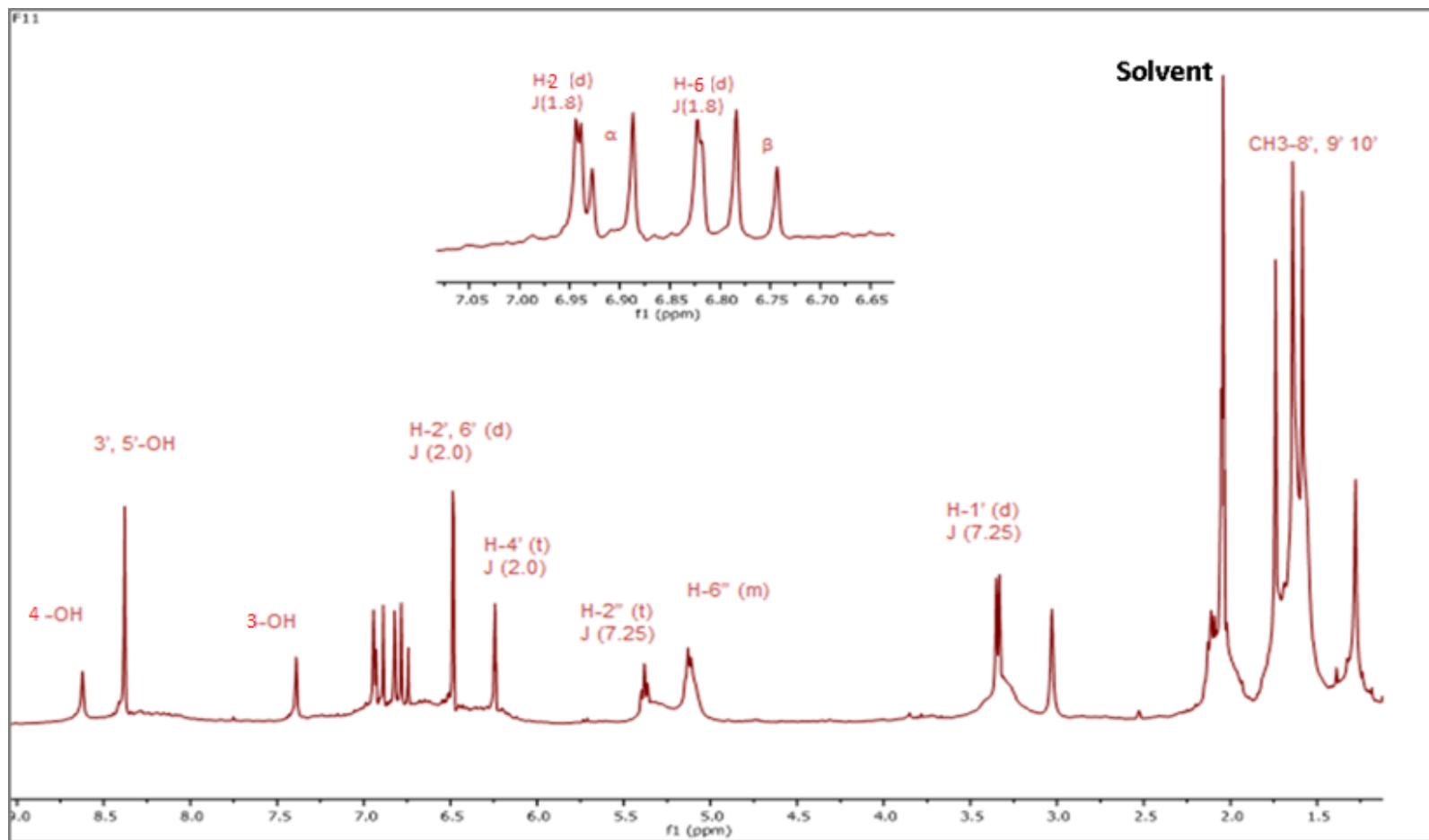


Figure 5.20: ^1H NMR of F13-11 (400 MHz, Acetone-d_6).

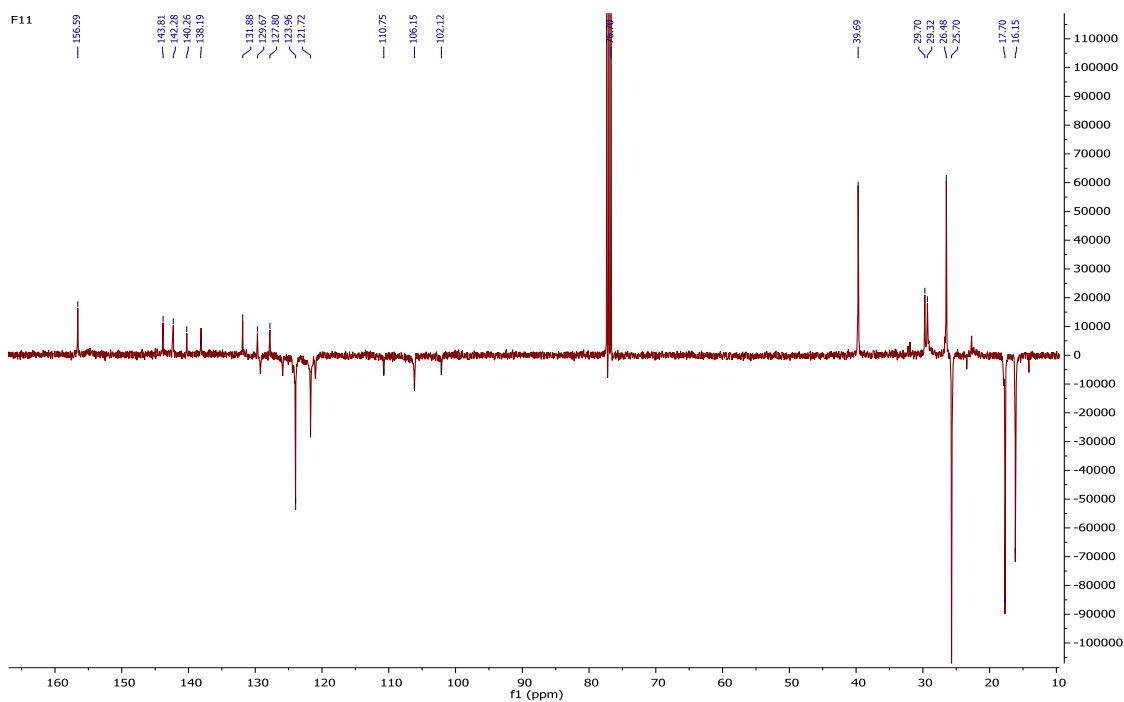


Figure 5.21: The DEPT ^{13}C NMR spectrum F13-11.

G:\19&11 UVf11

/2013 14:47:47

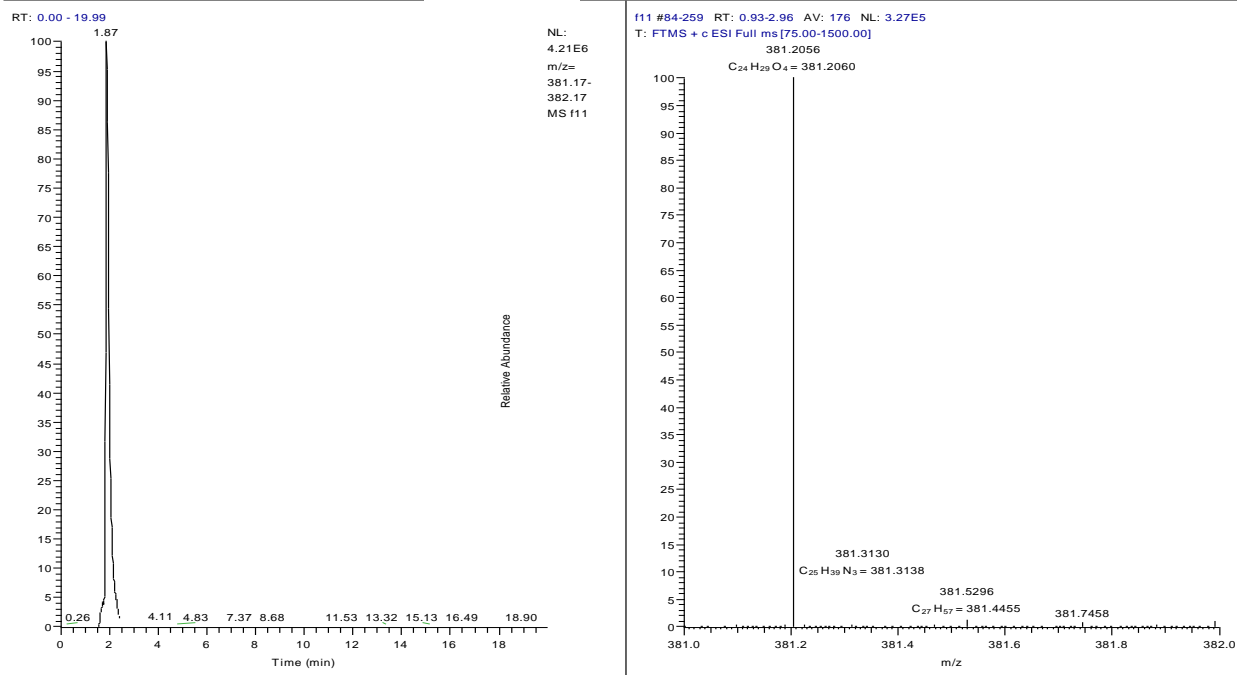


Figure 5.22: LC-MS trace and ESI mass spectrum of F13-11.

The major difference between the two isolated congeners 1 (F9-1) and 2 (F13-11), besides the absence of the isoprene unit on the resorcinol moiety as evidenced by the

additional broad triplet at δ_H 6.24 found in 1, was the disappearance of a 10 Hz coupling giving rise to methine doublets in 2 for H-1'' and H-2'' at δ_H 6.34 and 5.59, respectively. The 10 Hz doublets were replaced by a 7.2 Hz doublet-triplet coupling pair at δ_H 3.34 (d) and 5.36 (t), respectively for a methylene-methine (CH_2-CH) system. A further variation is the additional phenolic hydroxyl (OH) singlet at δ_H 8.62 at C-4. For compound 2, the methylene proton for H-1'' gave an HMBC correlation with the hydroxyl bound carbon at δ_C 143.5 for C-3 which was deshielded when compared to that in compound 1. When linking the trans-olefinic protons and the carbons of *meta*-coupled methine protons within the 6.0-7.0 ppm region, compound 2 yielded similar HMBC correlations to 1, as exhibited in Figure 5.23. This evidence suggested the opening of the chromenol ring in 1 yielding a catechol system in 2. A similar phenomenon has been observed for related geranyl stilbene derivatives known as pawhuskins B and C isolated from *Dalea purpurea* Vent. (Fabaceae) collected from a tall grass prairie preserve near Pawhuska, Oklahoma (Belofsky et al., 2004).

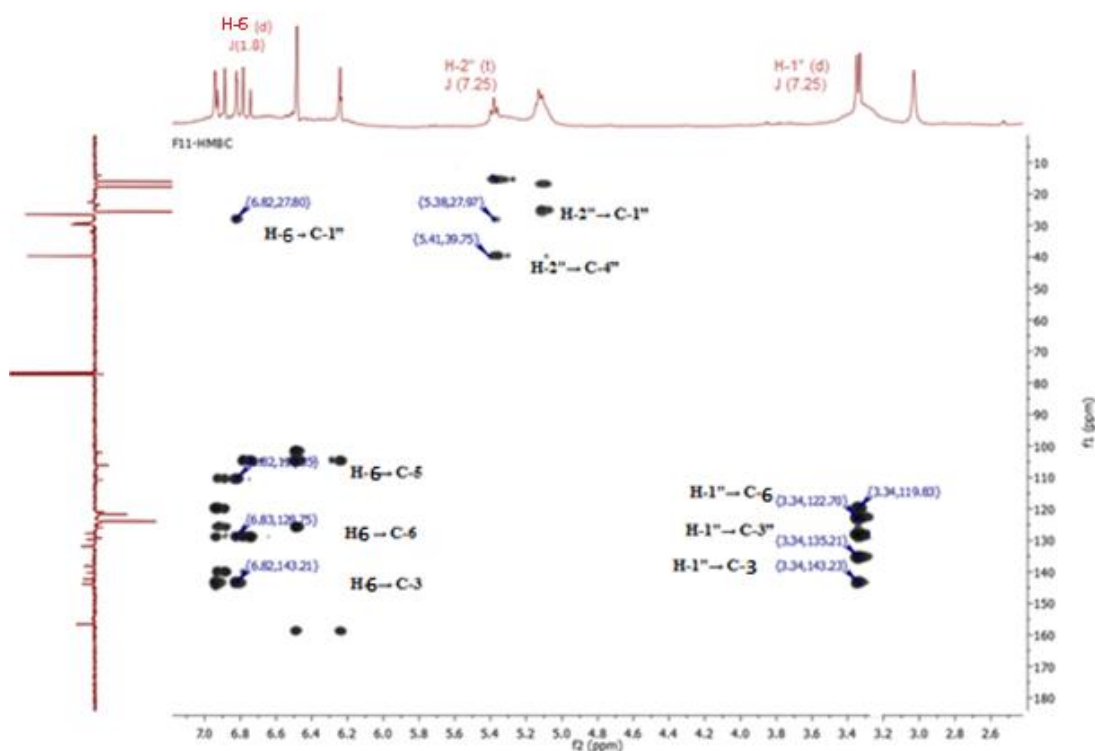


Figure 5.23: Expansion of the HMBC of F13-11. The labelled correlations show how the location of the signals for the open chromenol ring differs from those of F9-1.

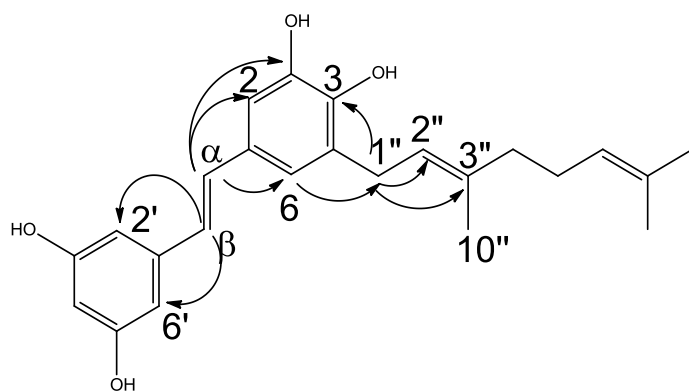


Figure 5.24: Key HMBC correlations (H → C) for compounds F13-11.

Overall, the Compound 2 (F13-11) was identified as 5-((E)-3, 5-dihydroxystyryl)-3-((E)-3, 7-dimethylocta-2, 6-dien-1-yl) benzene-1, 2-diol or the 4'-deprenylated congener of mappain which arises from the geranylation of tetrahydroxy stilbene.

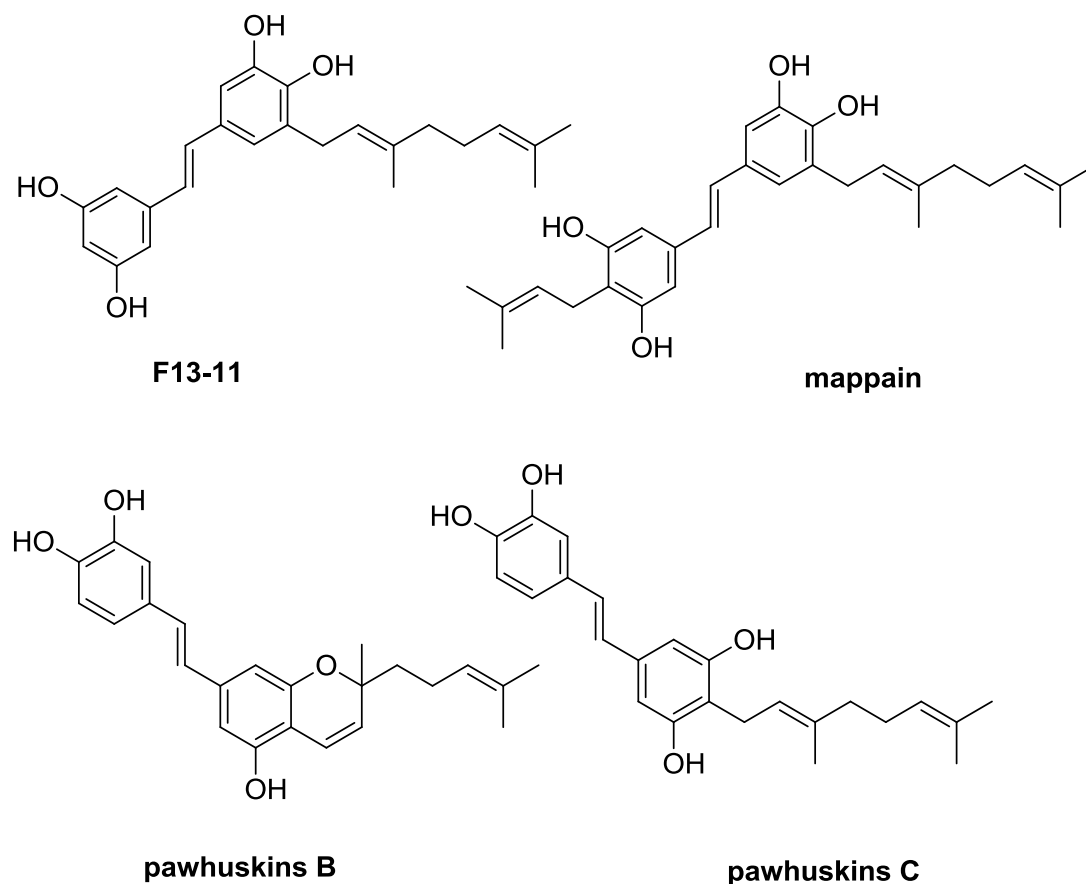


Figure 5.25: geranylated stilbenes f13-11 (2) and some Related Compounds.

5.7 Biological activities of new stilbenes

5.7.1 Anti-trypanosomal activity

The preliminary screening of 19 fractions (Table 5.2), including crude extracts of the S87 sample, was carried out in order to determine their biological activity *in vitro* against *T. brucei brucei* using the Alamar Blue™ 96-well microplate assay as explained in section (2.10.1). Some of these fractions (F9 and F13) which showed high to moderate potency were chosen to isolate the bioactive components. Two pure isolated compounds (F9-1, F13-11) were tested against *T. brucei brucei* to determine their minimum inhibitory concentrations which showed moderate potency as shown in Table 5.4. These MIC values were compared to those of hyperforin (Figure 3.3 Chapter 3) which also gave a moderate activity at 5.82 μM and suramin as a positive control with an MIC of 0.125 μM .

Table 5.4: MIC of the stilbenes isolated from Ghanian propolis along with positive controls against *T. brucei brucei*.

Compound	MIC (μM)
F9-1	6.73
F13-11	16.45
Hyperforin	5.82
Suramin ^[a]	0.125

[a] positive control

5.8 Discussion

Of all the MPLC fractions obtained from the ethyl acetate extract of sample S87, Fraction 9 showed the highest activity against the parasite *T. b. brucei* from screening tests. Further purification of this fraction led to the isolation of a prenylated stilbene as the main active component. Another stilbene with a geranyl substituent was obtained from Fraction 13 of the same extract. These compounds F9-1 (1) and F13-11 (2) were found to be moderately active against *T. b. brucei* with MICs of 6.73 μ M and 16.54 μ M respectively, using suramin (MIC 0.125 μ M) as a positive control in an *in vitro* anti-trypanosomal assay using Alamar Blue method.

Prenylated stilbenes are formed by prenylation of a tetrahydroxy stilbene while geranylation leads to formation of geranyl stilbenes. So far stilbenoids have rarely been isolated from propolis; however, few stilbenes have been identified as components. For example a stilbene congener has been reported from propolis of Western Australia by Ghisalberti (Ghisalberti et al., 1978); while recently, two geranyl stilbenes were described from Kenyan propolis (Petrova et al., 2010).

Stilbenes are compounds composed of two benzene rings connected by an exocyclic double bond. Despite being simple at the core, stilbene derivatives are considered to be of high complexity when produced as secondary metabolites (Yoder, 2005). Also, stilbene compounds are not highly predominant as natural products. However a variety of notable stilbene derivatives have been isolated from various plants such as *Macaranga alnifolia* (Yoder, 2005).

It is possible that the potential pharmacological value of propolis is the activity associated with a mixture of prenylated/geranylated stilbenes. However, the prenylated stilbene was found to have a higher potency than the geranylated one. So, the cyclization of prenylated substituents might also play a vital role in the biological activity of these compounds. Mappain is the most closely related compound to the geranylated stilbene (2), and it was reported to be cytotoxic to ovarian cancer cells with an IC₅₀ of 1.3 μ M (van der Kaaden et al., 2001).

CHAPTER 6:
METABOLOMIC PROFILING OF THE EFFECTS
OF PRENYLATED STILBENES ON *T. BRUCEI*

6 METABOLOMIC PROFILING OF THE EFFECTS PRENYLATED STILBENES ON *T. BRUCEI*

6.1 Introduction

It was the intention to carry out more extensive metabolomic profiling of anti-trypanosomal compounds from propolis. In the end there was only a chance to carry out some preliminary work. However, the results described below are sufficiently encouraging for further studies of this nature to be carried out in the future.

6.2 Materials and Methods

6.2.1 Chemicals and solvents

HPLC grade chloroform, methanol and acetonitrile were obtained from Fisher Scientific, UK. Ammonium carbonate, ammonia and all other compounds were purchased from Sigma-Aldrich, Dorset, UK. HPLC grade water was produced by a Direct-Q 3 Ultrapure Water System from Millipore, UK.

6.2.2 Cell extraction

Cultures of BSF *T. brucei brucei* S427 wild type were used at 4×10^7 cells/ml. They were incubated with different concentrations of compound F13-11 starting at the MIC (16.45 μ M) and higher than it. A concentration of 20 μ g/ml in DMSO was selected due to the fact that it clearly demonstrated an inhibitory effect on growth of *T. b. brucei* cells, and the growth curve was steady for 24 h. Cell cultures were rapidly cooled to 4°C by submersion of the flask in a dry ice/ethanol bath, and kept at 4°C for all subsequent steps. The cold cell culture was centrifuged at 1,000 RCF for 10 minutes, supernatant removed, and the pellet washed in 30 mL HEPES-free HMI-9. The washed cells were then centrifuged and the supernatant completely removed. Cell lysis and protein denaturation was achieved by addition of 200 μ L of cold chloroform/methanol/water (ratio 1:3:1), followed by vigorous mixing for 1 hour at 4°C. Each of the extract mixtures was centrifuged at 16,000 RCF for two minutes at a temperature of 4°C. The supernatant obtained was collected and stored frozen at -80°C until further analysis. This procedure was conducted in Parasitology lab of

Dr.Harry de Koning at the University of Glasgow in collaboration with Abdusalam Alkhaldi.

6.2.3 Mass spectrometry

LC-MS was carried out on an Accela 600 HPLC system combined with an Orbitrap Exactive instrument (Thermo Fisher Scientific, Germany) set at 30,000 resolution. A volume of sample (10 μ l) was injected onto a ZIC-pHILIC (150 \times 4.6mm, 5 μ m) HiChrom, Reading UK. The LC-MS system was run in binary gradient mode with the following conditions: A 20 mM ammonium carbonate pH 9.2 B Acetonitrile; 0 min 80% B 30 min 20% B, 36 min 20% B, 37 min 80% B, 46 min. 80% B. The ESI interface was operated in positive and negative ion switching mode, with +4.0 kV of spray voltage for positive mode and -3.5 kV for negative mode. The temperature of the ion transfer capillary was 270 $^{\circ}$ C and sheath and auxiliary gas was set at 57 and 17 arbitrary units, respectively. The full scan range of both positive and negative modes was set at 75 to 1200 m/z with AGC target and resolution as balanced and high (1E6 and 50,000), respectively. Before the analysis, mass calibration was performed for both ESI modes using the standard Thermo Calmix solution with some additional compounds to cover the low mass range, where the signals of 83.0604 m/z (2xACN+H) and 91.0037 m/z (2 x formate-H) were selected as lock masses for positive and negative mode, respectively. The data were recorded using the Xcalibur 2.1.0 software package (Thermo Fisher Scientific). MS² spectra were obtained using the same conditions listed for the Exactive on an LTQ Orbitrap instrument at 35 V.

Data obtained from Xcalibur software were exported into Sieve Software 1.3 (Thermo Fisher Co.) where extracted ion chromatograms were aligned in 0.02 amu windows. The features obtained in Sieve were then exported into an Excel based macro for searching against a data base of accurate masses taken from KEGG, Lipidmaps, Human Metabolome database and Metlin.

6.3 Metabolomics data processing

6.3.1 The Effect of compound F13-11 on the Metabolome of T. b. brucei

Metabolomic profiling can be used in order to get an understanding of mechanism of action of a drug. In any form of chemotherapy the more selective the chemotherapy

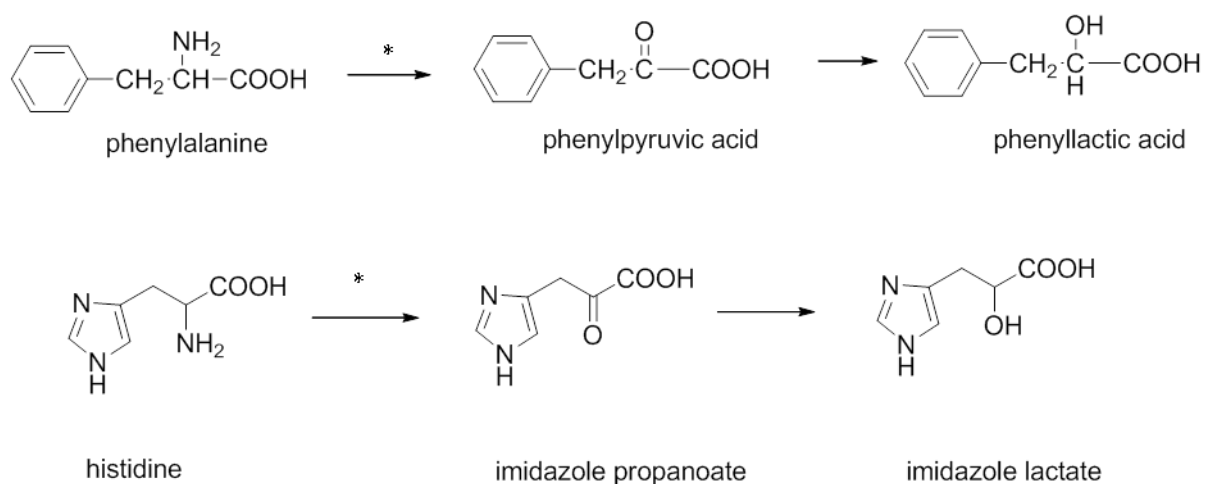
is for the target the less the host is going to be affected. In previous work the selectivity of eflornithine in treating *T. b. brucei* was explored via metabolomic profiling (Vincent et al., 2010) thus it was of interest to see if fraction 11 which contained mainly compound F13-11 had any selective effects on the metabolism of *T. b. brucei*. Treated *T. brucei* and controls were extracted at 0 h, 4 h and 24 h. Data extraction and data base searching revealed around 600 metabolites which were putatively identified by their accurate masses. In addition many of these compounds matched the retention times of standard compounds which have been run in previous studies (Zhang et al., 2014). The major differences in metabolism were observed after 24 h with very little perturbation of the metabolome up to 4 h. While many compounds were unaltered by treatment there are certain interesting metabolic themes running through the effect of F13-F11 on *T. b. brucei* metabolome. There is a clear effect on the metabolism of aromatic amino acids. For unknown reasons *T. b. brucei* produce large amounts of deamidated amino acids when grown in culture (Li et al., 2011, Creek et al., 2012). Most of the amino acids were deamidated and large amounts of the corresponding ketoacids and hydroxy acids are produced. Thus for example phenylalanine is deamidated to produce phenylpyruvic acid and phenyl lactic acid or histidine similarly produces imidazole propanoate and imidazole lactate (Figure 6.1). In the cases of valine, leucine, histidine, phenylalanine and tyrosine there appears to inhibition of the conversion of the amino acid to the keto acid with a corresponding rise in the amino acid. The most marked effect is on phenylalanine levels which are more than doubled in the treated cells. The only amino acid which is deamidated but which is not affected is arginine. There are a number of metabolites involved in DNA metabolism which are affected by treatment and the most marked effect is on sedoheptulose phosphate which is involved in the pentose phosphate pathway which provides the ribose group for incorporation into DNA bases. Sedoheptulose phosphate is elevated ten times in the treated cells. Figure 6.2 shows the extracted ion traces for sedoheptulose phosphate in treated *T. b. brucei* in comparison with untreated *T. b. brucei*. The elevation of metabolites in this pathway is not consistent but both cytidine and aspartic acid are involved in the pyrimidine pathway while adenine and xanthosine phosphate are in the purine biosynthesis pathway. Xanthosine phosphate is a precursor of guanosine phosphate. The

conversion of xanthosine phosphate to guanosine phosphate requires addition of an amine group. However, there was no effect of treatment on the levels of guanosine phosphate in *T. b. brucei*. Several metabolites of central carbon metabolism were affected by treatment with fraction F13-11 and most notably the level of pyruvate fell. *T. b. brucei* particularly rely on glycolysis to provide energy since they have a truncated Krebs cycle so that the metabolism of glucose beyond pyruvate is not as complete as in mammalian system (Coustou et al., 2008, Bringaud et al., 2006). This suggests that f13-F11 is inhibiting glycolysis in some way and this might explain the increase in sedoheptulose phosphate where some of the products of glycolysis are being diverted into the pentose phosphate pathway. The most complete effect of the treatment is on lipid metabolism. Choline, glycerol phosphate, choline phosphate and glycerol choline phosphate are all increased by treatment with fraction f13-11. This suggests either that phospholipids are being broken down or that synthesis of phospholipids is being inhibited. The levels of free fatty acids extracted from the samples were not affected by treatment which suggests that the effect may be on the inhibition of phospholipid formation. Many phospholipids are directly affected by the treatment and Table 6.1 shows the more abundant lipids which were altered by treatment. There are several ether lipids which are increased by treatment and some acyl lipids which are decreased. The ether lipids have an ether linkage at the 1-position of the glycerol backbone and means that the fatty acid chain attached to them cannot be removed by hydrolysis. This suggests that the organism is changing its membrane composition in order to reduce the effect of the treatment. The treated samples also contain higher levels of cholesterol sulphate (Figure 6.3). Trypanosomes incorporate cholesterol into their cell membranes and cholesterol sulphate formation could be a way of solubilising cholesterol so that it is removed from the membrane. This again suggests membrane remodelling is occurring. Looking at the structure of the prenyl stilbene which was isolated from fraction f13-11 the prenylated portion of the molecule would be likely to interact with cell membranes. This may be the basis of the toxicity of the molecule. The other metabolic changes observed may be a consequence of the alteration of the membrane structure. For instance the conservation of amino acids may be a consequence of reduced ability of the

trypanosomes to take them up from the growth medium as a consequence of alterations in the membrane structure.

6.3.2 Conclusion

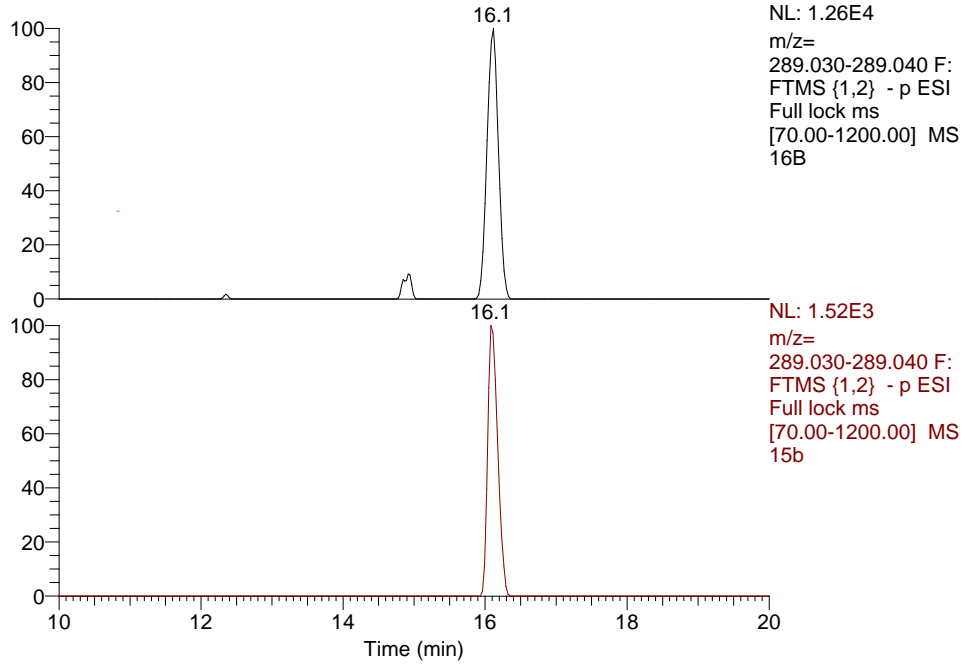
The effects of fraction f13-11 were very interesting since the extract seemed to target particular pathways. It is of interest to observe a selective effect against the target organism since a general toxic effect would be no use since it might affect the host as well as the parasite. The fact that many different samples of propolis have activity against protozoa must be an indication of the fact the bees are also susceptible to this type of parasite.



*Step is inhibited by compound F13-11

Figure 6.1: Deamidation of phenylalanine and histidine when normal grown in culture.

RT: 10.0 - 20.0 SM: 7G



16B #1172 RT: 16.12 AV: 1 SB: 1 6.29, 7.16 NL: 1.69E4
T: FTMS {1,2} - p ESI Full lock ms [70.00-1200.00]

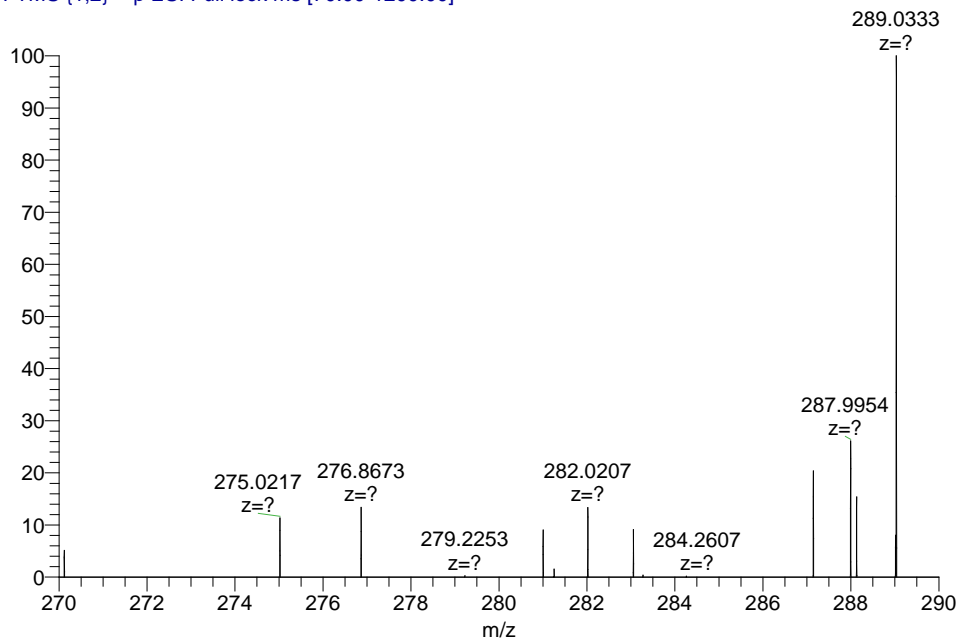


Figure 6.2: Extracted ion trace showing increased levels of sedoheptulose phosphate in *T. b. brucei* treated with fraction 11 for 24 h.

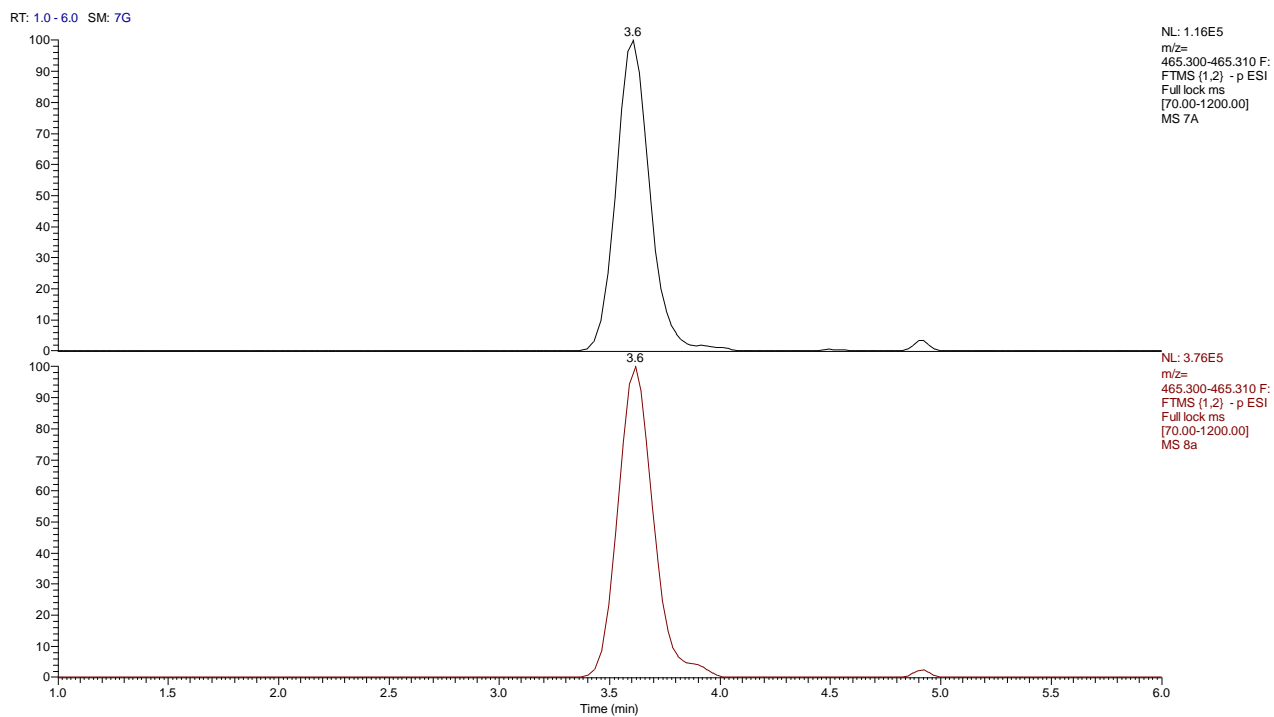


Figure 6.3 Extracted ion trace showing an increase in cholesterol sulphate in *T. b. brucei* treated with fraction 11 for 24 h (lower trace).

Table 6.1: The effects of fraction 11-13 on the metabolic profile of *T.brucei* comparison of 4 h or incubation fraction vs control and 24 h incubation fraction vs control

<i>ID</i>	<i>M/Z</i>	<i>RT</i>	<i>Name</i>	<i>Ratio treated/control</i>			
				At 24 h	P value	At 4 h	P value
Aromatic amino acid metabolism							
9	163.0404	4.8	Phenylpyruvic acid	0.21	2.20E-02	0.68	6.20E-02
19	166.0863	10.0	phenylalanine	2.51	2.10E-06	0.91	4.30E-01
385	165.0559	7.3	L-3-Phenyllactic acid	0.50	3.40E-02	0.68	4.30E-01
37	179.0355	8.1	3-Hydroxyphenylpyruvic acid	0.35	2.60E-02	0.96	8.70E-01
47	182.0812	12.8	Tyrosine	1.32	6.30E-03	1.00	9.90E-01
1405	195.03	11.5	3-(3,4-Dihydroxyphenyl)pyruvate	0.19	9.20E-03	ND	
2015	195.03	7.3	3-(3,4-Dihydroxyphenyl)pyruvate	0.06	2.90E-02	ND	
101	205.0972	11.3	Tryptophan	1.86	2.00E-03	1.02	9.40E-01

DNA/RNA Metabolism

395	134.0447	15.0	L-Aspartic acid	1.40	7.10E-03	0.83	2.40E-01
333	136.0619	9.3	Adenine	3.15	1.90E-04	1.11	7.90E-01
186	155.01	10.3	Orotic acid	0.64	7.0E-02	ND	
9							
619	244.0927	11.7	Cytidine	2.03	2.20E-03	1.15	5.70E-01
387	258.1082	10.8	5-Methylcytidine	1.24	2.90E-02	0.91	6.30E-01
370	289.0333	16.1	D-Sedoheptulose 7-phosphate	10.88	6.60E-03	ND	
9							
311	322.045	15.7	Cytidine monophosphate	2.27	1.40E-05	ND	
9							
994	363.0358	14.9	Xanthosine 5'-phosphate	10.04	1.20E-02	ND	

Proline/arginine metabolism							
2	116.0707	12.5	D-Proline	1.28	4.60E-03	1.05	5.50E-01
219	175.1078	13.1	N-Acetylornithine	1.63	3.10E-03	1.13	4.70E-01
257	174.0873	14.0	Oxoarginine	1.79	5.50E-02	1.13	4.70E-01
44	175.119	24.4	L-Arginine	1.24	5.00E-02	0.84	3.60E-01
517	176.103	15.6	Argininic acid	1.59	2.40E-02	0.98	9.20E-01
Leucine/isoleucine/valine metabolism							
76	115.0403	7.3	2-Methylacetoacetic acid	0.28	2.00E-02	0.88	4.40E-01
202	118.0862	13.6	valine	1.91	2.20E-02	1.02	9.60E-01
180	117.0558	7.4	5-Hydroxypentanoate	1.39	1.60E-02	1.04	6.20E-01
1							
7	129.0559	4.9	3-Oxohexanoic acid	0.28	1.90E-02	0.68	2.40E-01
258	131.0351	7.3	(S)-2-Acetolactate	0.48	6.30E-02	0.99	9.50E-01
6	132.1019	11.0	D-Leucine	1.28	2.10E-02	1.02	8.90E-01

Central Carbon Metabolism

2	87.00869	8.5	3-Oxopropanoate	0.46	3.60E-02	0.98	8.30E-01
168	89.02418	8.4	Lactic acid	0.37	4.70E-02	1.17	6.80E-01
7							
196	115.0037	16.0	Fumaric acid	1.48	2.20E-02	0.84	3.30E-01
586	166.9753	17.5	Phosphoenolpyruvic acid	3.72	4.50E-02	2.54	2.80E-02
29	179.0565	14.5	Glucose	1.23	1.90E-02	1.01	9.40E-01

Histidine metabolism

761	155.045	10.6	3-Imidazole-2-oxopropanoate	0.43	2.00E-03	1.04	9.00E-01
68	156.0767	14.5	L-Histidine	1.14	3.80E-01	1.11	6.20E-01
206	157.0607	11.1	(S)-3-(Imidazol-5-yl)lactate	6.84	3.50E-02	1.11	7.50E-01

Choline metabolism							
4	104.107	19.0	Choline	3.20	1.20E-03	0.54	1.00E-01
446	173.0207	14.9	Glycerol 3-phosphate	3.64	8.00E-03	1.60	2.80E-01
33	184.0733	14.8	Choline phosphate+	2.53	3.20E-03	0.92	7.90E-01
1	258.11	14.2	Glycerophosphocholine	2.00	1.80E-03	0.91	7.50E-01
Miscellaneous							
406	189.1598	20.7	N6,N6,N6-Trimethyl-L-lysine	1.71	2.70E-03	1.04	8.60E-01
78	189.1235	12.5	Acetyllysine	5.47	4.70E-05	1.51	2.60E-01
300	241.031	15.9	L-Cystine	1.50	1.70E-03	1.01	9.70E-01
315	190.0896	4.7	S-Prenyl-L-cysteine	3.38	3.10E-03	0.98	8.00E-01
336	465.3053	3.6	Cholesterol sulfate	3.16	4.00E-03	1.00	9.70E-01
Lipids							
156	730.575	3.9	PE 36:1	2.33	2.60E-04	1.09	7.70E-01

110	730.5387	3.9	PC 32:2	0.43	3.20E-03	1.33	1.90E-01
133	742.5752	3.9	PC 34:3 ether lipid	1.94	8.80E-04	0.80	2.00E-01
179	744.591	3.9	PC 34:2 ether lipid	2.67	2.10E-04	1.00	9.90E-01
174	756.5544	3.9	PC 34:3	0.41	2.80E-03	1.18	1.40E-01
169	760.5856	4.0	PC34:1	0.63	7.40E-03	1.15	2.40E-01
136	768.5906	3.9	PC 36:4 ether lipid	2.18	4.70E-04	0.84	4.10E-01
30	770.606	3.9	PC 36:3 ether lipid	2.36	1.50E-03	0.86	5.60E-01
21	772.6208	3.9	PC36:1 ether lipid	3.39	3.40E-03	0.91	7.00E-01
163	780.5544	4.0	PC 36:5	0.45	5.20E-03	1.38	2.10E-02

CHAPTER 7:
PROFILING, TESTING AND FRACTIONATION
OF SAUDI ARABIAN PROPOLIS

7 PROFILING, TESTING AND FRACTIONATION OF SAUDI ARABIAN PROPOLIS

7.1 Introduction

Ethanol extracts of Saudi propolis were chemically and biologically identified using different chromatographic techniques such as CC and flash chromatography. Four compounds were isolated and elucidated by HR-ESI-MS and 1D and 2D NMR.

Up to now, there have only been very limited studies on the chemical profiles of Saudi Arabian propolis and on the identification of lead compounds which are responsible of the bioactivity. Some flavonoids, phenolic acids and terpenes which have been isolated from Saudi Arabian propolis have been reported to include p-coumaric acid, caffeic acid, apigenin, kaempferol, quercetin, rutin, ferruginol, totarol and triterpene acetate (3'-acetoxy-19(29)-taraxasten-20a-ol) (El-Mawla and Osman, 2011, Jerz et al., 2014).

It has been reported that propolis samples collected from different geographical regions will produce unique chemical compounds that are dependent on the available plant resources visited by the honeybees (Peyfoon, 2009). The best region for collecting honey products is the mountainous region in south-western Saudi Arabia which is known as a honey production area (Jerz et al., 2014). This mountainous region includes Assir, ABaha and Taif (Figure 7-1) which are the most suitable areas for beekeepers and the class of local bee colonies is *Apis mellifera jemenitica* (Alqarni et al., 2011). This area is quite distinct from many other regions with regard to the plants growing there.

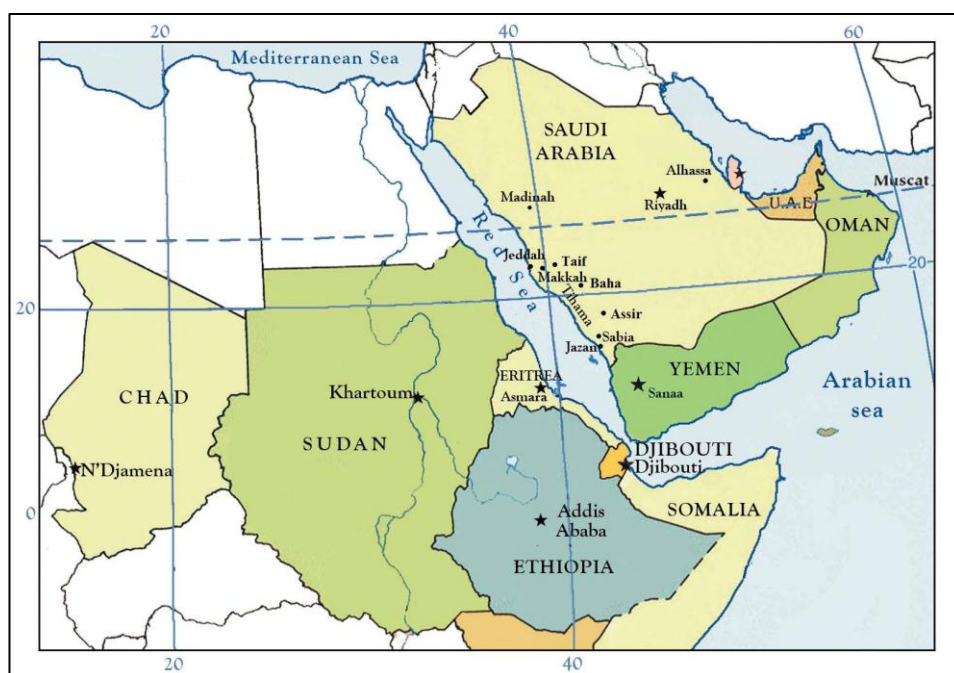


Figure 7.1: Distribution of *Apis mellifera jemenitica* Ruttner in the Arabian Peninsula and northeastern Africa (Alqarni et al., 2011).

7.2 Methodology

7.2.1 Saudi Arabian Propolis

Propolis samples in (shown in Figure 7.2) were collected in summer 2013 from Rijal Alma'a Village in Assir district in south-western Saudi Arabia ($42^{\circ}16' 14.726''\text{E} / 18^{\circ}11' 34.974''\text{N}$). The sample was provided by the local beekeeper and was stored at room temperature.



Figure 7.2: Saudi Arabian propolis.

7.2.2 Extraction of Saudi Arabian Propolis Metabolites

The propolis sample (7.05 g) was coarsely ground and dissolved in 100 ml of ethanol and was extracted for one hour by sonication at room temperature and this was repeated three times and the sample was filtered each time. The total crude extract was dried using a rotary evaporator and the residue was transferred to pre-weighed vials (50ml) and then re-dissolved twice in about 5 ml ethyl acetate. The ethyl acetate extract was dried under nitrogen and the vial was re-weighed to yield 4.8 g of extract which was subjected to further analysis.

7.2.3 Chromatographic Isolation of Components in Saudi Arabian propolis

Initially the crude extract obtained (4.8g) was fractionated by using column chromatography on silica gel (55g of silica gel in a 40x3 cm glass column). The extract was dissolved in a minimum amount of EtOAc and then mixed with a small quantity of silica. The mixture was then left to dry completely under a vacuum hood until the next day. The dried extract was then loaded onto the top of the column and then elution was carried out sequentially using a gradient profile with Hexane: EtOAc (90:10 to 100:0), followed by MeOH: EtOAc (60:40 to 100:0) as illustrated in Table 7.1).

Fractions were collected in 50 ml vials and produced a total of 32 fractions. Using LC-MS, besides TLC, as a guide, similar fractions were combined and the solvent was removed so that finally 10 fractions were obtained.

Table 7.1: Sequence of Column Chromatography Solvent Systems and propolis extracts collected

Hexane (%)	EtOAc(%)	MeOH(%)	M.P. volume (ml)	Fractions obtained
90	10	0	200	1-4
60	40	0	200	5-8
40	60	0	200	9-12
20	80	0	200	13-16
0	100	0	200	17-20
-	60	40	200	21-24
-	30	70	200	25-28
-	0	100	200	29-32

7.2.3.1 Isolation of bioactive fractions from CF6 using ColumnChromatography

Fractions which were found to possess strong biological activity were subjected to further fractionation.

Fraction number 6 (458.1 mg) which showed biological activity but was not completely pure was subjected to further purification and was re-chromatographed using a shorter column CC (40x 3cm glass column) with packed to 2/3 of the silica gel which was mixed in non-polar solvent (Hexane) to form a slurry then the homogenous mixture were poured into the column and allowed flow through the column. The sample (F6) was carefully added on top of the column and then elution

was performed using an isocratic system (40/60 Hexane/EtOAc) which was determined from the TLC results. Fractions were collected in 20 ml vials and TLC and LC-MS were performed in to combine fractions showing similar profiles and thus two pure compounds, compound 1 from C2F4, C2F5, C2F6 and compound 2 from C2F7 were obtained.

7.2.3.2 Isolation of bioactive fractions from CF7 using Reveleris® iES Flash Chromatography System

Fraction 7 was further purified with a Grace Reveleris® iES Flash Chromatography System equipped with a dual-UV wavelength detector set at 210 and 280 nm and an ELSD detector. This fraction (619.7 mg) was dissolved in a minimum amount of ethyl acetate and preadsorbed onto Celite® and was then left to dry under a fume hood. The dried mixture was put into the solid loader on the top of the Reveleris® 24 g/32 ml silica gel column and then fractionated by elution with isocratic conditions in hexane-ethyl acetate (40:60 v/v) for 90 min. All peaks were collected into tubes and tested the similarity of the fractions with ELSD and TLC in order to combine the similar ones. Nine sub-fractions were obtained from fraction 7, compound 3 (9.7 mg) was obtained in fraction 2 and Compound 4 (80.0 mg) was obtained in fractions 5, 6 and 7.

7.2.4 Analysis of Fractions from Saudi Arabian propolis using LC-MS, LC-UV-ELSD

Fractions containing the purified compounds were dissolved in methanol for LC-MS analysis to detect and confirm their mass and molecular formula as well as to know fragmentation pattern. The MSⁿ fragmentation was performed on using Collision Induced Dissociation (CID) at 35V, Activation Q and the activation time were set at 0.250ms and 30.00 ms, respectively on a LTQ-Orbitrap mass Spectrometer combined with HPLC. The ESI-MS conditions and chromatographic conditions were used as described in 2.6.1 for sample profiling and were also used a short method as a step-wise gradient elution with reversed phase column (4.6×50 mm, 3µm C18) (Atlantis, Ireland) from 95% A (0.1% v/v formic acid in water) and 5% B (0.1% v/v formic

acid in acetonitrile) to 70% B mobile phases at a flow rate of 0.400 $\mu\text{l}/\text{min}$ over 0-20 min then for a further 1-min for isocratic elution, and a return to starting conditions at 21 min for re-equilibration for the last 4 minutes, using up a total of 25 min for the run.

Each interesting or purified fraction was also subjected to a preliminary characterisation using HPLC–UV–ELSD with the same conditions as in 2.6.1 as for check the purity of compounds isolated by flash chromatography.

7.2.5 NMR experiment

Each sample was prepared by dissolving 10 mg in 700 μL of appropriate deuterated solvent, either DMSO- d_6 or CDCl_3 , and then transferred into standard NMR tubes. After this, the NMR experiments were then carried out as described in section 2.9.

7.3 Results

The ethanol extract of Saudi propolis 4.80 g was found to have antitrypanosomal activity with MIC (25 µg/ml) in the Almar Blue assay. Flavonoids and diterpenes were subsequently isolated from this crude extract. A sample of this extract (10 mg) was initially analysed by NMR to determine the general nature of components and LCMS profiling which was carried out by using the LC-MS method described in section 7.2.4

LC-MS analysis revealed the presence of diterpenes and flavonoids as the dominant components in the crude extract of Saudi propolis as summarised in Table 7.2. As well as the ¹H NMR spectra (Figure 7.3) revealed that the main components were terpenoids or fatty acids in the crude extract. Figure 7.4 shows the three most abundant compounds in the LC-MS analysis with their elemental compositions C₂₀H₃₁O₃, C₂₀H₂₁O₉ and C₂₀H₃₁O. From the initial information we can predict from the formula and RDB that these compounds are probably diterpenes and flavonoids.

The next interesting abundant compounds had a formulae corresponding to diterpenes with the compositions C₂₀H₂₉O₃ and C₂₀H₂₉O₂ (MS MH⁺ Figure 7.5) and could be abietanes which were among the diterpenes found in Egyptian propolis (Peyfoon, 2009). However, the NMR is always needed to determine the exact structure of compounds.

The fourth most abundant compound eluted later with RF C18 LCMS and it had an elemental composition C₁₉H₁₉O₈ (Figure 7.7) for the M+H⁺ spectrum. This composition could correspond to a casticin (Figure 7.8) which has been isolated from different plants and it has been reported to have biological activity against cancer and antioxidant activity (Rasul et al., 2014) but on further analysis by NMR, it was confirmed to be psiadiarabin 2 as described in section 7.3.3.

Further investigation for this sample was needed to identify the compounds responsible for the biological activity.

Table 7.2: The compounds in the crude extract of Saudi propolis which are the most abundant by response when analysed by reversed phase LC-MS in positive ion mode.

<i>Compound</i>	<i>m/z</i>	<i>Rt min</i>	<i>RDB*</i>	<i>Elemental composition</i>
1	319.2268	18.47	5.5	C ₂₀ H ₃₁ O ₃
2	405.1168	18.75	10.5	C ₂₀ H ₂₁ O ₉
3	317.2107	15.21	6.5	C ₂₀ H ₂₉ O ₃
4	375.1069	20.3	10.5	C ₁₉ H ₁₉ O ₈
5	287.2364	19.41	5.5	C ₂₀ H ₃₁ O
6	301.2158	14.53	6.5	C ₂₀ H ₂₉ O ₂
7	359.1122	22.8	10.5	C ₁₉ H ₁₉ O ₇
8	401.2680	25.8	7.5	C ₂₅ H ₃₇ O ₄
9	391.1021	16.6	10.5	C ₁₉ H ₁₉ O ₉
10	435.1281	21.10	10.5	C ₂₁ H ₂₃ O ₁₀
11	329.1743	26.06	8.5	C ₂₀ H ₂₅ O ₄

* RDB stands for relative double bond

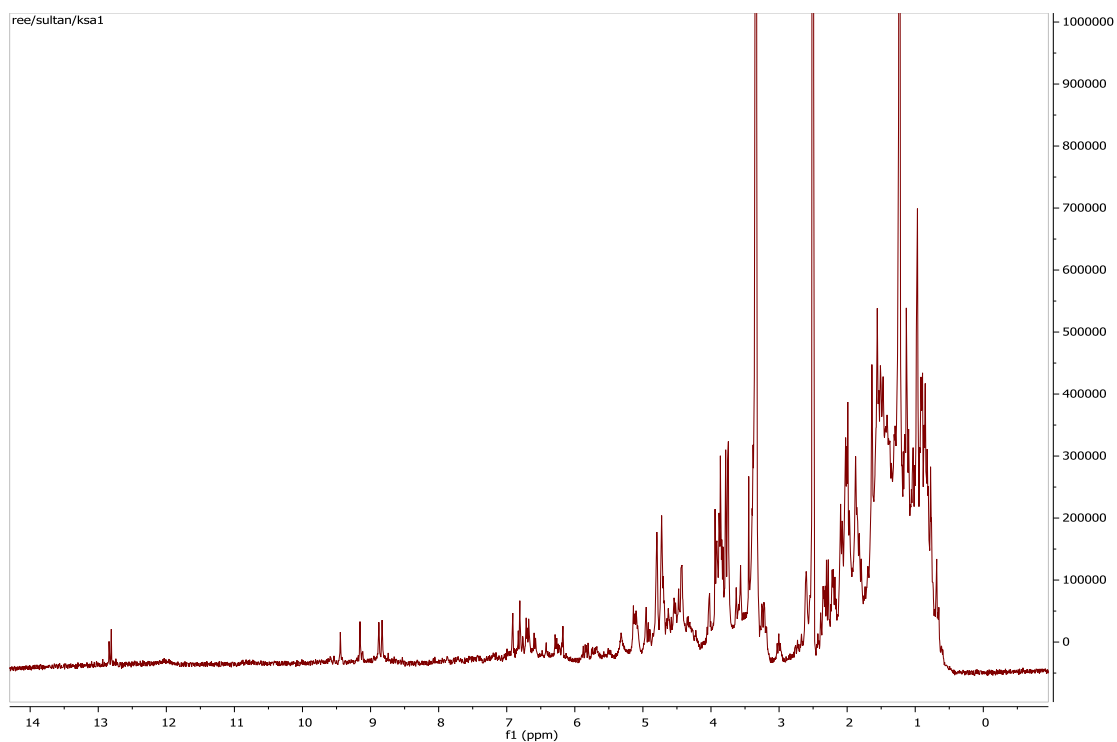


Figure 7.3: ¹H NMR spectrum (400 MHz, DMSO-d₆) of crude Saudi propolis.

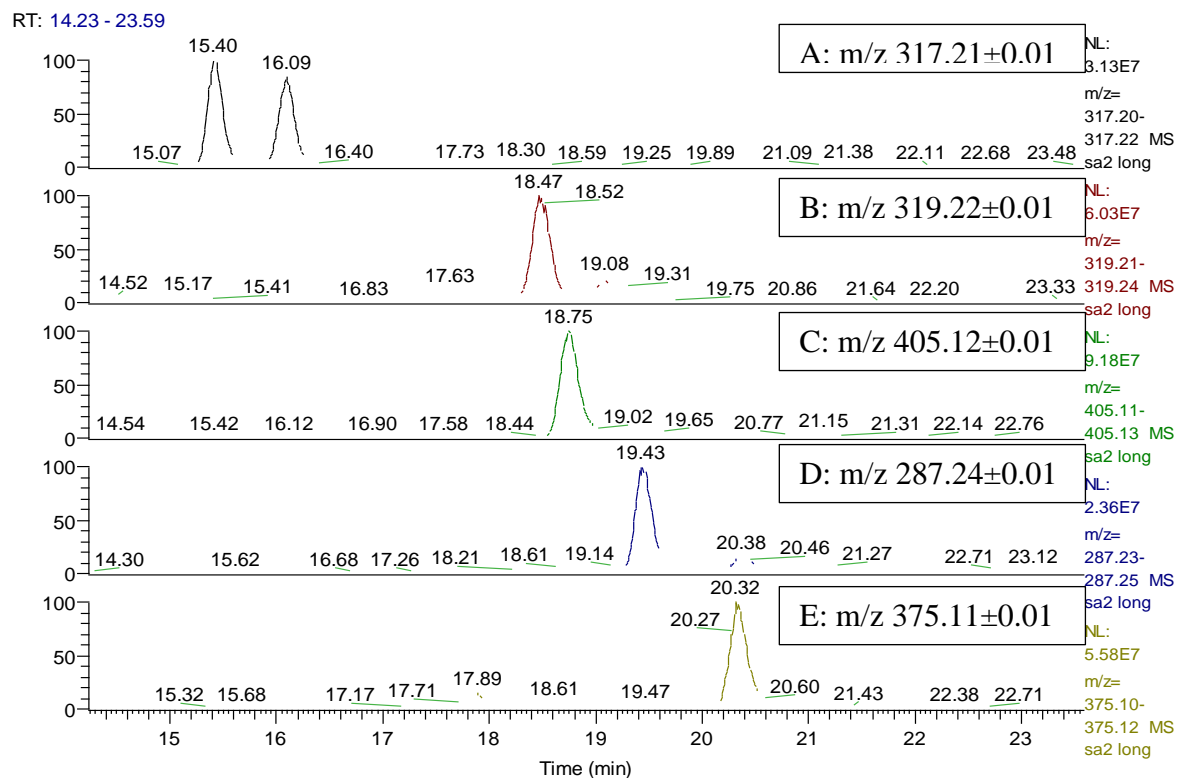


Figure 7.4: Extracted ion traces (A-E) for the the most abundant components in a crude extract of Saudi propolis. These elemental compositions could correspond to a range of structural type diterpenes and flavonoids as shown inTable 7.2

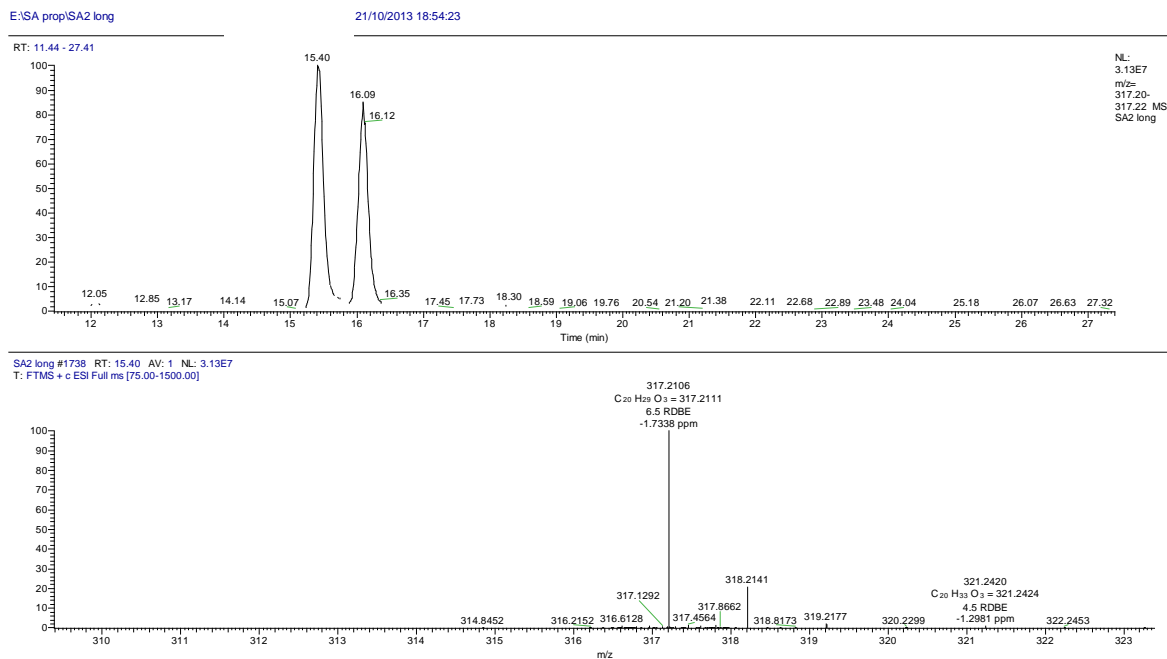


Figure 7.5: Extracted ion chromatogram and mass spectrum for the third most abundant compound by response in crude extract of Saudi propolis. The elemental composition corresponds to that of the diterpene abietic acid.

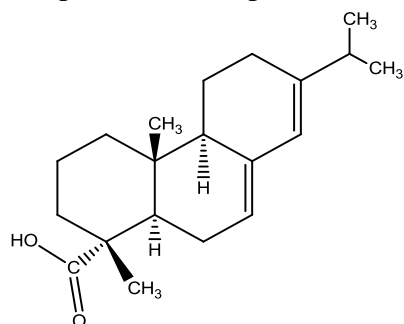
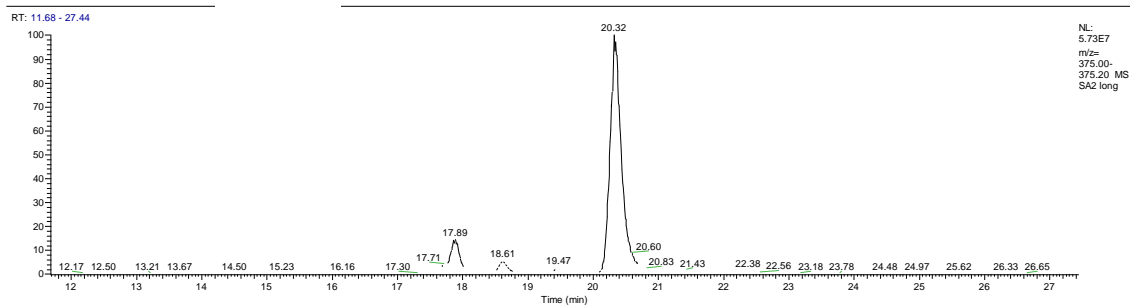


Figure 7.6: Structure of diterpene abietic acid.



SA2 long #2316 RT: 20.34 AV: 1 NL: 5.46E7
T: FTMS + c ESI Full ms [75.00-1500.00]

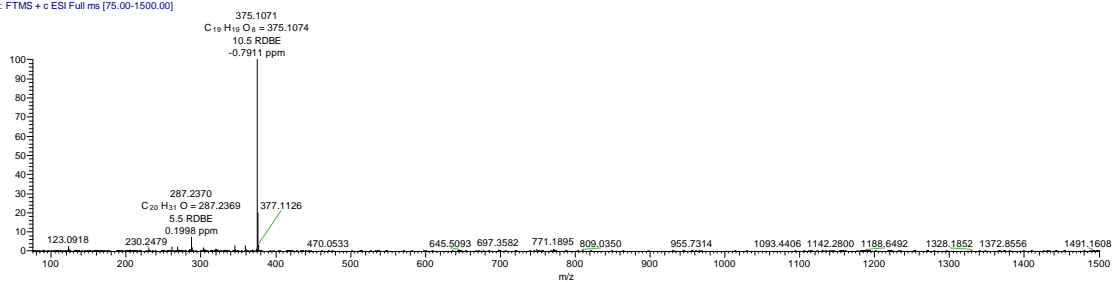


Figure 7.7: Extracted ion chromatogram and mass spectrum for the fourth most abundant compound by response in a crude extract of Saudi propolis. The elemental composition shown corresponds to casticin.

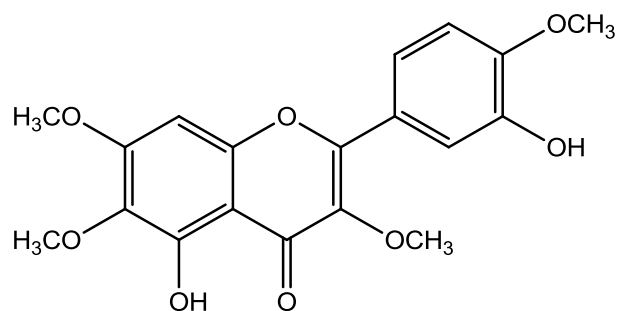


Figure 7.8: Structure of casticin.

7.3.1 The yields obtained and bioactivity fractions of KSA1 extracts

The Saudi Arabian propolis (7.05g) was successively extracted with absolute Ethanol. The metabolites were fractionated based on polarity using normal phase chromatography and the yields of fractions are listed in Table 7.3. Some of fractions which have interesting biological activity (highlighted in the table) were subjected to further preparative-scale isolation.

Table 7.3: Yields and activities of pooled fractions obtained from KSA1 extract the fractions which are highlighted had strong activity, while pink highlight indicates the compounds which were identified

Fractions No.	Pooled fractions	Yield (mg)	Anti-trypansomal activity	
			20µg/ml % D control	MIC (µg/ml)
CF1	SC1-7	352.2	102.7	
CF2	SC8-9	318.6	19.9	
CF3	SC10-11	150.7	-2.7	
CF4	SC12	124.8	-0.6	
CF5	SC13	100.8	4.4	
CF6	SC14-16	458.1	1.6	12.5
CF7	SC17-23	619.7	1.8	
CF8	SC24	825.5	115.6	50
CF9	SC25-27	294.5	135.4	
CF10	SC28-30	657.9	248.6	
CF11	SC31-32	-	-	
Crude Extract		4,800		25
Suramin	+Ve Control			0.162

Saudi propolis extract (4.80 g) was chromatographed through open column and thirty two fractions (table 7.3) were eluted successively starting with 90% hexane, and increasing the polarity in 10% increments with EtOAc, then finally increasing amounts of MeOH in EtOAc to 100% MeOH. A series of fractions were obtained

some of which had increased bioactivity in comparison to that of the crude extract. The fractions with the strongest bioactivity were F6 and 7 which eluted with a polar solvent system (60% EtOAc –MeOH for F7). Further investigations of these two fractions are presented in the next section. The earliest eluting active fraction eluted with 40 % Hexane –EtOAc (F3) but produced a low yield. Next active fraction was F4 (eluting in 40 % Hexane/ EtOAc) which from the LC-MS profile appeared to be quite pure and might be a casticin as the most abundant compound in this fraction. The last active fraction (F5) which eluted with 20% Hex-EtOAc showed considerable activity in the initial screening (4.4 µg/ml) and LC-MS result revealed the presence of four major components with RDB which would be expected for flavonoids as shown in Table 7.4.

Table 7.4: The most abundant in mixture fraction 5 when analysed by reversed phase LC-MS in positive ion mode

<i>Compound</i>	<i>m/z</i>	<i>Rt min</i>	<i>RDB*</i>	<i>Elemental composition</i>
1	361.0918	15.66	10.5	C ₁₈ H ₁₇ O ₈
2	375.1077	19.49	10.5	C ₁₉ H ₁₉ O ₈
3	419.1335	21.11	10.5	C ₂₁ H ₂₃ O ₉
4	387.2896	24.54	6.5	C ₂₅ H ₃₉ O ₃

* Relative double bound

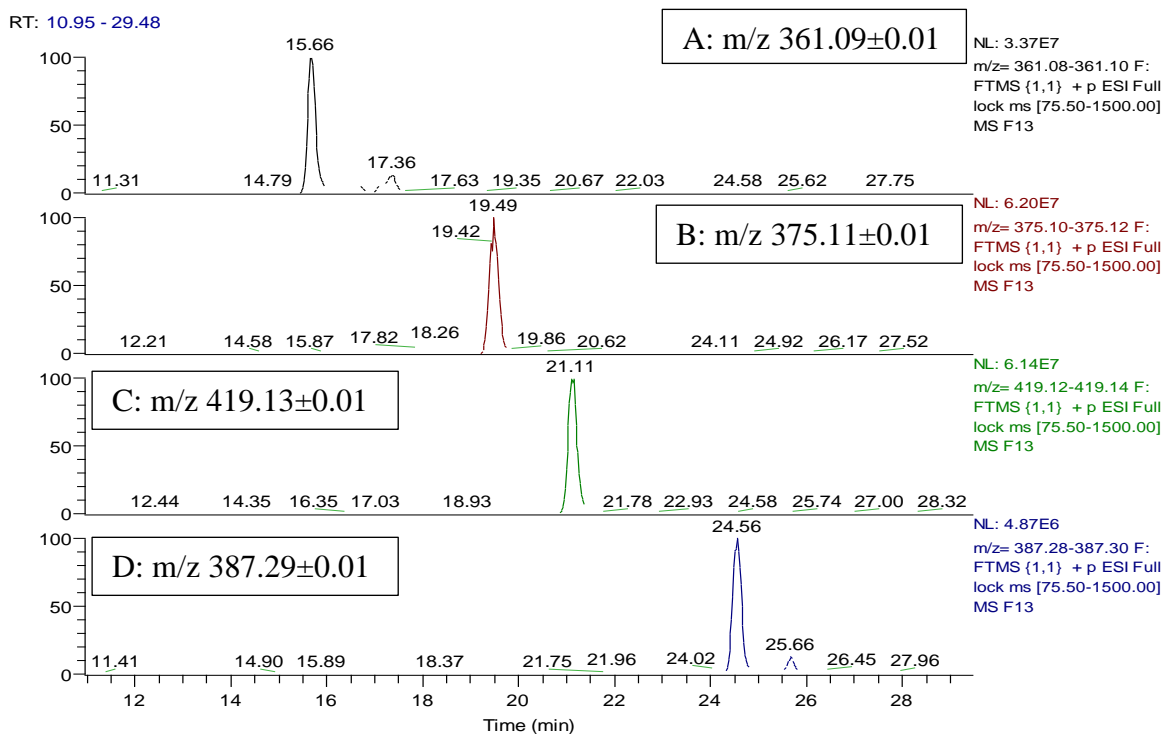


Figure 7.9: Extracted ion traces (A-D) for the main compounds present in fraction 5 run in positive ion mode. Their elemental composition are as shown in Table 7.4.

7.3.2 Identification and Structure Elucidation of main compound from fraction 4 (CF4)

Fraction 4 was found to be active against *T. b. brucie* as seen in Table 7.3. Further analysis employing LC-UV-ELSD showed only one major compound with UV absorption as seen in the chromatogram in Figure 7.10.

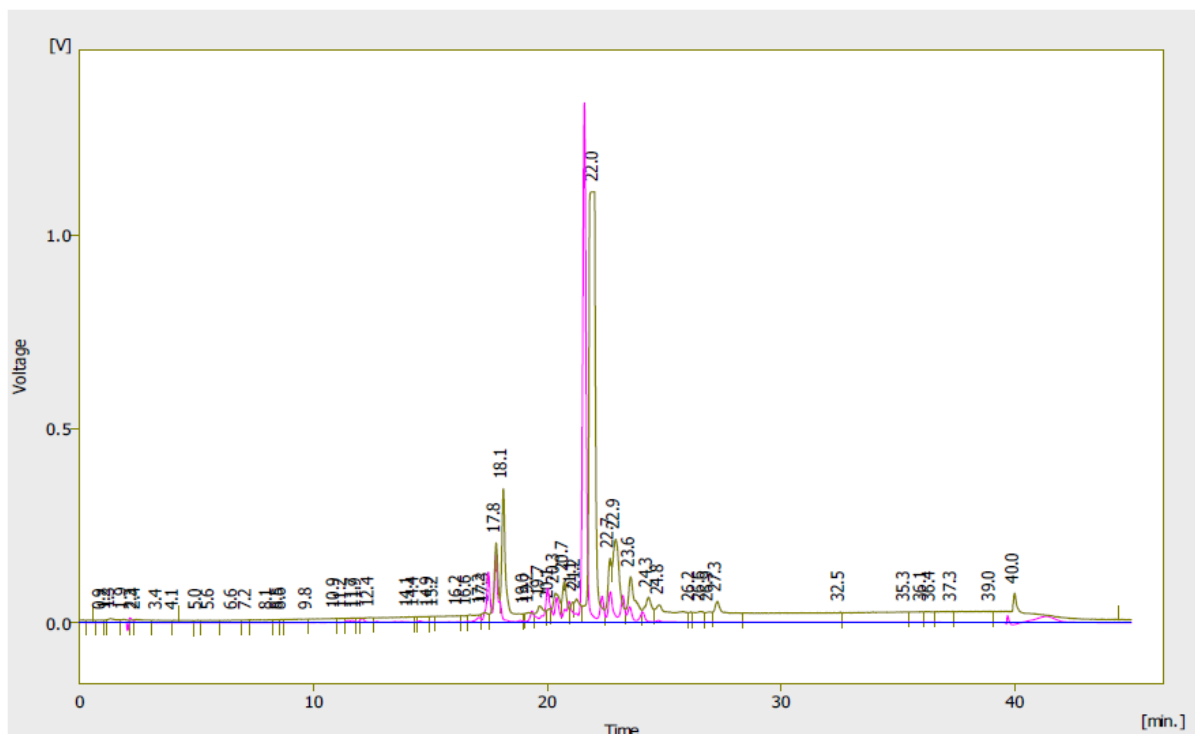


Figure 7.10: LC-UV-ELSD chromatogram of fraction 4 (CF4) methods as in section 7.2.3. Pink trace UV absorbance (290 nm) and brown trace ELSD response.

7.3.3 Characterisation of CF4 (Flavonoid compound)

The CF4 fraction appeared as a yellow, sticky material with yield of 124.8 mg. It was observed to be UV absorbing at $\lambda=290$ nm on liquid chromatography-UV-ELSD (figure 7.10). HR-ESIMS in positive ion mode (Figure 7.11) gave a molecular ion $[M + H]^+$ at m/z 375.1075 and suggested a molecular formula of $C_{19}H_{19}O_8$.

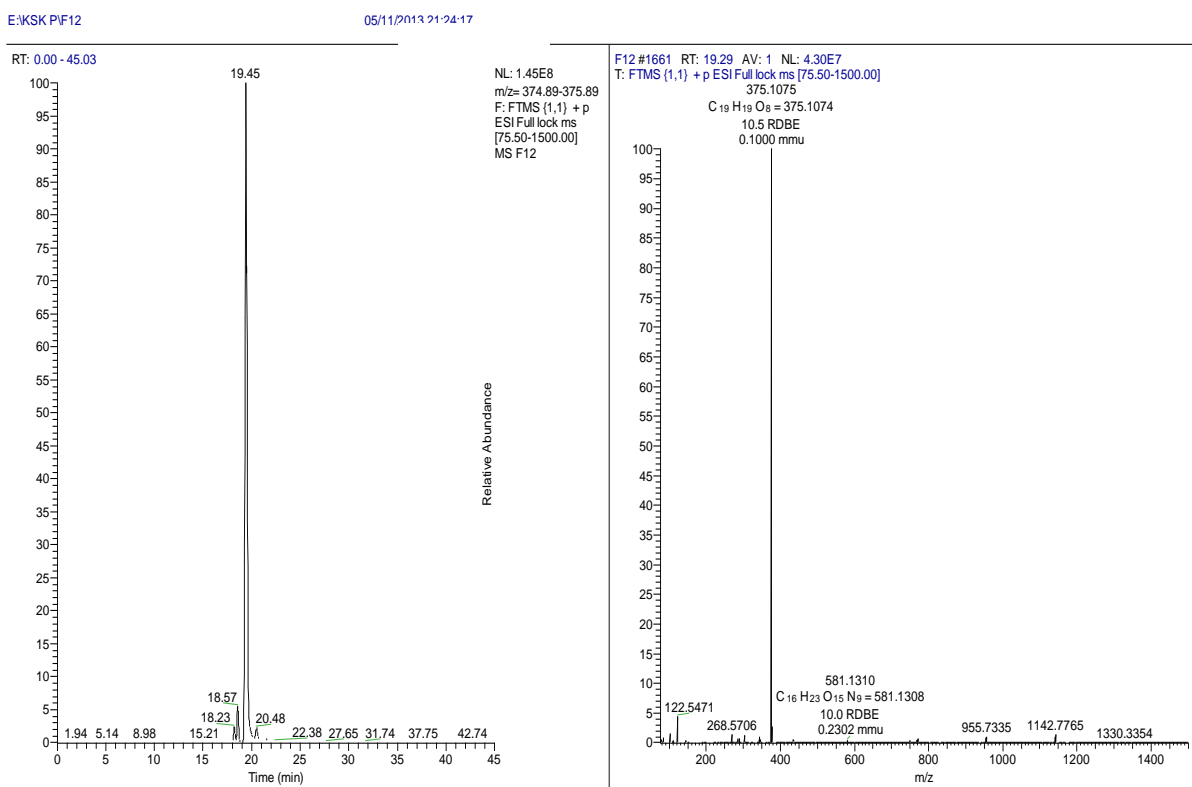


Figure 7.11: HR-ESIMS ion chromatogram and mass spectrum of the main component in CF4

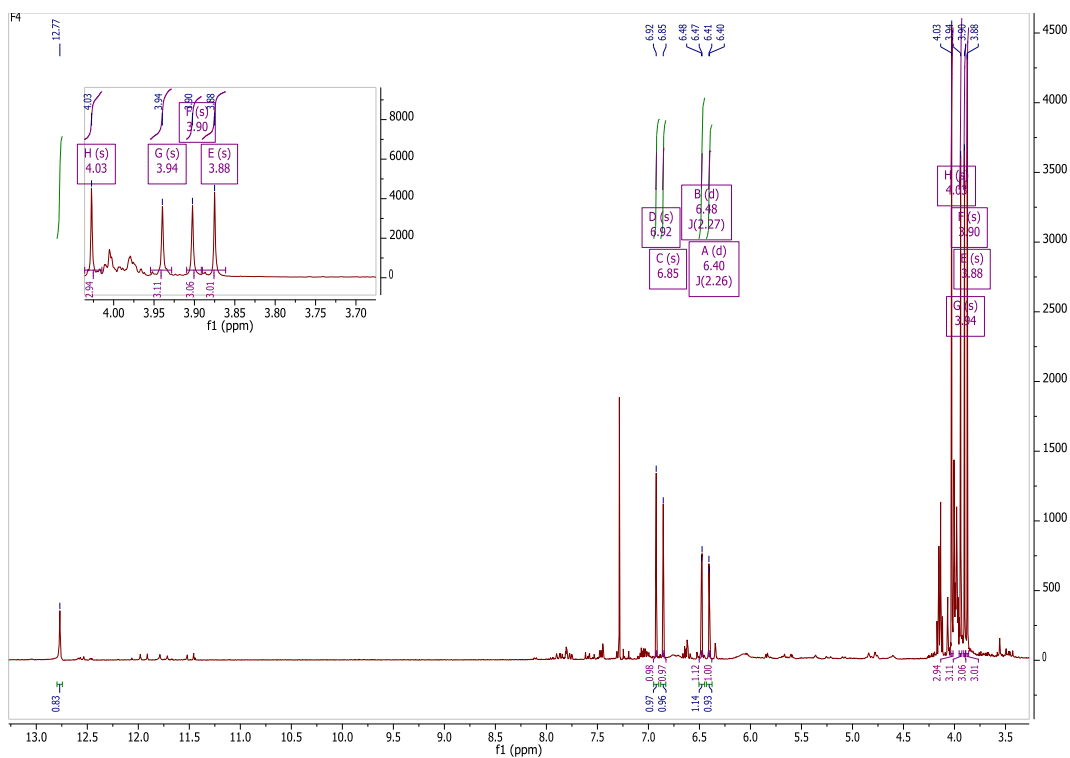


Figure 7.12: ^1H NMR of CF6-f6 (400 MHz, CDCl_3)

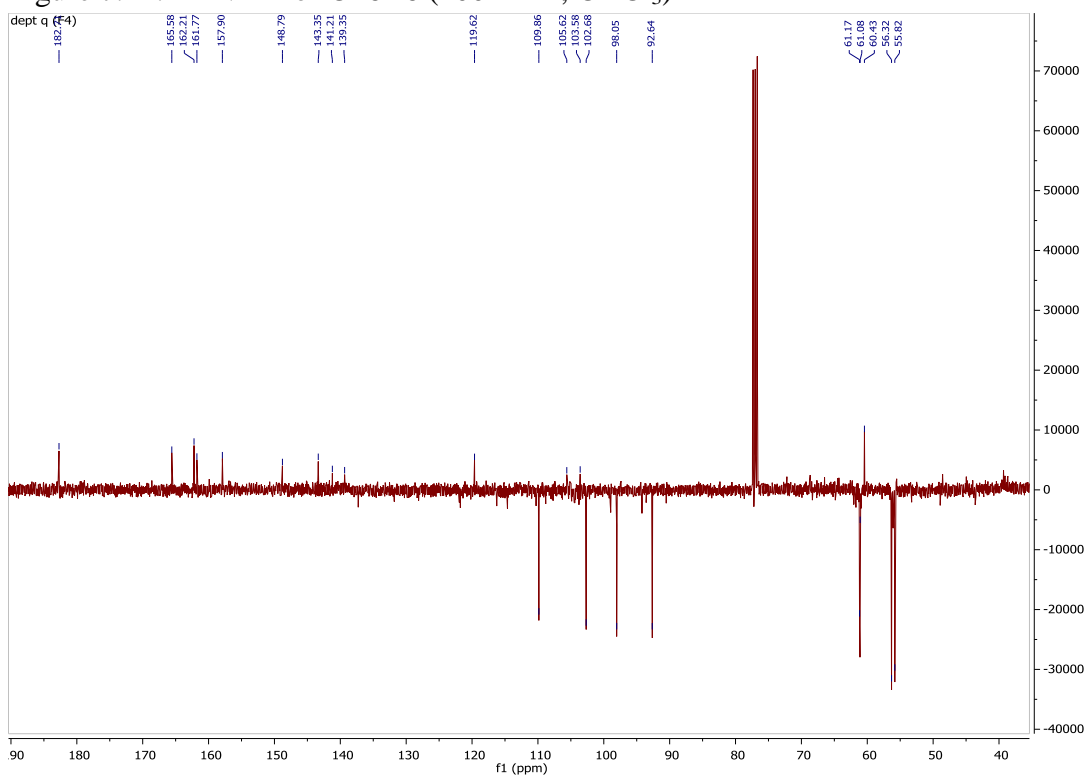


Figure 7.13: ^{13}C NMR spectrum of CF6-F6 (100 MHz, CDCl_3)

Table 7.5: ^1H and ^{13}C NMR data of compound CF4 (400 MHz, CHCl_3)

Experimental compound CF4				Psiadiarabin 2(El-Feraly et al., 1990)		
Position	δ_{H} (multiplicity, J)	δ_{C}	^{13}C Type	δ_{H} (multiplicity, J)	δ_{C}	^{13}C Type
1						
2		161.7	C		161.7	C
3	6.93 (1H, s)	109.8	CH	6.94 (1H, s)	109.9	CH
4		182.7	C		182.7	C
5		162.2	C		162.2	C
5-OH	12.77 s			12.78s		
6	6.40 (1H, d, 2.2)	98.0	CH	6.38 (1H, d, 2.0)	98.0	C
7	-	165.5	C		165.6	C
8	6.48 (1H, d, 2.2)	92.6	CH	6.45 (1H, d, 2.0)	92.6	CH
9	-	157.9	C		157.9	C

10	-	105.6	C		105.6	C
1'	-	119.6	C		119.6	C
2'	-	141.1	C		141.2	C
3'		143.3	CH		143.4	C
3'-OH	6.07, br s			6.12 s		
4'	-	139.4	C		139.4	C
5'	-	148.7	C		148.9	C
6'	6.86 (1H, s)	102.5	CH	6.84 (1H, s)	102.6	CH
4'-OMe	4.03 s	61.3	CH ₃	4.00 s	61.2	CH ₃
2'-OMe	3.88 s	61.1	CH ₃	3.92 s	61.1	CH ₃
5'-OMe	3.94 s	56.3	CH ₃	3.88 s	56.3	CH ₃
7-OMe	3.90 s	55.8	CH ₃	3.85 s	55.8	CH ₃

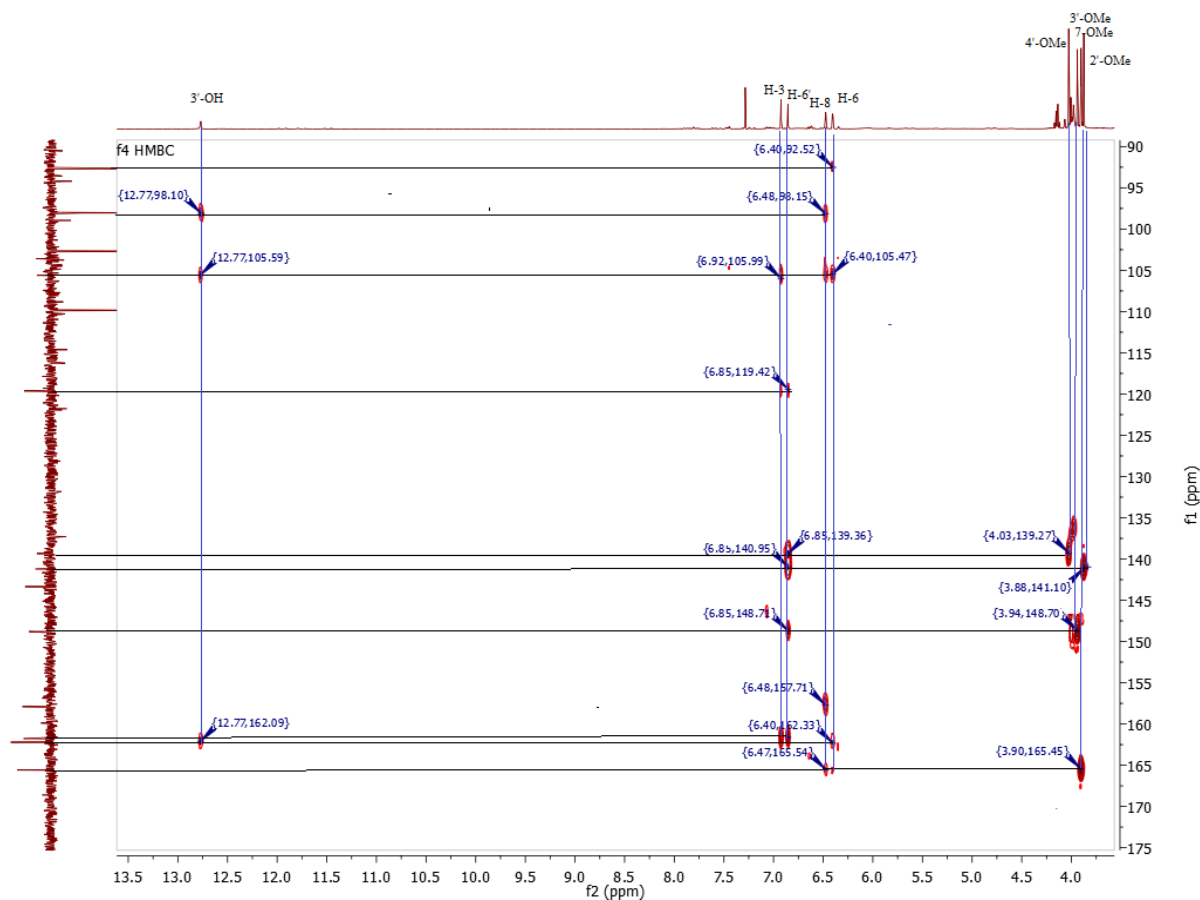


Figure 7.14: HMBC correlations (H → C) for compound in F4.

The ^1H and ^{13}C NMR spectra (Table 7.5) were consistent with a flavonoid skeleton and this data was compared with the data published for psiadiarabin 2 and exactly matched with the NMR data previously reported (El-Feraly et al., 1990, Alyahya et al., 1987) (Table 7.5). Psiadiarabin 2 was previously isolated from the aerial parts of *Psiada arabica* and has never been reported before in propolis samples.

The ^1H -NMR spectrum showed a doublet signal at 6.40 ppm (1H, d, $J=2.6$ Hz, H-6) due to the proton on C-6 at δC 98.2 ppm and a doublet at 6.48 ppm (1H, d, $J=2.7$ Hz, H-8) on C-8 at δC 92.5 ppm due to the protons on C6 and C8 meta coupling to each other. Two singlet protons H-3 at 6.93 ppm and H-6' at 6.86 ppm could be assigned to the protons in benzene ring B.

In addition, it was confirmed by HMQC and HMBC (Figure 7.14) experiments, which observed correlations involved OH -5 at 12.77 showing correlations to three signals at 98.0, 105.6 and 162.2 (C-6, C-10 and C-5) and a 3J correlation from the methoxy protons signals at 165.5, 141.2, 139.5 and 148.9 (C-7, C-2', C-4' and C-5'). In addition HMBC showed strong correlation for both aromatic protons H-6 and H-8 in benzene ring A at 105.6 (C-10), 165.5 (C-7) and 157.5 (C-9). While the aromatic protons H-6' in ring B showed strong correlation to C-5' at 148.9 and C-1' at 119.6 as well as to the heterocyclic aliphatic proton at C-3. This was confirmed by its HMBC correlations (3-H) to C-2 at 161.7 and C-3 at 119.6.

Based on the above evidence, the structure of F4 was confirmed to be psiadiarabin 2 (5, 3'-dihydroxy-7, 2', 4', and 5'-tetra-methoxyflavone (El-Feraly et al., 1990)

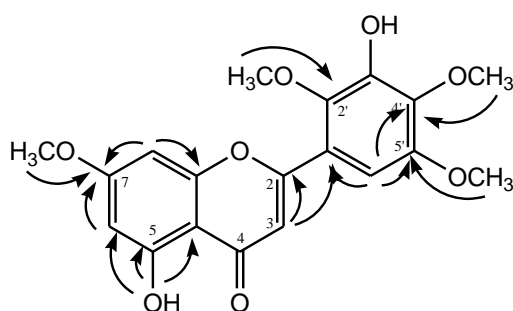


Figure 7.15: Structure of CF4 (psiadiarabin 2)

7.3.4 Further characterisation of bioactive Fractions obtained from KSA propolis extracts

Fractions 6 and 7 which appeared yellowish sticky solids and yielded 458.2, 619.7 mg, respectively and were obtained from silica gel column chromatography and eluted with 80% of EtOAc / Hexane. These fractions were found to be most active against Trypanosoma as seen in Table 7.3. Thus they were subjected to further analysis including TLC and ELSD as shown in (Figures 7.16 7.17) as well as NMR and ESI-MS in order to initially characterise and determine of the nature their constituents.

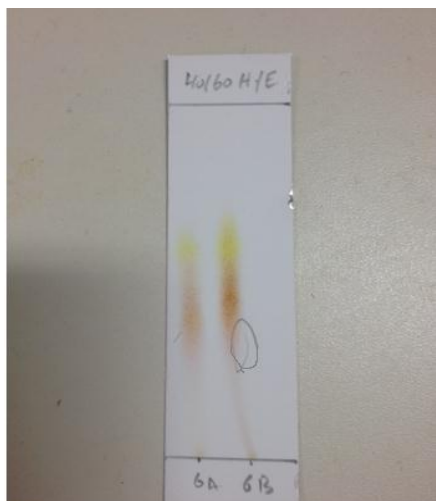


Figure 7.16: TLC analysis of CF 6 from a Saudi propolis extract using 60:40% EtOAc/ hexane as a mobile phase. The spots were observed with anisaldehyde spray and also under short UV light λ 254 nm.

A TLC plate and a LC-UV-ELSD chromatogram revealed that fraction 6 was still mixture of two main compounds one of which had conjugated bonds or benzene rings which was observed under UV light. The ^1H NMR spectrum showed the presence of a mixture and that both compounds seemed to have a similar skeleton structure. Therefore the fraction was re-chromatographed for further purification in order to identify these compounds using a short silica gel column as described in 7.2.3.1

^1H NMR spectra for Fraction 7 indicated that it contained at least two major compounds which did not contain any conjugated bonds based on the lack of absorbance by the analytes when TLC plate was viewed under UV light. In addition no UV peaks absorbing could be seen LC-UV-ELSD chromatogram (Figure 7.18). Hence, this fraction was re-fractionated using Grace Reveleris® iES Flash Chromatography System as described in methodology section 7.2.3.2.

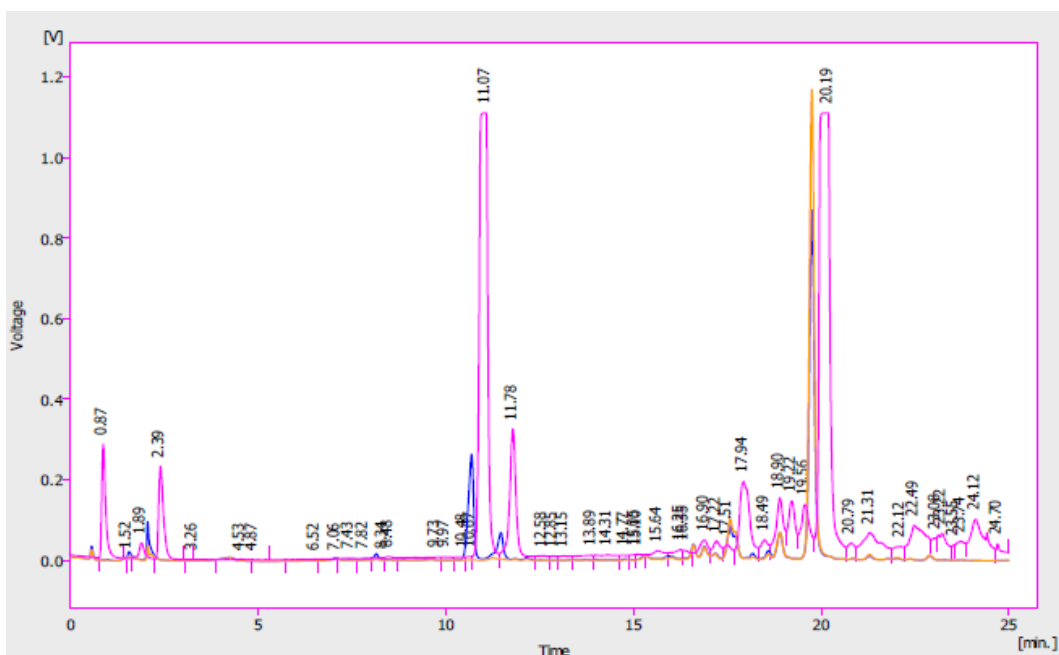


Figure 7.17: LC-UV-ELSD chromatogram of fraction 6(CF6) of KSA propolis extracts methods as in section 7.2.3 (Pink traces ELSD and blue trace UV at 290 nm).

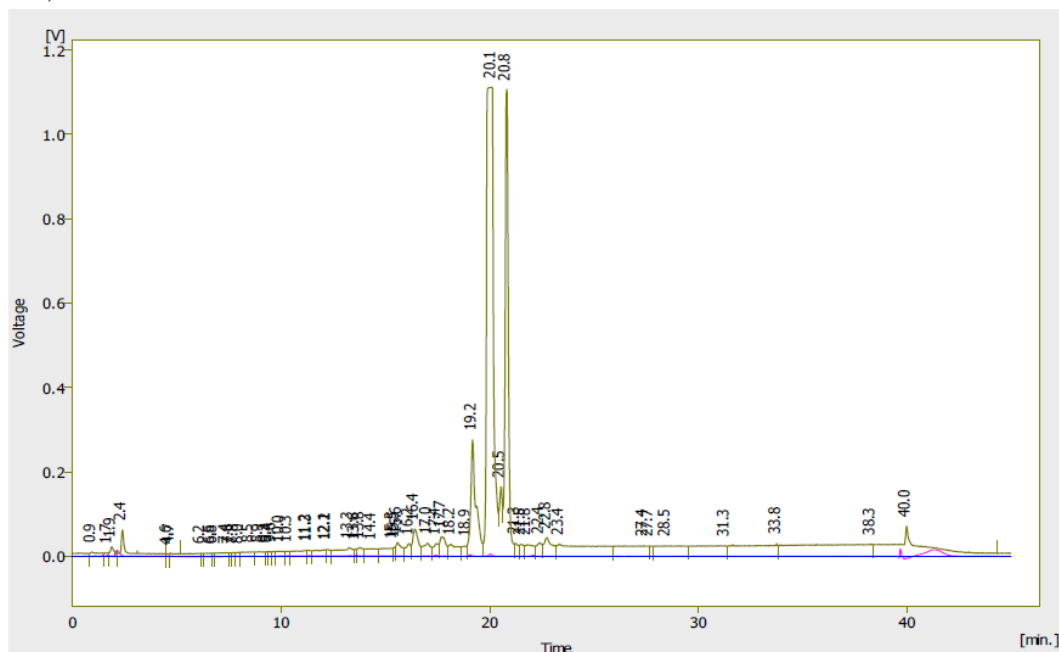


Figure 7.18: LC-UV-ELSD chromatogram of fraction 7(CF7) of KSA propolis extracts methods as in section 7.2.3 (brown trace ELSD and blue trace UV at 290 nm).

7.3.5 Identification and Structure Elucidation of Purified Compounds from CF6 and CF7

From further separation of CF 6 two compounds were obtained CF6-F5 and CF6-F6 by using column chromatography followed by re-chromatography with on a shorter silica column while fraction 7 produced compounds CF7M2 and CF7M5 from further purification using Grace Reveleris® flash chromatography on a silica gel column.

The elemental compositions for the compounds were obtained from LC-MS analysis using an Orbitrap Exactive mass spectrometer in positive/negative ion switching mode and their structures were identified by 1D and 2D NMR analysis.

7.3.5.1 Characterisation of CF6-F5 (Flavonoid compound)

CF6-F5 was obtained as colourless material with a yield of 10 mg. On TLC plate it appeared as violet when observed under UV at $\lambda=254$ nm and UV peaks absorbing at $\lambda=290$ nm on liquid chromatography-UV-ELSD (Figure 7.19). HR-ESIMS in positive ion mode (Figure 7.20) gave a molecular ion $[M + H]^+$ at m/z 275.0910 and suggesting a molecular formula of $C_{15}H_{15}O_5$.

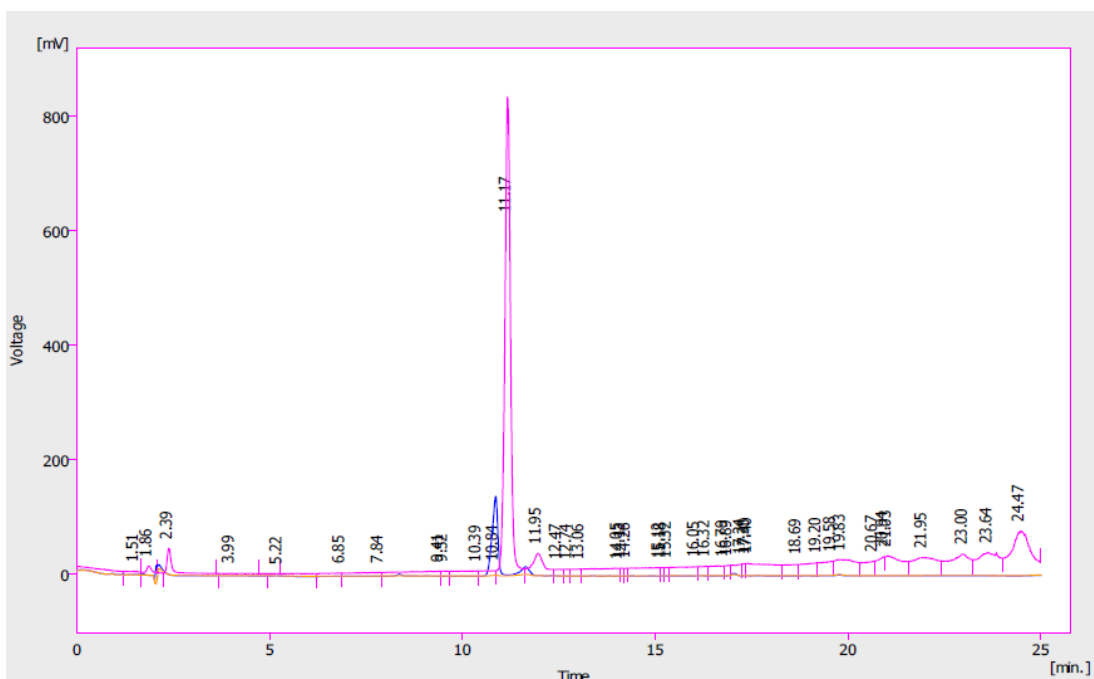


Figure 7.19: LC-UV-ELSD chromatogram of CF6-F5 purified from CC (Section 7.2.3.1) (Pink traces ELSD and blue trace UV at 290 nm).

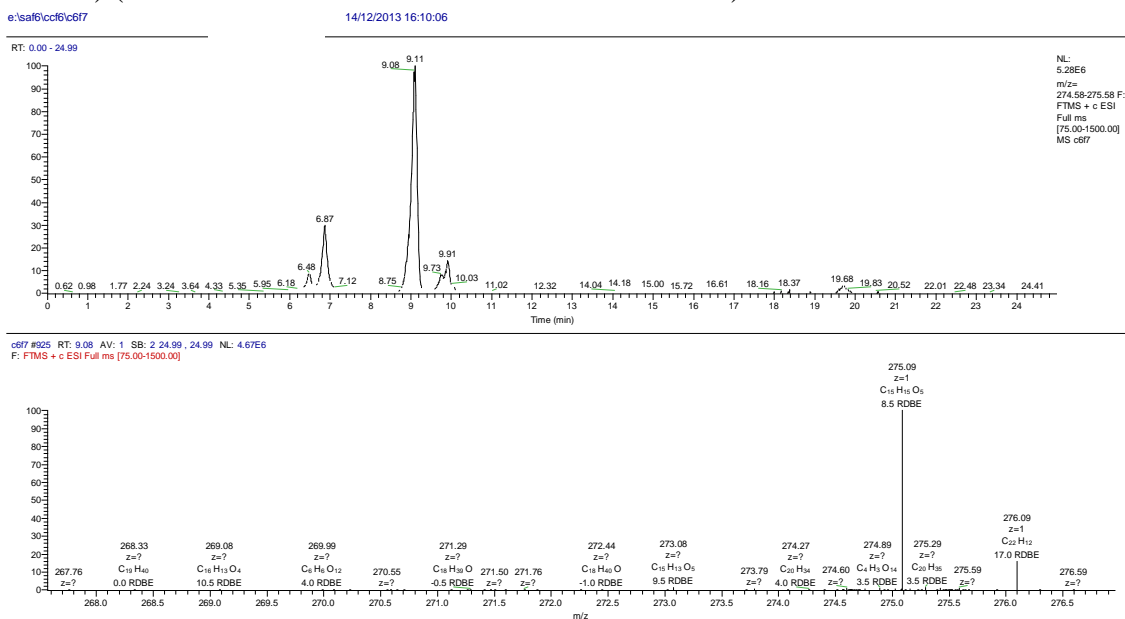


Figure 7.20: HR-ESIMS ion chromatogram and mass spectrum of CF6-F5

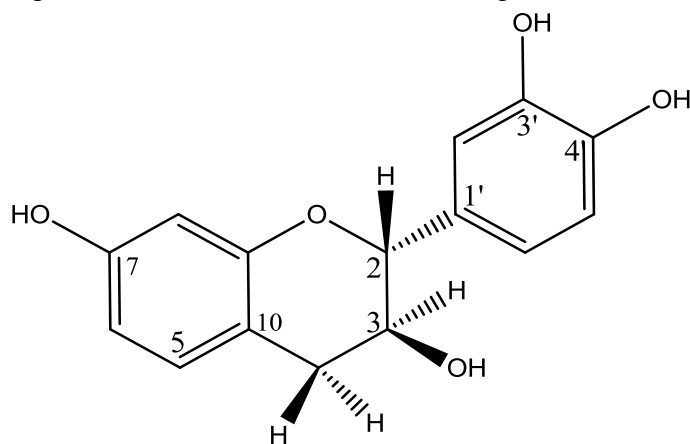


Figure 7.21: Structure of CF6-f5. (Fisetinidol): 3, 4-dihydro-2-(3, 4-dihydroxyphenyl)-2H-chromene-3, 7-diol.

The NMR data in Table 7.6 obtained for CF6-F5 was comparable to that of ananthoside (Piacente et al., 1999) previously isolated from the bark of *Anadenanthera macrocarpa*.

Compound 1 differed from ananthoside by the presence of a free hydroxyl group which in ananthoside is bound to a xylose unit at C-3 ($\delta_{\text{C}} = 67.26$) with the hydroxyl proton of the C-3 occurring $\delta_{\text{H}} 4.96$ (d, $J = 7.08$ Hz).

The COSY spectrum, (Figure 7.22), clearly showed coupling between the proton of the hydroxyl group and broad multiplets at $\delta_{\text{H}} 3.87$ (m) and they were both coupled to the C-4 protons at 2.74 ppm (dd, 5.1, 15.7 Hz) and 2.58 ppm (dd, 8.0, 15.9 Hz) as well as coupled to the C-2 proton at 4.57 ppm (d, 4.6 Hz). This correlation would be attributed to the heterocyclic aliphatic ring of a flavonol skeleton (Bae et al., 1994). In addition the J values for assigned signal to H-2 ($J = 4.6$ Hz) and H-4 ($J = 5.1, 15.7$ and 8.0, 15.9) of the heterocyclic aliphatic ring at C-2 and C-3 suggested the same stereochemistry as in ananthoside.

Also HMBC showed that the OH-proton at C3 gave a long range (HMBC) correlation to C-2 signal at 81.9 ppm, therefore the protons were assigned to a heterocyclic aliphatic ring.

Table 7.6: ^1H and ^{13}C chemical shifts for Anadanthoside and CF6-F5 (400MHz, d_6 -DMSO)

<i>Experimental compound 1 of CF6-F5</i>				<i>Anadanthoside (Piacente et al., 1999)</i>		
Position	δH , multiplicity (J)	δC	^{13}C Type	δH , multiplicity(J)	δC	^{13}C Type
1						
2	4.57, d, (4.6)	81.9	CH	4.97, d (5.9)	80.7	CH
3	3.87 m	67.3	CH	4.15, m	76.9	CH
3-OH	4.96, d, (7.1)	-	-	-	-	-
4	2.74, dd (5.1, 15.7)	33.2	CH_2	2.82, dd (6.2, 15.6)	31.0	CH_2
	2.58, dd (8.0, 15.9)			2.87, dd (4.8, 15.6)		
5	6.82, d (8.2)	131.1	CH	6.85, d (8.3)	131.5	CH
6	6.28, dd (2.4, 8.2)	109.1	CH	6.36, dd (2.0, 8.3)	109.6	CH
7	-	158.8	C	-	158.0	C
7-OH	9.16, s	-	-			

8	6.18, d (2.4)	103.3	CH	6.33, d (2.0)	103.5	CH
9	-	155.9	C	-	155.9	C
10	-	112.4	C	-	112.4	C
1'	-	131.7	C	-	132.2	C
2'	6.72, d (2.0)	115.7	CH	6.82, d (2.0)	114.8	CH
3'	-	146.5	C	-	146.3	C
3'-OH	8.88, s	-	-	9.45 s	-	-
4'	-	146.3	C	-	146.4	C
4'-OH	8.84, s	-	-	-	-	-
5'	6.67, d (8.0)	116.0	CH	6.76, d (8.3)	116.3	CH
6'	6.59, dd (2.0, 8.0)	119.2	CH	6.72, dd (2.0, 8.3)	119.6	CH
Xylose	-	-	-	data of Anadanthoside from (Piacente et al., 1999)		

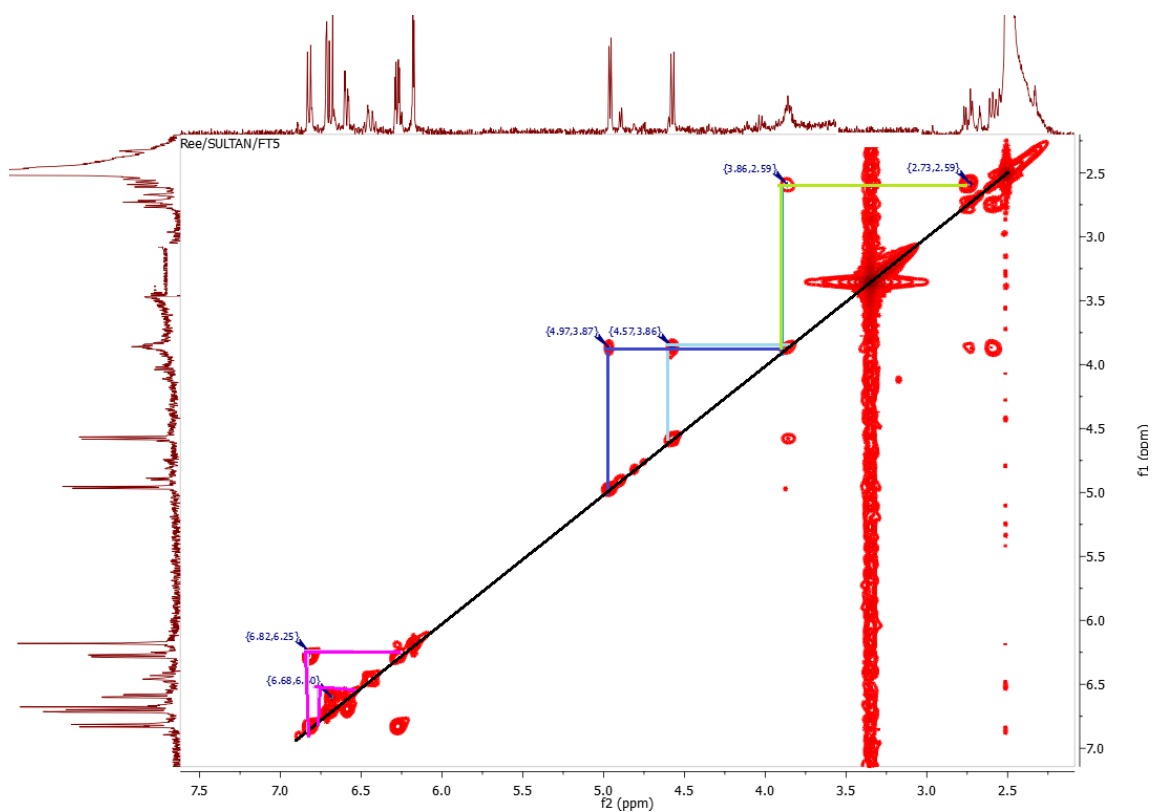


Figure 7.22: COSY spectrum of the compound present in CF6-F5 (400 MHz, d-DMSO)

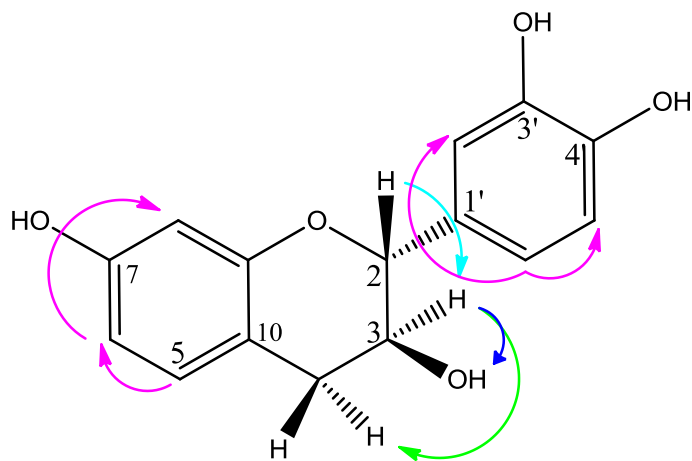


Figure 7.23: COSY correlations of F6-f5. The coloured arrows show the correlations corresponding COSY correlations in Figure 7-22.

From ^1H NMR spectra there were signals of aromatic protons at 6.82 ppm (1H, *d*, $J=8.2$ Hz, H-5), at 6.28, (1H, *dd*, $J= 2.4, 8.2$ Hz, H-6) and at 6.18 ppm (1H, *d*, $J=2.4$

Hz, H-8) and also a hydroxyl protons at 9.16 ppm, s on C-7. It was also possible to assign aromatic region protons in the B ring at 6.72(1H, d, J=2.0 Hz, H-2'), 6.67 (1H, d, J=8.0 Hz, H-5') and 6.59 (1H, dd, J=2.0, 8.0 Hz, H-6') referable to 1', 3', 4' -tri-substituted ring B of flavonoids skeleton.

The summary of NMR data in Table 7.6 indicates that most of the data for the compound in F6-F5 corresponded to those reported previously for the compound anadanthoside (Piacente et al., 1999). Thus the structure of compound 1 (CF6-F5) was elucidated as 3, 4-dihydro-2-(3, 4-dihydroxyphenyl)-2H-chromene-3, 7-diol.

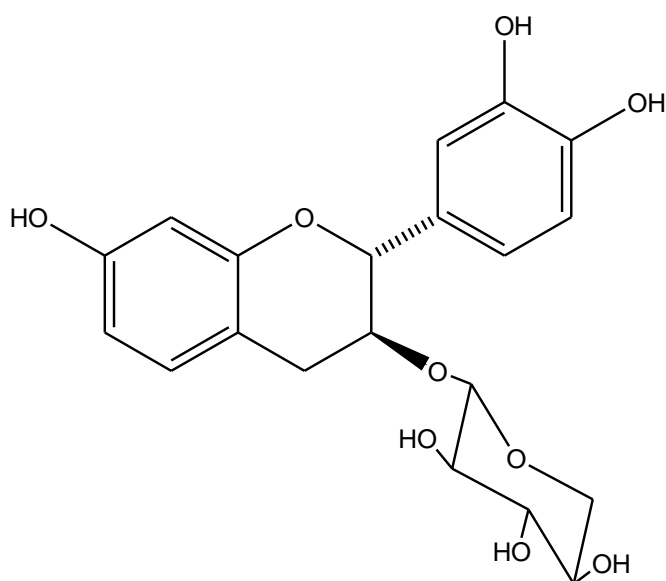


Figure 7.24: The structure anadanthoside (Piacente et al., 1999) that data were compared to proposed structure for F6-F5.

7.3.5.2 Characterisation of Flavonoids compound (CF6-F6)

The CF6-F6 was obtained as a sticky yellow solid $[\alpha]_{\text{D}}^{-16^{\circ}}$ (*c.* 0.1, CHCl_3) and yielded 25.7 mg. It had a molecular formula $\text{C}_{20}\text{H}_{21}\text{O}_9$ and a molecular ion $[\text{M} + \text{H}]^+$ at m/z 405.1170 was detected using Orbitrap high-resolution mass spectrometer (Figure 7.27) and were eluted as non-polar compounds on liquid chromatography - UV-ELSD (Figure 7.26).

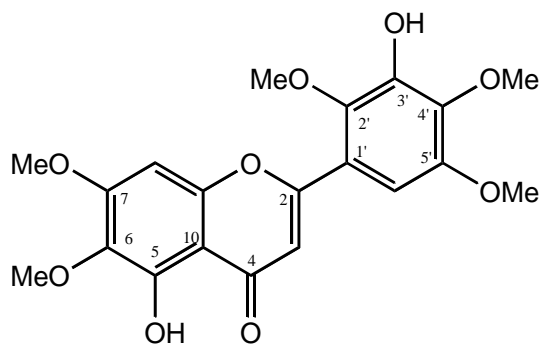


Figure 7.25: Structure of CF6-F6 psiadiarabin 1

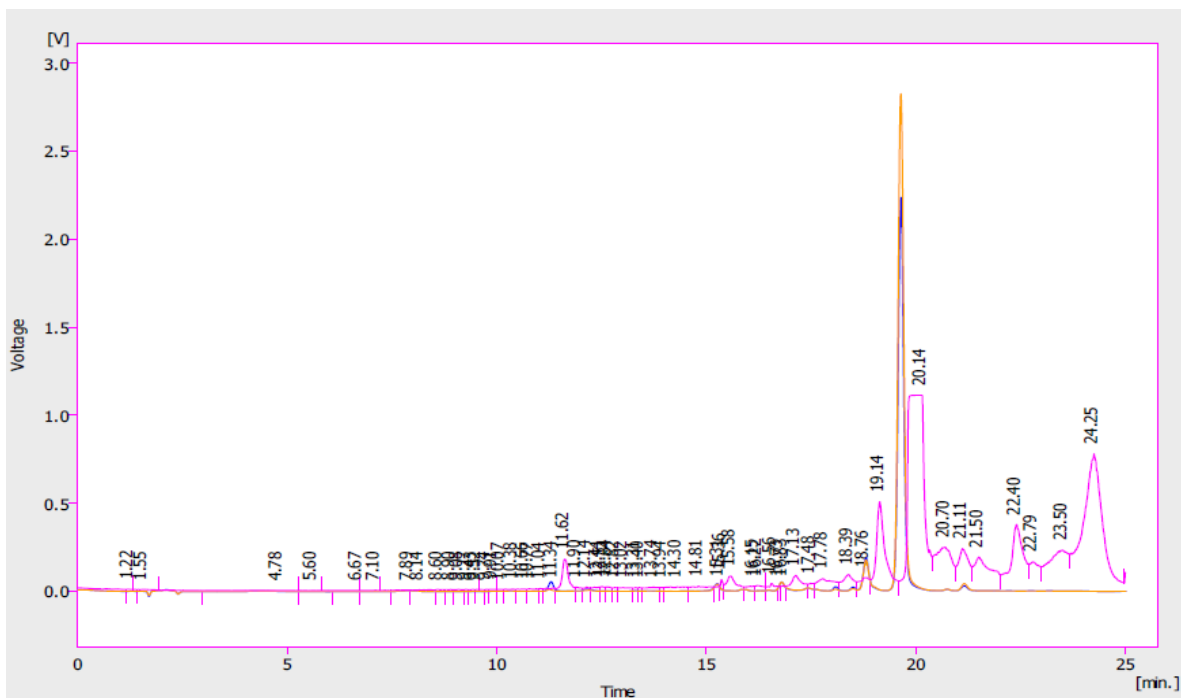
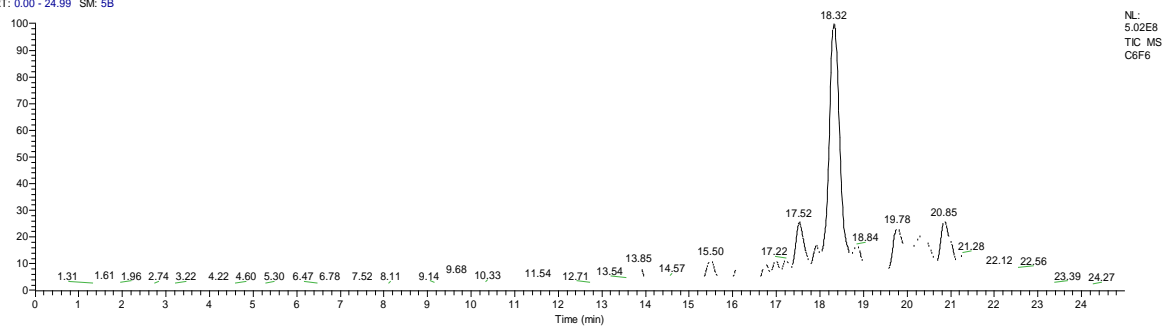


Figure 7.26: LC-UV-ELSD chromatogram of CF6-F6 purified from CC (conditions in section 7.2.3.1)

RT: 0.00 - 24.99 SM: 5B



NL:
5.02E8
TIC MS
C6F6

C6F6 #1968 RT: 18.34 AV: 1 NL: 2.75E8
T: FTMS + c ESI Full ms [75.00-1500.00]

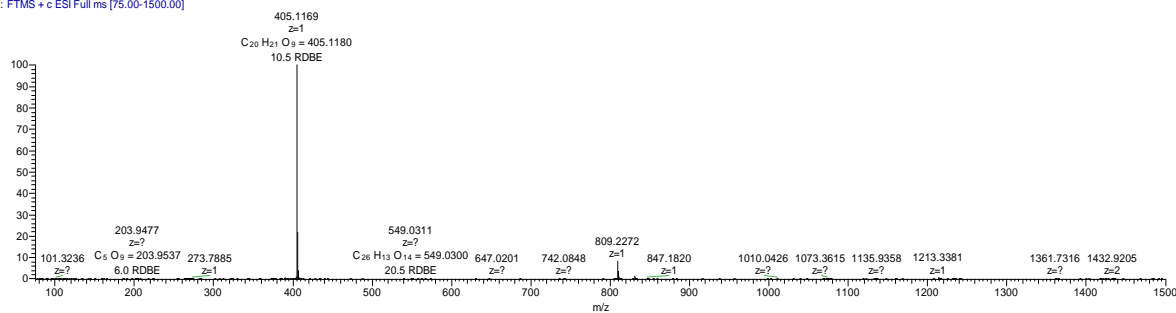


Figure 7.27: HR-ESIMS ion chromatogram and mass spectrum of CF6-F6

Table 7.7: ^1H NMR (400 MHz) and ^{13}C NMR (100 MHz) data of compounds CF6-F6 (400 MHz, DMSO- d_6)

<i>Experimental compound 2 CF6-F6</i>				<i>Psiadiarabin1(El-Feraly et al., 1990)</i>	
Position	δ_{H} , mult.	δ_{C}	^{13}C Type	δ_{C}	^{13}C Type
1					
2	-	162.9	C	161.7	C
3	6.81s	109.2	CH	109.6	CH
4	-	182.5	C	182.9	C
5	-	152.4	C	153.0	C
5-OH	12.8 s				
6	-	132.2	C	132.7	C
7	-	159.1	C	158.9	C
8	6.90 s	92.1	CH	90.6	CH
9	-	153.4	C	153.5	C
10	-	105.7	C	106.2	C
1'	-	119.8	C	119.6	C
2'	-	140.9	C	141.3	C
3'	-	145.0	C	143.5	C
3'-OH		9.45 s			
4'	-	142.3	C	139.5	C
5'	-	149.8	C	148.9	C
6'	6.92 s	102.4	CH	102.6	CH
6-OMe	3.74 s	61.0	CH ₃	61.2	CH ₃
7-OMe	3.93 s	57.0	CH ₃	61.1	CH ₃
2'-OMe	3.80 s	60.9	CH ₃	60.8	CH ₃
4'-OMe	3.76 s	60.5	CH ₃	56.5	CH ₃
5'-OMe	3.87s	56.6	CH ₃	56.4	CH ₃

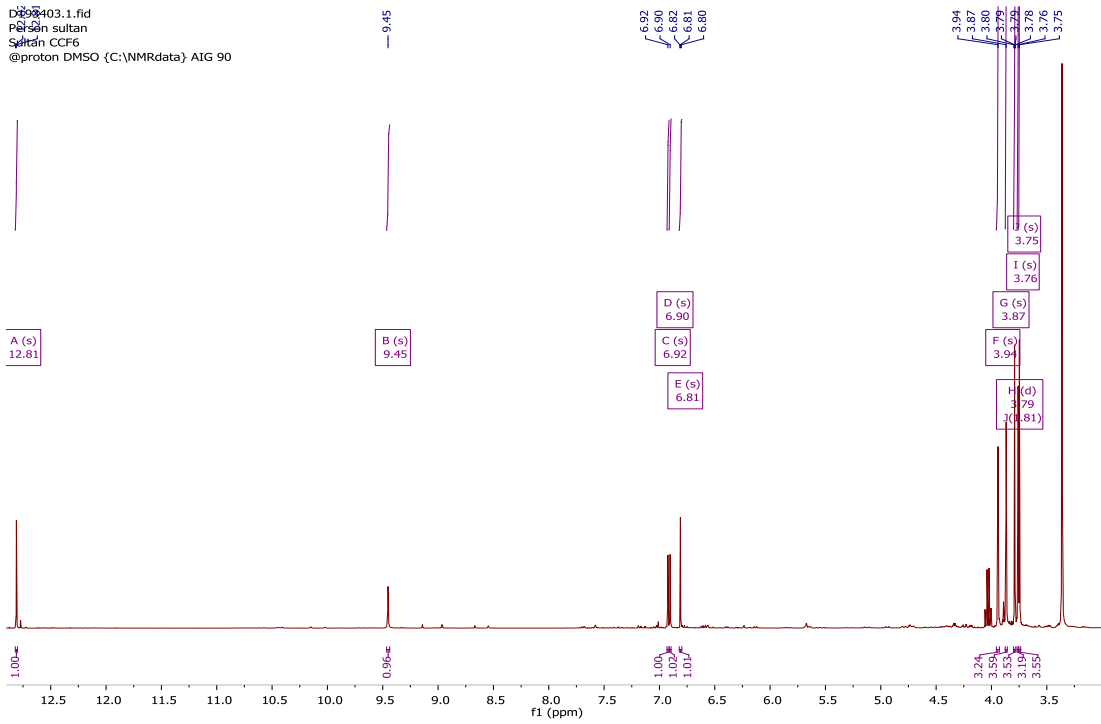


Figure 7.28: ^1H NMR of CF6-f6 (400 MHz, DMSO- d_6).

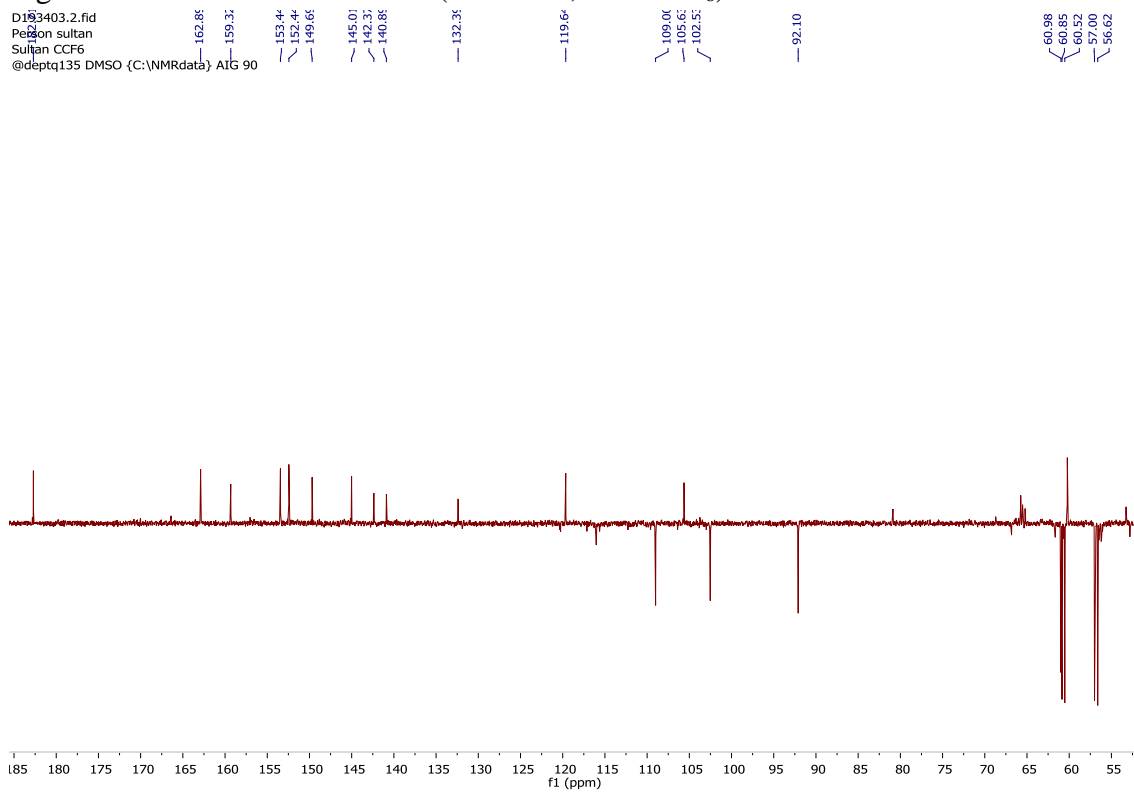


Figure 7.29: ^{13}C NMR spectrum of CF6-F6 (100 MHz, $-\text{DMSO-d}_6$).

The NMR data (400 MHz, DMSO-d_6) were compared to those of psiadiarabin which exactly matched those reported for psiadiarabin 1 (El-Feraly et al., 1990, Alyahya et al., 1987) previously isolated from the aerial parts of *Psiada arabica*.

From ^1H NMR and ^{13}C NMR spectra (Figures 7-28, 7-29) revealed the presence of five methoxyl groups at C-6, C-7, C-2', C-3', C-4' and C-5' were clearly observed as well as the presence of a keto group at δ_{C} 182.5 ppm.

Three aromatic protons at 6.81, 6.92 and 6.90 as singlet and two exchangeable hydroxyl group at 12.8 (s, C-5) and 9.45 (s, C-3') were shown on ^1H NMR and

This suggests that the compound was identical to be psiadiarabin 1 (5, 3'-dihydroxy-6, 7, 2', 4', 5'-pentamethoxyflavone, 1) Figure 7-30 (El-Feraly et al., 1990, Piacente et al., 1999, Mossa et al., 1992).

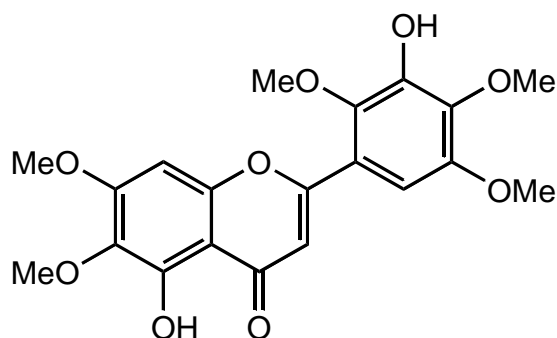


Figure 7.30: Psiadiarabin 1 structure (El-Feraly et al., 1990).

7.3.5.3 7.3.5.3 Characterisation of diterpene compound CF7-M1

CF7-M1 (compound 3) was obtained as a yellow solid [α]_D -65° (*c.* 0.1, CHCl₃) and yield (9.5 mg). On the TLC plate, it appeared as violet spot when sprayed with anisidine but without any spot being observed under UV light. As the chromatographic trace obtained on liquid chromatography -UV-ELSD is shown in figure 7.33 and indicates that the fraction is more or less composed of a single component. The HR-ESI-MS in positive mode displayed an [M+H]⁺ ion at 319.2256 (calc 319.2268) suggesting the molecular formula of C₂₀H₃₁O₃.

Compound 3 showed a set of deshielded protons typical of an exomethylene (CH₂) group at δ_{H} 4.81 and 4.86 ppm and a methine proton δ_{H} 4.16 ppm attached to an oxygen bearing carbon at δ_{C} 68.6 ppm. It also showed two methyl singlets at δ_{H} 1.26 and 1.35 and a set of methylene protons (on an oxygen bearing carbon at δ_{C} 69.0) at 3.41, 4.12 ppm (2H, m).

The number of carbons in its ¹³C spectrum was typical of a diterpene and based on its COSY, HMBC (Fig. 7.36, 7.38) and HMQC correlations the compound was identified as a kaurane type diterpene as follows: The methyl group at 1.35 ppm showed long range correlations (HMBC) to the methylene at 52.1 ppm and the oxymethylene carbon at 69.0 ppm thus this methyl group must be at C-4. The correlations from the methylene protons at 4.12 ppm and 3.41 ppm (H-19) to the methyl at δ_{C} 31.1 ppm (C-18) indicated that this oxymethylene group was also at C-4. The position of the second oxygenated carbon was obtained by the correlations from the methine proton at 1.36 ppm (H-5) to an oxygenated carbon at δ_{C} 67.6 ppm. The COSY spectrum as well as HMBC correlations indicated methylene protons at C-1, C-3 and C-7 therefore this oxymethine carbon must be at C-6. Correlations to and from the rest of the protons and carbons indicated that the exomethylene group was on a kaurane ring moiety and this was confirmed by correlations observed for the exomethylene protons as well as correlations to the quaternary double bonded carbon. The structure was confirmed by comparison with previous literature reports (Eldomiaty et al., 1993, Mossa et al., 1992) for similar compounds (psiadin, 2). Accordingly, compound 3 (propsiadin) was identified as (ent)-2-oxokaur-16-en-6,

18-diol. Thus it was proposed that the structure was as shown in Figure 7.31. The proposed structure of this compound was not matched in any databases but it was closely similar to Psiadin [118]. Thus it is a novel diterpene.

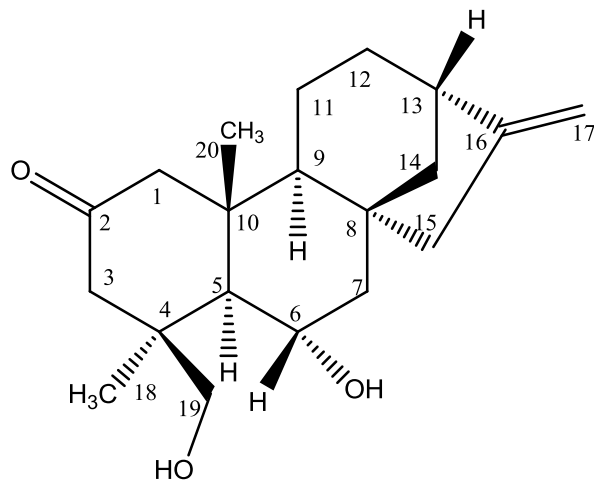


Figure 7.31: Chemical structure of CF7-M1.

Table 7.8: ^{13}C NMR (100 MHz) and ^1H NMR (400 MHz) chemical shifts for CF7-M2 (400MHz, CDCl_3) and Diterpene 3 (75MHz, pyridine- d_5).

(CF7-M1) Compound 3				Diterpene 3 (Eldomiaty et al., 1993)
Chemical shift δ in ppm				
Position	δ_{H}	δ_{C}	Type ^{13}C	δ_{C}
1	1.94, 2.55	56.0	CH_2	46.6 t
2	-	211.5	$\text{C}=\text{O}$	211.8 s
3	2.11, 2.40	52.1	CH_2	55.7 t
4	-	42.4	C	47.3 s
5	1.36	58.0	CH	53.6 d
6	4.16	67.6	CH	67.9 d
7	1.69, 1.82	50.6	CH_2	50.6 t
8	-	44.2	C	44.0 s
9	1.27	54.8	CH	54.1 d
10	-	44.0	C	43.0 s
11	1.45, 1.74	18.4	CH_2	18.8 t
12	1.57	32.7	CH_2	32.9 t
13	2.71	44.1	CH	44.1 d
14	1.34, 1.92	39.6	CH_2	39.6 t
15	2.19, 2.15	48.6	CH_2	49.0 t
16	-	154.0	C	154.0 s
17	4.81, 4.86	104.1	CH_2	104.0 t
18	3.41, 4.12	69.0	CH_2	70.1 t
19	1.35	31.1	CH_3	65.1 t
20	1.26	20.3	CH_3	20.5 q

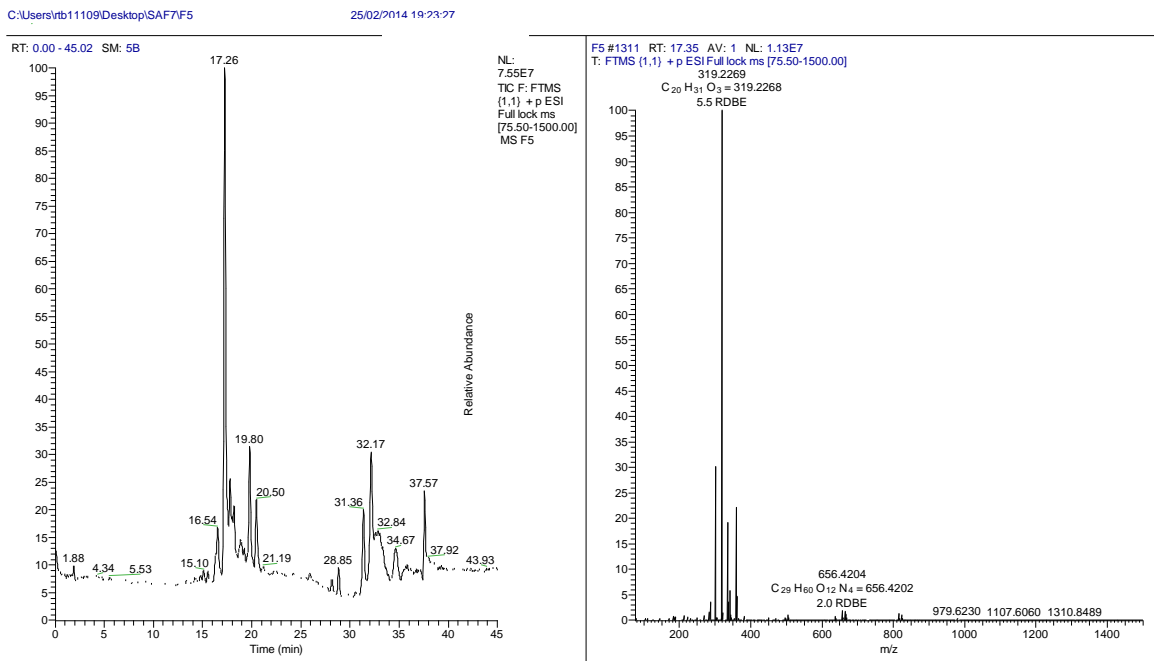


Figure 7.32: Positive ion HR-ESIMS extracted ion chromatogram and mass spectrum of CF7-M1

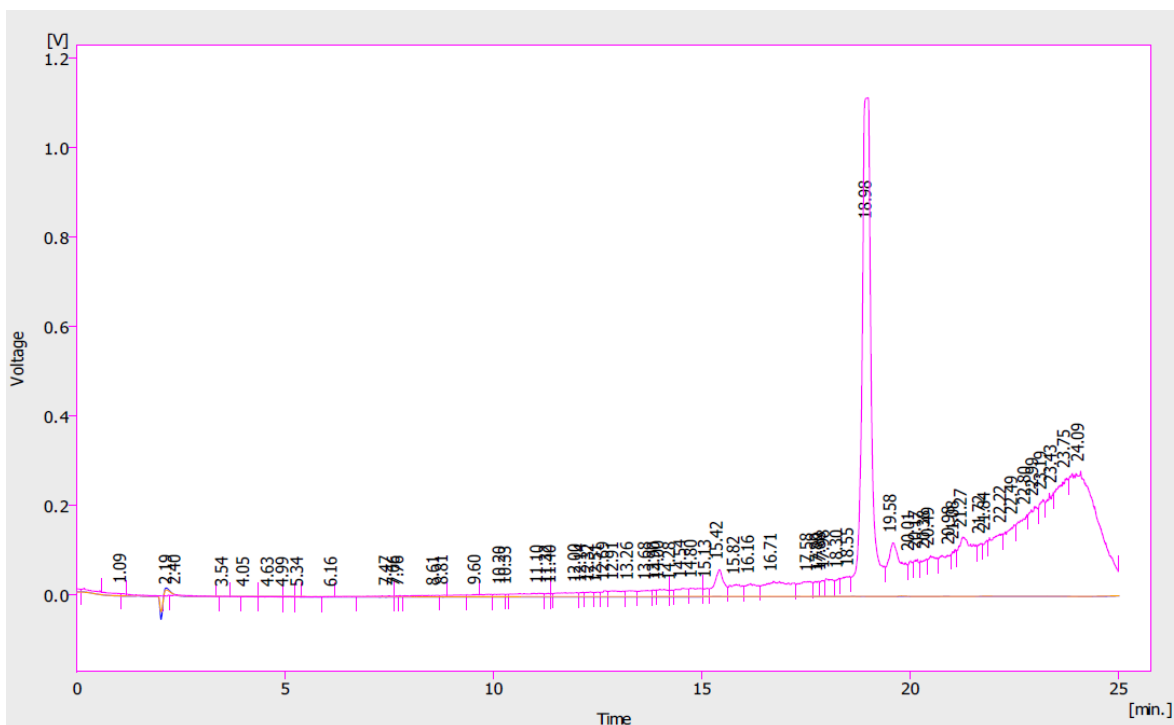


Figure 7.33: LC-UV-ELSD Chromatogram of CF7-M1 Purified from Grace flash chromatography (in section 7.2.3.2) ELSD trace in pink.

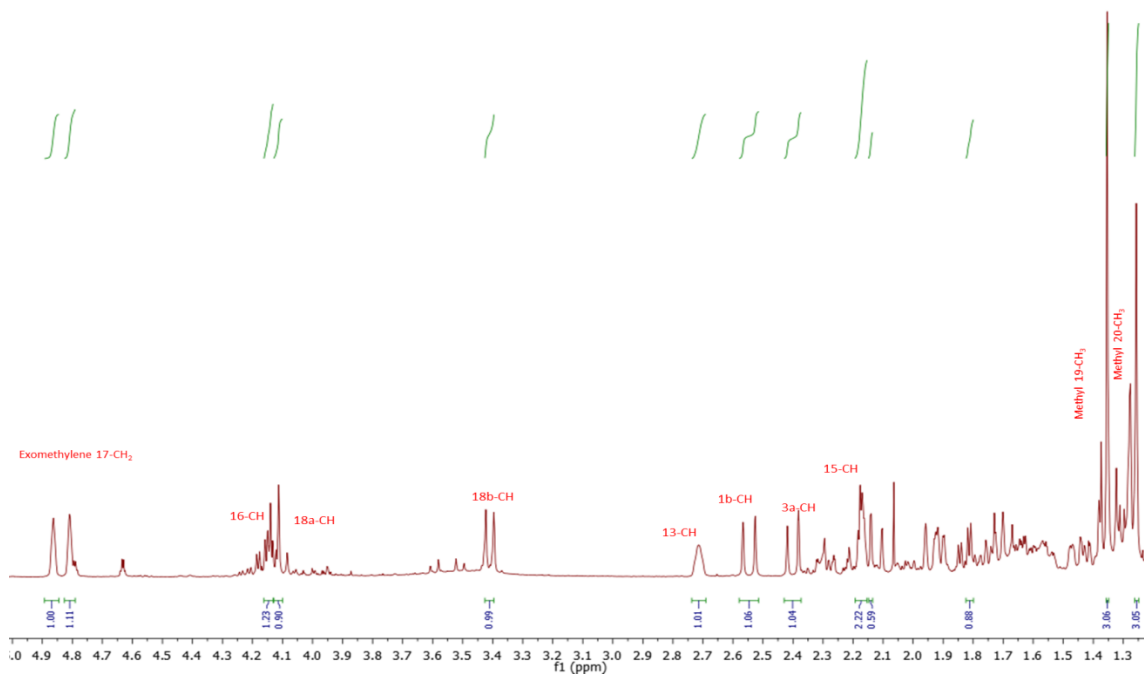


Figure 7.34: ^1H NMR of CF7-M1 (400 MHz, CDCl_3)

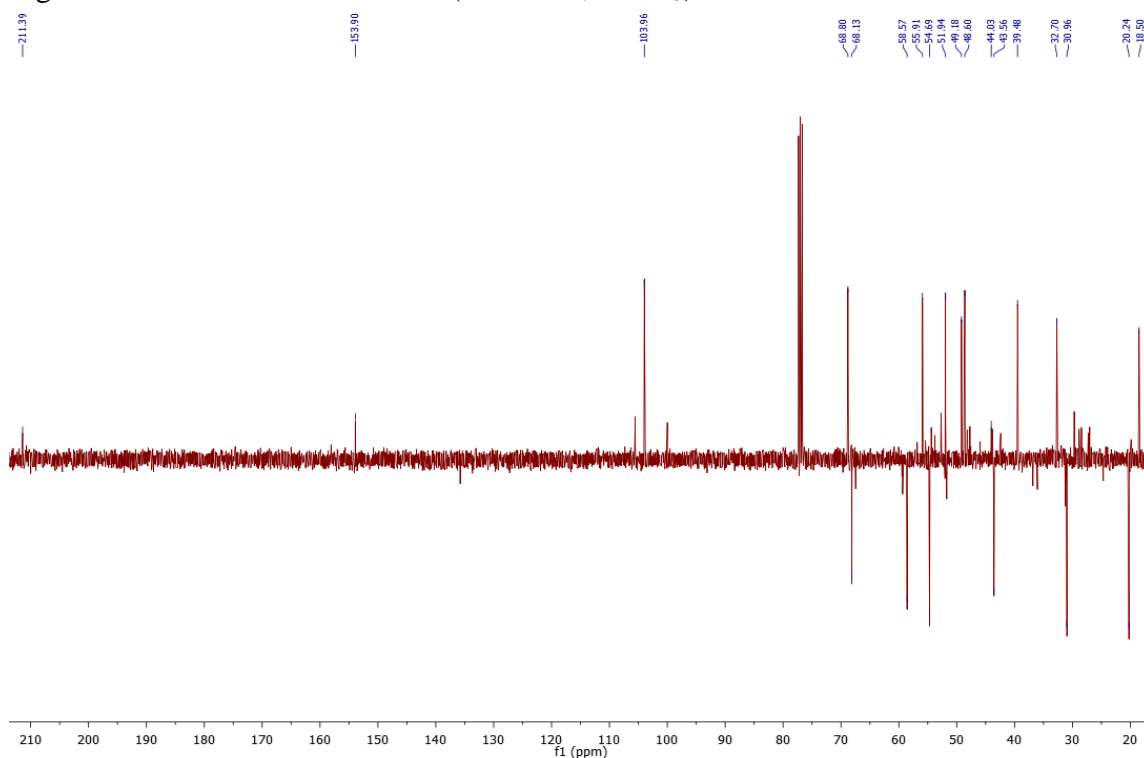


Figure 7.35: The DEPT Q ^{13}C NMR spectrum of CF7-M1 (100 MHz, CDCl_3)

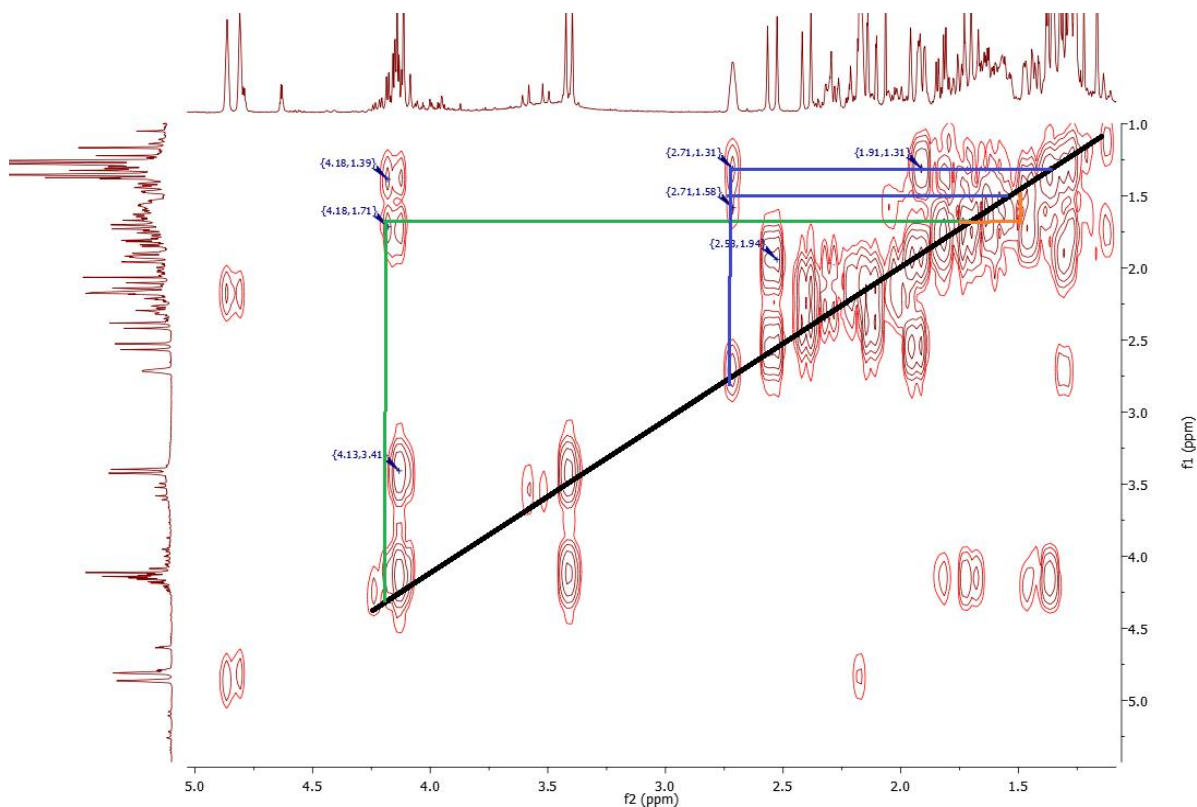


Figure 7.36: COSY spectrum of the CF7-M1 structure showing the correlations mentioned in the discussion above and shown in figure 7-31.

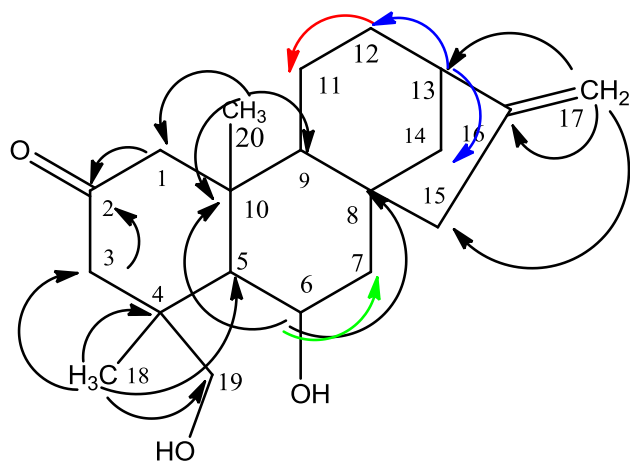


Figure 7.37: Key HMBC (\rightarrow) and COSY correlations. The colours arrows show the corresponding to the COSY correlations in Figure 7-36.

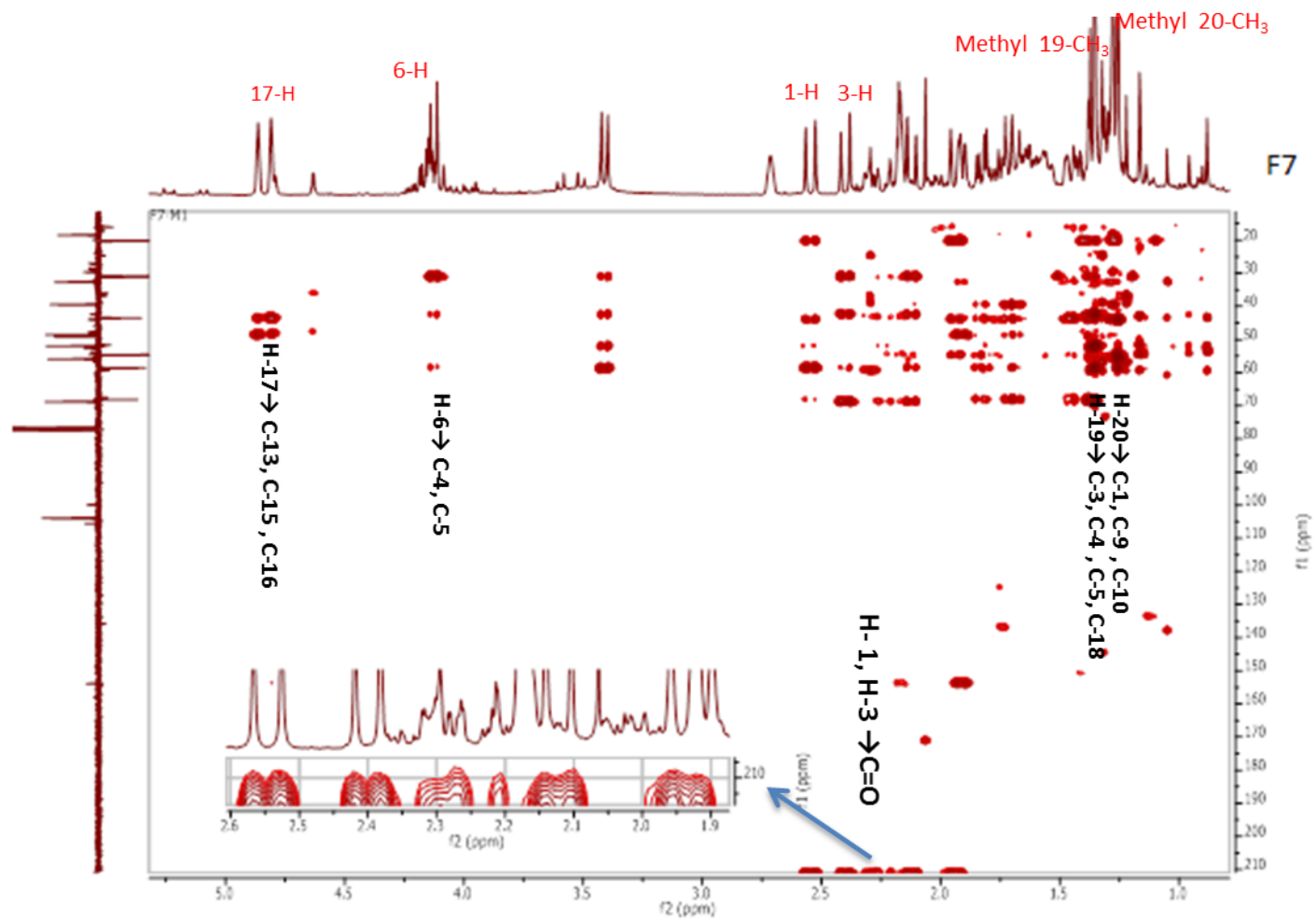


Figure 7.38: HMBC correlations of CF7-M1.

The NOESY spectrum of the compound gave its relative stereochemistry as follows: The H-20 at 1.26 ppm gave strong correlations to one of the H-19 (CH₂OH) protons and H-6 proton thus they are all axial. Therefore the C-18 methyl and C-6 OH are equatorial. The C-5 proton must be trans-diaxial with the C-20 methyl as no correlation was observed between them in the nOe spectrum of the compound (Figure 7.39). Figure 7.40 shows the MS² data obtained for compound 3.

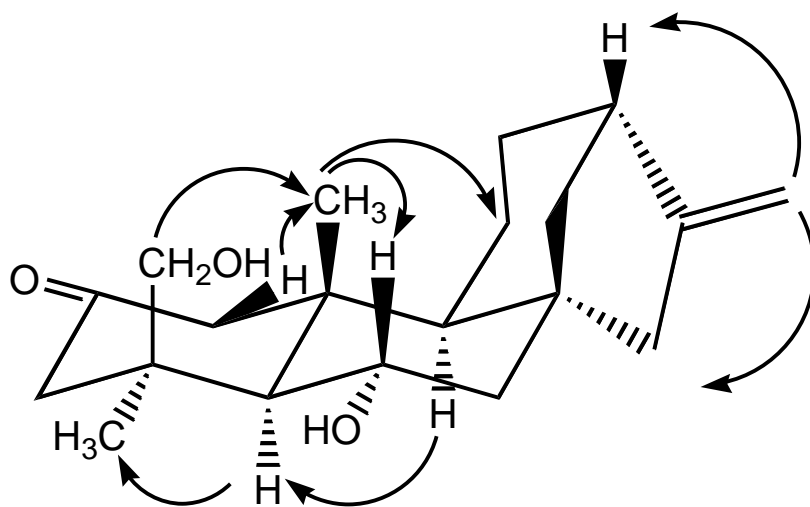
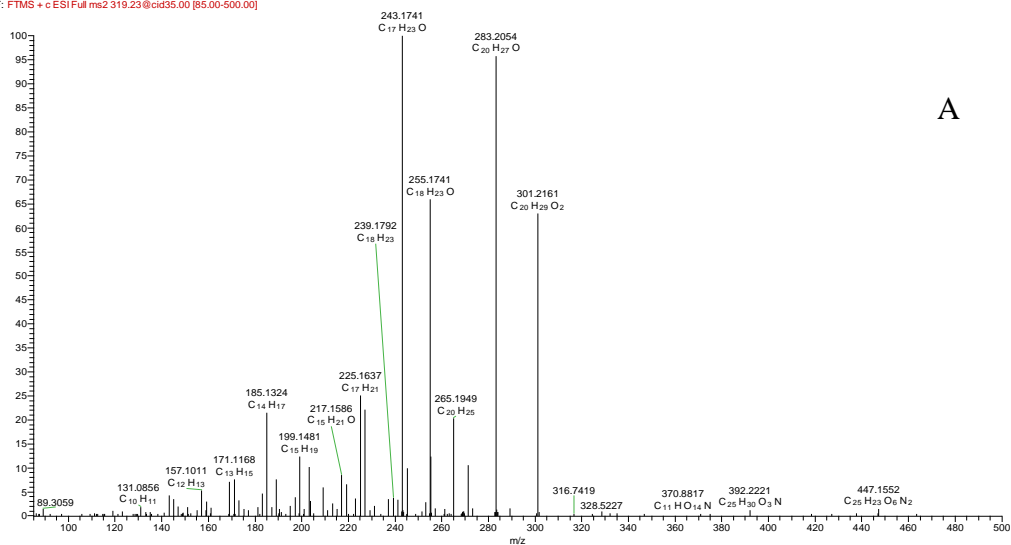
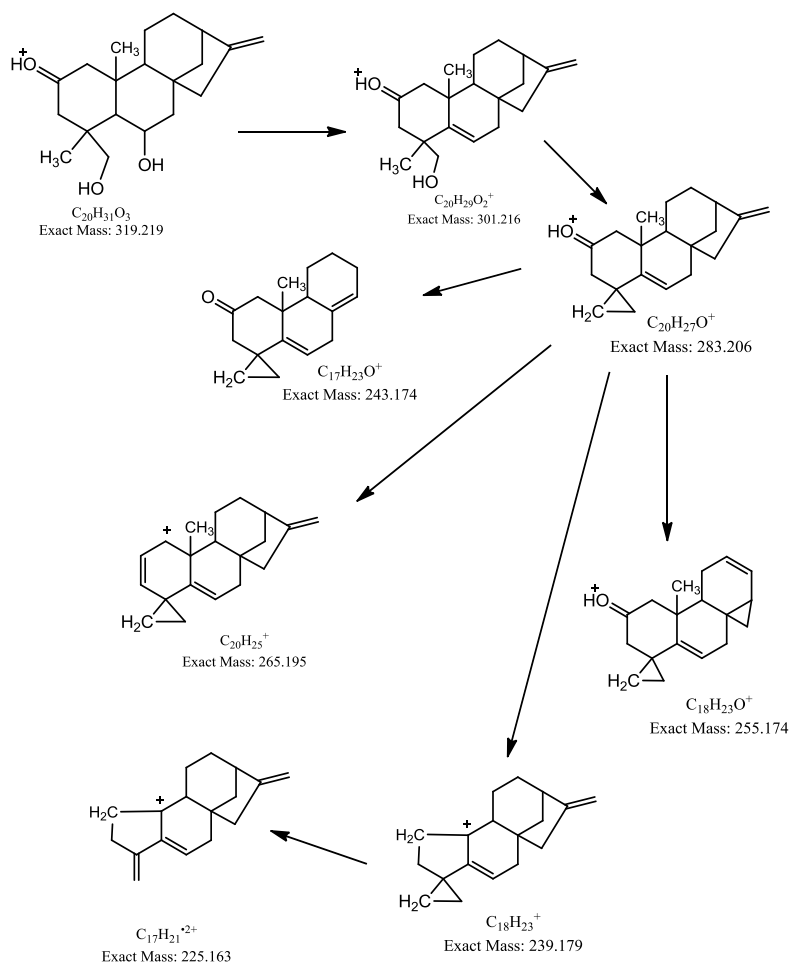


Figure 7.39: nOe interactions observed in the NOESY spectrum for CF7-M1 (compound 3)



A



B

Figure 7.40: Fragmentation of m/z 319.2256 $[M+H]^+$. (A) Mass spectrum for ion using the LTQ-Orbitrap. (B) The proposed fragmentation pathway of compound 3 ($C_{20}H_{31}O_3$).

7.3.5.4 Characterisation of diterpene compound CF7-M5

CF7-M5 (compound 4) was obtained as a white powder $[\alpha]_D -169^\circ$ (*c.* 0.1, CHCl_3) and the weight of the fraction was 80.0 mg. It displayed a protonated molecular ion which like that of compound 3 corresponded to the molecular formula $\text{C}_{20}\text{H}_{30}\text{O}_3$ obtained from HRESI MS $[\text{M}+\text{H}]^+$ ion at 319.2256 ($\text{C}_{20}\text{H}_{31}\text{O}_3$ calc 319.2268). The NMR data of 4 showed that the second hydroxy group was not in position C-6 as in 3 but at C-19. The mutual correlations in the HMBC spectrum between the hydroxymethyl groups showed that they were geminal. Thus it was proposed that the structure corresponded to the diterpene psiadin which had previously been isolated from *Psiada arabica* (Eldomiaty et al., 1993, Mossa et al., 1992). The ^{13}C and ^1H data for compound 4, psiadin comparable to the literature (Table 7.9). The key differences from compound 3 in the NMR spectra were due to the presence of two oxymethylene groups at 65.2 and 70.8 ppm and the absence of the methyl group which was at 31.1 ppm in compound 3. The oxymethine proton at position which was at 4.16 ppm (attached to an oxygen bearing carbon at 68.3 ppm) in compound 3 is absent and is replaced by a methylene group with protons at 1.76 and 1.48 ppm and the carbon at position 7 is further up field in 4 shifting from 50.6 to 40.4 ppm. In the HMBC spectrum these protons correlate with the proton at C-5. The protons attached to carbon 7 are now in a more symmetrical environment and form a broad incompletely resolved signal rather than having two distinct shifts as in compound 3. Otherwise the spectrum of 4 was similar to that of 3 and the ^{13}C shifts corresponded to those in the literature (Midiwo et al., 1997). None of these compounds had been isolated from propolis before.

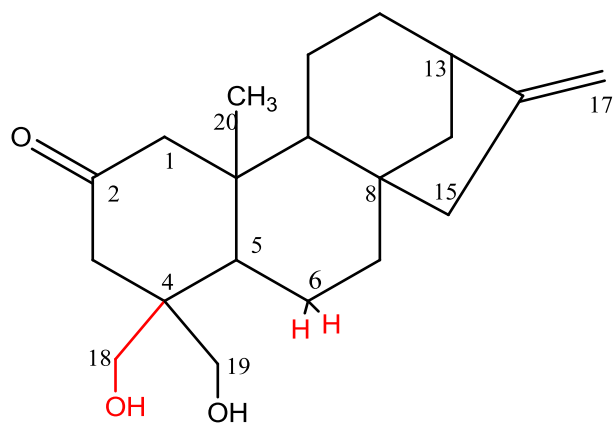


Figure 7.41: CF7-M5 structure compound 4. The differences between this compound and Compound 3 are highlighted.

Table 7.9: ^1H NMR (400 MHz) and ^{13}C NMR (100 MHz) data of compound 4 in CDCl_3 . Highlighted rows indicate the differences from Compound 3.

Experimental compound 4 CF7-M5			
Position	δ_{H} in ppm	δ_{C}	Multiplicity
1	2.59, 1.96	55.9	CH_2
2	-	213.3	C
3	2.67, 2.39	44.7	CH_2
4	-	46.4	C
5	1.60	50.4	CH
6	1.76, 1.48	20.9	CH_2
7	1.57	40.4	CH_2
8	-	44.0	C
9	1.34	54.7	CH
10	-	43.9	C
11	1.70, 1.47	18.4	CH_2
12	1.54, 1.65	32.6	CH_2
13	2.67	43.4	CH
14	1.15, 1.90	39.2	CH_2
15	2.11	48.5	CH_2
16	-	154.7	C
17	4.86, 4.81	103.7	CH_2
18	3.87, 3.53	70.8	CH_2
19	3.77, 3.75	65.2	CH_2
20	1.09	19.3	CH_3

7.4 Biological Testing of Components Isolated from Saudi Arabian Propolis

7.4.1 Anti-Trypanosomal and Anit-mycobacterium activity

Screening of both pure compounds, crude extracts and fractions were performed in vitro to determine their activity against the bloodstream form of *Trypanosoma brucei brucei* using an Alamar Blue™ assay as previously described in 2.10.1. Initially the tests were carried out at a single concentration of 20µg/ml and the results obtained are presented in Table 7.3.

The concentration range of isolated compounds (in µg/mL) from Saudi propolis were tested against organisms to determine the minimum inhibitory concentration (MIC) values, where the concentrations at which cell inhibition was more than 90% were taken and converted to µM (Table 7.10).

Table 7.10: MIC against *M. marinum* and *T. brucei*

Compound	%	<i>D</i>	MIC	%	<i>D</i>	MIC
	<i>Control</i> 100µg/ml	(µM) <i>M. marinum</i>		<i>Control</i> (20µg/ml)	(µM) <i>T. brucei</i>	
Fisetinidol	111.2	-	-	64.5	-	-
Psiadiarabin 1	3.4	61.9	30.9	4.2	78.1	30.9
propsiadin	13.7	312.1	78.1	7.2	78.1	78.1
psiadin	-0.9	312.1	78.1	1.0	78.1	78.1
Psiadiarabin 2	-	-	-	4.4	-	-
Suramin						0.125
Gentamycin			13.48			-

7.5 Discussion

The fractionation and purification of the ethanol extract of Saudi propolis using different chromatographic techniques led to the isolation of a new diterpene propsiadin ((ent)-2-oxo-kaur-16-en-6,18-diol) (3) along with known flavonoids 3, 4-dihydro-2-(3, 4-dihydroxyphenyl)-2H-chromene-3,7-diol (1), 5, 3'-dihydroxy-7, 2', 4', 5'-tetra-methoxyflavone (2), diterpene psiadin (4) and psiadiarabin 2 (5). These were isolated from the Saudi Arabian propolis using silica gel column chromatography to obtain pure compounds 1, 2 and 5, while from fraction no. 7 compounds 3 and 4 were isolated by using Grace Reveleris® iES Flash Chromatography. Three compounds (2, 3 and 4) exhibited moderate activity against *T. b. brucei* and *M. Marinum* while Compound 1 was inactive against these organisms

It is suggested that one of the potential plant sources visited by *Apis mellifera* in Assir region could be the Compositae family (*P. arabica* and *P. punctulata*, *P. Coronopus*, *P. Salviifolia*), some of whose species (e.g. *P. punctulata*) are widespread in East Africa and the leaf extracts are used in alternative medicine for treating conditions such as fevers, colds, stomach ulcers and ectoparasites from cattle (Midiwo et al., 1997). The term Psiadis is derived from the Greek word *psiados* (a drop) which describes the exudate from the leaves of this plant (Quattrocchi, 2012) and this exudate might be readily obtained by the bees. Some of the isolated compounds of types *P. Trinervia* were found to possess biological activity against some bacteria and fungi (Albar, 2014).

Thus, the profiles of chemical compounds reported in this study showed similarities to the results for the compounds that were isolated from *P. punctulata* in Saudi Arabia that were published in 2009 (Albar, 2014) in which it was shown that the major components of *Psiadia* species were flavones and kaurene type of diterpenes as summarised Figure 7.42.

Two pure diterpenes F7-M1 and F7-M5 of the kaurene type were obtained from fraction no.7 and it was found that M7-M1 (compound 3) was a novel diterpene which made it necessary to perform intensive analysis in order to determine its

structure using HR-ESI-MS, 1D and 2D NMR. The F7-M5 was identified as being related to compound 3 (F7-M1) and was found to be psiadin which had earlier been isolated from *Psiadia* species.

The diterpene compounds displayed moderate activity against *M. marinum*. However, in its partially isolated form, fraction (CF7) showed a higher activity against *T. b. brucei* at the initial concentration tested (20µg/ml) where cell viability corresponded to 1.8% of control (Table 7.3). The fact that on further purification the activity decreased might be explained by the possibility that there might be synergistic activity between the two compounds against the organism's *bloodstream* forms. Compound 4 (psiadin) was observed to be the most active with MIC of 78.1µM against *T. b. brucei*. Previous studies on the biological activity of kaurene diterpenes isolated from *Psiadia* species have reported that these diterpenes have a stimulating effect on uterine contraction and on the brain (El-Shafae and Ibrahim, 2003).

The flavonoid compounds 1 and 2 (Fisetinidol and Psiadiarabin 1) were isolated from fraction 6 (CF6) and tested against *T. b. brucei*. It was observed that compound 2 was significantly active at 20µg/ml concentration and with a MIC of 30.9 µM, while the compound 1 was not active against the same organism.

The psiadiarabin flavonoids (compounds 2 and 5) are of a new type distinct from those that had previously been isolated from propolis. Compound 1 was first isolated in 1987 from *P. Arabica* (Alyahya et al., 1987) and the current study reports for the first time the testing of this compound against microorganisms. However, some studies have reported on the biological activity of 3-methoxyl flavones which possess activity against some of bacteria and fungi (Wang et al., 1989). The activity of compound 2 against *M. marinum* is quite high and is of interest since anti-mycobacterial activity has not been reported very widely for propolis extracts. It is likely there are many other components yet to be isolated from this type of propolis. Returning to the data in table 7-4 it is possible to see two more flavonoids in the LC-MS run which are closely related to compound 1. The compound with a formula $C_{18}H_{17}O_8$ suggests a structure in which compound 1 has one less methyl group and

the formula $C_{21}H_{23}O_9$ suggests addition of an extra methyl group and a methoxy group. Neither of these compounds corresponds to any of the structures shown in Figure 7-42.

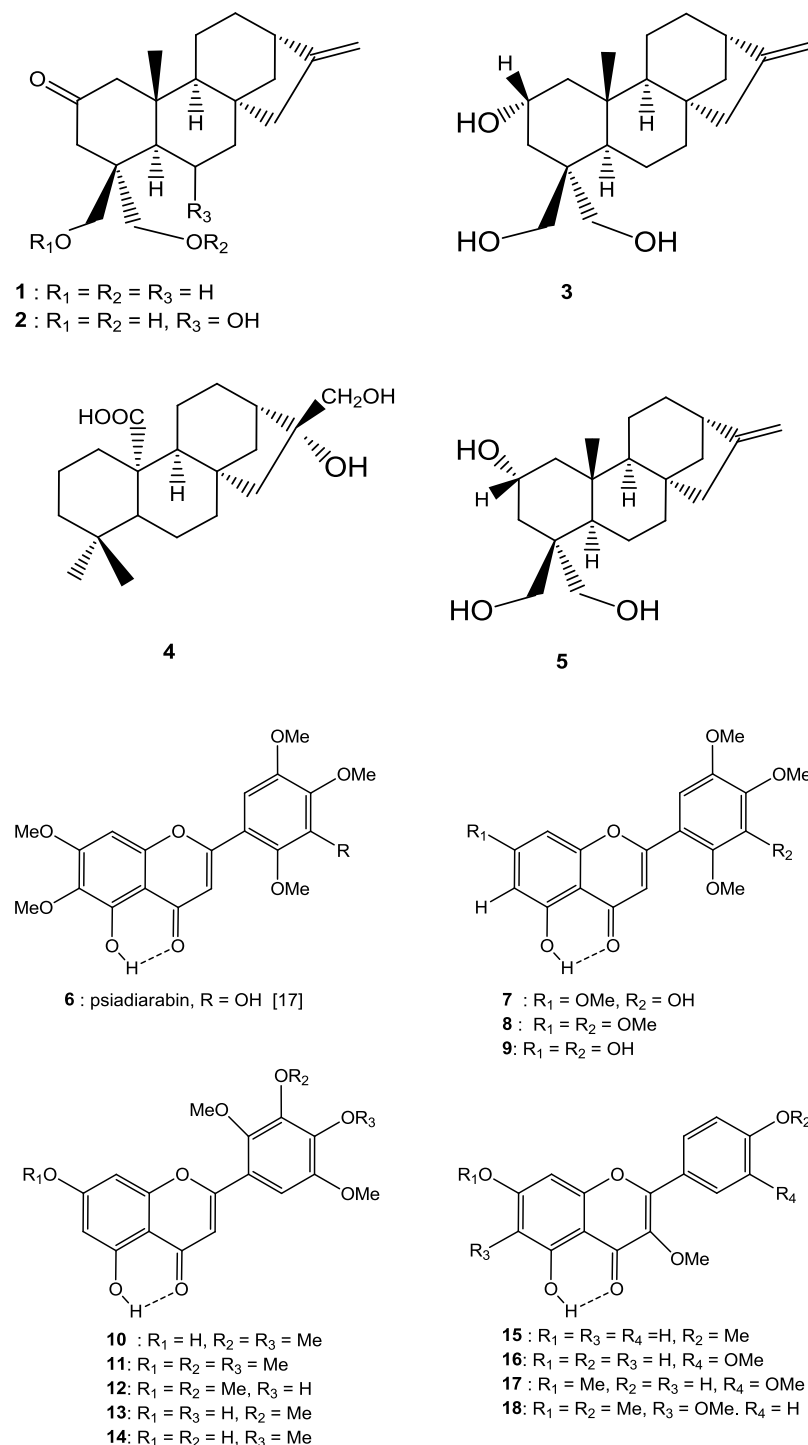


Figure 7.42: Flavonoids and diterpenes isolated of *Psiadia* species (Albar, 2014)

CHAPTER 8:
GENERAL DISCUSSION

8 GENERAL DISCUSSION

Patients who become infected by trypanosomiasis still have to rely on a limited number of medicines that have restricted efficacy and substantial side effects. Increasing the number of options of available safe and efficacious medicines for managing this disease is an essential medical research intervention. The demand for discovery of novel anti-trypanosoma medicines has led to many researchers across the world seeking solutions from naturally occurring substances.

Propolis, which is one of several products produced by honeybees, was selected for investigation in this work because some of its components have been previously reported to possess potential activity against parasites and against mycobacteria *in vitro*. The exciting finding, from previous studies that a phloroglucinone isolated from Cameroonian propolis (Almutairi et al., 2014) was strongly potent (with an MIC of 0.348 μM *in vitro*) against *T. brucei* led us to initially attempt isolation of this compound from other African propolis samples. Ninety one (n=91) propolis samples from different geographical origins (mainly Africa) were initially screened, following extraction with ethyl acetate, by liquid chromatography/mass spectrometry profiling. At the same time, minimum inhibitory concentrations (MICs) for these extracts were determined against *T. brucei*. As can be seen in Table 3.1, Chapter 3 page 52 the samples displayed varying degrees of activity against the parasite. LC-MS screening indicated that some of them might contain propolones although this information was inconclusive. This was mainly because of the possibility of other active lead compounds being present in some of the propolis samples from other classes of natural products such as prenylated flavonoids or terpenoids. These compounds have similar elemental composition and levels of unsaturation with high oxygenation levels as phloroglucinones, although in terpenoids there is generally less unsaturation (RDB < 10). Thus it was hypothesized that there might be more than one target class of compounds responsible for the activity against *T. brucei* with MIC values similar to those of the propolones.

The three most active extracts were CU29, S95 (Nigerian) and S87 (Ghanian) which exhibited highest activity against *T. brucei*. The amounts of S95 and S87 available

were sufficient for fractionation but there was not enough of CU29 to carry out fractionation. The S95 and S97 extracts were subjected to further fractionation in order to isolate the compounds responsible for anti-trypanosomal activity. The targeted compounds in the extracts were expected to display levels of potency against *T. brucei* similar to those of propolones even if propolones themselves were not in the final extracts. Following this idea, thirteen fractions were obtained from the Nigerian sample (S95) through medium pressure liquid chromatographic (MPLC) fractionation on a normal phase silica column. Fractions eluting early from the column at 50-40% of ethyl acetate/hexane (fraction 3-4) were found to contain compounds putatively assigned to propolones based on their elemental composition and the level of unsaturation detected in their molecular structure. Although putative assignment was based on the consideration that although elemental compositions matched propolone structures they could also correspond to compounds such as lignans. Moreover, the most highly active fractions eluted after fraction 5 thus suggesting the possibility of the presence of more than one target compound with the same level of biological activity.

The ethyl acetate extract of Ghanian propolis (S87) displayed the highest anti-trypanosomal activity based on MIC (0.78 μ g/ml) wherefore; it was subsequently investigated through both Medium Pressure Liquid Chromatography (MPLC) and HPLC in order to isolate highly bioactive fractions (shown in Table 5.2). This led to the identification of two main components which were found to be new stilbenes. Fractions 9, 12, 13 and 15 not only displayed relatively good anti-trypanosomal activity (Table 5.2) but also showed significant activity against *M. marinum*. Since the crude extract had not shown any significant anti-mycobacterial activity, it was hypothesized that the observed activity in the fractions had possibly manifested owing to increased concentration of extractable active compounds after fractionation of the crude material. Preliminary chemical screening of the crude extracts by reversed phase LC-MS in positive ion mode had detected that the most common abundant components might prenyl or geranyl flavanones (Chapter 5, Figure 5.1) which mainly appeared in fraction 15. These types of compounds are usually abundant in propolis samples from Africa and the Pacific regions (Huang et al.,

2014). In addition, the presence of the prenylated group in these compounds has been reported to enhance antimicrobial activity due to the lipophilic prenyl chain which enables them to penetrate into cell membranes and rapidly damage it (Raghukumar et al., 2010). However, in order to confirm the presence of these components in this fraction, further investigations are needed.

The two new prenylated stilbenes from the Ghanaian sample were obtained following further fractionation of fractions 9 and 13, obtained from MPLC, using different chromatographic techniques, and subsequently confirmed by the use of various spectrophotometric techniques including HR-ESI-MS, 1D, 2D NMR, optical rotation and UV. The pure compounds F9 (1) and F13-11(2) (Section 5.6, Figure 5.13) were thus identified as (*E*)-5-(2-(8-hydroxy-2-methyl-2-(4-methylpent-3-en-1-yl)-2*H*-chromen-6-yl) vinyl)-2-(3-methylbut-2-en-1-yl) benzene-1, 3-diol (1) and 5-((*E*)-3,5-dihydroxystyryl)-3-((*E*)-3,7-dimethylocta-2,6-dien-1-yl) benzene-1,2-diol (2) respectively. Both of these compounds are considered to be derivatives of mappain which had earlier been described as a cytotoxic agent from the leaves of a Hawaiian species of *Macaranga mapp* (Euphorbiaceae) (van der Kaaden et al., 2001). However, this class of phenolic stilbenoid is very difficult to produce as a natural secondary metabolite and because of this it is rarely predominant as a natural product (Yoder, 2005). A small number of studies have reported stilbenes to have been isolated from propolis. In 2010 Petrova et al reported two geranyl stilbenes (schweinfurthin A and B) isolated from Kenyan propolis and showed that they possessed anti-antibacterial activity against *S. aureus* (Petrova et al., 2010). In addition, the report also suggested that the plant source for these stilbenes was *Macaranga schweinfurthii* and it hypothesised that honeybees probably gathered the material from the plant species *Macaranga mapp* and *M. schweinfurthii* which are widespread in the Sub-Saharan African region. In addition, other prenylated stilbenes have been previously isolated from propolis originating from Kangaroo Island, in Australia, which showed antioxidant activity (Ghisalberti et al., 1978, Abu-Mellal et al., 2012). Both pure prenylated stilbenes (F9-1 and F13-11) exhibited activity against *T. brucei brucei* with MICs of 6.73 and 16.45 μ M, respectively.

The prenylated stilbene (F13-11) (Fig 1.13) was subjected to a metabolomic profiling study in order to try to gain an understanding of its effects on the metabolic system of trypanosomes or its mechanism of action in the organism. For that reason it was used to treat *T. b. brucei* (with appropriate controls) and metabolites were extracted at 0, 4 and 24 hours. Metabolites which demonstrated major effects were observed only at 24 h. The level of deamidation of the amino acids phenylalanine and histidine was reduced while arginine was not affected. In addition the level of sedoheptulose phosphate, which is in the pentose phosphate pathway, was elevated in the treated compared to untreated *T. brucei*. Also, the level of pyruvate which is the end product of glycolysis pathway was decreased. This implies that glycolysis, the pathway which provides energy during cell respiration, was inhibited which might have produced and increased level of sedoheptulose phosphate. Moreover, it was noticed that many phospholipids were altered by treatment with F13-11 which meant that either catabolism or synthesis had been occurring. This suggests that the cell membrane of the organism is altered by treatment in order to reduce the effect of the treatment and it suggests that the prenylated portion of structure F13-F11 could be interacting with the cell membrane.

Of special note are the results that were obtained from investigations of Saudi propolis which have been reported for the first time in this current study. There are a limited number of studies on propolis obtained from Saudi Arabia. It was found that in spite of the geographical source of the propolis being new, the isolated compounds exhibited interesting activity against both bacteria and trypanosoma. Furthermore the active compounds found in these samples were isolated for the first time from propolis and among these was a new diterpene. This fact evidently relates due to the diversity in the type of flora which grows in the mountainous regions of Southern Saudi Arabia and which is foraged by honeybees and may also be due to the unique strain of bees, *Apis mellifera jemenitica*, which are kept in Saudi Arabia. Crude extracts of Saudi propolis were initially screened using LC-ESI-MS and revealed that the main components were flavonoids, phenolics and terpenes (Section 7, Table 7.2), all of which are obviously common compounds in propolis originating from temperate regions. The crude extracts also showed significant biological activity. To

confirm this, the crude extracts were further purified in order to isolate individual components using different techniques including conventional chromatographic methods. The resulting earlier fractions (F4 and sub-F6) revealed three pure known flavonoids which were identified as psiadiarabin 1, psiadiarabin 2 and fisetinidol. Additionally, one new diterpene and another known diterpene were also obtained from sub-fraction 7. These compounds displayed varying but moderate activity against *T. brucei* and *M. marinum* and for the first time biological activity was tested on the compounds psiadiarabin 1 and 2 which had high potency values. However, no activity was observed for fisetinidol neither against trypanosomes nor bacteria. The most biologically active compound isolated was psiadin (Diterpene 2, Fig. 7.41. Pg. 166) with MIC values of 30.9 and 61.9 μM for *T. brucei* and *M. marinum*, respectively. It can be suggested that the antimicrobial activity displayed not only relates to the flavonoid class of compounds but also to terpenoids. Additionally, it is evident that these compounds obtained from propolis originated from *Psiadia* species which is their only plant source according to previous studies (El-Feraly et al., 1990, Eldomiaty et al., 1993, Mossa et al., 1992). A study by Albar (2009) reported in addition other compounds isolated from this plant species and their biological activity which included antibacterial and antifungal activities. Therefore, propolis constituents can be considered to be extracted from the plants by bees for their biological activity.

These pure compounds have been submitted for testing for anti-cancer and anti-leishmania activity, but the results have not been received yet.

CHAPTER 9:
CONCLUSIONS AND FUTURE WORK

9 CONCLUSIONS AND FUTURE WORK

The research described in this study investigated the main composition and biological activity of various propolis samples collected from different regions mainly in Africa. The primary aim of these investigations was to evaluate which of the sample constituents making up the propolis were the most active against trypanosoma.

During the preliminary stages, we developed a new method for rapid qualitative analysis of these propolis samples to determine their main components using various chromatographic and spectroscopic techniques. This was followed by conducting a series of chromatographic separations and aided with spectroscopic detection methods in order to fractionate and identify biologically active compounds from propolis extracts. Three novel compounds including two prenylated stilbenes (1) as (*E*)-5-(2-(8-hydroxy-2-methyl-2-(4-methylpent-3-en-1-yl)-2*H*-chromen-6-yl) vinyl)-2-(3-methylbut-2-en-1-yl) benzene-1, 3-diol and (2) as 5-((*E*)-3,5-dihydroxystyryl)-3-((*E*)-3,7-dimethylocta-2,6-dien-1-yl) benzene-1,2-diol and one diterpene (3) as (ent)-2-oxokaur-16-en-6, 18-diol (propsiadin) were isolated from Ghanian propolis and Saudi propolis (for diterpene 3). In addition, four known flavonoids and diterpene compounds were isolated from Saudi propolis samples including psiadiarabins 1, 2 which were isolated for the first time from propolis. These pure compounds all exhibited activity against *T. brucei* and *M. marinum in vitro* using the Alamar Blue assay technique.

The metabolomics study for stilbene 2 in trypanosomes revealed many changes in the cell metabolome of the organism caused by the compound which might give some insights into the mechanism of action of propolis in the typanosoma cell system. Most of the present study has already been published in the three papers listed at the beginning of the thesis (page xxii).

Overall, this work has revealed new propolis constituents which possess potential biological activity and has confirmed the presence of some interesting compounds which could be employed as lead compounds for new drug discovery. For new pure

compounds further investigations are needed to study SARs in relation to Trypanosoma and Mycobacteria in order to determine the effect of changes in functional groups on their biological activity. For compounds psiadiarabin 1 and 2, it is further recommended that these should be tested against *M. tuberculosis* and *Leishmania*. There are many more exciting components in Saudi propolis which could be isolated, characterised and tested and this research will certainly be continued.

10 REFERENCES

- ABRAHAM, R. & MOBLI, M. 2009. *Modelling 1H NMR Spectra of Organic Compounds : Theory, Applications and NMR Prediction Software*, Chichester, GBR, John Wiley & Sons.
- ABU-MELLAL, A., KOOLAJI, N., DUKE, R. K., TRAN, V. H. & DUKE, C. C. 2012. Prenylated cinnamate and stilbenes from Kangaroo Island propolis and their antioxidant activity. *Phytochemistry*, 77, 251-259.
- ALBAR, P. H. A. H. 2014. *Chemical constituent of P. punctulata from Saudi Arabia* [Online]. Saudi Arabia. Available: http://www.kau.edu.sa/Show_Res.aspx?Site_ID=0001866&Lng=EN&RN=34463 [Accessed 11 July 2014].
- ALMUTAIRI, S., EAPEN, B., CHUNDI, S. M., AKHALIL, A., SIHERI, W., CLEMENTS, C., FEARNLEY, J., WATSON, D. G. & EDRADA-EBEL, R. 2014. New anti-trypanosomal active prenylated compounds from African propolis. *Phytochemistry Letters*, 10, 35-39.
- ALQARNI, A. S., HANNAN, M. A., OWAYSS, A. A. & ENGEL, M. S. 2011. The indigenous honey bees of Saudi Arabia (Hymenoptera, Apidae, *Apis mellifera jemenitica* Ruttner): Their natural history and role in beekeeping. *Zookeys*, 83-98.
- ALYAHYA, M. A., HIFNAWY, M. S., MOSSA, J. S., ELFERALY, F. S., MCPHAIL, D. R. & MCPHAIL, A. T. 1987. X-RAY STRUCTURE OF PSIADIARABIN, A FLAVONE FROM PSIADIA-ARABICA. *Phytochemistry*, 26, 2648-2649.
- ANON 2008. Parasite Database. 16 July ed.: Lifecenter.
- BAE, Y.-S., BURGER, J. F. W., STEYNBERG, J. P., FERREIRA, D. & HEMINGWAY, R. W. 1994. Flavan and procyanidin glycosides from the bark of blackjack oak. *Phytochemistry*, 35, 473-478.
- BANSKOTA, A. H., TEZUKA, Y. & KADOTA, S. 2001. Recent progress in pharmacological research of propolis. *Phytotherapy Research*, 15, 561-571.
- BARRETT, M., BOYKIN, D., BRUN, R. & TIDWELL, R. 2007. Human African trypanosomiasis: pharmacological re-engagement with a neglected disease. *British journal of pharmacology*, 152, 1155-1171.
- BARRETT, M. P., BAKKER, B. M. & BREITLING, R. 2010. Metabolomic systems biology of trypanosomes. *Parasitology*, 137, 1285-1290.
- BARRETT, M. P., BURCHMORE, R. J., STICH, A., LAZZARI, J. O., FRASCH, A. C., CAZZULO, J. J. & KRISHNA, S. 2003. The trypanosomiasis. *The Lancet*, 362, 1469-1480.
- BELOFSKY, G., FRENCH, A. N., WALLACE, D. R. & DODSON, S. L. 2004. New geranyl stilbenes from *Dalea purpurea* with in vitro opioid receptor affinity. *Journal of Natural Products*, 67, 26-30.
- BERTELLI, D., PAPOTTI, G., BORTOLOTTI, L., MARCAZZAN, G. L. & PLESSI, M. 2012. 1H-NMR Simultaneous Identification of Health-Relevant Compounds in Propolis Extracts. *Phytochemical Analysis*, 23, 260-266.

- BOUTEILLE, B., OUKEM, O., BISSER, S. & DUMAS, M. 2003. Treatment perspectives for human African trypanosomiasis. *Fundamental & clinical pharmacology*, 17, 171-181.
- BREITLING, R., PITT, A. R. & BARRETT, M. P. 2006. Precision mapping of the metabolome. *TRENDS in Biotechnology*, 24, 543-548.
- BREITMAIER, E. 1993. *Front Matter*, Wiley Online Library.
- BRINGAUD, F., RIVIÈRE, L. & COUSTOU, V. 2006. Energy metabolism of trypanosomatids: adaptation to available carbon sources. *Molecular and biochemical parasitology*, 149, 1-9.
- BRUN, R., BLUM, J., CHAPPUIS, F. & BURRI, C. 2010. Human african trypanosomiasis. *The Lancet*, 375, 148-159.
- BURDOCK, G. A. 1998. Review of the biological properties and toxicity of bee propolis (propolis). *Food and Chemical Toxicology*, 36, 347-363.
- CEBOLLA, V. L., MEMBRADO, L., VELA, J. & FERRANDO, A. C. 1997. Evaporative light-scattering detection in the quantitative analysis of semivolatile polycyclic aromatic compounds by high-performance liquid chromatography. *Journal of chromatographic science*, 35, 141-150.
- CHEN, C., GONZALEZ, F. J. & IDLE, J. R. 2007. LC-MS-based metabolomics in drug metabolism. *Drug metabolism reviews*, 39, 581-597.
- CHENG, Y., LIANG, Q., HU, P., WANG, Y., JUN, F. W. & LUO, G. 2010. Combination of normal-phase medium-pressure liquid chromatography and high-performance counter-current chromatography for preparation of ginsenoside-Ro from panax ginseng with high recovery and efficiency. *Separation and Purification Technology*, 73, 397-402.
- CHOU, C. C., CHEN, Y. W. & LU, L. C. 2005. Antibacterial activity of propolis against *Staphylococcus aureus*. *Int J Food Microbiol*, 100, 213-220.
- CLAESON, P., TUCHINDA, P. & REUTRAKUL, V. 1993. Some empirical aspects on the practical use of flash chromatography and medium pressure liquid chromatography for the isolation of biologically active compounds from plants. *J Sci Soc Thailand*, 19, 73-86.
- COUSTOU, V., BIRAN, M., BRETON, M., GUEGAN, F., RIVIÈRE, L., PLAZOLLES, N., NOLAN, D., BARRETT, M. P., FRANCONI, J.-M. & BRINGAUD, F. 2008. Glucose-induced remodeling of intermediary and energy metabolism in procyclic *Trypanosoma brucei*. *Journal of Biological Chemistry*, 283, 16342-16354.
- CRANE, E. 1990. *Bees and Beekeeping Science Practice and World Resources*, Oxford, Heinemann Professional Publishing Ltd.
- CREEK, D. J., ANDERSON, J., MCCONVILLE, M. J. & BARRETT, M. P. 2012. Metabolomic analysis of trypanosomatid protozoa. *Molecular and biochemical parasitology*, 181, 73-84.
- CUMMINS, H. & JONES, A. 2000. Nuclear magnetic resonance: a quantum technology for computation and spectroscopy. *Contemporary Physics*, 41, 383-399.
- DE CASTRO ISHIDA, V. F., NEGRI, G., SALATINO, A. & BANDEIRA, M. F. C. 2011. A new type of Brazilian propolis: Prenylated benzophenones in propolis from Amazon and effects against cariogenic bacteria. *Food chemistry*, 125, 966-972.

- DE CHAGAS, M. 2009. Transmission and Life Cycle.
- DE GROOT, A. C., POPOVA, M. P. & BANKOVA, V. S. 2014. AN UPDATE ON THE CONSTITUENTS OF POPLAR-TYPE PROPOLIS. 11.
- DETTMER, K., ARONOV, P. A. & HAMMOCK, B. D. 2007. Mass spectrometry-based metabolomics. *Mass spectrometry reviews*, 26, 51-78.
- DUMAS, M., BOUTEILLE, B. & BUGUET, A. 1999. *Progress in human African trypanosomiasis, sleeping sickness*, Springer-Verlag France.
- DVOŘÁČKOVÁ, E., ŠNÓBLOVÁ, M. & HRDLIČKA, P. 2014. Carbohydrate analysis: From sample preparation to HPLC on different stationary phases coupled with evaporative light-scattering detection. *Journal of separation science*, 37, 323-337.
- EL-FERALY, F. S., MOSSA, J. S., AL-YAHYA, M. A., HIFNAWY, M. S., HAFEZ, M. M. & HUFFORD, C. D. 1990. Two flavones from *Psiadia arabica*. *Phytochemistry*, 29, 3372-3373.
- EL-MAWLA, A. M. A. A. & OSMAN, H. E. H. 2011. HPLC analysis and role of the Saudi Arabian propolis in improving the pathological changes of kidney treated with monosodium glutamate. *Spatula DD*, 1, 119-127.
- EL-SHAFAR, A. M. & IBRAHIM, M. A. 2003. Bioactive kaurane diterpenes and coumarins from *Fortunella margarita*. *Die Pharmazie - An International Journal of Pharmaceutical Sciences*, 58, 143-147.
- ELDOMIATY, M. M., ELFERALY, F. S., MOSSA, J. S. & MCPHAIL, A. T. 1993. DITERPENES FROM *PSIADIA-ARABICA*. *Phytochemistry*, 34, 467-471.
- ELLIS, D. I., DUNN, W. B., GRIFFIN, J. L., ALLWOOD, J. W. & GOODACRE, R. 2007. Metabolic fingerprinting as a diagnostic tool.
- FAIRLAMB, A. H. 2002. Metabolic pathway analysis in trypanosomes and malaria parasites. *PHILOSOPHICAL TRANSACTIONS-ROYAL SOCIETY OF LONDON SERIES B BIOLOGICAL SCIENCES*, 357, 101-108.
- FAIRLAMB, A. H. 2003. Chemotherapy of human African trypanosomiasis: current and future prospects. *Trends in parasitology*, 19, 488-494.
- FALCÃO, S. I., VILAS-BOAS, M., ESTEVINHO, L. M., BARROS, C., DOMINGUES, M. R. & CARDOSO, S. M. 2010. Phenolic characterization of Northeast Portuguese propolis: usual and unusual compounds. *Analytical and bioanalytical chemistry*, 396, 887-897.
- FIEHN, O. 2001. Combining genomics, metabolome analysis, and biochemical modelling to understand metabolic networks. *Comparative and Functional Genomics*, 2, 155-168.
- FIEHN, O. 2002. Metabolomics—the link between genotypes and phenotypes. *Plant molecular biology*, 48, 155-171.
- FRANZBLAU, S. G., WITZIG, R. S., MCLAUGHLIN, J. C., TORRES, P., MADICO, G., HERNANDEZ, A., DEGNAN, M. T., COOK, M. B., QUENZER, V. K., FERGUSON, R. M. & GILMAN, R. H. 1998. Rapid, low-technology MIC determination with clinical *Mycobacterium tuberculosis* isolates by using the microplate Alamar Blue assay. *Journal of Clinical Microbiology*, 36, 362-366.
- FRIEDHEIM, E. A. 1949. Mel B in the treatment of human trypanosomiasis. *The American journal of tropical medicine and hygiene*, 1, 173-180.

- GHISALBERTI, E. L., JEFFERIES, P. R., LANTERI, R. & MATISONS, J. 1978. Constituents of propolis. *Experientia*, 34, 157-158.
- GOODACRE, R., VAIDYANATHAN, S., DUNN, W. B., HARRIGAN, G. G. & KELL, D. B. 2004. Metabolomics by numbers: acquiring and understanding global metabolite data. *TRENDS in Biotechnology*, 22, 245-252.
- GREEK, A. 1997. WHAT IS PROPOLIS ? . *Helicobacter*, pp.1-11.
- HAANSTRA, J. R., VAN TUIJL, A., KESSLER, P., REIJNDERS, W., MICHELS, P. A., WESTERHOFF, H. V., PARSONS, M. & BAKKER, B. M. 2008. Compartmentation prevents a lethal turbo-explosion of glycolysis in trypanosomes. *Proceedings of the National Academy of Sciences*, 105, 17718-17723.
- HAMILTON, M. 2014. *While world focuses on Ebola, Chagas disease surges ahead* [Online]. Available <http://www.digitaljournal.com/news/world/while-world-focuses-on-ebola-chagas-disease-surges-ahead/article/410080#ixzz3afwpCdX1> [Accessed 5-2015].
- HAUSEN, B., WOLLENWEBER, E., SENFF, H. & POST, B. 1987. Propolis allergy. *Contact dermatitis*, 17, 163-170.
- HERNÁNDEZ, I. M., FERNANDEZ, M. C., CUESTA-RUBIO, O., PICCINELLI, A. L. & RASTRELLI, L. 2005. Polyprenylated benzophenone derivatives from Cuban propolis. *Journal of Natural Products*, 68, 931-934.
- HOET, S., OPPERDOES, F., BRUN, R. & QUETIN-LECLERCQ, J. 2004. Natural products active against African trypanosomes: a step towards new drugs. *Natural Product Reports*, 21, 353-364.
- HU, Q., NOLL, R. J., LI, H., MAKAROV, A., HARDMAN, M. & GRAHAM COOKS, R. 2005. The Orbitrap: a new mass spectrometer. *Journal of mass spectrometry*, 40, 430-443.
- HUANG, S., ZHANG, C.-P., WANG, K., LI, G. Q. & HU, F.-L. 2014. Recent Advances in the Chemical Composition of Propolis. *Molecules*, 19, 19610-19632.
- IKEGAKI, M. & KOO, H. 2013. Antimicrobial and antiproliferative activities of stingless bee *Melipona scutellaris* geopropolis. *BMC Complementary and Alternative Medicine*, 13, 23-34.
- INUI, S., HOSOYA, T., SHIMAMURA, Y., MASUDA, S., OGAWA, T., KOBAYASHI, H., SHIRAFUJI, K., MOLI, R. T., KOZONE, I. & SHIN-YA, K. 2012. Solophenols B–D and Solomonin: New Prenylated Polyphenols Isolated from Propolis Collected from The Solomon Islands and Their Antibacterial Activity. *Journal of Agricultural and Food Chemistry*, 60, 11765-11770.
- JERZ, G., ELNAKADY, Y. A., BRAUN, A., JÄCKEL, K., SASSE, F., AL GHAMDI, A. A., OMAR, M. O. M. & WINTERHALTER, P. 2014. Preparative mass-spectrometry profiling of bioactive metabolites in Saudi-Arabian propolis fractionated by high-speed countercurrent chromatography and off-line atmospheric pressure chemical ionization mass-spectrometry injection. *Journal of Chromatography A*, 1347, 17-29.

- KANG, J.-S. Principles and Applications of LC-MS/MS for the Quantitative Bioanalysis of Analytes in Various Biological Samples. *Tandem Mass Spectrometry—Applications and Principles*, 441-492.
- KANG, J.-S. 2012. Principles and Applications of LC-MS/MS for the Quantitative Bioanalysis of Analytes in Various Biological Samples. *Tandem Mass Spectrometry—Applications and Principles*, 441-492.
- KORFMACHER, W. A. 2005. Foundation review: Principles and applications of LC-MS in new drug discovery. *Drug Discovery Today*, 10, 1357-1367.
- KRAUSS, M., SINGER, H. & HOLLENDER, J. 2010. LC-high resolution MS in environmental analysis: from target screening to the identification of unknowns. *Analytical and Bioanalytical Chemistry*, 397, 943-951.
- KÜHL, O. 2008. Phosphorus-31 NMR Spectroscopy. Springer-Verlag, Berlin–Heidelberg.
- LEE, C. W. & MAURICE, J. M. 1983. The African trypanosomiases : methods and concepts of control and eradication in relation to development. *The African trypanosomiases*. Washington, D.C., U.S.A: World Bank, c1983.
- LEGROS, D., OLLIVIER, G., GASTELLU-ETCHEGORRY, M., PAQUET, C., BURRI, C., JANNIN, J. & BÜSCHER, P. 2002. Treatment of human African trypanosomiasis—present situation and needs for research and development. *The Lancet infectious diseases*, 2, 437-440.
- LEWIS, G. D., WEI, R., LIU, E., YANG, E., SHI, X., MARTINOVIC, M., FARRELL, L., ASNANI, A., CYRILLE, M. & RAMANATHAN, A. 2008. Metabolite profiling of blood from individuals undergoing planned myocardial infarction reveals early markers of myocardial injury. *The Journal of clinical investigation*, 118, 3503-3512.
- LI, F., AWALE, S., TEZUKA, Y. & KADOTA, S. 2008. Cytotoxic constituents from Brazilian red propolis and their structure–activity relationship. *Bioorganic & medicinal chemistry*, 16, 5434-5440.
- LI, J. V., SARIC, J., WANG, Y., UTZINGER, J., HOLMES, E. & BALMER, O. 2011. Metabonomic investigation of single and multiple strain *Trypanosoma brucei brucei* infections. *The American journal of tropical medicine and hygiene*, 84, 91-98.
- LINDON, J. C., NICHOLSON, J. K. & HOLMES, E. 2011. Metabolic Profiling: Applications in Plant Science. *The Handbook of Metabonomics and Metabolomics*, 443.
- LOONEY, P. M. 2012. *QUANTIFICATION AND CHARACTERIZATION OF BIOLOGICALLY ACTIVE COMPONENTS OF ACTAEA RACEMOSA L.(BLACK COHOSH) FOR IDENTIFYING DESIRABLE PLANTS FOR CULTIVATION*. Western Carolina University.
- LOTFY, M. 2006. Biological activity of bee propolis in health and disease. *Asian Pac J Cancer Prev*, 7, 22-31.
- LU, L.-C., CHEN, Y.-W. & CHOU, C.-C. 2005. Antibacterial activity of propolis against *Staphylococcus aureus*. *International journal of food microbiology*, 102, 213-220.
- MARCUCCI, M., C. 1995. Propolis: chemical composition, biological properties and therapeutic activity. *Apidologie*, 26, 83-99.

- MATSUHISA, M., SHIKISHIMA, Y., TAKAISHI, Y., HONDA, G., ITO, M., TAKEDA, Y., SHIBATA, H., HIGUTI, T., KODZHIMATOV, O. K. & ASHURMETOV, O. 2002. Benzoylphloroglucinol Derivatives from *Hypericum s cabrum*. *Journal of Natural Products*, 65, 290-294.
- MIDIWO, J. O., OWUOR, F. A. O., JUMA, B. F. & WATERMAN, P. G. 1997. Diterpenes, from the leaf exudate of *Psiadia punctulata*. *Phytochemistry*, 45, 117-120.
- MIDORIKAWA, K., BANSKOTA, A. H., TEZUKA, Y., NAGAOKA, T., MATSUSHIGE, K., MESSAGE, D., HUERTAS, A. A. G. & KADOTA, S. 2001. Liquid chromatography–mass spectrometry analysis of propolis. *Phytochemical Analysis*, 12, 366-373.
- MOORE, A. & RICHER, M. 2001. Re-emergence of epidemic sleeping sickness in southern Sudan. *Tropical Medicine & International Health*, 6, 342-347.
- MOREDA-PIÑEIRO, A., FISHER, A. & HILL, S. J. 2003. The classification of tea according to region of origin using pattern recognition techniques and trace metal data. *Journal of Food Composition and Analysis*, 16, 195-211.
- MORENO, B., URBINA, J. A., OLDFIELD, E., BAILEY, B. N., RODRIGUES, C. O. & DOCAMPO, R. 2000. ³¹P NMR spectroscopy of *Trypanosoma brucei*, *Trypanosoma cruzi*, and *Leishmania major* Evidence for high levels of condensed inorganic phosphates. *Journal of Biological Chemistry*, 275, 28356-28362.
- MOSSA, J. S., ELDOMIATY, M. M., ALMESHAL, I. A., ELFERALY, F. S., HUFFORD, C. D., MCPHAIL, D. R. & MCPHAIL, A. T. 1992. A FLAVONE AND DITERPENE FROM *PSIADIA-ARABICA*. *Phytochemistry*, 31, 2863-2868.
- NIELSEN, J. & JEWETT, M. C. 2007. *Metabolomics: a powerful tool in systems biology*, Springer.
- OLDIGES, M., NOACK, S. & PACZIA, N. 2013. Metabolomics in Biotechnology (Microbial Metabolomics). *Metabolomics in Practice: Successful Strategies to Generate and Analyze Metabolic Data*, 379-391.
- OLIVEIRA, A. P., FRANÇA, H., KUSTER, R., TEIXEIRA, L. & ROCHA, L. 2010. Chemical composition and antibacterial activity of Brazilian propolis essential oil. *Journal of Venomous Animals and Toxins including Tropical Diseases*, 16, 121-130.
- PAVIA, D. L., LAMPMAN, G. M., KRIZ, G. S. & VYVYAN, J. R. 2009. *Introduction to Spectroscopy*, Washington Brooks/ Cole.
- PEPIN, J. & MILORD, F. 1994. The treatment of human African trypanosomiasis. *Advances in parasitology*, 33, 1-47.
- PETROVA, A., POPOVA, M., KUZMANOVA, C., TSVETKOVA, I., NAYDENSKI, H., MULI, E. & BANKOVA, V. 2010. New biologically active compounds from Kenyan propolis. *Fitoterapia*, 81, 509-514.
- PEYFOON, E. 2009. *Chemical and biological properties of propolis*. Ph.D, University of Strathclyde.
- PIACENTE, S., BALDERRAMA, L., DE TOMMASI, N., MORALES, L., VARGAS, L. & PIZZA, C. 1999. Anadanthoside: a flavanol-3-O-beta-D-xylopyranoside from *Anadenanthera macrocarpa*. *Phytochemistry*, 51, 709-711.

- PICCINELLI, A. L., CAMPONE, L., DAL PIAZ, F., CUESTA-RUBIO, O. & RASTRELLI, L. 2009. Fragmentation pathways of polycyclic polyisoprenylated benzophenones and degradation profile of nemorosone by multiple-stage tandem mass spectrometry. *Journal of the American Society for Mass Spectrometry*, 20, 1688-1698.
- PLUSKAL, T., CASTILLO, S., VILLAR-BRIONES, A. & ORESIC, M. 2010. MZmine 2: Modular framework for processing, visualizing, and analyzing mass spectrometry-based molecular profile data. *Bmc Bioinformatics*, 11.
- POPOVA, M. P., GRAIKOU, K., CHINOU, I. & BANKOVA, V. S. 2010. GC-MS profiling of diterpene compounds in Mediterranean propolis from Greece. *Journal of Agricultural and Food Chemistry*, 58, 3167-3176.
- QUATTROCCHI, U. 2012. *CRC World Dictionary of Medicinal and Poisonous Plants: Common Names, Scientific Names, Eponyms, Synonyms, and Etymology (5 Volume Set)*, CRC Press.
- RAGHUKUMAR, R., VALI, L., WATSON, D., FEARNLEY, J. & SEIDEL, V. 2010. Antimethicillin-resistant *Staphylococcus aureus* (MRSA) activity of 'pacific propolis' and isolated prenylflavanones. *Phytotherapy Research*, 24, 1181-1187.
- RAI, M., CORDELL, G. A., MARTINEZ, J. L., MARINOFF, M. & RASTRELLI, L. 2012. *Medicinal plants: biodiversity and drugs*, CRC Press.
- RASUL, A., ZHAO, B.-J., LIU, J., LIU, B., SUN, J.-X., LI, J. & LI, X.-M. 2014. Molecular Mechanisms of Casticin Action: an Update on its Antitumor Functions. *Asian Pacific journal of cancer prevention: APJCP*, 15, 9049.
- RÄZ, B., ITEN, M., GREYER-BÜHLER, Y., KAMINSKY, R. & BRUN, R. 1997. The Alamar Blue® assay to determine drug sensitivity of African trypanosomes (*T.b. rhodesiense* and *T.b. gambiense*) in vitro. *Acta Tropica*, 68, 139-147.
- ROBINSON, K., PRINS, J. & VENKATESH, B. 2011. Clinical review: adiponectin biology and its role in inflammation and critical illness. *Crit Care*, 15, 221.
- ROESSNER, U. & BOWNE, J. 2009. What is metabolomics all about? *Biotechniques*, 46, 363.
- SALATINO, A., FERNANDES-SILVA, C. C., RIGHI, A. A. & SALATINO, M. L. F. 2011. Propolis research and the chemistry of plant products. *Natural Product Reports*, 28, 925-936.
- SALOMAO, K., PEREIRA, P. R. S., CAMPOS, L. C., BORBA, C. M., CABELLO, P. H., MARCUCCI, M. C. & DE CASTRO, S. L. 2008. Brazilian propolis: correlation between chemical composition and antimicrobial activity. *Evidence-Based Complementary and Alternative Medicine*, 5, 317-324.
- SCALBERT, A., BRENNAN, L., FIEHN, O., HANKEMEIER, T., KRISTAL, B. S., VAN OMMEN, B., PUJOS-GUILLOT, E., VERHEIJ, E., WISHART, D. & WOPEREIS, S. 2009. Mass-spectrometry-based metabolomics: limitations and recommendations for future progress with particular focus on nutrition research. *Metabolomics*, 5, 435-458.
- SCHMIDT, J. B., S. 1992. Research Entomologists, Carl Hayden Bee Research Center.

- SEIDEL, V., PEYFOON, E., WATSON, D. G. & FEARNLEY, J. 2008. Comparative study of the antibacterial activity of propolis from different geographical and climatic zones. *Phytotherapy Research*, 22, 1256-1263.
- SHAW, D., LEON, C., KOLEV, S. & MURRAY, V. 1997. Traditional remedies and food supplements. *Drug safety*, 17, 342-356.
- SHIMADZU 2015. Principles and Practical Applications of Shimadzu's ELSD-LT 2 Evaporative Light Scattering. Japan.
- SHIN, M. H., LEE, D. Y., LIU, K.-H., FIEHN, O. & KIM, K. H. 2010. Evaluation of sampling and extraction methodologies for the global metabolic profiling of Saccharophagus degradans. *Analytical chemistry*, 82, 6660-6666.
- SMITH, D. H., PEPIN, J. & STICH, A. H. 1998. Human African trypanosomiasis: an emerging public health crisis. *British Medical Bulletin*, 54, 341-355.
- SNIDER, J. 2014. *Overview of Mass Spectrometry* [Online]. UK: Thermo Scientific. Available: <http://www.piercenet.com/method/overview-mass-spectrometry> [Accessed OCTOBER 2014 2014].
- STILL, W. C., KAHN, M. & MITRA, A. 1978. Rapid chromatographic technique for preparative separations with moderate resolution. *The Journal of Organic Chemistry*, 43, 2923-2925.
- SUZUKI, A., SHIROTA, O., MORI, K., SEKITA, S., FUCHINO, H., TAKANO, A. & KUROYANAGI, M. 2009. Leishmanicidal active constituents from Nepalese medicinal plant Tulsi (*Ocimum sanctum* L.). *Chemical and Pharmaceutical Bulletin*, 57, 245-251.
- T'KINDT, R., JANKEVICS, A., SCHELTEMA, R. A., ZHENG, L., WATSON, D. G., DUJARDIN, J.-C., BREITLING, R., COOMBS, G. H. & DECUYPERE, S. 2010. Towards an unbiased metabolic profiling of protozoan parasites: optimisation of a Leishmania sampling protocol for HILIC-orbitrap analysis. *Analytical and Bioanalytical Chemistry*, 398, 2059-2069.
- TEZUKA, Y., KADOTA, S. & BANSKOTA, A. H. 2001. Recent progress in pharmacological research of propolis. *Phytotherapy Research*, 15, 565-575.
- THEODORIDIS, G. A., GIKA, H. G. & WILSON, I. D. 2013. LC-MS-Based Nontargeted Metabolomics. *Metabolomics in Practice*. Wiley-VCH Verlag GmbH & Co. KGaA.
- TOMITA, M. & NISHIOKA, T. 2006. *Metabolomics: the frontier of systems biology*, Springer.
- TRYGG, J., HOLMES, E. & LUNDSTEDT, T. 2007. Chemometrics in metabolomics. *Journal of proteome research*, 6, 469-479.
- TSOPMO, A., TENE, M., KAMNAING, P., NGNOKAM, D., AYAFOR, J. F. & STERNER, O. 1998. Geranylated flavonoids from *Dorstenia poinsettifolia*. *Phytochemistry*, 48, 345-348.
- VAN DER KAADEN, J. E., HEMSCHEIDT, T. K. & MOOBERRY, S. L. 2001. Mappain, a new cytotoxic prenylated stilbene from *Macaranga mappia*. *Journal of Natural Products*, 64, 103-105.
- VINCENT, I. M., CREEK, D., WATSON, D. G., KAMLEH, M. A., WOODS, D. J., WONG, P. E., BURCHMORE, R. J. & BARRETT, M. P. 2010. A molecular mechanism for eflornithine resistance in African trypanosomes. *PLoS pathogens*, 6, e1001204.

- VOLPI, N. & BERGONZINI, G. 2006. Analysis of flavonoids from propolis by on-line HPLC–electrospray mass spectrometry. *Journal of pharmaceutical and biomedical analysis*, 42, 354-361.
- WAGH, V. D. 2013. Propolis: A Wonder Bees Product and Its Pharmacological Potentials. *Advances in pharmacological sciences*, 2013.
- WANG, Y., HAMBURGER, M., GUEHO, J. & HOSTETTMANN, K. 1989. Antimicrobial flavonoids from *Psiadia trinervia* and their methylated and acetylated derivatives. *Phytochemistry*, 28, 2323-2327.
- WEBER, P., HAMBURGER, M., SCHAFFROTH, N. & POTTERAT, O. 2011. Flash chromatography on cartridges for the separation of plant extracts: Rules for the selection of chromatographic conditions and comparison with medium pressure liquid chromatography. *Fitoterapia*, 82, 155-161.
- WHO. 2013. *Trypanosomiasis, human African (sleeping sickness)*, factsheet 259 [Online].
- WISHART, D. S. 2008. Applications of metabolomics in drug discovery and development. *Drugs in R & D*, 9, 307-322.
- WOJTYCZKA, R. D., KEPA, M., IDZIK, D., KUBINA, R., KABAŁA-DZIK, A., DZIEDZIC, A. & WĄSIK, T. J. 2013. In vitro antimicrobial activity of ethanolic extract of Polish propolis against biofilm forming *Staphylococcus epidermidis* strains. *Evidence-Based Complementary and Alternative Medicine*, 2013.
- XIAN, F., HENDRICKSON, C. L. & MARSHALL, A. G. 2012. High resolution mass spectrometry. *Analytical chemistry*, 84, 708-719.
- YODER, B. J. 2005. *Isolation and structure elucidation of cytotoxic natural products from the rainforests of Madagascar and Suriname*. PhD, Faculty of the Virginia Polytechnic Institute and State University.
- YOUNG, C. S. & DOLAN, J. W. 2003. Success with evaporative light-scattering detection. *LC-GC*, 21, 120-128.
- ZHANG, R., WATSON, D. G., WANG, L., WESTROP, G. D., COOMBS, G. H. & ZHANG, T. 2014. Evaluation of mobile phase characteristics on three zwitterionic columns in hydrophilic interaction liquid chromatography mode for liquid chromatography-high resolution mass spectrometry based untargeted metabolite profiling of *Leishmania* parasites. *Journal of Chromatography A*, 1362, 168-179.

11 Appendix I: Publication